



HAL
open science

Sedimentological and structural evolution of the Tertiary Dévoluy Basin, external western Alps, SE France

Laurence Daniel Meckel

► **To cite this version:**

Laurence Daniel Meckel. Sedimentological and structural evolution of the Tertiary Dévoluy Basin, external western Alps, SE France. Tectonics. Eidgenössische Technische Hochschule Zürich (ETHZ), 1997. English. NNT: . tel-00799329

HAL Id: tel-00799329

<https://theses.hal.science/tel-00799329v1>

Submitted on 12 Mar 2013

HAL is a multi-disciplinary open access archive for the deposit and dissemination of scientific research documents, whether they are published or not. The documents may come from teaching and research institutions in France or abroad, or from public or private research centers.

L'archive ouverte pluridisciplinaire **HAL**, est destinée au dépôt et à la diffusion de documents scientifiques de niveau recherche, publiés ou non, émanant des établissements d'enseignement et de recherche français ou étrangers, des laboratoires publics ou privés.



MECKEL (L.D.)

1997

DISS. ETH Nr. 12008

**Sedimentological and structural evolution of the Tertiary Dévoluy Basin,
external western Alps, SE France**

A dissertation submitted to the
SWISS FEDERAL INSTITUTE OF TECHNOLOGY ZÜRICH

for the degree of
Doctor of Natural Sciences

UNIVERSITE DE GRENOBLE
INSTITUT DE GÉOLOGIE
DOCUMENTATION
15, RUE MAURICE GIGNOUX
F 38031 GRENOBLE CEDEX
TÉL. (33) 76 63 59 66
FAX. (33) 76 87 02 43

presented by
Lawrence Daniel Meckel, III
Master of Arts, The University of Texas, Austin, Texas, U.S.A.

born April 1st, 1967
citizen of The United States of America

accepted on the recommendation of
Prof. Dr. D. Bernoulli
Dr. M. Ford
Prof. Dr. P. Homewood

examiner
1. co-examiner
2. co-examiner

1997

(A.S.) MECKEL (D.V.)

FRAT

DISS. ETH Nr. 12008

**Sedimentological and structural evolution of the Tertiary Dévoluy Basin,
external western Alps, SE France**

A dissertation submitted to the
SWISS FEDERAL INSTITUTE OF TECHNOLOGY ZÜRICH

for the degree of
Doctor of Natural Sciences

presented by
Lawrence Daniel Meckel, III
Master of Arts, The University of Texas, Austin, Texas, U.S.A.

born April 1st, 1967
citizen of The United States of America

accepted on the recommendation of
Prof. Dr. D. Bernoulli
Dr. M. Ford
Prof. Dr. P. Homewood

UNIVERSITÉ DE GRENOBLE I
INSTITUT DE GÉOLOGIE
DOCUMENTATION
15, RUE MAURICE GIGNOUX
F 38031 GRENOBLE CEDEX
TEL. (33) 76 83 59 66
FAX. (33) 76 87 82 43

examiner
1. co-examiner
2. co-examiner

1997

no: 10190703

i
TABLE OF CONTENTS

ABSTRACT	iv
RESUMÉ	vi
ACKNOWLEDGEMENTS	viii
CHAPTER 1: Introduction	1
1.1. Overview	1
1.1.1. Objectives and aims	1
1.1.2. Methods	2
1.2. The external Western Alps	4
1.2.1. Geographical and geological setting	4
1.2.2. General evolution	5
1.3. Dévoluy	9
1.3.1. Location and physiography	9
1.3.2. Stratigraphic and sedimentary setting	9
1.3.3. Structural and tectonic setting	13
PART I: STRATIGRAPHY AND SEDIMENTOLOGY OF THE PALEOGENE DÉVOLUY BASIN	16
CHAPTER 2: The Pierroux Conglomerate Formation	17
2.1. Lithofacies analysis and stratigraphy	21
2.2. Paleocene/Eocene folding and Eocene normal faulting	26
2.3. Depositional setting and provenance	30
CHAPTER 3: The Dévoluy Nummulitic Limestone Formation	32
3.1. The Nummulitic Conglomerate Member	33
3.1.1. Lithofacies analysis and stratigraphy	35
3.1.2. Syndepositional extensional faulting and associated topography	44
3.1.3. Depositional setting and provenance	46
3.2. The Nummulitic Calcarene Member	47
3.2.1. Lithofacies analysis and stratigraphy	48
3.2.2. Depositional setting	49
CHAPTER 4: The Queyras Marlstone Formation	50
4.1. Lithofacies analysis and stratigraphy	54
4.2. Depositional setting	60
CHAPTER 5: The Souloise Greywacke Formation	61
5.1. Lithofacies analysis and stratigraphy	63
5.2. Petrography and provenance	75
5.3. Depositional setting	75
CHAPTER 6: The St-Disdier Arenite Formation	78
6.1. Lithofacies analysis and stratigraphy	79
6.2. Rupelian thrusting and uplift: the development of the western Dévoluy unconformity	89
6.3. Petrography and provenance	89
6.4. Depositional setting	91
CHAPTER 7: The St-Disdier Siltstone Formation	94
7.1. Lithofacies analysis and stratigraphy	94
7.2. Petrography and provenance	104

Univ. J. Fourier - O.S.U.G.
MAISON DES GEOSCIENCES
DOCUMENTATION
F. 38041 B.P. 53
Tél. 04 76 63 54 27 - Fax 04 76 51 40 58
Mail: platour@ujf-grenoble.fr

UNIVERSITÉ DE GRENOBLE
INSTITUT DE GÉOLOGIE
DOCUMENTATION
14, RUE MATHIEU GOMBEAU
F. 38041 GRENOBLE CEDEX
TÉL. (04) 76 63 54 27
FAX (04) 76 51 40 58

7.3. Depositional setting	106
CHAPTER 8: The Montmaur Conglomerate Formation	107
8.1. Lithofacies analysis and stratigraphy	107
8.2. Provenance	112
8.3. Depositional setting	112
CHAPTER 9: The sedimentary evolution of the Dévoluy basin within the framework of the western Alpine foreland basin	114
9.1. The evolution of the southern Chaînes Subalpines	115
9.1.1. Initial stages of foreland basin development: Provençal-phase fold- ing, extensional faulting, subaerial erosion, and development of the dis- tal forebulge	115
9.1.2. Eocene continental deposition	118
9.1.3. The underfilled stage of foreland basin development: Deepening- up, carbonate-dominated deposition	119
9.1.4. Marine flooding	120
9.1.5. The transition from underfilled to overfilled conditions: Shallowing-up, siliciclastic marine sedimentation and syndepositional deformation	121
9.1.6. The "overfilled" stage of foreland basin development: Re- establishment of continental conditions and terminal subaerial erosion	124
9.2. Correlation with the Swiss Molasse Basin	124
9.3. Summary	127
PART II: NEOGENE STRUCTURAL GEOLOGY OF THE DÉVOLUY BASIN	128
CHAPTER 10: Late Alpine structures	129
10.1. Folds in northern Dévoluy	129
10.2. The Median Dévoluy Thrust and the Lucles Fault	131
10.2.1. The Median Dévoluy Thrust	131
10.2.2. The Lucles Fault	135
10.3. Structures in central Dévoluy	135
10.3.1. North-south oriented faults	136
10.3.2. North-northeast — south-southwest oriented faults: the St-Etienne Fault Zone	143
10.3.3. Folds	143
10.4. Structures in southeastern Dévoluy	146
10.5. Cleavage	150
10.6. Fission track evidence for early Miocene tectonic burial of Dévoluy	151
10.7. Late Alpine tectonics of the Dévoluy Basin	154
10.7.1. The transition from the Median Dévoluy Thrust to the Aspres- lès-Corps Fault	155
10.7.2. The transition from the Median Dévoluy Thrust to the Digne Thrust	155
10.7.3. Conclusions	156
CHAPTER 11: The tectonic evolution of the external western Alpine arc	158
11.1. Kinematics at the bend of the western Alpine arc	158
11.2. Models	162
11.2.1. Case 1: Partitioning	162
11.2.2. Case 2: Independent Movement	164
11.2.3. Discussion	166
11.3. Timing of formation of the external arc	167
11.4. Conclusions	167

CHAPTER 12: Conclusions	168
REFERENCES	173
APPENDIX A1: Sedimentary petrography	185
CURRICULUM VITAE	189

Abstract

This thesis documents the synorogenic sedimentary and structural evolution of the 80 km² Dévoluy basin (Hautes-Alpes, southeastern France), a remnant of the Alpine foreland basin, during the Paleogene and Neogene. Dévoluy is located at a critical break in the depositional and kinematic patterns of the external Alpine domains. Therefore, another component of the thesis is to discuss the history of Dévoluy in the context of the Alpine foreland basin as a whole.

During the Priabonian, carbonate-dominated, transgressive marine formations (the Queyras Group) were deposited in Dévoluy. They unconformably overlie Provençal phase (Eocene), NNW-SSE oriented, W-facing folds that are best developed in N Dévoluy. The continental Pierroux Conglomerate Formation (10 - 150 m thick) occurs in NE and central Dévoluy, in the hanging-walls of NNE-SSW oriented, syndepositional extensional faults. Southward decreases in stratigraphic thickness and average maximum clast size, and increases in channelization, rounding, and sorting, document a transition from sedimentologically immature, unconfined flow (alluvial fan) to channelized flow and texturally more mature deposition (braidplain). The Priabonian marine Dévoluy Nummulitic Limestone Formation is 20-25 m thick, except in NE Dévoluy, where it is 100 m thick in the downthrown E block of the synsedimentary Lucles Fault. The formation is subdivided into the lower Nummulitic Conglomerate Member (upper shoreface, foreshore, or flanks of shallow tidal bars) and the upper Nummulitic Calcarenite Member (medium-energy ramp-type shelf). The upper Priabonian Queyras Marlstone Formation consists of up to 200 m of interbedded silty lime wackestone and very fine-grained marly limestones deposited on a moderately deep shelf or slope populated by a *Zoophycos* ichnofauna. Very fine- to medium-grained turbidites in the upper part of the formation indicate shelf instabilities towards the end of deposition. A carbonaceous mud- to siltstone at the top of the formation documents the first significant influx of siliciclastic debris in the foreland basin.

From the latest Priabonian through the late Oligocene, siliciclastic-dominated, regressive marine and continental formations (the Souloise Group) were deposited. The uppermost Priabonian - lowermost Oligocene Souloise Greywacke Formation (≈ 70 m thick) consists of interbedded fine-grained sandstones and mud- and siltstones interpreted as the deposits of fine-grained, N-flowing turbidity currents, perhaps in a distal fan or distal delta setting. Sedimentary structures document an upsection shallowing from below storm wave base to above fair weather wave base. The lower Oligocene St-Disdier Arenite Formation (≈ 100 m thick) is composed primarily of well-sorted, medium-grained sandstones with planar, trough, and tabular cross bedding and asymmetrical, symmetrical, and climbing ripples (medium- to high-energy, upper to middle shoreface). Paleocurrents are bidirectional (W-E). The formation occurs above a progressive unconformity, the hiatus of which decreases from west to east, indicating syndepositional uplift of the western margin

of the basin. The upper Oligocene St-Disdier Siltstone Formation (> 63 m thick) consists of alluvial floodplain muds and silts, isolated or vertically stacked, mixed-load, fluvial channels with a wide spread of paleocurrent directions, very fine-grained overbank (crevasse) splays, and paleosols. The upper Oligocene Montmaur Conglomerate Formation (several hundred meters thick), which consists of crudely-bedded, poorly stratified conglomerate beds with occasional sandy lenses, is interpreted as having been deposited in an alluvial fan or braidplain setting. The petrography of the Souloise Group documents an upsection increase in internal Alpine debris.

The complete sedimentary succession is compatible with that of the Alpine foreland basin, and indicates that Dévoluy occupied a position at the distal edge of the marine basin and the proximal edge of the ensuing continental basin. Changes in depositional trends appear to be related primarily to local and regional tectonic effects.

During the Mio-Pliocene, the sediments were deformed into a N-S trending, W-facing, 10 km wide synclorium cut by the E-dipping Median Dévoluy Thrust, which links to the north to the Aspres-lès-Corps Fault and, to the south, to the Digne Thrust. Slickenfibers on the Median Dévoluy Thrust and minor related faults show W-directed compression. An apatite fission track age (16.2 ± 1.4 Ma) from the St-Disdier Siltstone Formation in the immediate foot-wall of the Median Dévoluy Thrust indicates that the thrust was active before the middle of the early Miocene. Zones of pressure solution cleavage occur in close proximity to faults and are interpreted to be fault-related. Second-order, km-scale folds are S-plunging and W-facing in N Dévoluy, and NW-plunging and SW-facing in SE Dévoluy. The folds, which are cut by the Median Dévoluy Thrust, postdate emplacement towards the W and SW of a thrust sheet, preserved today as the overturned Banards and Grand-Combe Klippen in SE Dévoluy. In central Dévoluy, N-S and NNE-SSW oriented faults that occur in the hanging wall of the Median Dévoluy Thrust record dextral strike-slip and downthrow to the west. The faults were probably contemporaneously active with the thrust. The NNE-SSW faults form the St-Etienne Fault Zone, interpreted as a hanging-wall drop fault zone which accommodated northward stratigraphic climb on the Median Dévoluy Thrust.

The SW-directed thrusting recorded in SE Dévoluy is consistent with thrusting directions throughout the southern Chaînes Subalpines, and is interpreted to have been partitioned to the N into components of W-directed compression on the Median Dévoluy Thrust and dextral strike-slip in central Dévoluy. The partitioning occurs where the Median Dévoluy Thrust begins to steepen and horizontal displacement decreases. Models to explain SW-directed transport in the southern Chaînes Subalpines include regional partitioning of large-scale tectonic forces on NE-SW oriented strike-slip faults, or the occurrence of SW-directed transport independent of overall NNW- or NW-directed transport.

Cette thèse présente l'évolution sédimentaire et structurale du bassin du Dévoluy au cours du Paléogène et du Néogène. Ce bassin, d'une superficie de 80 km², est un fragment du bassin tertiaire d'avant-chaîne des Alpes occidentales, situé à l'endroit où les conditions de dépôt et les critères cinématiques des Alpes externes changent. C'est pourquoi, l'histoire du bassin du Dévoluy a également été intégrée à celle du bassin d'avant-chaîne des Alpes.

Le Priabonien, dominé par des dépôts carbonatés, est marqué par la transgression marine des formations du Groupe du Queyras. Il repose en discordance sur des plis orientés NNW-SSE et déversés vers l'W attribués à la phase "Provençale" (Éocène). Ces plis se retrouvent essentiellement dans le N du Dévoluy. Les dépôts continentaux du Conglomérat de Pierroux se sont déposés au dessus de failles normales syn-sédimentaires orientées NNE-SSW. Cette unité atteint son épaisseur maximale (150 m) dans le Dévoluy du NE et du centre et s'amincit vers le S. Parallèlement, la taille des éléments clastiques diminue et s'homogénéise, leur forme s'arrondit, et des chenaux se développent. Cette formation est interprétée comme le passage de sédiments déposés dans un cône alluvial à des dépôts de chenaux. Les dépôts marins priaboniens de Calcaires Nummulitiques, épais de 20 - 25 m en moyenne, atteignent 100 m d'épaisseur au toit de la faille synsédimentaire de Lucles. Ces calcaires se divisent en deux termes: le Conglomérat Nummulitique à la base (dépôts d'avant-côte supérieure, de basse plage, ou de bordures des barres tidales peu profondes) et les Calcarénites Nummulitiques (dépôt de moyenne énergie sur un "shelf" carbonaté à géométrie de rampe). Les Marnes du Queyras (Priabonien supérieur) peuvent atteindre plus de 200 m d'épaisseur. Il s'agit d'une séquence de lits répétitifs de calcaires marneux fins et de "lime wackestones" contenant des débris siliciclastiques en quantité variable ainsi que des ichnofaunes de type "Zoophycos". Ces marnes sont des dépôts de plate-forme ou de pente continentale assez profonde. La présence de turbidites à grain fin et moyen dans la partie supérieure de cette formation, montre l'instabilité de la plate-forme à la fin du dépôt. Au sommet, des argiles à débris charbonneux sont les premiers éléments siliciclastiques du bassin.

La sédimentation, du Priabonien terminal à l'Oligocène supérieur, est dominée par des dépôts siliciclastiques de type marin régressif à continental (Groupe de la Souloise). Les Grauwackes de la Souloise (Priabonien terminal à Oligocène inférieur), épais de 70 m, forment une séquence de lits répétitifs de grès à grain fin ou moyen, de silts, et de boues. Ces lits sont attribués à des courants de turbidité dirigés vers le N, peut-être devant un delta ou un cône distal. La formation commence sous le niveau de base des vagues et finit au-dessus de ce niveau. Les Arénites de St-Disdier (= 100 m d'épaisseur) sont composées de grès de grain moyen et homogène. Les structures sédimentaires incluent des stratifications planes et obliques (arquées et tabulaires), des rides symétriques, asymétriques, ou en aggradation verticale ou oblique. L'analyse des figures de paléocourants révèle un écoulement de direction E-W à composante oscillatoire. Ces observations montrent que les

Arénites de St-Disdier se sont déposées dans un bassin peu profond. Leur limite inférieure est une discordance progressive le long de laquelle la lacune érosive diminue de l'ouest vers l'est, ce qui indique que la bordure occidentale du Dévoluy était suffisamment haute pour être érodée avant ou pendant ce dépôt. Les Silts de St-Disdier, datés de l'Oligocène supérieur (plus de 63 m d'épaisseur) sont caractérisés par quatre lithofacies: des boues et silts de plaine d'inondation, des chenaux fluviaux isolés ou superposés montrant des directions d'apport variés, des dépôts fins d'ébrasement, et des paléosols. Cette association est typique d'une plaine d'inondation alluviale. Le Conglomérat de Montmaur, d'âge Oligocène supérieur et épais de plusieurs centaines de mètres, est formé de lits mal stratifiés contenant parfois des nodules gréseux et s'interprète comme un dépôt de cône alluvial ou de chenaux en tresse. L'analyse pétrographique indique que la quantité de débris du domaine interne des Alpes augmente progressivement dans les sédiments du Groupe de la Souloise.

Cette stratigraphie est comparable avec celle du bassin d'avant-chaîne des Alpes, et indique que le Dévoluy occupait une position distale dans le bassin marin, mais proximale dans le bassin continental. Le remplissage du bassin apparaît comme lié à la tectonique locale et régionale.

Au cours du Mio-Pliocène, les sédiments sont déformés par un synclorium de près de 10 km de large, de direction N-S à vergence W qui est recoupé du NE au SW par le Chevauchement Médian du Dévoluy, plongeant vers l'E et qui se connecte au N à la Faille de Aspres-lès-Corps et au S au Chevauchement de Digne. Les stries associées au Chevauchement Médian et aux failles mineures accompagnant ce chevauchement témoignent d'un transport tectonique vers l'W. L'âge (16.2±1.4 Ma) obtenu par la méthode des traces de fission sur des apatites prises dans les Silts de St-Disdier, 40 m sous le chevauchement, indique que ce chevauchement était actif avant la première partie du Miocène moyen. Près des failles, on observe des schistosités par dissolution-cristallisation, probablement induites par ces mêmes failles. Les plis de deuxième ordre, d'échelle kilométrique, sont à vergence W et plongent vers le S, au N du Dévoluy, alors que dans la partie SE, ils ont une vergence SW et plongent vers le NW. Ces plis, recoupés par le Chevauchement Médian du Dévoluy, sont postérieurs à la mise en place W-SW d'une nappe, préservée aujourd'hui sous formes de klippes renversée au SE du Dévoluy (Klippes des Banards et de la Grande-Combe). Dans le Dévoluy central, le toit du Chevauchement Médian présente des failles N-S et NNE-SSW décrochantes dextres à composante inverse et rejet vers l'W, probablement contemporaines du chevauchement. Les failles NNE-SSW forment la Zone de Failles de St-Etienne qui est interprétée comme une zone d'accommodation de l'amincissement du toit du chevauchement en direction du N. La direction de transport SW enregistrée dans le SE du Dévoluy est compatible avec celles des Chaînes Subalpines Méridionales. Elle résulte de décrochements dextres dans la partie centrale du Dévoluy et d'un raccourcissement E-W sur le Chevauchement Médian du Dévoluy, qui se verticalise vers le N alors que les déplacements horizontaux diminuent. Cette direction de transport NE-SW dans les Chaînes Subalpines Méridionales peut s'expliquer par une décomposition des forces tectoniques en failles décrochantes NE-SW, ou par deux directions de transport tectonique distinctes, l'une NE-SW, l'autre NNW-SSE à NW-SE.

 Acknowledgements

Despite my name alone on the title page, many other people have helped with aspects of the evolution of this thesis.

In the spring of 1991, Bert Bally suggested I call Dan Bernoulli in Zürich to inquire about doctoral positions at the ETH. I had no clue about Switzerland then (some would say I still don't), but I took Bert's gracious advice and contacted Dan, who was then, as has always been since, enthusiastic and supportive about this project (as well as, to his credit, a meticulous proofreader). My next contact at the ETH was Mary Ford, my advisor, colleague, and friend. In Dévoluy, I learned from her, Dan, John Ramsay, Wilfried Winkler, Ed Williams, Hugh Sinclair, Di and Terry Seward, Hermann Lebit, Catalina Lüneburg, Zoë Sayer, Judith Bürgisser, and others the wonderful world of Alpine geology. Thank you all for a unforgettable education, and also for so much other help at numerous steps along the way! Other people who have helped immeasurably in different scientific aspects of the thesis include Jean-Pierre Burg, Katharina von Salis Perch Nielsen, Hanspeter Funk, Rolf Schmid (IMP) and Henry Lickorish. Special thanks are also due to Peter Homewood, for having taught me about the Swiss Molasse Basin (and its fabulous wines), and for being a co-examiner on this thesis.

I was blessed for three summers to spend time in the Gîte de St-Disdier in Dévoluy, where Eric Giudice, Isabelle Petite, and their fantastic daughter, Annabelle (la petite dinosaure) made my time there not only fun and pleasurable, but also one of the best experiences of my life. I'll never forget you three. À bientôt!!! Other people in the Dévoluy valley were also incredibly receptive to a Texan who spoke a bizarre concoction of French, English, Spanish, and German, and who was fascinated by life in your unique world. En particulier, merci beaucoup à Isabelle (St-Etienne) et sa famille, les habitants des Gicons, le postier, les boulangers, et les jeunes de St-Disdier, Anne (Gîte des Renards), le personnel des Neyrettes, et "Scraps", mon compagnon de travail le premier été. Je ne vous ai pas oublié.

Many of the the thoughts presented in this thesis represent the fruits of endless discussions with my colleagues at one of the most receptive and supportive geology departments on the planet: the ETH-Zürich. In four and a half years here, I think I've asked everyone here for advice on *some* aspect of my thesis, and every single one has been magnificently helpful. So, to everyone who has taken her or his time to share expertise and knowledge, I offer my gratitude and indebtedness. How can I thank you all enough without naming the whole department?

I would, however, like to single out four non-scientific heroes who have helped me immeasurably - Eva Sauter, who has been like a second mother to me during my time here, Urs Gerber, who consistently provided me with spectacular slides, Silvia Bonadurer, whose help in so many ways is especially appreciated, and Rita de Cia, who made dealing with the administration a pleasure - and also those people who have taken their time to help me translate my English into presentable French

 - Jean-Pierre Burg, Alex Mauler, and Jogi Graf.

My father once told me that I would make many of the greatest friends of my life in graduate school. Without question, it happened here. So, here's a "prost" at the bar of your choice to all of you who have shared themselves with me. You're welcome at The Green Frog Café wherever I am! In particular, let me mention my officemates - Alex, Andrea, Christian, Graham, Jan Henk, and Teresa, who put up with my messes, bizarre musical tastes, and endless need for coffee, and who provided me with countless good times - and remember a few other special friends who will always have a place deep in my Texas heart - Ali, Barbara, Bill, Caroline, Catalina, Cris, Daniel, Daniela, Flavio, Guy, Hermann, Jane, Jogi, JP, Judy, Katja, Mara, Maria, Markito, Markus, Martin, Michi, Piotr, Steve, and Véro.

Finally, I'd like to remember the people who have contributed to my "European (and elsewhere) experience" outside of the institute. Here's to Marion, Oli, Maurizio, Sabine, Chris, Sue, the "Latin mafia", the staff at Jimmy's, Caro, Gret Feldmann, Deanna, Erin, Luisa, Steph, Dave, Mike, Steve, Will, KathArine, Jeff, Andrew, Kim, KathErine, Geary, the Gawendas, the van Konijnenburgs, the Ohlendorfs, the Artonis, the Maulers, and, above all else, my family - Baba, Larry, Bret, Tip, and Kit - without whom I'm nothing.

This thesis was originally funded by the Swiss National Science Foundation. Additional support was provided by ETH. Money may not be everything, but it sure helps.

To all the above, and to anyone I've neglected to mention, my warmest love for your having made these the best years of my life. Vaya con Dios, y'all.

For my parents,
for everything

CHAPTER 1

Introduction

1.1. Overview

1.1.1. Objectives and aims

This thesis documents the dynamic sedimentary and tectonic evolution of the Dévoluy basin, a remnant of the Tertiary Alpine foreland basin, from the late Eocene to the Mio-Pliocene. Dévoluy, located near the bend of the external western Alpine arc in the Hautes-Alpes of southeastern France (Fig. 1.1), was chosen as a study area because it occupies a critical location for understanding the origin of the arc and the evolution of the Alpine foreland basin. Significant geologic differences exist north and south of the bend in the arc, including the thicknesses of the Tertiary sediments and the direction of tectonic transport, and yet the origin of the arc and its effects on the development of the foreland basin is poorly understood. Therefore, determining the geologic evolution of Dévoluy, the foreland basin remnant closest to the bend in the arc, may provide insight into the timing and nature of the development of the arc. Furthermore, Dévoluy is one of only four areas (including also the Barrême and Bargême basins and the easternmost portion of the western Molasse Basin) in the external western Alps (Fig. 1.2) to record both early marine and late continental conditions in the Alpine foreland basin. Dévoluy's location relative to the other areas (Fig. 1.2) makes it the westernmost preserved fragment of the Alpine foreland basin to record both marine transgression and the transition from marine to continental conditions. Thus, the location of Dévoluy and its history of evolution impose significant restrictions on both the geometry and the evolution of the larger Alpine foreland basin.

In addition to increasing the understanding of the Alpine foreland basin, this study also provides quantitative and qualitative information concerning the more general aspects of foreland basin evolution. The theory of using foreland deposits to bracket the age of deformation in orogenic belts and to track tectonic evolution is well-established. However, new data improve efforts to constrain temporal and spatial variations in these factors, as well as helping to refine the rates and magnitudes of processes such as subsidence, uplift, and sediment supply. Based on such data, improved models of foreland basin evolution may be developed.

The objectives of this thesis are therefore the following:

- (1) to describe the upper Eocene-Oligocene stratigraphy, sedimentology, and syn-depositional structural geology of Dévoluy and to discuss the implications of these observations in relationship to the evolution of the western Alpine foreland basin (Part I);
- (2) to quantitatively describe the post-depositional Mio-Pliocene structural geology of Dévoluy and to use these data to evaluate proposed models of the formation of the western Alpine

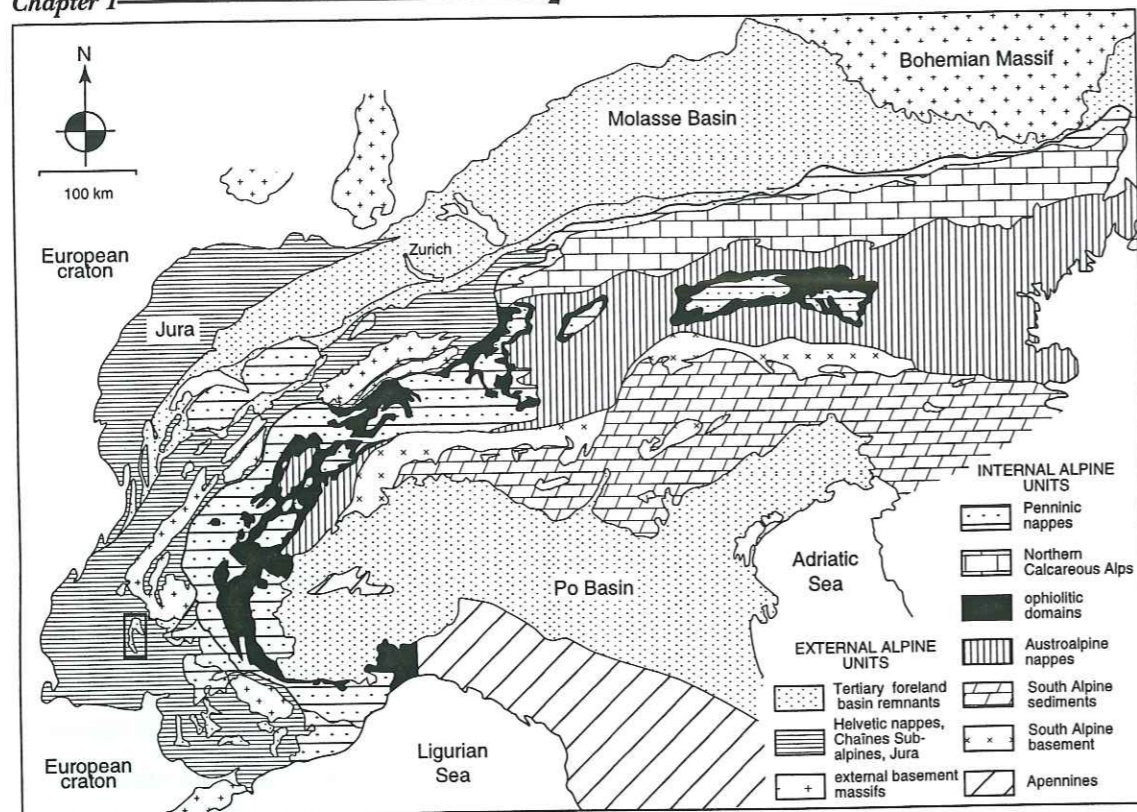


Fig. 1.1. Simplified map of the Alpine orogenic belt (after Homewood *et al.*, 1986; Ricou & Siddans, 1986; Coward & Dietrich, 1989; and Polino *et al.*, 1990). Box indicates the location of Dévoluy.

arc (Part II).

1.1.2. Methods

Field data presented in this thesis were collected by mapping Tertiary structures and sediments at a scale of 1:10,000. Quaternary, as well as most Cretaceous and older sediments, were not mapped. Instead, these data, where presented, were taken from the 1:50,000 BRGM geologic maps *St-Bonnet* (BRGM, 1980d, Carte géologique de la France à 1/50 000. Feuille XXXIII-37) and *Gap* (BRGM, 1971, Carte géologique de la France à 1/50000. Feuille XXXIII-38). Measured sedimentary sections were logged at a scale of 1:50. Hand samples were collected in the field for petrographic analysis.

Orientation data were collected for bedding, cleavage, fracture, fault planes, and slickenfibers on fault surfaces. All stereonet plots of these data are on lower hemisphere, equal area projections. Data were plotted using *Stereonet* v. 3.9.6a (Allmendinger, 1988-1995). All fault kinematic analyses were performed using the Macintosh program *FaultKin* v. 3.8a (Allmendinger *et al.*, 1989-1994).

Paleocurrent data were collected in the field from sole marks, imbricated pebbles, ripple, trough, and tabular foresets, ripple crests, and trough axes. Folded data were later corrected for the plunges of the fold axes and the tilting of bedding in the fold limbs using *Stereonet* v. 3.9.6a

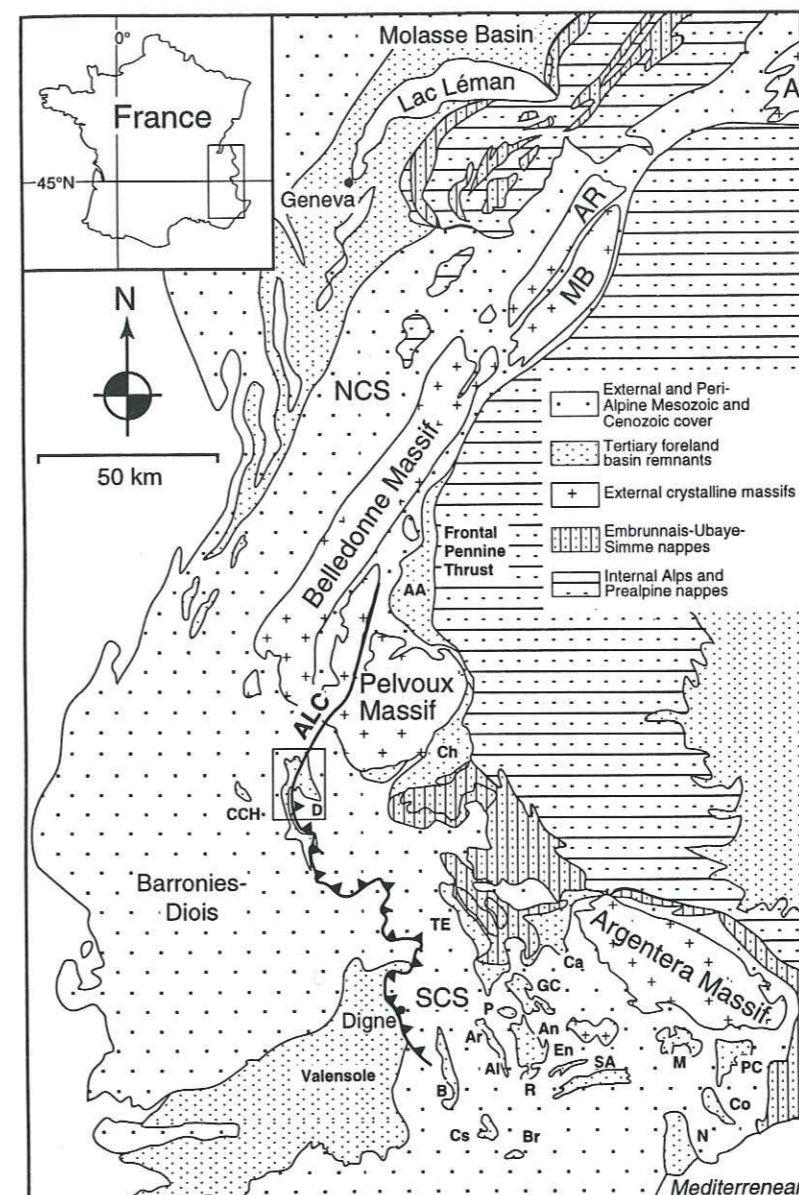


Fig. 1.2. Map of the external western Alps. Box indicates the location of Dévoluy. A = Aar Massif; AA = Aiguilles d'Arves basin; Al = Allons basin; ALC = Aspres-lès-Corps Fault; An = Annot basin; AR = Aiguilles Rouges Massif; Ar = Argens basin; B = Barrême basin; Br = Bargême basin; Ca = Cayolle basin; CCH = Col de la Croix Haute basin; Ch = Champsaur basin; Co = Contes basin; Cs = Castellane basin; D = Dévoluy basin; En = Entrevaux basin; GC = Grand Coyer basin; M = Monoinas basin; MB = Mont Blanc Massif; N = Nice basin; NCS = Northern Châines Subalpines; P = Peyresq basin; PC = Peira Cava basin; R = Rouaine basin; SA = St-Antonin basin; SCS = Southern Châines Subalpines; TE = Trois Evêches basin.

(Allmendinger, 1988-1995). The corrected data were plotted on rose diagrams using *Stereonet* v. 3.9.6a (Allmendinger, 1988-1995).

The petrography of the Tertiary siliciclastic sediments was determined by optical analysis of standard thin sections under a polarizing, transmitted light microscope. Preliminary inspection of the thin sections identified 25 basic categories to be counted (Appendix A-1). Approximately 300 non-cement, non-matrix grains were counted in each thin section to assure that a statistically valid population would be counted (van der Plas, 1962; Frangipane & Schmidt, 1974). The grains were counted using a variation of the Gazzi-Dickinson point-counting method (Appendix A-1). The advance-stage interval selected on the point counting stage was equal to the average largest width of the largest grain found in an initial inspection of each thin section (as suggested by, e.g., Frangipane & Schmid, 1974).

Carbonate terminology is based on Dunham (1962) and Embrie & Klovan (1971).

All numerical geologic ages are from the Haq *et al.* (1988) time scale unless otherwise noted.

Fission track analysis of one sample was performed by D. Seward (ETH-Zürich) to determine its burial and exhumation history.

Structural cross sections were drawn at the scale of 1:10,000. One of these sections was preliminarily balanced and restored according to the rules of Dahlstrom (1969) and Woodward *et al.* (1989).

1.2. The external western Alps

1.2.1. Geographical and geological setting

Dévoluy is part of the external western Alps, one of the best-studied parts of the Alps (dating back to the early studies of Termier, Haug, Schardt, Lugeon, and Argand in the 1890s and early 1900s). This area, a broad, arcuate zone of crystalline basement "massifs" and Mesozoic and Cenozoic sediments, occurs between the internal Alps to the east and the European craton to the west (Figs. 1.1, 1.2).

The internal Alps include rocks that belonged to the Adriatic microcontinent, the Tethyan ocean, and part of the southeastern margin of the European continental plate prior to collision with the African plate in the latest Cretaceous or early Tertiary. These rocks are now juxtaposed across the Frontal Pennine Thrust (*sensu* Ramsay, 1963) with the external Alps, which also belonged to the southern margin of the pre-collisional European plate (Fig. 1.2). The European craton west of the external Alps remained relatively undeformed by Alpine orogenesis.

The basement massifs of the external western Alps are composed of Variscan crystalline basement and Mesozoic low-grade metasediments. The history of emplacement of the basement massifs is not well-understood (see discussion in Coward & Dietrich, 1989). For example, the Belledone massif (Fig. 1.2) has been interpreted as a complex of allochthonous post-Eocene imbricate thrust sheets (Boyer & Elliot, 1982; Butler, 1983; Butler *et al.*, 1986), whereas the adjacent Pelvoux Massif (Fig. 1.2) has been interpreted as either an "autochthonous" Mesozoic extensional block that was partially inverted during late Alpine compression (Lemoine *et al.*, 1986; Gillchrist *et al.*, 1987; Coward *et al.*, 1991), or a Cretaceous-early Eocene basement "pop-up" structure (Ramsay, 1963; Ford, 1996) that was buried 6-8 km after the middle Oligocene (Waibel, 1990) and re-exhumed at approximately 4 Ma (D. Seward, pers. comm.).

The sedimentary cover of the external western Alps is composed of thin Triassic siliciclastics, evaporites, and carbonates, lower and middle Jurassic shales, sandstones, and limestones, upper Jurassic limestones, lower Cretaceous shale and limestone cycles, upper Cretaceous limestones with subordinate sandstones and shales, and Tertiary carbonates and siliciclastics (Trümpy, 1980; Lemoine *et al.*, 1986). The sediments are relatively unmetamorphosed, but locally reach laumontite, prehnite-pumpellyite, and even greenschist metamorphic facies (e.g., Ivaldi, 1989, his Fig. 27).

Tertiary sediments, middle Eocene to Miocene in age, occur in the Molasse Basin and a series of geographically isolated basins that parallel the external western Alpine arc (Figs. 1.1, 1.2). These basins, which are considered to be remnants of a larger foreland basin (e.g., Kerckhove *et al.*, 1980;

Pairis *et al.*, 1984a; Pairis *et al.*, 1984b; Elliott *et al.*, 1985; Homewood *et al.*, 1985; Homewood *et al.*, 1986; Pairis, 1988), record the progressive migration of the orogenic load and its related deformation toward the foreland.

The arc of the external western Alps, delineated by the basement massifs and structures in the sedimentary cover, is roughly semi-circular and has a radius of approximately 150 km (Figs. 1.1, 1.2). The northern arm of the arc, the Northern Chaînes Subalpines, trends NE-SW. It extends approximately 200 km from the Prealps in western Switzerland to the south end of the Belledonne massif in southeastern France (Fig. 1.2). The southern arm of the arc, the Southern Chaînes Subalpines, trends NW-SE, and extends approximately 175 km from the Pelvoux massif to southeast of the Argentera Massif in southeastern France (Fig. 1.2). The transition from the Northern Chaînes Subalpines to the Southern Chaînes Subalpines occurs in less than 50 km in the area southwest of the Belledonne massif and west of the Pelvoux massif (Fig. 1.2).

The timing and nature of the development of the arc is not well understood and numerous theories have been proposed to explain its genesis (e.g., Graham, 1978; Siddans, 1979; Tricart, 1984; Butler *et al.*, 1986; Fry, 1989a, b; Gratier *et al.*, 1989; Platt *et al.*, 1989; Laubscher, 1991; Ford *et al.*, 1995). Coward & Dietrich (1989) summarize many of these models. The controversy arises from the empirical observation that the direction of late Alpine (Oligocene - Holocene) tectonic transport diverges dramatically around the arc (e.g., Platt *et al.*, 1989; Fry, 1989b). From 40-15 Ma, deformation in the Helvetic Alps was NNW- to NW-directed (Fig. 1.3; Dietrich & Casey, 1989; Platt *et al.*, 1989; Ramsay, 1989); in the Northern Chaînes Subalpines, it was NW- to WNW-directed (Fig. 1.3; Butler, 1985, 1992; Platt *et al.*, 1989); around the bend of the arc, it was WNW- to W- to SW-directed (Fig. 1.3; Fry, 1989a; Gratier *et al.*, 1989; Ford *et al.*, 1995); and in the Southern Chaînes subalpines and northern Provençal Alps, it was SW-directed (Fig. 1.3; Siddans, 1979; Fry, 1989a, b; Platt *et al.*, 1989). From 15 Ma until the present, NW- and SW-directed deformation has occurred in the northern and central Jura Mountains (Platt *et al.*, 1989, their Fig. 1).

Hypotheses to explain this divergence in thrusting directions include crustal-scale models — counter-clockwise rotation of a rigid indenter (Gratier *et al.*, 1989; Laubscher, 1991) or locally-generated body forces associated with the emplacement of an indenter (Platt *et al.*, 1989, their Fig. 3) — and decollement models, where the divergence is an upper crustal response — orogenic collapse and extrusion (Siddans, 1979), sidewall collapse during over NW convergence (Butler *et al.*, 1986), partitioning of relative plate motion (Fry, 1989b), and the occurrence of two distinct, more or less synchronous tectonic transport directions, one toward the W-WNW and one toward the SW-WSW (Ford *et al.*, 1995).

1.2.2. General evolution

The external western Alps (Figs. 1.1, 1.2) record aspects of much of the evolution of the larger Alpine orogen: extension, passive margin subsidence and deposition, continent-continent collision, the creation of a load-induced foreland basin, and post-foreland basin folding and thrusting

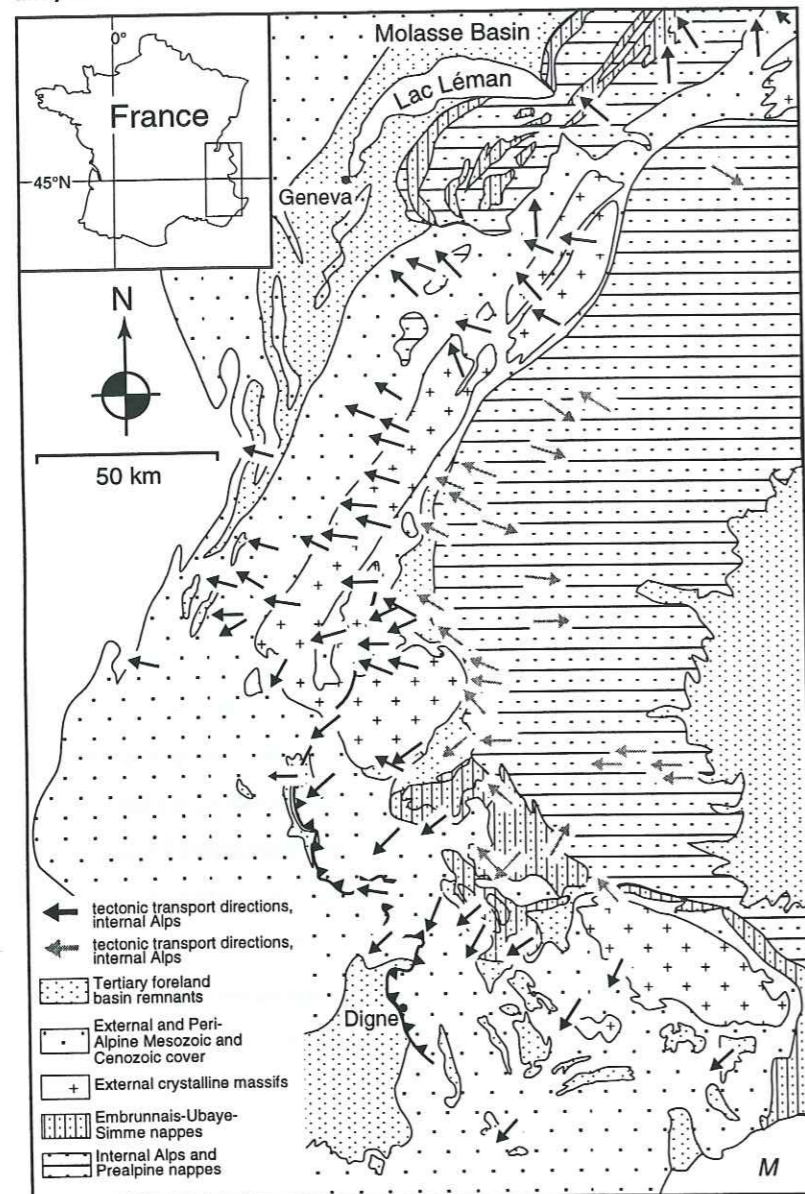


Fig. 1.3. Directions of late Alpine tectonic transport from 40-15Ma (compiled from Siddans, 1979, Butler *et al.*, 1986, Fry, 1989a, Platt *et al.*, 1989, Coward & Dietrich, 1989, Mugnier & Rosetti, 1990, Coward *et al.*, 1991, Butler, 1992, and Meckel *et al.*, 1996).

(Fig. 1.4).

The earliest Mesozoic sedimentary deposits of the external western Alps were deposited on the subsiding distal European Tethyan passive continental margin (i.e., Variscan continental basement). The sedimentation took place during Triassic to early Cretaceous (Aptian - Albian) extension associated with ESE movement of the African continental plate relative to Europe (Dewey *et al.*, 1989). The extension caused Paleozoic NE-SW trending zones of crustal weakness to be reactivated as a series of passive margin faults (Lemoine *et al.*, 1986; Coward & Dietrich, 1989).

At the end of the extensional phase, at about 110-80 Ma, the African plate began to move to the NE relative to Europe (Fig. 1.4; Dewey *et al.*, 1989). This movement resulted in south-directed subduction of oceanic crust, followed by the obduction of some oceanic crust, now preserved as ophiolites in the internal Alps (Fig. 1.1; Coward and Dietrich, 1989; Avigad *et al.*, 1993) and the partial subduction of European continental crust beneath the African plate in the internal Alps.

PERIOD	PLATE MOTION	INTERNAL ALPS	EXTERNAL ALPS	DÉVOLUY
Holocene				
Pliocene	←			
Miocene	9 Ma	Cleavage-related metamorphism	Jura folding	
	-19 Ma		Helvetic thrusting	W-, SW-directed folding and thrusting
Oligocene	38 Ma	pumpellyite-actinolite metamorphism emplacement of Parpaillon nappe emplacement of Autapie nappe		gradual uplift of western Dévoluy subsidence
				siliciclastic deposition
Eocene	51 Ma	Penninic/Austro-Alpine thrusting	"Pyreneo-Provençal" event	E-W extensional faulting NNW-SSE oriented folds (pre-Bartonian, post-late Maastrichtian)
				carbonate deposition
Paleocene	very slow motion		"Paleocene restoration"	subaerial erosion
Cretaceous	65 Ma	Thrusting, HP/LT metamorphism, and subduction of continental crust		Senonian limestones
	-84 Ma			W-E oriented folds (early Turonian - Coniacian)
	92 Ma	emplacement of Penninic-Ligurian domain		
Jurassic		ophiolites	Extensional basins/oceanic spreading	
Triassic			rifting	
	-220 Ma		pre-rift	

Fig. 1.4. Important events in the formation of the Alps (modified from Dewey *et al.*, 1989) and Dévoluy. Plate motion arrows show movement of Africa relative to the stable European craton.

Contemporaneous with the earliest phases of continent-continent collision, which occurred mainly in the eastern Alps, a NE-SW trending zone of W-E to NE-SW trending, upright to N- or NW-facing folds (Figs. 1.4, 1.5) developed in SE France during the Turonian (Siddans, 1979; Debrand-Passard *et al.*, 1984; Lemoine *et al.*, 1986) to late Coniacian (Arnaud, 1974). These folds are well-known in the Barronies-Diois and Dévoluy regions (e.g., Glangeaud & d'Albissin 1958; Mercier, 1958; Debelmas & Lemoine 1970; Gidon *et al.* 1970; Arnaud 1974; Baudrimont & Dubois, 1977; Siddans, 1979; BRGM, 1980d; Debrand-Passard *et al.*, 1984;

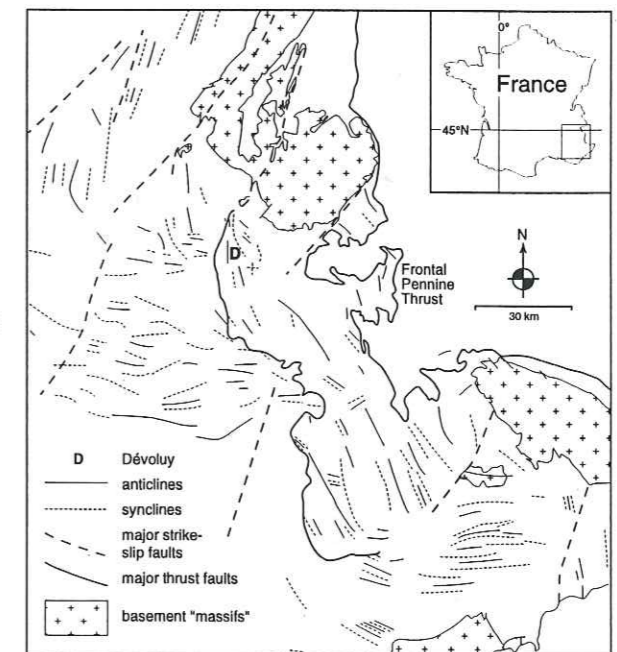


Fig. 1.5. Folding patterns in southeastern France (after Siddans, 1979).

Odonne & Vialon 1987; Ford & Stahel, 1995; Huyghe & Mugnier, 1995), where they are well dated as Turonian-Coniacian by a stratigraphic unconformity. The deformation in Dévoluy has been linked to N-S oriented compression (Siddans 1979).

After the Turonian-Coniacian deformation, a poorly understood phase of Senonian (Campanian-Maastrichtian) sedimentation (Baudrimont & Dubois, 1977) occurred locally in the Dévoluy region (Fig. 1.4). The sediments, 500-700m thick in Dévoluy, consist of deeper marine cherty limestones to continental carbonate conglomerates that reflect a relatively rapid marine shallowing followed by continental conditions (BRGM, 1980d).

This sedimentation was followed by a period of uplift from the Paleocene to the early Eocene during which widespread subaerial erosion occurred throughout the external Alps (Trümpy, 1980; Dewey *et al.*, 1989). The erosion was probably associated with a reduction in the rate of northward movement of Africa at the same time (e.g., Fig. 1.4), but has also been interpreted as a response to the inception of forebulge uplift at the distal edge of the western Alpine foreland basin (Crampton & Allen, 1995).

North to northeast directed motion of the African plate relative to Europe resumed in the Eocene (Laubscher & Bernoulli, 1982; Vialon *et al.*, 1989; Stampfli, 1993), followed by N-directed motion during the Oligocene (Fig. 1.4), leading to renewed tectonic activity and sedimentation in the external Alps. In Provence, Eocene W-E oriented folds record the Pyrenean-Provençal orogeny (Lemoine, 1972; Siddans, 1979; Kerckhove *et al.*, 1980; Lemoine *et al.*, 1986; Ricou & Siddans, 1986; Coward *et al.*, 1991; Fry, 1989a; Ford, 1996). Elsewhere in the external domain, Mesozoic NE-SW oriented passive margin faults were reactivated, primarily as sinistral strike-slip faults (e.g., Gidon & Pairis, 1976; Laubscher & Bernoulli, 1982; Lemoine *et al.*, 1986; Gillchrist *et al.*, 1987; Coward & Dietrich, 1989; Gratier *et al.*, 1989; Coward *et al.*, 1991). Eocene extensional faults, commonly parallel to the passive margin faults have been related to their sinistral reactivation (Tricart, 1984; Ford & Stahel, 1995; Meckel *et al.*, 1996). The former faults may also reflect the early response of the external Alps to the onset of loading in the internal Alps.

At the same time, orogenic upbuilding in the internal Alps led to increased loading of the crust, which caused flexural subsidence and the formation of the Alpine foreland basin in the external domain. A wave of tectonically-generated subsidence migrated outward, resulting in a northward and westward marine transgression and deepening in the foreland basin during the middle to late Eocene (Elliot *et al.*, 1985; Pairis, 1988), referred to as the Alpine Nummulitic transgression. It is characterized by the deposition of a succession of shallow marine limestones and deeper marine carbonate marls.

The transgression was followed by a rapid infill of the foreland basin during the Oligocene (Trümpy, 1980; Elliott *et al.*, 1985; Homewood *et al.*, 1985; Pairis, 1988) by siliciclastic turbidites and shallow marine and continental siliciclastic sediments. This infill was synchronous with shortening in the Helvetic domain of the central external Alps (Fig. 1.4; Trümpy, 1980; Pfiffner, 1986; Dewey *et al.*, 1989). Thrusting and folding of Mesozoic basement and its sedimentary cover had affected the

rest of the external western Alps by the post-mid Oligocene (Dewey *et al.*, 1989; Gratier *et al.*, 1989). Northwest to southwest-directed deformation led to the emplacement of the Penninic nappes at the eastern margin of the external western Alps (Trümpy, 1980; Laubscher & Bernoulli, 1982; Dewey *et al.*, 1989; Fry, 1989a).

Continued compression in the Miocene caused west- and southwest-directed displacement in the external western Alps with a counter-clockwise component of rotation (Fig. 1.4; Laubscher & Bernoulli, 1982; Gratier *et al.*, 1989). Regional cleavage was developed and low-grade metamorphism occurred locally in the more proximal parts of the Chaînes Subalpines during this time (Siddans, 1979). The depocenter of the Alpine foreland basin shifted outward in response to this more proximal tectonism, resulting in the deposition of more "molasse" sediments in the distal parts of the foreland basin.

During the Pliocene to Holocene, deformation extended to the Jura (located in Fig. 1.1) in response to continued northwest-directed movement of the African plate (Fig. 1.4; Dewey *et al.*, 1989). The cover rocks were detached along a series of thin-skinned thrusts in incompetent middle and upper Triassic evaporites (Laubscher, 1965).

1.3. Dévoluy

1.3.1. Location and physiography

Dévoluy is situated 15 km southwest of the Pelvoux Massif in southeastern France, slightly south of the bend of the western Alpine arc (Figs. 1.1, 1.2). The 80 km² area is covered by the *St-Bonnet* (BRGM, 1980) and *Gap* (BRGM, 1971) 1:50,000 geologic maps and the *Dévoluy* (IGN map 33337 OT) 1:25,000 topographic map.

The Dévoluy valley lies approximately 1200 m above sea level. It is bounded to the east by the N-S to NW-SE trending Faraud-Grande Combe ridge, and to the west by the NNE-SSW trending L'Obiou ridge (Fig. 1.6), both of which are composed of Senonian limestone. The north end of the valley drops off abruptly in a sub-vertical cliff of Senonian limestone. The south end is bounded by the Senonian limestones of the Auroze Plateau (Fig. 1.6), which also drops off in a steep cliff.

1.3.2. Stratigraphic and sedimentary setting

The oldest sediments in the Dévoluy region are Jurassic black shales and marls and lower through middle Cretaceous limestones and marls (pre-Senonian strata, Fig. 1.6; BRGM, 1980d). These sediments are unconformably overlain by upper Cretaceous (predominantly Senonian) limestones (Fig. 1.6), with or without chert interbeds, and calcareous conglomerates (BRGM, 1980d).

The Mesozoic sediments are in turn unconformably overlain by upper Eocene through Oligocene sediments (Fig. 1.6). The composite thickness of the Tertiary sediments is approximately 500m (Fig. 1.7). Dubois (1962), BRGM (1980), Pairis *et al.* (1983, 1984a, 1984b), Fabre & Pairis (1984), Fabre *et al.* (1986), Pairis (1988), Waibel (1990), and Meckel *et al.* (1996) describe aspects

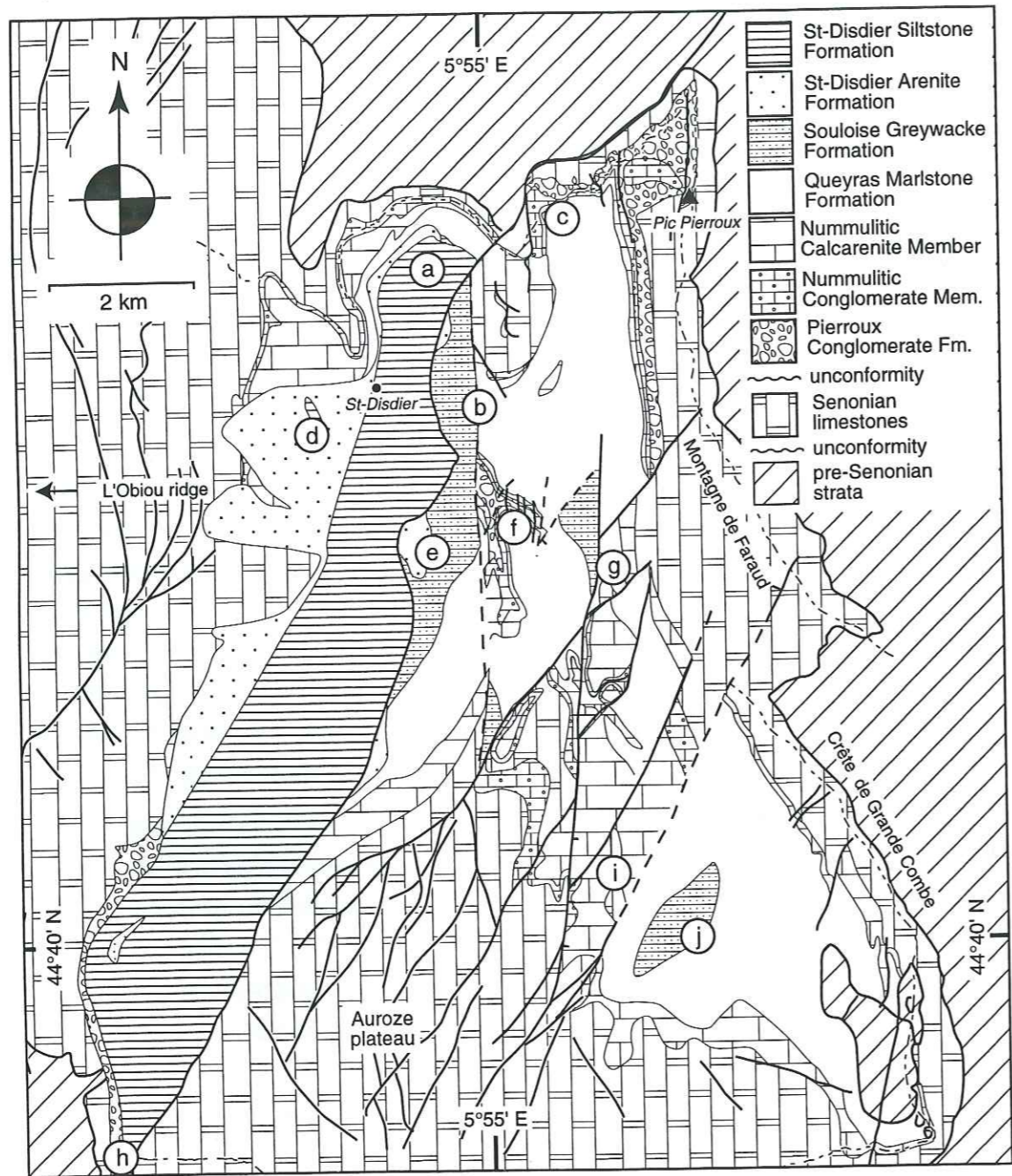


Fig. 1.6. Simplified geologic map of the Dévoluy basin. Circled letters indicate locations of composite sections shown in Fig. 1.7.

of the Tertiary succession. Field mapping allowed two stratigraphic groups to be distinguished within the Tertiary. These are the carbonate-dominated upper Eocene Queyras Group and the siliciclastic-dominated uppermost Eocene - Oligocene Souloise Group (Table 1-I).

The Queyras Group, named after the Queyras River in northern Dévoluy, consists of the Pierroux Conglomerate (Eocene?), Dévoluy Nummulitic Limestone (Priabonian), and Queyras Marlstone Formations (upper Priabonian) (Table 1-I). The Dévoluy Nummulitic Limestone Formation is subdivided into two members (Table 1-I).

Ma	Age	Formal stratigraphic nomenclature, this study	Members	BRGM, 1980d	Pairs et al., 1983	Fabre et al., 1986	Pairs, 1988 p. 236	Pairs, 1988 p. 241
25	Oligocene	Soulaise Group	Montmaur Conglomerate Formation	Grès de St-Disdier	Molasse rouge	Grès de St-Disdier	Grès de St-Disdier	Molasse rouge
30			St-Disdier Siltstone Formation					
35	Eocene	Queyras Group	Souloise Greywacke Formation	Marnes à Calcaires priaboniens	Marnes nummulitiques	Calcaires intermédiaires	Calcaires intermédiaires	Argillites noires
40			Queyras Marlstone Formation					
			Nummulitic Calcarenite Member Nummulitic Conglomerate Member	Poudingues et formations continentales de la base du Tertiaire	Conglomérats/couches infranummulitiques			

Table 1-I. Stratigraphic nomenclature of the Dévoluy basin, with comparison to previous nomenclature. Time scale (non-linear) after Haq et al. (1987). Solid lines indicate precisely located boundaries; dashed lines are less precisely located.

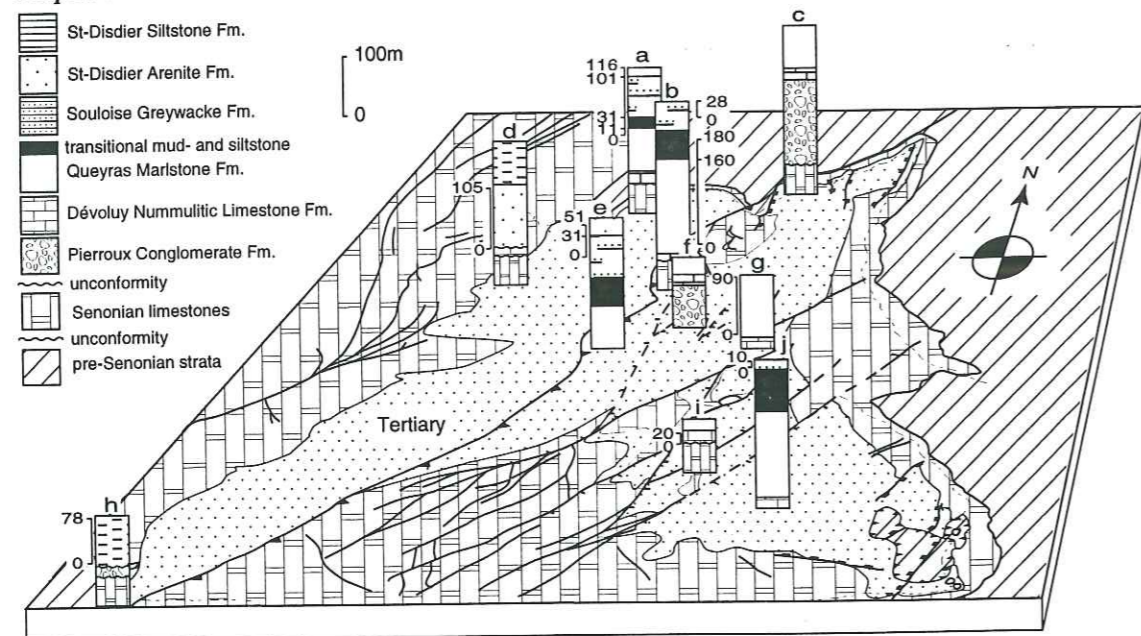


Fig. 1.7. Perspective map showing measured and estimated thicknesses of Tertiary sediments in Dévoluy. The composite thickness of the Tertiary sediments is approximately 500m.

The Souloise Group, named after the Souloise River in central Dévoluy, consists of the Souloise Greywacke, St-Disdier Arenite, St-Disdier Siltstone, and Montmaur Conglomerate Formations (Table 1-I).

The formal nomenclature established in this thesis is modified after the informal nomenclature proposed by Meckel *et al.* (1996). The latter was proposed because much of the nomenclature used previously in literature concerning Dévoluy was contradictory to Alpine nomenclature established elsewhere, or was internally inconsistent (Table 1-I).

Although the introduction of new nomenclature is generally to be avoided, it was considered to be necessary in this case in order to unambiguously define the Tertiary formations in Dévoluy. Therefore:

- the Pierroux Conglomerate Formation is named after its type locality in northwestern Dévoluy and its predominant lithology;
- the Dévoluy Nummulitic Limestone Formation receives only a modifying locality name;
- the two members of the Dévoluy Nummulitic Limestone Formation, as identified by Meckel *et al.* (1996), are named based on their predominant respective lithologies;
- the Queyras Marlstone Formation is named after the Queyras River, along which the formation outcrops abundantly, and its predominant lithology;
- the name of the Souloise Greywacke Formation is modified after "Flysch de la Souloise" (Parris, 1988, p. 236);
- the St-Disdier Arenite and St-Disdier Siltstone Formations, which were previously considered to be parts of either the "Grès de St-Disdier" or the "Grès de St-Disdier" and the "Molasse Rouge" (Table 1-I), are defined as separate mappable formations and are named according

to their predominant lithologies;

- the Montmaur Conglomerate Formation, which is only present south of the mapped field area, is considered as a separate formation based on field observations and the Gap geologic map (BRGM, 1971); it is named after the village of Montmaur, where it outcrops extensively, and its predominant lithology.

1.3.3. Structural and tectonic setting

Pre-Senonian (Albian-Cenomanian and older) strata in Dévoluy are deformed by a series of W-E to NE-SW oriented folds that crop out north, east, and southwest of the mapped study area (Glangeaud & d'Albissin, 1958; Mercier, 1958; Debelmas & Lemoine, 1970; Gidon *et al.*, 1970; Arnaud, 1974; Baudrimont & Dubois, 1977; Siddans, 1979; BRGM, 1980d; Debrand-Passard *et al.*, 1984; Odonne & Vialon, 1987; Huyghe & Mugnier, 1995). These folds are unconformably overlain by Senonian sediments. The age of these folds, as constrained by the unconformity, is early Turonian-Coniacian (Mercier, 1958; BRGM, 1980d). These pre-Senonian folds are locally overprinted by later Alpine folding (Odonne & Vialon, 1987).

NNW-SSE trending, W-facing folds occur locally in the Senonian limestones of northern and central Dévoluy. These folds are contemporaneous with Eocene folding in Provence (Flandrin, 1966) and predate deposition in Dévoluy of the Pierroux Conglomerate Formation, which overlies the eroded folds (Glangeaud & d'Albissin, 1958; BRGM, 1980d).

The principal Tertiary structural features of the Dévoluy basin are the east-dipping Median Dévoluy Thrust (Gidon & Parris, 1976), numerous folds in northern and southeastern Dévoluy, N-S and NNE-SSW oriented faults in the hanging wall of the Median Dévoluy Thrust in central Dévoluy, and the Grand-Combe and Banards Klippen in southeastern Dévoluy (Fig. 1.8).

The Median Dévoluy Thrust divides Dévoluy into two distinct sedimentary domains: east of the fault, in its hangingwall (eastern Dévoluy), carbonate sediments of the Queyras Group are more common; west of the fault, in its footwall (western Dévoluy), siliciclastic sediments of the Souloise Group prevail (Figs. 1.6, 1.7). The Median Dévoluy Thrust is interpreted as being the northern continuation of the Digne Thrust (Fig. 1.2; Gidon & Parris, 1976; BRGM, 1980d; Fabre *et al.*, 1986; Meckel *et al.*, 1996). It in turn links northward into the NE-SW oriented, subvertical Aspres-les-Corps Fault (Fig. 1.2; Gidon & Parris, 1976; BRGM, 1980d; Fabre *et al.*, 1986).

The large-scale fold geometry of Dévoluy is of a N-S trending, W-facing, 10 km wide (half-wavelength) periclinal synclorium (BRGM, 1980d). This first-order geotectonic feature involves smaller, km-scale folds (Fig. 1.8) that are approximately N-S oriented and W-facing in northern Dévoluy, and NW-SE oriented and SW-facing in southeastern Dévoluy. Folding is interpreted to have occurred before displacement on the Median Dévoluy Thrust and after the emplacement of the Banards and Grand-Combe Klippen in southeastern Dévoluy.

The NNE-SSW oriented faults in the hanging wall of the Median Dévoluy Thrust, which form the St-Etienne Fault Zone, divide eastern Dévoluy into northeastern, central, and southeastern zones

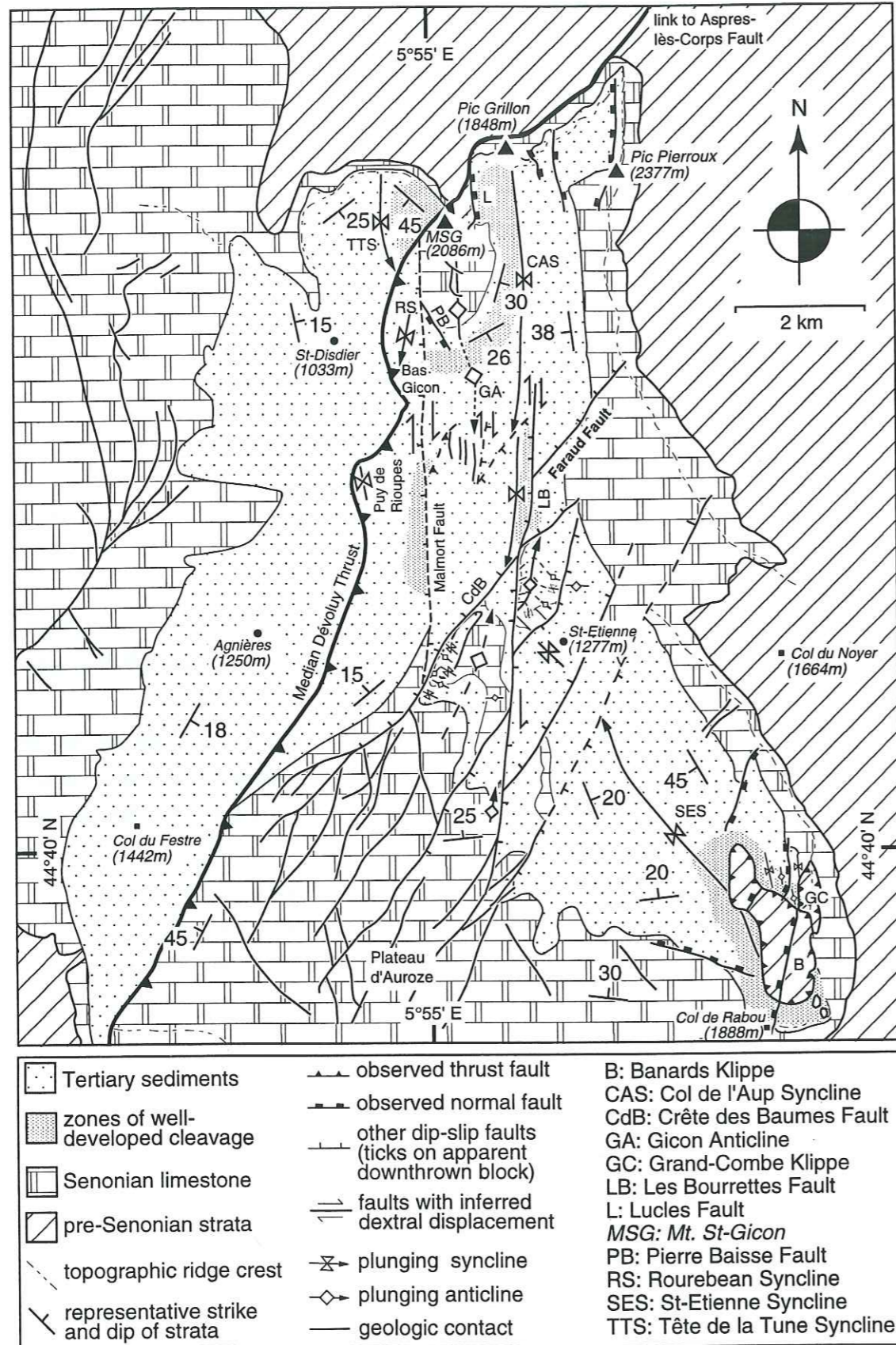


Fig. 1.8. Simplified tectonic map of Dévoluy.

(Fig. 1.8). The intersection of the NNE-SSW oriented faults with N-S oriented faults in the same area causes central Dévoluy to be divided into lozenge-shaped blocks containing minor folds. Both sets of faults were probably active at the same time as the Median Dévoluy Thrust.

The Banards and Grand-Combe klippen in southeastern Dévoluy (Fig. 1.8) consist of overturned, E-dipping Cretaceous and upper Eocene strata. They tectonically overlie Tertiary deposits (Fig. 1.8) that were folded after the emplacement of the thrust sheet.

Other structural features include the Pic Grillon, Lucles, Pierre Baisse and unnamed faults in northern Dévoluy, and isolated zones of well-developed cleavage in close proximity to faults (Fig. 1.8). A progressive unconformity associated with uplift of the western margin of Dévoluy exists between the Lower St. Disdier Arenite Formation and underlying formations (Fig. 1.6).

PART I
STRATIGRAPHY AND SEDIMENTOLOGY OF THE
PALEOGENE DÉVOLUY BASIN

CHAPTER 2

The Pierroux Conglomerate Formation

The Pierroux Conglomerate Formation, the lowermost Tertiary formation in the Dévoluy basin, is the basal formation of the Queyras Group (Table 1-I). The formation as defined here corresponds to the "poudingues et formations continentales de la base du Tertiaire" (BRGM, 1980d) and the "conglomérats et/ou couches infranummulitiques" (Pairis *et al.*, 1983; Fabre *et al.*, 1986) (Table 1-I). Similar conglomerates at the bases of Tertiary successions elsewhere in the external western Alps are referred to as the Infranummulitic conglomerates or "Infranummulitique" (Mayoraz, 1995).

The age of the Pierroux Conglomerate Formation is poorly constrained. The formation contains rare Jurassic and abundant Senonian (Campanian-Maastrichtian) clasts and therefore post-dates the Maastrichtian (BRGM, 1980d). Moreover, because it occurs below the Priabonian Dévoluy Nummulitic Limestone Formation, it is older than latest Eocene. However, it does not contain fossils which allow it to be dated more precisely, nor is the exact age of the folds it overlies known. Its age is given as Lutetian to Priabonian (Eocene) on the *St-Bonnet* geologic map (BRGM, 1980d), while Pairis *et al.* (1983, 1984a) give its dates as mid-Bartonian to mid-Priabonian.

Outcrops of the Pierroux Conglomerate Formation occur in northeastern, eastern, central, and southwestern Dévoluy (Fig. 2.1). These outcrops are not continuous except in northeastern Dévoluy. Although it is difficult to constrain the complete extent and depositional geometry of the formation, certain observations can be made: (1) the formation is thickest in northeastern Dévoluy, and thins to the south and west (Fig. 2.1); (2) the average maximum clast size (i.e., the arithmetic mean of the long axes of the 25 largest clasts visible in outcrop) decreases from 50 cm in the northeast to 41 cm in central Dévoluy (Fig. 2.2) to medium- to coarse-grained sand in the southwest.

East of the Median Dévoluy Thrust, the formation is 30 - 150 m thick and consists of clast-supported carbonate conglomerate beds. West of the Median Dévoluy Thrust, a 10 m thick exposure of calcite-cemented quartzarenite occurs in an analogous stratigraphic position. However, the quartzarenite is only present in a single isolated exposure in southwestern Dévoluy (Fig. 2.1), and cannot be definitely correlated to the conglomerates east of the Median Dévoluy Thrust. Nevertheless, the two units are considered here to be lateral equivalents (as indicated by BRGM, 1980d). South of the study area, outcrops of lithologies equivalent to the Pierroux Conglomerate Formation contain Jurassic limestone clasts (BRGM, 1980d). The formation is stratigraphically missing in northwestern and southeastern Dévoluy (Fig. 2.1), but it is not known whether this absence is the result of non-deposition or erosion.

The lower boundary of the Pierroux Conglomerate Formation is an erosional unconformity. Folded Jurassic through upper Cretaceous sediments below the formation are strongly truncated, particularly the hinges of km-scale anticlines (e.g., Fig. 10.3a). The resulting surface is generally

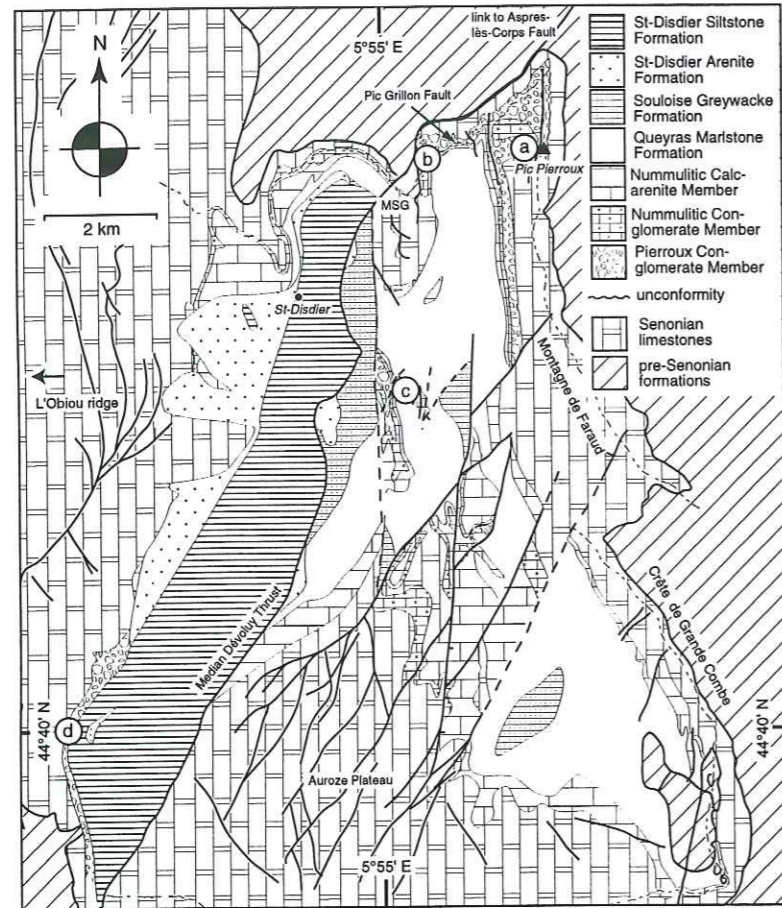


Fig. 2.1 Geologic map of Dévoluy, indicating localities mentioned in the text and estimated thicknesses of the Pierroux Conglomerate Formation at four points (a (Pic Pierroux) = 150m; b (Pic Grillon) = 100m; c (Puits des Bans) = 75m; d (Les Coutières) = $\leq 10\text{m}$). The type section is located at (a), near Pic Pierroux. MSG = Mt. St-Gicon.

Lithofacies	Description	Interpretation
PC-1	Clast-supported conglomerate with subangular clasts	unconfined to poorly channelized alluvial sheet flows
PC-2	Clast-supported conglomerate with subrounded clasts	bedload-dominated, braided alluvial stream channels
PC-3	Heterolithic calclithite, calcisiltite, and calcilitite	alluvial; interchannel/overbank sand or finer-grained unconfined flow
PC-4	Non-conglomeratic quartzite	continental? unconfined flows?
Lithofacies Associations		
PC-I	Interbedded PC-1, PC-2, and PC-3	alluvial fan/braidplain

Table 2-I. Summary of lithofacies and lithofacies associations of the Pierroux Conglomerate Formation.

concave-up to subplanar, and reflects local channelized incision on a broad, planar surface. In one outcrop in northern Dévoluy, the Pierroux Conglomerate Formation lies above a Senonian conglomerate (BRGM, 1980d). In this case, the lower bounding surface is indistinct and is locally characterized by either the occurrence of *Microcodium* in the matrix of the Senonian conglomerate or the presence of better-rounded clasts in the Pierroux Conglomerate Formation.

The upper boundary of the Pierroux Conglomerate Formation is either a transgressive surface, where the formation is overlain by the marine Priabonian Dévoluy Nummulitic Limestone Forma-

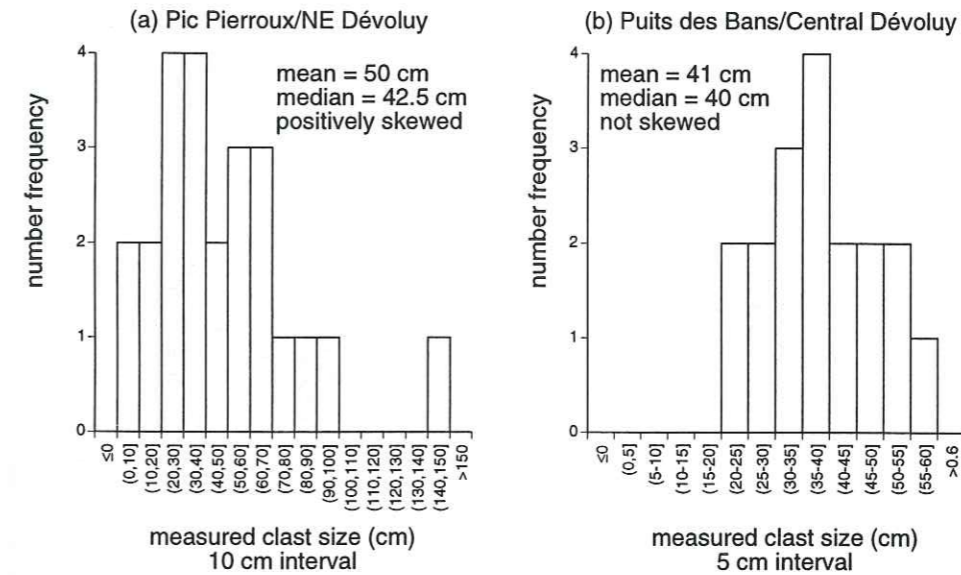


Fig. 2.2. Measured long axes of clasts in the Pierroux Conglomerate Formation at (a) Pic Pierroux and (b) Puits des Bans (localities indicated in Fig. 2.1). (a) Predominantly lithofacies PC-1. (b) Predominantly lithofacies PC-2. The "average maximum clast size" discussed in the text is the mean of the data at each locality. The distribution of data at Pic Pierroux may represent bimodal distribution of clasts.

tion, or is an unconformity, where the formation is overlain by the Chatian Upper St-Disdier Siltstone Formation. In both cases, the surface is broadly planar and does not show significant erosion.

No type section is proposed for the Pierroux Conglomerate Formation, as vertical sections of more than a few meters are inaccessible. The most representative section is on the southern side of Pic Pierroux in northeastern Dévoluy (Fig. 2.1), where up to 150 m of conglomerates crop out (Fig. 2.3a) in a vertical cliff section. Photomosaics allow synthetic sections (e.g., Fig. 2.3b) to be constructed.

The most obvious feature of the Pic Pierroux section is the predominance of lenticular to tabular, crudely-bedded conglomerate layers, usually a few meters thick (Fig. 2.3). The tabular layers are continuous along outcrop strike for hundreds of meters. The lenticular layers often show evidence of channeling (Fig. 2.3). Calcareous siltstones and fine- to medium-grained calcarenite beds are interbedded with the conglomerates, but are discontinuous over tens of meters along outcrop strike, usually because they are eroded by channelized conglomeratic beds (e.g., Fig. 2.4). The silt- and sandstone beds have a characteristic red to yellow-grey weathering color in outcrop.

Three lithofacies are found in this formation (Table 2-I): clast-supported conglomerate with subangular clasts (lithofacies PC-1), clast-supported conglomerate with subrounded clasts (lithofacies PC-2), and heterolithic calclithite, calcisiltite, and calcilitite (lithofacies PC-3). These three lithofacies characterize the Pierroux Conglomerate Formation east of the Median Dévoluy Thrust and do not occur west of it, where, instead, a non-conglomeratic quartzarenite (lithofacies PC-4) occurs at the same stratigraphic level.

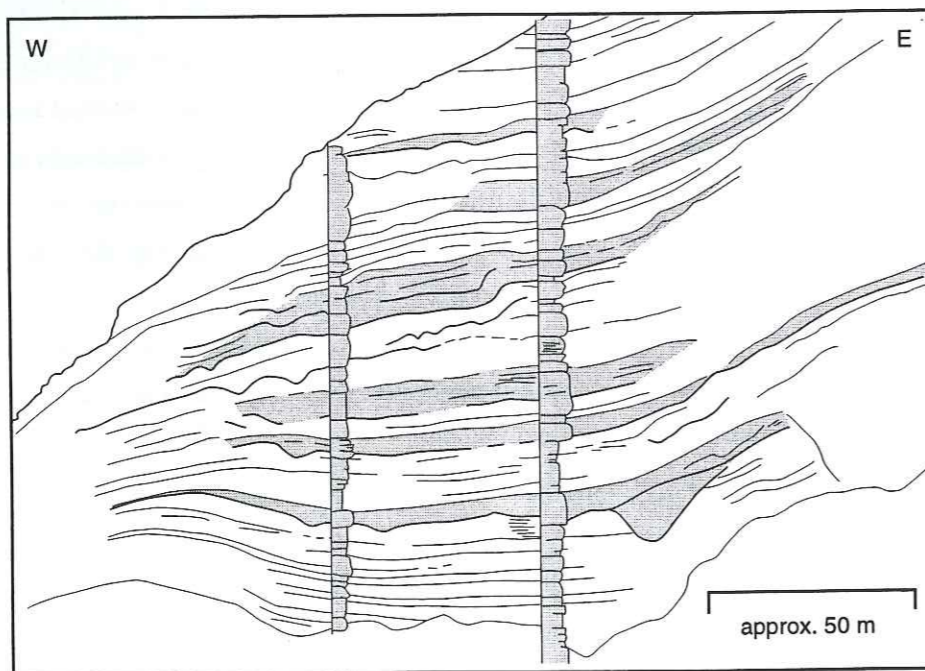
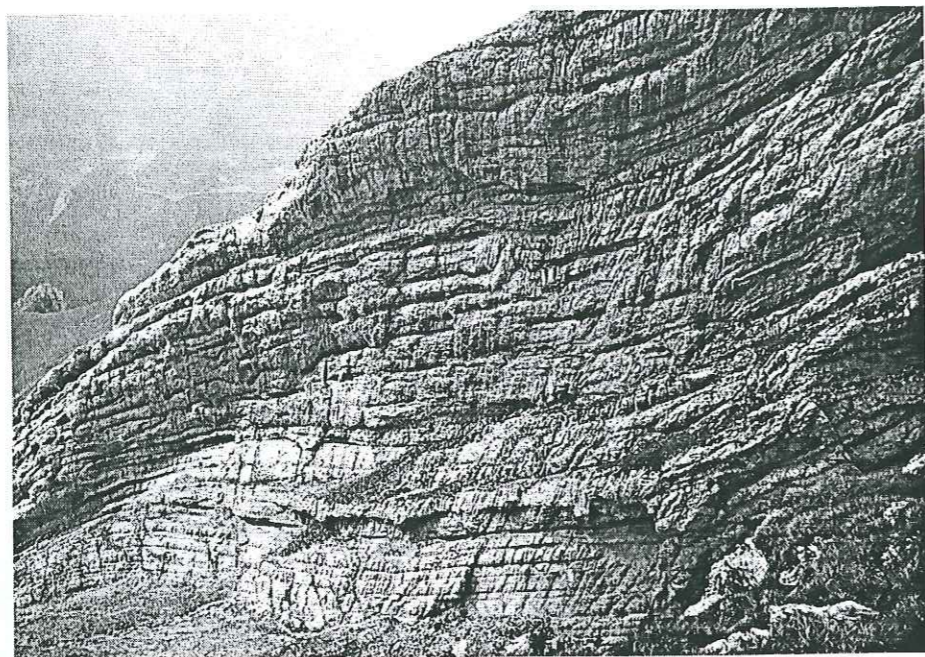


Fig. 2.3. Type section of the Pierroux Conglomerate Formation, south face of Pic Pierroux, northeastern Dévoluy. Location indicated in Fig. 2.2. (a) The Pierroux Conglomerate Formation at Pic Pierroux. Note the well-bedded nature of the formation at this locality. (b) Line drawing of (a) with synthetic stratigraphic sections (not measured, i.e., scale is relative) of the Pierroux Conglomerate Formation at Pic Pierroux, as determined from field observations and photomosaics. Note the incised channels, shown in grey.



Fig. 2.4. Truncation of a siltstone bed (lithofacies PC-3) by an overlying conglomerate bed (lithofacies PC-1). Photograph taken west of Fig. 2.5a. 50 cm hammer for scale.

2.1. Lithofacies analysis and stratigraphy

Lithofacies PC-1: Clast-supported conglomerate with subangular clasts

The most characteristic lithofacies of the Pierroux Conglomerate Formation is a mono- to oligomictic, clast-supported carbonate conglomerate with subangular grey limestone clasts, brown, partially to totally chertified limestone clasts* and a calcareous sand matrix. This lithofacies occurs most commonly in northeastern Dévoluy. The clasts are predominantly Senonian limestone (BRGM, 1980d) and are presumably locally sourced, given the prevalent Senonian limestone substratum. No basement clasts have been observed, although the Pelvoux basement massif presently lies less than 15 km to the east-northeast of Dévoluy and was a source of clasts for the stratigraphically equivalent conglomerates in the Champsaur region (Crampton, 1992).

The clasts have diameters ranging from a few centimeters up to 150 cm, with a mean diameter of 50 cm (Fig. 2.2a). They are poorly sorted, and vary from angular to moderately-rounded, although most are subangular to subrounded and are subequant in shape (Fig. 2.4). There is no apparent clast-size dependency on roundness. The matrix of this lithofacies is a moderately sorted, medium- to coarse-grained calcarenite to calcareous marl. It is often distinctly red to orange-yellow, but may also be grey or yellow-buff.

This lithofacies occurs in poorly- to well-bedded layers 1 to 5 m thick (Fig. 2.3b). Beds of this lithofacies are internally massive or crudely graded. Clasts do not display a preferred orientation. Bed distinctions are best made when the underlying layer is crudely fining-up, as evidenced by a decrease in overall clast size or, more commonly, an increase in matrix, and the overlying layer has larger clasts. Alternatively, some beds are identified by a change in average clast size when the beds

* The chertified clasts are characterized by variably penetrative replacement of limestone by chert, which typically occurs as "rinds" around the clasts. The chertification must have occurred after the erosion of the Senonian limestone, as chert horizons in the Senonian limestones are generally complexly bifurcating "layers" with non-penetrative chert rims that these would presumably not have yielded the well-rounded, rimmed clasts. Also, the chertification must predate deposition of the clasts, as the matrix of conglomerate beds is not chertified. This observation also applies to the chertified limestone clasts of the Nummulitic Conglomerate Member.

have no grading. There is no bed-by-bed variation in the composition of clasts, sorting, roundness, or fabric.

The bases of beds are sharp and subhorizontal and show little or no evidence of erosional incision above conglomerate layers. In contrast, when a bed of lithofacies PC-I overlies a relatively finer-grained layer, the base is concave-up and strongly erosional, usually truncating the underlying bed (Fig. 2.4).

Upper surfaces are subhorizontal and sharp to rapidly gradational (Fig. 2.3). Bedding surfaces often become indistinct along strike and beds become amalgamated (Fig. 2.3a). However, when bedding surfaces are discernible, bed thicknesses are constant along outcrop strike (Fig. 2.3). Therefore, the beds are characterized as large, poorly defined tabular to broadly lenticular bodies hundreds of meters wide in two-dimensional sections. The actual three-dimensional geometry of the beds cannot be determined.

Because clasts are not imbricated and no directional sedimentary structures were observed, no paleocurrent directions have been determined for this lithofacies. No body fossils, trace fossils, or plant material are present (BRGM, 1980d).

Limited outcrops prevent a specific interpretation of lithofacies PC-1. However, the distinctive red color of some beds is strong evidence for subaerial exposure (Nilsen, 1982), and the lithofacies is considered to have been deposited in a continental setting (BRGM, 1980d). The inferred tabular to broadly lenticular geometries of the beds suggests that the lithofacies may represent unconfined to poorly channelized sheet flows, such as are deposited in alluvial settings (Nilsen, 1982). Such flows can cover many square kilometers (Galloway & Hobday, 1983).

Lithofacies PC-2: Clast-supported conglomerate with subrounded clasts

Lithofacies PC-2 is a clast-supported conglomerate with moderately rounded, predominantly grey upper Cretaceous (?) limestone clasts and a calcareous sand matrix. Relatively few chertified limestone clasts are present, and, again, there are no basement clasts. The clasts are from 20-60 cm across, with a mean of 41 cm (Fig. 2.2b). They are moderately sorted, moderately- to well-rounded, and subequant in shape. The matrix is fine- to medium-grained calcareous sand and contains occasional quartz. The lithofacies weathers a grey to yellow-buff color.

Beds of lithofacies PC-2 vary in thickness from tens of centimeters to approximately 5 m. These beds are typically massive and ungraded. However, in some beds, an upward increase in the amount of matrix between clasts gives them an appearance of fining-up, although the clast size remains the same.

The beds have well-defined lower and upper surfaces. Lower bounding surfaces are sharp and may incise underlying layers as channels (Fig. 2.5). This incision is apparent even where two beds have similar clast sizes because of the common occurrence of coarser layers immediately above the scour surfaces. Upper bounding surfaces are sharp and possibly truncated when overlain by another bed of lithofacies PC-2. Alternatively, conglomerate beds sometimes grade into the calcare-

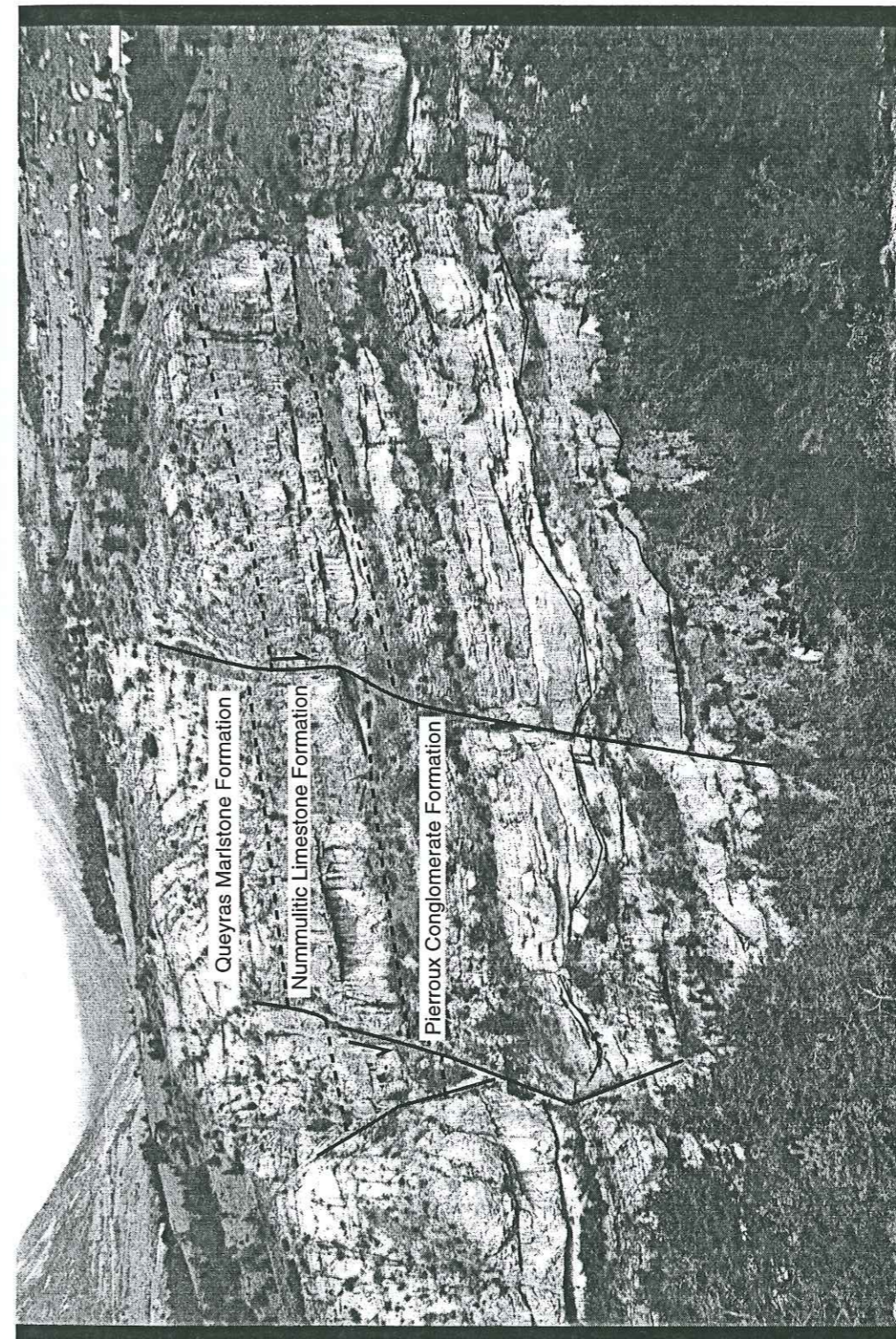


Fig. 2.5. 100 m high cliff exposure (looking NNE) at Puit des Bans (located in Fig. 2.2) showing the Pierroux Conglomerate and Nummulitic Limestone Formations, and the lower part of the Queyras Marlstone Formation. Formation boundaries indicated by dashed lines. Incised channel bases within the Pierroux Conglomerate Formation indicated by heavy lines. N-S oriented faults with dip-slip displacement also indicated. The faults are interpreted to cut the Tertiary succession (e.g., Fig. 2.2).

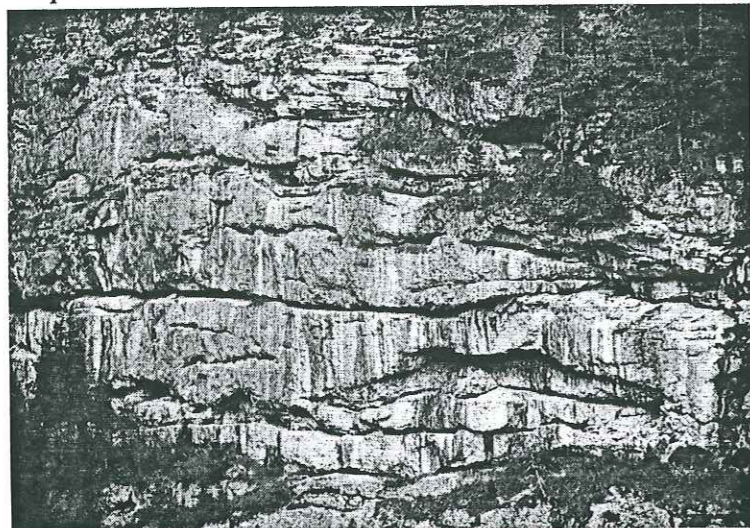


Fig. 2.6. Stacked channels with conglomerate fill in the Pierroux Conglomerate Formation at Puits des Bans (located in Fig 2.2). Most beds consist of lithofacies PC-2.

ous sandstone beds of lithofacies PC-3 (see description below).

This lithofacies crops out spectacularly in two cliff sections (e.g., Fig. 2.5) on either side of the Souloise River in central Dévoluy. The two-dimensional geometries exposed here are broadly lenticular, with gently concave-up bases and flatter tops (e.g., Fig. 2.6). Individual beds have widths of 10-500 m, but are often stacked laterally and vertically such that several beds are amalgamated into what appears to be one larger bed. The three-dimensional geometry of the beds cannot be determined in the sections, but the channelized two-dimensional geometries imply that the beds are elongate in a generally north-south direction.

Paleocurrents could not be determined because of a lack of directional sedimentary structures. There are no fossils present in this lithofacies.

The two-dimensional geometries and occasional fining-up nature of this lithofacies are indicative of alluvial or fluvial channels. The vertical and lateral amalgamation of the beds suggests that the channels were part of a braided river system.

Lithofacies PC-3: Heterolithic calclithite, calcisiltite, and calcilutite

Lithofacies PC-3 of the Pierroux Conglomerate Formation occurs in outcrops east of the Median Dévoluy Thrust as massive to fining-up beds 2 to 100 cm thick, between conglomeratic layers of lithofacies PC-1 and PC-2 (e.g., Fig. 2.4). The beds are composed of calcilutite, calcisiltite, and well-sorted, fine- to medium-grained, moderately- to well-rounded calcarenite. This lithofacies varies in color from red to pale yellow-grey. The variation in color does not appear to be related to macroscopic differences in the lithofacies (e.g., grain size).

Beds have sharp or rapidly gradational lower surfaces (Fig. 2.4). The upper surfaces of beds of lithofacies PC-3 are sharp and typically eroded (e.g., Fig. 2.4). Although upper surfaces that are apparently conformable are also found, such surfaces can generally be followed laterally to places where erosion is evident.

The beds are broadly lenticular, with flat to undular bases and convex to concave tops associated

with erosional truncation by the overlying layer. They are continuous over distances of 1 to 100 m along strike. Their three-dimensional geometry could not be determined. Internally, the beds have fine laminations or are structureless.

As with lithofacies PC-1 and PC-2 (Table 2-1), paleocurrents could not be determined, and no fossils were observed.

Lithofacies PC-3 always occurs above lithofacies PC-1, interpreted as unconfined sheet flows, or PC-2, interpreted as alluvial channels. Where the contact with the underlying lithofacies is abrupt, lithofacies PC-3 is interpreted as either an interchannel or overbank deposit or the deposit of a finer-grained unconfined flow. Where the contact with the underlying lithofacies is transitional, lithofacies PC-3 is interpreted as the deposits of waning flow associated with the underlying lithofacies.

Lithofacies PC-4: Non-conglomeratic quartzite

Lithofacies PC-4 is a medium- to coarse-grained, well-sorted quartzarenite with a sparry calcite cement. Limestone rock fragments and feldspar grains are present in minor (< 5%) proportions. The lithofacies occurs only in southwestern Dévoluy, in the footwall of the Median Dévoluy Thrust (Fig. 2.1). Therefore, the age and geometric relationship of this lithofacies to the lithofacies east of the Median Dévoluy Thrust is not known. However, this lithofacies ("Eocene continental sands and sandstone") is shown as the time-equivalent of the lithofacies east of the Median Dévoluy Thrust (BRGM, 1980d).

The lithofacies occurs as a 10m thick deposit that crops out for several hundred square meters. Bedding surfaces may be well-defined over less than 3 m, but become indistinct along strike. The beds are 1-10 cm thick, when discernible. They are internally massive or, less commonly, fining up. When visible, lower and upper bounding surfaces of beds are sharp and planar. Laterally continuous, meter-scale bedsets occur infrequently. These are tabular in two-dimensional outcrops, but three-dimensional constraints are rare. Paleocurrents are not available for this lithofacies, and there are no fossils. The lithofacies has a white, dirty yellow, or light pink color.

The interpretation of lithofacies PC-4 is problematic because it does not have any diagnostic sedimentary structures, nor does it occur in a large enough outcrop to determine its relationship to its substratum. It is assumed that this lithofacies was deposited in a continental setting, as were lithofacies PC-1, PC-2, and PC-3 (BRGM, 1980d). The discontinuity of individual bedding surfaces along strike suggests that many of the beds are amalgamated. The two-dimensional tabular nature of bedsets suggests that they are possibly the deposits of unconfined flows, as was lithofacies PC-1.

The quartz-rich composition and the sedimentological characteristics of lithofacies PC-4 distinguishes it readily from the other three lithofacies; therefore, this lithofacies is probably part of a different depositional system; alternatively, it may have been deposited at a different time. Its unique quartz-rich composition indicates that its source area was clearly different from that of lithofacies PC-1, PC-2, or PC-3. However, no source has been identified.

One lithofacies association (lithofacies association PC-I) has been determined for the Pierroux Conglomerate Formation, consisting of interbedded deposits of lithofacies PC-1, PC-2, and PC-3 (Table 2-I). The relative amounts of lithofacies PC-1 and PC-2 vary locally. In northeastern Dévoluy, lithofacies PC-1 (ca. 50%) is more common than lithofacies PC-2 (ca. 30%). In central Dévoluy (locality C, Fig. 2.1), lithofacies PC-2 (ca. 70%) is more common than lithofacies PC-1 (ca. 10%), which occurs only in the lower part of the formation.

The proportion of lithofacies PC-3 at both localities is relatively constant and is always subordinate to lithofacies PC-1 and PC-2. An exception to this observation occurs in northeasternmost Dévoluy, where a 30m outcrop of this lithofacies is reported to occur at the base of the formation (BRGM, 1980d).

The change from a predominance of lithofacies PC-1 in northeastern Dévoluy to a predominance of lithofacies PC-2 in central Dévoluy (Fig. 2.7) indicates an increased propensity for well-defined channels and an overall increase in rounding and sorting south from northern Dévoluy. The increases in channelization, rounding, and sorting are concomitant with decreases in both formation thickness and average maximum clast size to the southwest (Figs. 2.2, 2.7).

Thus, lithofacies association PC-I documents a southwestward transition from largely unconfined flow with a few channels and sedimentologically immature deposition in the northeastern part of Dévoluy to channelized flow and texturally more mature deposits in central Dévoluy (Fig. 2.7). It is proposed that these transitions, as well as the stratigraphic thinning to the south, reflect a change from a proximal alluvial fan setting, where distributary channels incised sheet flows, to a braidplain setting in the central to distal part of the fan (Fig. 2.7; see also discussion below).

2.2. Paleocene/Eocene folding and Eocene normal faulting

In northern Dévoluy, the Pierroux Conglomerate Formation unconformably overlies NNW-SSE trending, W-facing folds in the Senonian limestones. Here, the folds have steeply-dipping to overturned limbs (Fig. 10.3a), but they are less well-developed elsewhere in Dévoluy. In central Dévoluy, for instance, Senonian strata are gently folded such that there is an angular unconformity of 10-20° with the overlying Tertiary strata, while further south, the angular unconformity is typically less than 10°.

The "post-Senonian" folding was therefore most intense in northern Dévoluy, and died out to the south. The proximity of this tectonism to the NE-SW oriented Aspres-lès-Corps Fault zone, and the relative lack of early tectonism to the south, strongly suggest that the Aspres-lès-Corps Fault may have been active as a strike-slip fault. One component of the early movement on this fault is reported to have been dextral (Gidon & Pairis, 1976), which is consistent with the approximately W-E compression recorded in the folds. The age of the folds can be no better constrained than pre-mid Bartonian and post-late Maastrichtian, as the age of the Pierroux Conglomerate Formation is uncertain.

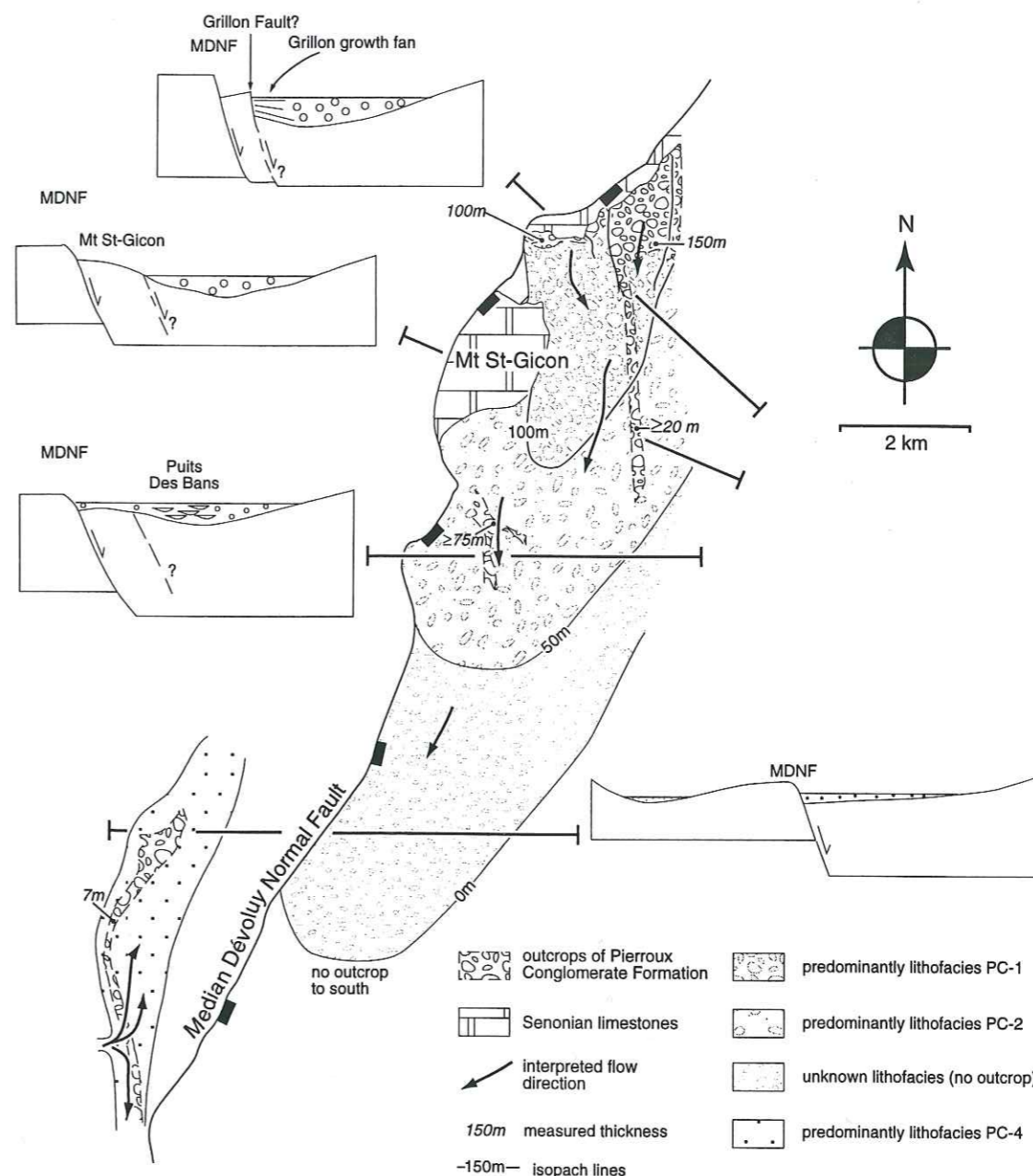


Fig. 2.7. Map and schematic cross sections showing possible relationship between northern Dévoluy, where lithofacies PC-1 is dominant, central Dévoluy, where lithofacies PC-2 is dominant, and southwestern Dévoluy, where lithofacies PC-4 is dominant. Based on sedimentological trends, the depocenter of the formation is inferred to be in the northeast (see text for details).

Extensional faults that cut the post-Senonian folds, and therefore postdate them, occur in northeastern Dévoluy. These faults, which were active before and during the deposition of the Pierroux Conglomerate Formation (Gidon & Pairis, 1976; Fabre *et al.*, 1985a; Meckel *et al.*, 1996) are: (i) the Median Dévoluy Normal Fault, which had pre-Priabonian downthrow to the east before being inverted as the Median Dévoluy Thrust in the Mio-Pliocene (Gidon & Pairis, 1976; see Section 10.3) and (ii) the Pic Grillon Fault, northeast of Mt. St-Gicon (Fig. 2.1). The Lucles Fault (Figs. 2.1, 10.3a)

may also have been active at this time. These three faults developed immediately south of the Aspries-Corps Fault in the vicinity of Mt. St-Gicon (Fig. 2.1).

The Median Dévoluy Normal Fault

Three lines of evidence point to down-to-the-east extensional displacement on the Median Dévoluy Thrust prior to or during deposition of the Pierroux Conglomerate Formation (Meckel *et al.*, 1996). In order to distinguish this early extensional displacement from the later Mio-Pliocene compressional displacement, the early fault is referred to here as the Median Dévoluy Normal Fault.

(1) An extensional stratigraphic offset is preserved in the Jurassic and Cretaceous sediments north of Mt. St-Gicon. This offset places Senonian limestones in the eastern (hanging) wall against lower Cretaceous and Jurassic sediments in the western (foot) wall (Fig. 2.1; Gidon & Pairis, 1976, their Fig. 3). The same sense of dip-slip offset is also preserved along strike to the east on the Aspries-Corps Fault (BRGM, 1980d).

(2) The Senonian limestones are dramatically thicker in the hanging wall than in the foot wall. In northern Dévoluy, the thickness difference is approximately 150 m across the fault (Figs. 10.3a, b; Gidon & Pairis, 1976, their Fig. 4a). In southwestern Dévoluy, the Senonian limestones are locally completely eroded in the foot wall, but are several hundred meters thick on the Auroze Plateau in the hanging wall (Fig. 2.1). The thickness difference across the fault indicates that it was a growth fault with down-to-the-east movement during deposition of the Senonian limestones or that post-Senonian displacement resulted in relative uplift and erosion of the foot wall.

(3) Two km to the south of Les Couitières, in the foot wall of the Median Dévoluy Normal Fault, the Pierroux Conglomerate Formation is in contact with Jurassic sediments (Fig. 2.1) and contains Jurassic clasts (BRGM, 1980d). This indicates that the Senonian limestones were completely eroded at this locality before deposition of the Pierroux Conglomerate Formation, and that the formation was sourced from the underlying Jurassic sediments. The most logical way to explain such a relationship is that the foot wall block was uplifted and the Senonian limestones were eroded before or, at latest, during deposition of the Pierroux Conglomerate Formation.

The above evidence suggests that down-to-the-east movement on the Median Dévoluy Normal Fault occurred prior to or during deposition of the Pierroux Conglomerate Formation. The thickness of the Priabonian Dévoluy Nummulitic Limestone Formation, which overlies the Pierroux Conglomerate Formation, does not vary significantly across the fault (Figs. 10.3a, b), indicating that the fault was not active during the Priabonian.

The Pic Grillon Fault

The second early extensional feature is observed at Pic Grillon in northern Dévoluy (Figs. 2.1, 2.8). Pic Grillon is a pillar-like Senonian limestone block with a 60°S dipping southern face. Beds of the Pierroux Conglomerate thicken away from the southern face and onlap it at a high angle (Fig. 2.8; Gidon and Pairis, 1976, their fig. 7). The angle of onlap steepens progressively downsection

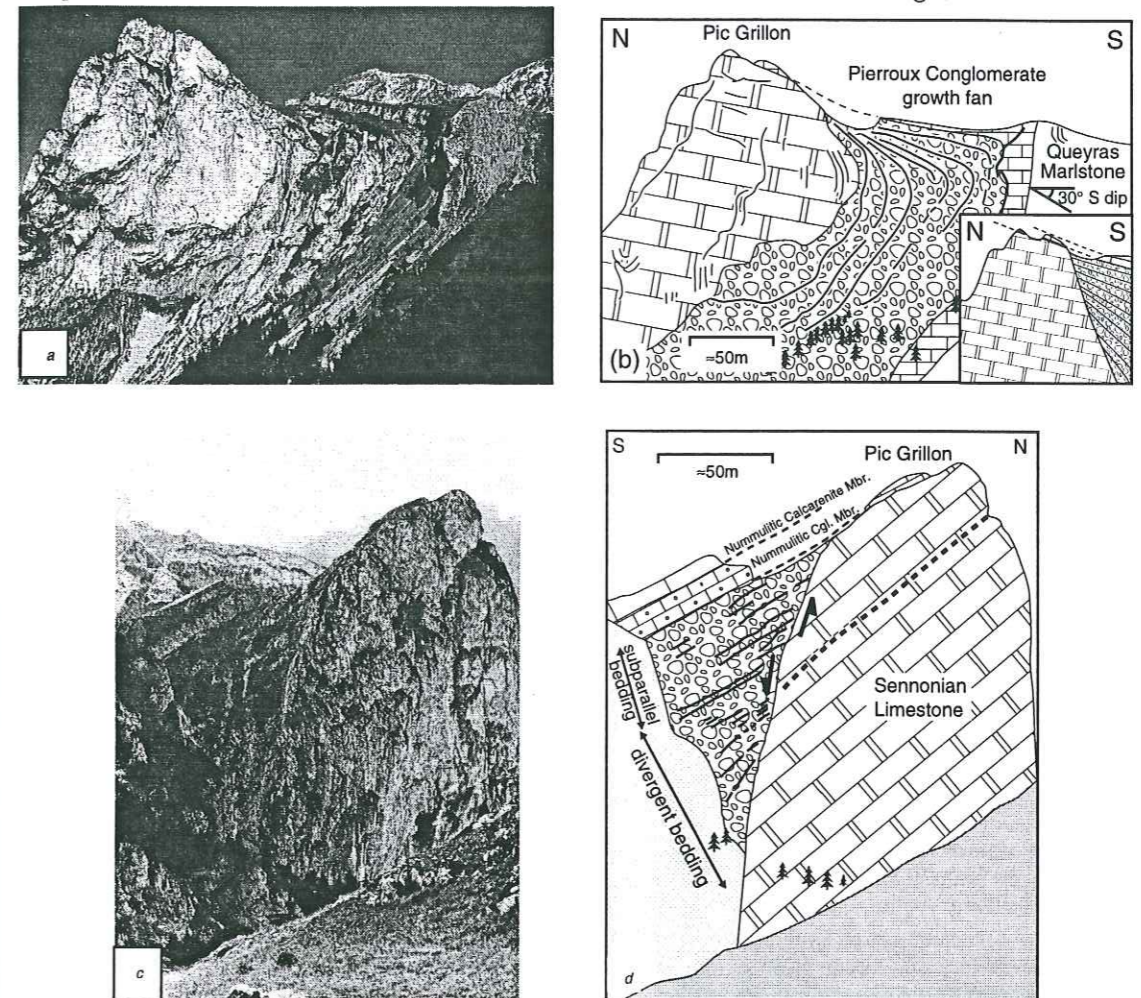


Fig. 2.8. The Pic Grillon growth structure. (a), (c) Views looking east and west, respectively, of progressive steepening of beds against the southern face of Pic Grillon. (b) Line drawing of (a). Curved lines in the Pierroux Conglomerate Formation show bedding traces in outcrop; these appear to be overturned because of three-dimensional cutting effects. The true geometric relationship is indicated in the inset (after Gidon & Pairis, 1976). (d) Line drawing of (c). Note that the Nummulitic Conglomerate Member (LNC) seals the structure and is not offset across the Pic Grillon Fault. UNC = Nummulitic Calcarenite Member. Dashed line in (d) indicates approximate trace of bedding.

(rotative onlap) such that the sediments form a cumulative wedge (*sensu* Riba, 1976a, b). In other areas, such features have been shown to be related to syndepositional uplift (Riba, 1976a, b; Anadon *et al.*, 1986; Miall, 1995). The relative uplift of Pic Grillon may have been caused by down-to-the-southeast displacement on a synthetic normal fault of the Median Dévoluy Normal Fault (the "Pic Grillon Fault" of Gidon & Pairis, 1976).

The uppermost beds of the Pierroux Conglomerate Formation do not thicken away from Pic Grillon (Fig. 2.9). Therefore, uplift ceased towards the end of deposition, which is supported by the facts that the overlying Dévoluy Nummulitic Limestone Formation also does not thicken across the Pic Grillon Fault, nor is it offset (Fig. 2.8). Therefore, uplift on Pic Grillon is considered to have ceased by the late Priabonian.

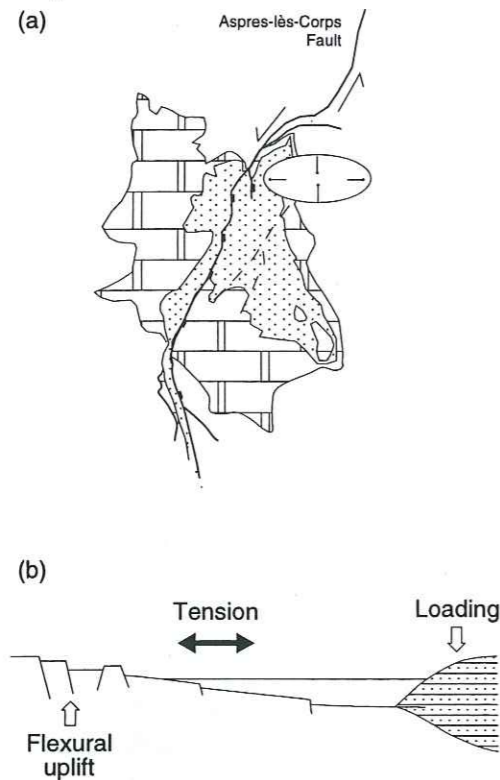


Fig. 2.9. Hypotheses to explain pre-Priabonian down-to-the-east faults in Dévoluy. (a) Simplified map of the Dévoluy region: sinistral strike-slip activity on the Aspres-lès-Corps Fault results in a regional strain ellipse that has an approximately W-E oriented extensional axis. Double brick pattern = Senonian limestones, stippled pattern = Tertiary sediments. Heavier lines are faults. The basement block is the (b) Cross section across the external Alps: loading of the lithosphere in the internal Alps causes tensional flexure in the external Alps and flexural uplift in the distal foreland. Dot-dash pattern = internal Alps.

1974; Debelmas, 1975; Gidon & Pairis, 1976) is consistent with the W-E extension recorded on the normal faults (Fig. 2.9a). As the faults postdate the "post-Senonian" folds associated with dextral movement on the Aspres-lès-Corps Fault, this sinistral movement must have postdated an earlier phase of dextral movement. An alternate explanation for the extension is that it reflects tensional response of the lithosphere to loading in more internal Alpine domains (Fig. 2.9b; Pfiffner, 1986; Miall, 1995; P. Tricart, personal communication).

2.3. Depositional setting and provenance

Sedimentological trends in the Pierroux Conglomerate Formation and its close association with pre-or syn-depositional extensional faults suggests that it is part of a locally-sourced alluvial fan/braidplain system, with a depocenter in the northeastern hanging wall of the Median Dévoluy Normal Fault. Although the Pelvoux Massif was a topographic high in the early Tertiary (Crampton,

The Lucles Fault

The Lucles Fault may also have been active before or during deposition of the Pierroux Conglomerate Formation, as the formation occurs only in its hanging wall (Figs. 2.1, 10.3a, b). By analogy with the Median Dévoluy Normal Fault (see above), this occurrence suggests movement prior to or synchronous with deposition of the Pierroux Conglomerate Formation. However, no other evidence has been found for activity on the fault at this time, and, because the formation could also have been deposited in the footwall and been eroded during subsequent uplift in the Priabonian, it is discussed below (section 3.1.2) with reference to its syn-Nummulitic movement.

In summary, the Median Dévoluy Normal Fault and Pic Grillon Fault, and perhaps the Lucles Fault, document a period of down-to-the-east extension in Dévoluy possibly before, and certainly during, deposition of the Pierroux Conglomerate Formation. The proximity of these faults to the Aspres-lès-Corps Fault and their apparent northward termination into it (Fig. 2.1) strongly suggest that pre-Priabonian strike-slip activity on the NE-SW oriented Aspres-lès-Corps Fault (Gidon & Pairis, 1976) may have influenced this early tectonism. Pre-Priabonian sinistral movement on the eastern branch of the Aspres-lès-Corps Fault (Vialon,

1992; Ford, 1996), and its uplift may have been connected with early tectonism in Dévoluy (Gidon & Pairis, 1976; Meckel *et al.*, 1996), a lack of basement clasts indicates that Dévoluy was sedimentologically separated from Pelvoux.

The fan/braidplain system was constrained to the west by the Median Dévoluy Normal Fault, and a second, smaller, siliciclastic depositional system occurred in the footwall of the Median Dévoluy Normal Fault (Fig. 2.7).

A modern analogue for the deposits of the Pierroux Conglomerate Formation occurs immediately south of the Dévoluy valley, where the Béoux River has deposited a thick conglomeratic alluvial fan of Senonian debris against the vertical southwestern face of Pic de Bure. This fan thins rapidly to the southwest, and the alluvial deposits become a braidplain less than a kilometer away from the fan.

Univ. J. Fourier - O.S.U.G.
 MAISON DES GEOSCIENCES
 DOCUMENTATION
 B.P. 53
 F. 38041 GRENOBLE CEDEX
 Tél. 04 76 63 54 27 - Fax 04 76 51 40 58
 Mail: ptalour@ujf-grenoble.fr

CHAPTER 3

The Dévoluy Nummulitic Limestone Formation

The Dévoluy Nummulitic Limestone Formation lies stratigraphically between the Pierroux Conglomerate and Queyras Marlstone Formations. It was deposited during a widespread marine transgression in the external western Alps (e.g., Pairis, 1988). The formation is also known as the "calcaires à Nummulites" (BRGM, 1980d), the "calcaires nummulitiques" (Fabre *et al.*, 1986; Pairis, 1988), and the Nummulitic Limestone (Meckel *et al.*, 1996) (Table 1-I). Similar deposits are documented along the northern margin of the Alps as far east as the western Carpathian Mountains in Poland.

In Dévoluy, the formation is dated as Priabonian (correlated with planktonic biochronozone P16) based on a foraminiferal assemblage that includes *Nummulites boulei*, *N. budensis*, *N. garnieri*, *N. incrassatus*, *N. stellatus*, *N. striatus*, *N. vascus*, rare *N. fabianii*, other foraminifera including *Heterostegina*, *Asterigerina*, *Sphaerogypsina*, *Chapmanina* (BRGM, 1980d; Pairis *et al.*, 1983, 1984a; Fabre & Pairis, 1984; Fabre *et al.*, 1986; Pairis, 1988), and probable *Discocyclina* fragments (Dubois, 1962).

The formation is present throughout the Dévoluy basin apart from southwestern Dévoluy (Fig. 3.1). It has a fairly uniform thickness of 20-25 m except in northeastern Dévoluy, where it is a thickness of 100 m.

The formation is deposited on either the Pierroux Conglomerate Formation or, more commonly, on Senonian limestone (Figs. 3.1, 3.2). The lower bounding surface of the formation is a transgressive surface that is a paraconformity above the Pierroux Conglomerate Formation and an angular unconformity above the Senonian limestones. The formation is conformably overlain by the Queyras Marlstone Formation. However, in northwestern Dévoluy, it is unconformably overlain by the St-Disdier Arenite Formation.

The type section of the Dévoluy Nummulitic Limestone Formation (Fig. 3.2) is located approximately 500 m ENE of the Superdévoluy ski resort (Fig. 3.1). Four sections were measured at this locality to constrain lateral variations in thickness and facies (Fig. 3.2). The type section is column III of figure 3.2.

The sections at Superdévoluy (Fig. 3.2) document several significant aspects of the formation. (1) The Nummulitic Limestone Formation consists of two distinct units, named here the Nummulitic Conglomerate Member and the Nummulitic Calcarenite Member. The two members are distinguished by the presence or absence, respectively, of pebble-sized clasts. These members are the equivalents of the Nummulitic Conglomerate and Nummulitic Calcarenite of Meckel *et al.* (1996). (2) Major bedding surfaces (e.g., surfaces a, b, c, and d, Fig. 3.2) in the Dévoluy Nummulitic Limestone Formation are continuous for hundreds of meters, but may be locally obscured, as are more minor bedding surfaces (e.g., other correlated surfaces, Fig. 3.2). (3) The basal surface of the formation locally incises the Senonian limestones.

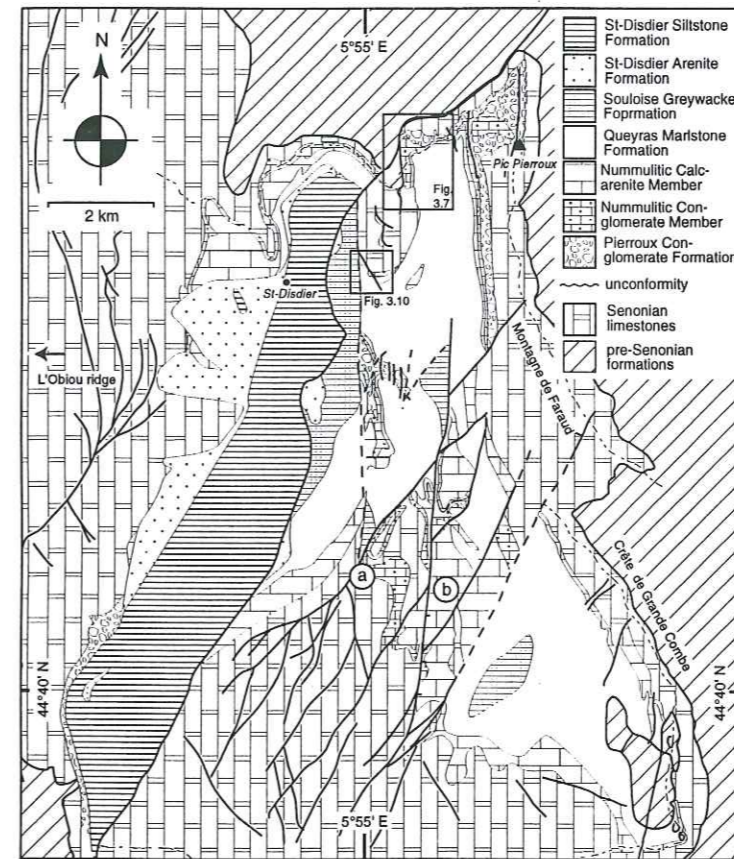


Fig. 3.1. Geologic map of Dévoluy, indicating locations of measured sections of the Dévoluy Nummulitic Limestone Formation. a = Le Collet du Tat section; b = Superdévoluy sections (including type section).

3.1. The Nummulitic Conglomerate Member

The Nummulitic Conglomerate Member is present throughout northern Dévoluy (Fig. 3.1). It is not present in southwesternmost Dévoluy. It may be present in southeastern Dévoluy, but outcrops are inaccessible, so it has not been mapped there.

The lower boundary of the member varies according to the substratum. Above the Pierroux Conglomerate Formation, the lower boundary is defined as the bottom of the lowermost bed containing visible *Nummulites* or, if *Nummulites* are not visible, as the bottom of the first matrix-supported conglomerate bed with well-rounded pebble-sized clasts. Above Senonian limestones, the lower surface of the Nummulitic Conglomerate Member is an irregular and locally incisive angular unconformity (Figs. 3.2, 3.3).

In northern Dévoluy, there is a Senonian conglomerate between the well-bedded Senonian limestone and the Nummulitic Conglomerate Member (BRGM, 1980d). Here, the Nummulitic Conglomerate Member is identified by the presence of *Nummulites*, a shift from clast-supported to matrix-supported fabric, or the abrupt appearance of characteristic brown chertified rinds around some Senonian clasts. Another distinguishing feature, if present, is *Microcodium* in the matrix of the Senonian conglomerate (BRGM, 1980d). *Microcodium*, an indicator of subaerial exposure (Esteban & Klappa, 1983), is not found in the Nummulitic Conglomerate Member.

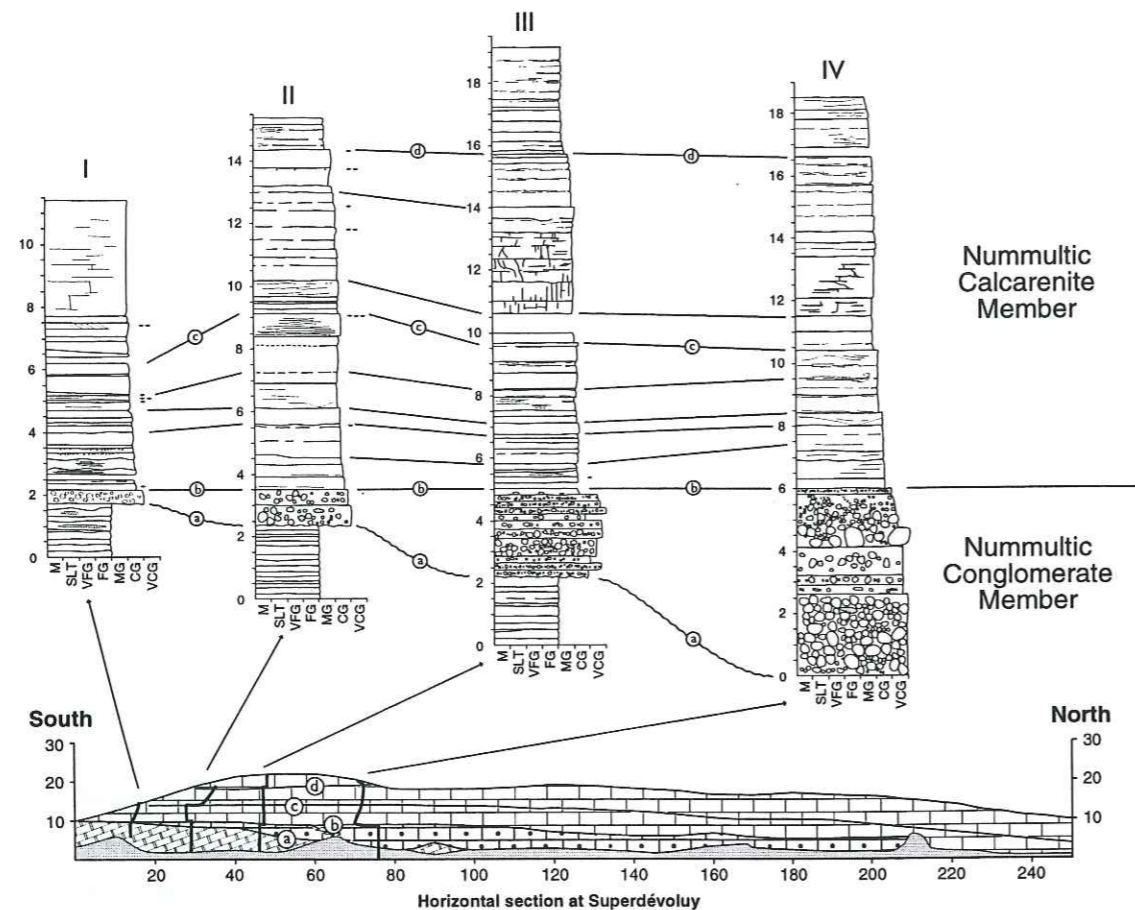


Fig. 3.2. Measured sections (thicknesses in meters) of the Dévoluy Nummulitic Limestone Formation at Superdévoly (locality b, Fig. 3.1), showing lateral relationships between beds as discerned in the field. Column III is the type section of the formation. Senonian limestones occur beneath surface a. Note the angular nature of this contact. Surfaces a, b, c, and d are internally correlatable surfaces of unknown significance. Black dots to the right of measured sections represent *Nummulites* content (1 dot = scarce, 3 dots = abundant). Patterns in lower cross section as in Fig. 3.1, except grey is foreground.

The upper boundary, with the Nummulitic Calcarenite Member, is often abrupt. It is defined as the top of the uppermost bed containing at least 5% of clasts visibly larger than the surrounding matrix (Fig. 3.2). The clasts tend to weather a different color than the matrix, and protrude from the weathered matrix.

In northwestern Dévoluy, the contact between the Lower St. Disdier Arenite Formation and the Nummulitic Conglomerate Member does not crop out, but, based on bedding dips, appears to be a low-angle angle unconformity.

The Nummulitic Conglomerate Member is usually 1-10 m thick. However, northeast of Mt. St-Gicon, it is 90-95 m thick and contains numerous large Senonian limestone blocks (Fig. 3.4). The unusual thickness and the presence of the Senonian blocks is attributed to syndepositional extensional faulting in this area (Gidon & Pairis, 1976).

The Nummulitic Conglomerate Member has four lithofacies (Table 3-I): angular to well-rounded rudstone (lithofacies LN-1); rounded fossiliferous floatstone (lithofacies LN-2); subrounded fossiliferous lime wackestone to packstone (lithofacies LN-3); and fossiliferous lime packstone (lithofacies

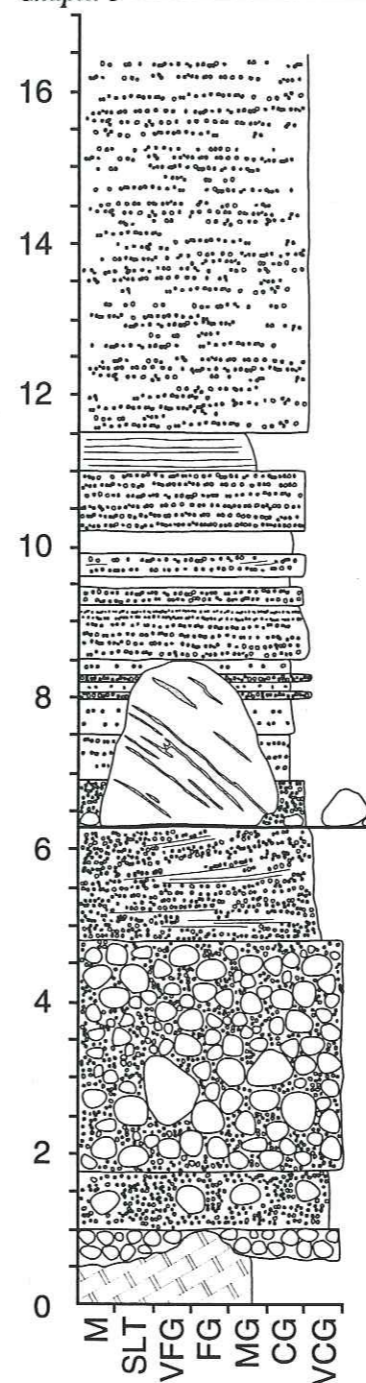


Fig. 3.3. Measured section (scale in meters) of the Nummulitic Conglomerate Member at Le Collet du Tat (locality a, Fig. 3.1). Note that the member is significantly thicker at this locality than at Superdévoly (Fig. 3.2). The lowermost bed in this section is lithofacies LN-1, as is the bed from 1.75 - 4.75 m. Other beds are lithofacies LN-2 and LN-3 (with pebbles) and lithofacies LN-4 (without pebbles). Most of the beds of lithofacies LN-2 and LN-3 have been shown as single layers for graphic convenience (e.g., the beds from 10.25 - 11 m and from 11.5 m to the top of the section). The bed from 4.75 - 6.25 m shows low angle inclined stratification. Above this bed, an anomalously large block occurs, which may be a lag deposit. The Senonian limestones beneath the member are shown with a double brick pattern.

LN-4).

3.1.1. Lithofacies analysis and stratigraphy

Lithofacies LN-1: Carbonate conglomerate with angular to well-rounded clasts

A poorly-sorted, clast-supported carbonate conglomerate with angular to well-rounded clasts occurs occasionally in the lowermost part of the Nummulitic Conglomerate Member. This lithology is composed of grey Senonian limestone clasts, brown chertified Senonian limestone clasts, brown

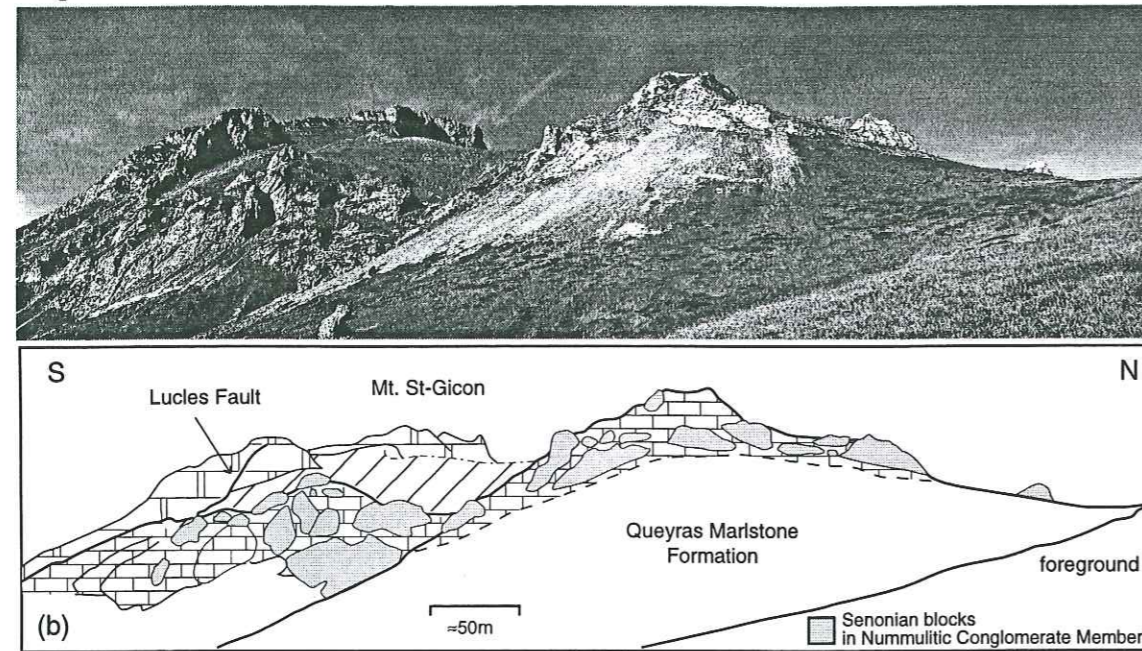


Fig. 3.4. (a) Photograph and (b) line drawing of large Senonian blocks (grey) within the Nummulitic Conglomerate Member of the Dévoluy Nummulitic Limestone. Other patterns as in Fig. 3.1.

Lithofacies	Description	Interpretation
LN-1	Carbonate conglomerate with angular to well-rounded clasts	transgressive lag; shallow marine, high energy; coarse sediment flows
LN-2	Fossiliferous carbonate conglomerate with rounded clasts	shallow marine, high energy shoreface
LN-3	Fossiliferous wackestone to packstone	lower energy equivalent of Lithofacies LN-2
LN-4	Fossiliferous calcarenite	lower energy, slightly deeper equivalent of lithofacies LN-3
Lithofacies associations		
LN-I	Interbedded lithofacies LN-1 and LN-2	shallow marine, high energy; LN-2 reworks LN-1?
LN-II	Interbedded lithofacies LN-2, LN-3, and LN-4	composite shoreface/shallow marine deposits
LN-III	Interbedded lithofacies LN-3 and LN-4	transgressive, shallow shelf deposits
Lithofacies		
UN-1	Fossiliferous grainstone	moderately deep (20-40m), relatively calm carbonate ramp "background" settling of finer-grained sediment; moderately deep-water
UN-2	Lime mudstone	

TABLE 3-I. Summary of lithofacies and lithofacies associations of the Nummulitic Limestone Formation.

or grey chert clasts, and a medium-grained, grey carbonate sand matrix.

The clasts have long axes that typically vary in length from 1 mm to 1 m, with limestone and chertified limestone clasts usually larger than 5 cm and chert clasts, from 1 to 5 mm. The limestone clasts may reach boulder-size: for instance, in one bed at Le Collet du Tat in central Dévoluy, a 2.75

m clast occurs (Fig. 3.3), and in northeastern Dévoluy, Senonian blocks up to 50 m in length occur. All clasts show decreasing roundness with increasing size: clasts 1 mm to 20 cm in size are subrounded to well-rounded, clasts 20 to 25 cm in size are subrounded, and clasts larger than 25 cm are subangular to angular. Some limestone clasts smaller than 25 cm are also subangular to angular, especially in northeastern Dévoluy.

This lithofacies typically occurs as the basal bed of the member, and also occurs in a second bed at Le Collet du Tat (6.25 m, Fig. 3.3). Beds vary in thickness from 3 m or less in southern Dévoluy to approximately 30m in northeastern Dévoluy. The beds are usually structureless, although occasionally they exhibit a poorly-developed, fining-up internal structure. The upper and lower bounding surfaces are sharp.

When beds of this lithofacies overlie Senonian bedrock, they thicken into topographic lows and have channelized or broadly lenticular three-dimensional geometries with concave-up bases and flat tops. Over topographic highs, beds may be no more than thin veneers of scattered clasts lying on gently undular surfaces, or may be completely absent (Fig. 3.3). In contrast, there is little evidence of erosional incision when this lithofacies overlies the Pierroux Conglomerate Formation or other lithofacies of the Nummulitic Conglomerate Member. The beds have tabular geometries in these cases. The upper surfaces of beds do not show signs of erosion.

Local concentrations of small *Nummulites* and their fragments occur in the matrix of this lithofacies. In northern Dévoluy, this lithofacies also contains abundant red algal rhodoliths and dasycladacean fragments. The *Nummulites* in the matrix indicates deposition in a shallow marine, high energy setting.

The erosional features in the Senonian limestone are similar to those developed on modern rocky shorelines, where irregular coast-perpendicular depressions and ridge-and-runnel topography are well-documented. Therefore, the Nummulitic Conglomerate Member may be interpreted as a transgressive deposit above the Senonian limestone. The stratigraphically higher bed at Collet du Tat (Fig. 3.3) may be the winnowed deposits of a storm surge (cf. Jones & Desrochers, 1992).

Where lithofacies LN-1 occurs above the Pierroux Conglomerate Formation, it may also be a transgressive lag deposit that reworks the older conglomerates. Although this hypothesis cannot be conclusively proven in Dévoluy, similar Nummulitic conglomerate deposits at the top of underlying continental conglomerates at a single outcrop (St-Jacques) near Barrême, 50 km southeast of Dévoluy, provide valuable insight into the nature of the contact. Here, the uppermost clasts of the continental conglomerates have been bored by marine fauna, documenting shoreline conditions (Evans, 1987; cf. Jones & Desrochers, 1992). Similar shoreline bored clasts have been reported in Champsaur, 15 km east of Dévoluy (Crampton, 1992). The overlying Nummulitic conglomerates thus record the initial stages of transgression. These bored clast horizons may be analogous to the deposits at the base of the Nummulitic Conglomerate Member in Dévoluy.

The lack of bored clasts in Dévoluy may reflect a difference in wave energy between Dévoluy and the other two areas. Such a situation occurs in the modern environment at Zumaia, northwestern



Fig. 3.5. Sub-spherical clasts in lithofacies LN-2 of the Nummulitic Conglomerate Member of the Dévoluy Nummulitic Limestone Formation. Note the bimodal distribution of grain sizes.

Spain, where *Lithophaga* molluscs preferentially populate rocky outcrops in protected coves and bore the rocky substrate (personal observation). The same molluscs are absent at rocky outcrops less than 500 m away that are exposed to extremely high wave energy. The niche occupied by the molluscs is clearly related to the lower wave energy, as all other conditions (water temperature, salinity, water chemistry, etc.) are presumably identical. The bored clasts in the protected coves strongly resemble those at St-Jacques in Barrême (personal observation), whereas those in the exposed areas resemble those in Dévoluy (personal observation). This modern analogue suggests that Dévoluy was subjected to higher wave energy than St-Jacques, which may reflect small-scale differences in the paleogeography of the Nummulitic coastline.

Lithofacies LN-2: Fossiliferous carbonate conglomerate with rounded clasts

Lithofacies LN-2 of the Nummulitic Conglomerate Member is a matrix-supported carbonate conglomerate composed of Senonian clasts (grey limestone, brown, chertified limestone, and brown and grey chert), fossiliferous carbonate sand, and some interstitial micrite.

The clasts range in size from less than 1 mm to 5 cm in diameter. The light brown chert and chertified limestone clasts are significantly more common than limestone clasts in sizes from 1 mm to 3 cm. These clasts are well-rounded in some beds and subangular in others. Most clasts in a given bed have the same degree of rounding. Limestone is more common than chert in the size range from 3 to 5 cm. Clasts are subangular to extremely well-rounded and are subspherical in this size range (Fig. 3.5). Subangular clasts are much more common than subrounded to well-rounded ones. Overall, the clasts from 1 mm to 3 cm are better rounded than the clasts from 3 to 5 cm. The size ranges of the clasts varies from bed to bed. It is also possible to have several distinct clast populations within a given bed, in which case the most common populations are less than 1 cm and greater than 2 cm. These two clast populations are not arranged in systematic layers of coarser- and finer-grained clasts within the bed; rather, the clasts are poorly sorted throughout the bed.

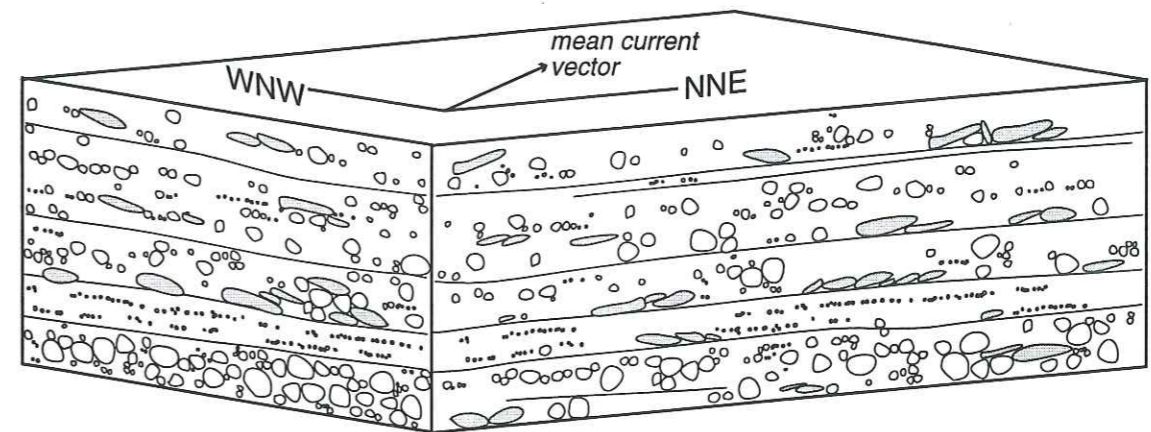


Fig. 3.6. Schematic block diagram of crudely imbricated clasts (grey) in lithofacies LN-2 of the Nummulitic Conglomerate Member of the Dévoluy Nummulitic Limestone Formation. The mean current vector based on the orthogonal outcrops (indicated) was to the NNW here. The sketch is based on field observations near the Superdévoluy ski resort in south-central Dévoluy (locality b, Fig. 3.1).

The carbonate sand is medium-grained, moderately-rounded, and well-sorted. Other elements include abundant *Nummulites*, red algae, *Dasycladaceae*, subrounded grains of sparry calcite, carbonate rock fragments, and micrite. The fossils are usually more complete than in lithofacies LN-1.

Beds in lithofacies LN-2 are 0.5 - 300 cm thick. Thinner beds do not have well-developed internal structures, but thicker beds often have crudely developed low-angle planar stratification (Fig. 3.3) and larger, flat pebbles, when present, show crude imbrication (Fig. 3.6). Fining-up sequences occur, but are not common. When developed, such sequences are usually the result of increasing amounts of carbonate sand, rather than decreasing clast size.

Lower bounding surfaces of beds are sharp, with little evidence of erosional incision into underlying layers. Upper bounding surfaces are sharp to gradational. The geometries of the beds are sheet-like to lenticular for thin beds and tabular to broadly lenticular for thicker beds. Thinner beds sometimes fill small depressions and are discontinuous along the exposure profile.

The low-angle planar stratification within beds is slightly discordant to subparallel with the upper and lower bounding surfaces (Fig. 3.3). Measured divergences are never more than 5°, so no current directions were determined from the planar surfaces. However, the imbricated clasts show a preferred flow direction. In the vicinity of Superdévoluy in south central Dévoluy, imbricated clasts are exposed in a set of semi-orthogonal cliff faces trending 030 - 210° and 100 - 280° (Fig. 3.6). Approximately 85% of the imbricated clasts in beds on the NNE-SSW face show flow to the NNE; the remaining 15% show flow to the SSW (Fig. 3.6). In the WNW-ESE oriented face, 100% of clasts show flow to the WNW (Fig. 3.6). These orientations indicate a primary flow to the NNW and a secondary flow to the WSW in this locality (Fig. 3.6). Nearby, at the type section of the Dévoluy Nummulitic Limestone Formation, imbricated pebbles indicate a general northward flow.

Lithofacies LN-2, the diagnostic lithofacies of the Nummulitic Conglomerate Member, is interpreted as having been deposited in a shallow marine, high energy shoreface setting. This interpretation is based on: (1) the faunal assemblage preserved in the carbonate sand, which indicates a

marine environment; (2) the bimodal sorting of the beds and bidirectional paleocurrents, which indicates a swash-backwash type of environment; (3) the very well-rounded nature of many of the clasts, in combination with the large size of many of the clasts, which indicate that the clasts were probably not transported a significant distance, but were subject only to reworking within the depositional environment (in comparison, the clasts of the Pierroux Conglomerate Formation do not display the same degree of rounding); (4) the low-angle planar stratification, which is considered diagnostic of shoreface deposits (Inden & Moore, 1983); and (5) the fact that the clasts are not bored, which indicates a high-energy, wave-dominated setting (see pp. 36-37). The lithofacies is interpreted as a shallow marine, and not a beach deposit, because there is no evidence of subaerial exposure (e.g., characteristic cement textures). Similar lithofacies are common in modern shoreface settings (Inden & Moore, 1983).

Lithofacies LN-3: Fossiliferous wackestone to packstone

Lithofacies LN-3 of the Nummulitic Conglomerate Member is a grey carbonate lime wackestone to packstone containing scattered ($\geq 5\%$), angular to subrounded (most commonly subangular), brown or dark grey chert clasts 1 to 3 mm in size. The matrix is a fine- to medium-grained carbonate sand composed of diverse fossil fragments (nummulitids, other foraminifera, and algae), limestone grains, and interstitial micrite. The limestone grains are micrites and fossiliferous wackestones and packstones, apparently eroded from the Senonian bedrock.

Beds are 2 to 300 cm thick. They are structureless and display no grain size trends. The clasts are scattered randomly within the matrix.

Lower bounding surfaces are sharp to abruptly gradational. There is no evidence of erosion into underlying layers. Upper surfaces are sharp, and may be slightly undular or even eroded when overlain by lithofacies LN-1 or LN-2. The beds are tabular to sheet-like when continuous, and are lenticular with convex-up upper surfaces when the upper surface is eroded.

This lithofacies is interpreted as being a lower energy equivalent of Lithofacies LN-2. It may have been deposited in slightly deeper or calmer waters, thereby decreasing the capacity of the system to (1) transport large volumes of clasts, (2) transport clasts larger than 3mm, and (3) significantly round the clasts.

Lithofacies LN-4: Fossiliferous calcarenite

This lithofacies is a well-sorted, medium-grained, grey lime wackestone, packstone, or grainstone. The limestones are composed of subrounded carbonate lithic fragments, diverse fossil fragments, including abundant nummulitids, red algae, and *Dasycladaceae*, and interstitial micrite. The carbonate grains are micrites and fossiliferous wackestones and packstones.

Beds are 1 to 100cm thick. They do not display internal structures, nor do they exhibit grain size trends.

Lower bounding surfaces are sharp and slightly undular, with no evidence of erosion into un-

derlying layers. Upper surfaces are also sharp to undular. The beds are tabular to sheet-like.

Lithofacies LN-4 is interpreted as being a relatively lower energy and slightly deeper water equivalent of lithofacies LN-3. The *Nummulites* and other marine fossils indicate a shallow marine setting. However, the lack of pebble-sized clasts indicates relatively calm water conditions, which is interpreted as being a depth-related factor. The well-sorted nature and occasional lack of mud in this lithofacies indicate that it was partially winnowed, either during or following deposition.

LITHOFACIES ASSOCIATIONS

Three lithofacies associations have been determined for the Nummulitic Conglomerate Member. These are interbedded lithofacies LN-1 and LN-2 (lithofacies association LN-I), interbedded lithofacies LN-2, LN-3, and LN-4 (lithofacies association LN-II), and interbedded lithofacies LN-3 and LN-4 (lithofacies association LN-III) (see Table 3-I for a summary of these lithofacies).

Lithofacies association LN-I: Interbedded lithofacies LN-1 and LN-2

This association occurs only in northeastern Dévoluy, where the Nummulitic Conglomerate Member is 90 - 95 m thick. Here, the two lithofacies are interbedded in the hanging wall of a syndepositional normal fault, the Lucles Fault (see section 3.1.2). Lithofacies LN-1, which occurs in beds up to 30 m thick, makes up approximately 75% of the section, while lithofacies LN-2, which occurs in beds up to 2 m thick, makes up the remainder of the section. The typical association is of a bed or beds of lithofacies LN-1 to be overlain by a bed of lithofacies LN-2.

Lithofacies LN-1 contains large oblong Senonian blocks that are elongate parallel to bedding. These blocks may reach up to 50 m in length, and are generally a few meters to 10s of meters thick (Figs. 3.4, 3.7). The size of these blocks and their proximity to the Lucles Fault suggests that they were shed from the fault scarp (Figs. 3.8a, b).

Several of the larger blocks are colonized on their upper surfaces by populations of red algae. Smaller clasts surrounding these large blocks are not encrusted, suggesting that the colonies preferred the slightly shallower water depths or higher wave energies afforded on the tops of these blocks (Crampton, 1992). Such algal colonies on boulders and cobbles have been identified as forming in water depths from 0 - 70 m (Bosence, 1983).

Beds of lithofacies LN-2 that occur above the beds of lithofacies LN-1 do not contain the large blocks, and their higher degree of rounding may reflect reworking of the clasts of the underlying bed in a shallow marine environment (Fig. 3.8c).

Therefore, lithofacies association LN-I appears to represent an interplay between input of coarse clastics, possibly as debris flows, (lithofacies LN-1) and reworking of these deposits in a high-energy, shallow marine environment (lithofacies LN-2).

Lithofacies association LN-II: Interbedded lithofacies LN-2, LN-3, and LN-4

Lithofacies LN-2 (ca. 50% of the association), LN-3 (ca. 30%), and LN-4 (ca. 20%) are regularly

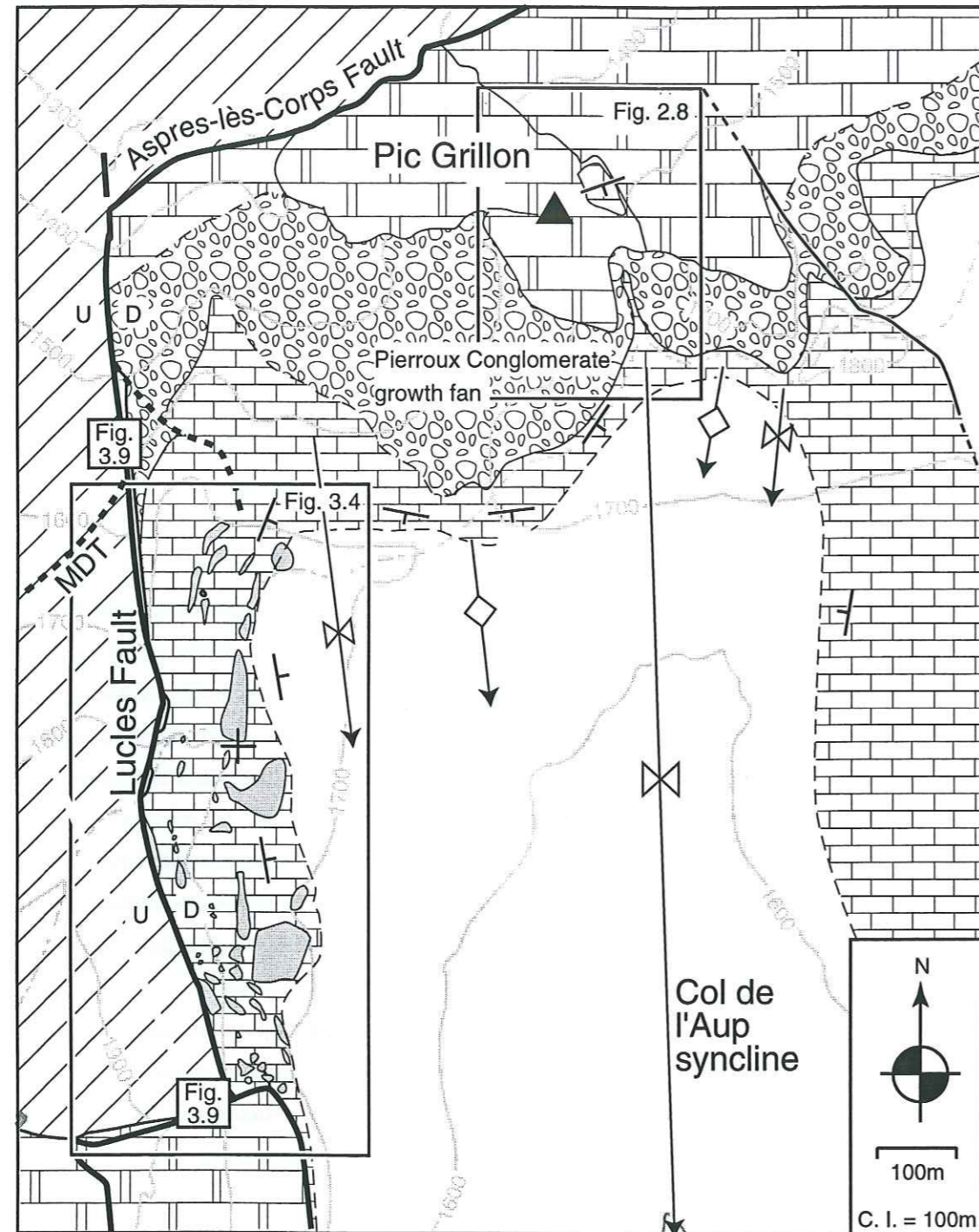


Fig. 3.7. Detailed map of northeastern Dévoluy showing elongate Senonian blocks in the Lower Nummulitic Limestone. These blocks occur at the bases of beds of lithofacies LN-1 (Fig. 3.8) and are occasionally encrusted by red algal colonies. Location of map indicated in Fig. 3.1. Locations of Figs. 2.8 and 3.4 indicated. Patterns as in Fig. 3.1, except Senonian blocks are shown in grey.

interbedded in most outcrops of the Nummulitic Conglomerate Member (e.g., Figs. 3.2, 3.3). This lithofacies association (LN-II) typifies the Nummulitic Conglomerate Member. There is no predictable vertical arrangement of the three lithofacies within the association. Rather, the three lithofacies

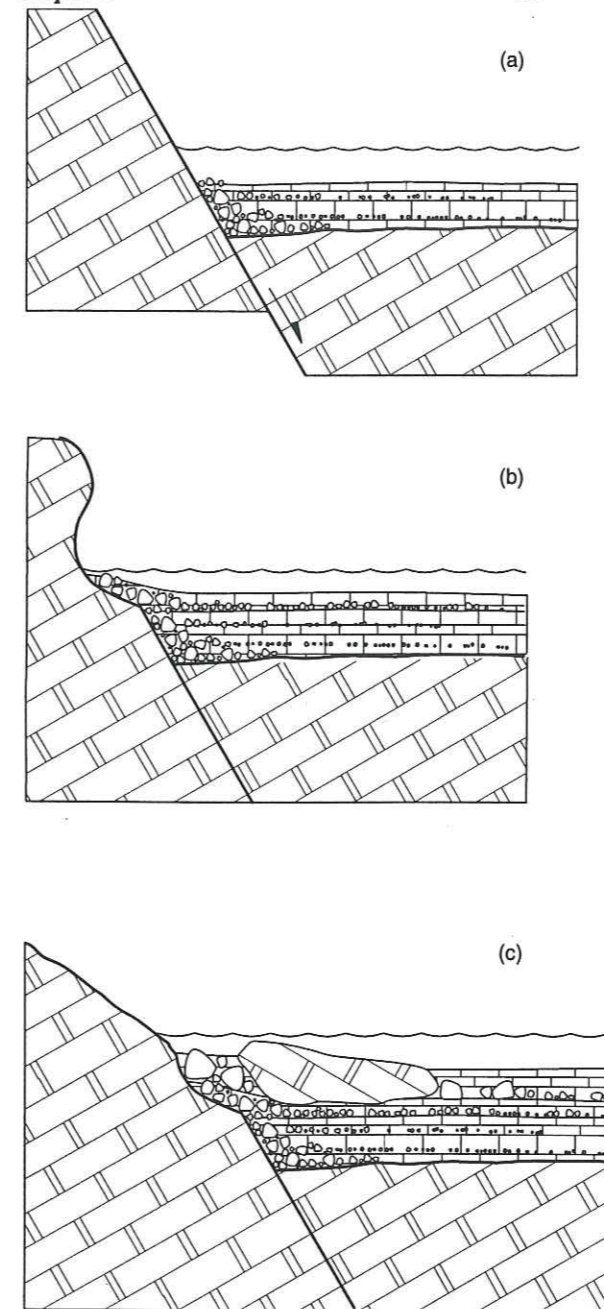


Fig. 3.8. Interpretive drawing of the deposition of the large Senonian blocks in the Nummulitic Conglomerate Member in northeastern Dévoluy. (a) Movement on the Lucles Fault created a scarp. Wave action eroded the scarp and reworked the pebbles (lithofacies LN-2). (b) Continued wave activity created an overhang. (c) The overhang collapsed, depositing a large block and associated debris (lithofacies LN-1). Continued wave activity caused the process to repeat (lithofacies association LN-I) until the scarp was completely eroded. Patterns as in Fig. 3.1, except that pebble-sized clasts are shown in the Nummulitic Conglomerate Member.

occur randomly throughout the association.

As discussed above, the high degree of rounding, the bimodal sorting, and the bidirectional paleocurrents of lithofacies LN-2 are best interpreted as representing a swash-backwash environment above wave base, where the clasts were probably subjected to repeated episodes of surf reworking. Larger and smaller clasts indicate that the wave energy of the system fluctuated regularly. The increase in rounding with decreasing grain size probably indicates that the smaller clasts were reworked for longer periods of time.

In this interpretation, the occurrences of the pebble-poor beds of lithofacies LN-3 and the pebble-free beds of lithofacies LN-4 represent either temporary deepening conditions at the shoreface, and resulting calmer water conditions, or lateral shifting of clast input.

This lithofacies association is interpreted as the composite deposits of a shallow marine and/or shoreface depositional system.

Lithofacies association LN-III: Interbedded lithofacies LN-3 and LN-4

Lithofacies association LN-III is composed of stacked beds of lithofacies LN-3 and LN-4. This association commonly occurs in the uppermost Nummulitic Conglomerate Member. As with lithofacies association LN-II, there is no predictable vertical arrangement of the two facies. Generally, though, a bed of lithofacies LN-3 (20 - 40% of the association) will occur

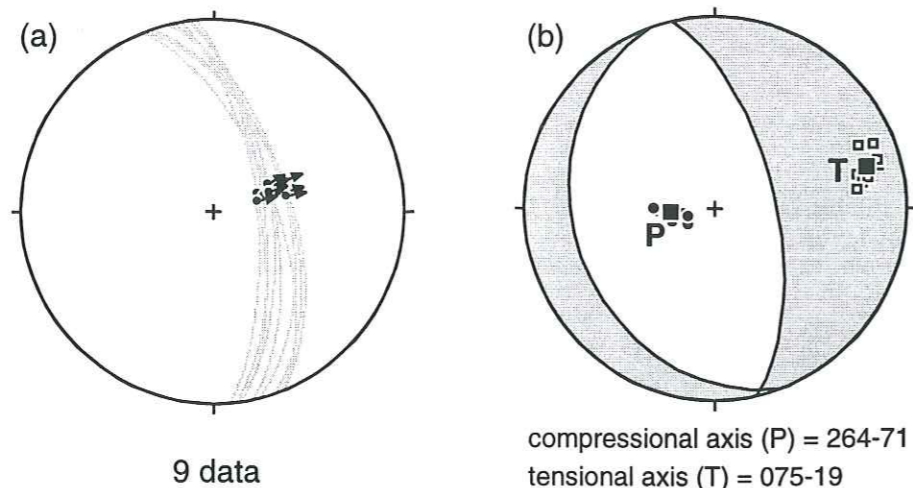


Fig. 3.9. Lower hemisphere, equal area projections of (a) fault and slickenfiber data associated with the Lucles Fault, and (b) fault plane solution (linked Bingham axis) of the data presented in (a). Locations of data indicated in Fig. 3.7.

between sets of 2 to 5 beds of lithofacies LN-4 (60 - 80% of the association).

The dominance of lithofacies LN-4 in this lithofacies association, and the total absence of conglomeratic lithofacies (LN-1 or LN-2) indicates that this association represents lower energy conditions such as would be present in a calmer water setting. Because the Dévoluy Nummulitic Limestone Formation is overall a transgressive deposit representing deepening marine conditions (e.g., Pairis, 1988), it seems reasonable to interpret the calmer water conditions represented by lithofacies association LN-III as being caused by relative flooding of a shallow shelf, such that the lithofacies association was deposited in slightly deeper water.

3.1.2. Syndepositional extensional faulting and associated topography

There is evidence that extensional faults were active in northern Dévoluy during deposition of the Nummulitic Conglomerate Member. The faults are the Lucles Fault, on the eastern and north-eastern side of Mt. St-Gicon (Fig. 3.7), and the Pierre Baisse Fault, on the southwestern side of Mt. St-Gicon (Fig. 3.10).

The Lucles Fault

The Lucles Fault (Fig. 3.7; Gidon & Pairis, 1976) has an average strike and dip of 349-64E (Fig. 3.9a). Stratigraphic offset of the Senonian limestone indicates that down-to-the-east displacement of at least 500m occurred at the northern end of the fault (Figs. 10.3a, b). The offset decreases to the south and the fault tips out at the southern end of Mt. St-Gicon (Fig. 3.1; Gidon & Pairis, 1976). Down-dip grooves several centimeters deep and up to 1 m long show pure dip-slip displacement to the east and give a kinematic solution with a tensional axis of 19-075 (Fig. 3.9b).

In the foot wall of the Lucles Fault, on the top of Mt. St-Gicon, lithofacies LN-3 and LN-4 (lithofacies association LN-III) of the Nummulitic Conglomerate Member occur in outcrops < 5 m

thick (shown schematically in Fig. 10.3b). These deposits are limited to the northeast by two NW-SE trending normal faults (Fig. 3.1), each with less than 5 m of down-to-the-southwest throw (Gidon & Pairis, 1976).

In contrast, next to the fault in its hanging wall, the Nummulitic Conglomerate Member is composed of interbedded layers of Lithofacies LN-1 and LN-2 (lithofacies association LN-I) in a 100 m thick succession (Fig. 10.3b). The large Senonian blocks that occur at this locality (Figs. 3.4, 3.7; see also discussion of lithofacies association LN-I above) are interpreted as slide blocks (Gidon & Pairis, 1976) that were calved from the fault scarp during deposition of the Nummulitic Conglomerate Member (Fig. 3.8).

Less than a kilometer to the east in the hanging wall, the member is only approximately 10m thick (Fig. 10.3b), and is characterized by lithofacies association LN-II.

These observations lead to the following conclusions: (1) the relative thicknesses of the Nummulitic Conglomerate Member in the foot and hanging walls of the Lucles Fault indicates that the foot wall was a topographic high during deposition of the Nummulitic Conglomerate Member (Fig. 10.3b). (2) The presence of the Senonian slide blocks immediately adjacent to the fault in its hanging wall implies that the footwall block was eroded during deposition. Finally, (3) the rapid thinning of the member away from the fault in the hanging wall suggests that it may have acted as a syndepositional growth fault (Fabre *et al.*, 1985a).

The Pierre Baisse Fault

The Pierre Baisse Fault (Gidon & Pairis, 1976) trends NW-SE and dips steeply to the SW. It crops out for approximately 500 m along the SW corner of Mt. St-Gicon (Figs. 3.10a, b). Maximum throw on the fault is approximately 100 m and occurred at its northwestern end. Vertical displacement on the fault decreases to the southeast (Fig. 3.10b).

At its northwestern extremity, the fault confines the Dévoluy Nummulitic Limestone Formation in its southern (hanging) wall. Limited outcrops up to 20 m thick of the Nummulitic Conglomerate Member abut the fault scarp at this locality (Figs. 3.10a, b). Along strike to the southeast, a bed of lithofacies LN-2 of the Nummulitic Conglomerate Member seals the fault (Gidon & Pairis, their Fig. 6).

The beds of lithofacies LN-2 that seal the Pierre Baisse Fault grade into beds of Lithofacies LN-3 and LN-4 less than 5 m thick towards the top of Mt. St-Gicon (Fig. 3.1). This occurrence of lithofacies association LN-III was previously mentioned with regard to the Lucles Fault. The thinness of these beds relative to those in the hanging walls of the Pierre Baisse and Lucles faults suggests that Mt. St-Gicon was a fault-bounded topographic high during deposition of the Nummulitic Conglomerate Member.

Four hundred meters southeast of the location where the fault is sealed, there are syndepositional microfaults in the Nummulitic Conglomerate Member which Gidon & Pairis (1976) interpreted as the lateral continuation, as micro-splays, of the Pierre Baisse Fault. These microfaults are sealed by

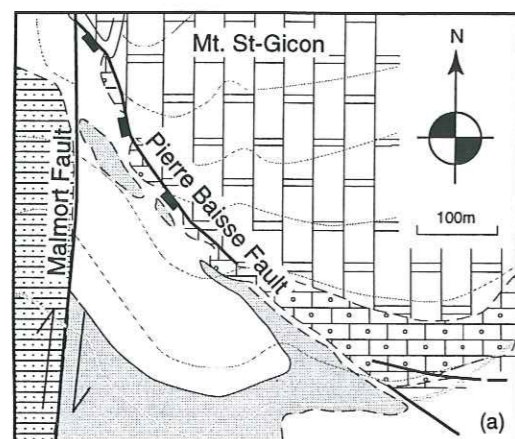
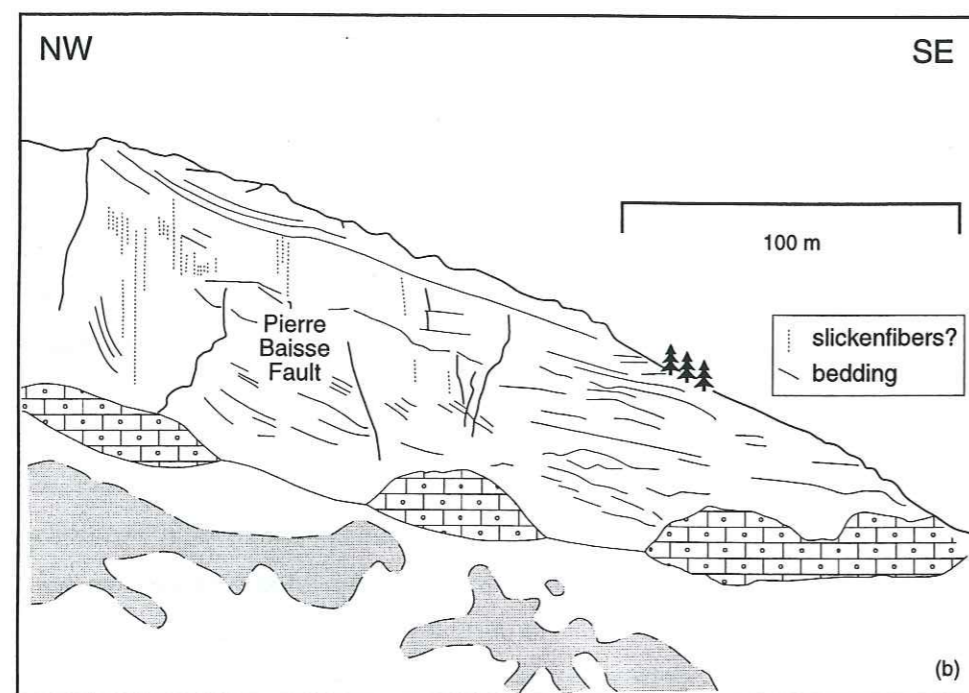


Fig. 3.10. The Pierre Baisse Fault, north central Dévoluy. (a) Map of the fault, located in Fig. 3.1. (b) Field sketch of the fault showing localized deposits of the Nummulitic Conglomerate Member adjacent to the fault. Patterns as in Fig. 3.1, except that white areas indicate no outcrop, and grey indicates the Queyras Marlstone Formation.



deposits of Lithofacies LN-2 (Gidon & Pairis, 1976, their Fig. 5). This along-strike relationship indicates that downthrow to the southwest on the Pierre Baisse Fault occurred during deposition of the Dévoluy Nummulitic Limestone Formation (Gidon & Pairis, 1976).

The syndepositional activity on the Lucles and Pierre Baisse faults in northern Dévoluy documents extension in the late Eocene. The localization of these faults immediately south of the Aspres-les-Corps Fault is probably related to strike-slip movement on the Aspres-les-Corps Fault (Meckel *et al.*, 1996) and flexural loading of the crust. Because the orientations of the syn-Nummulitic faults are similar to those of the pre- or syn-Pierroux Conglomerate Formation faults, it is probable that normal faulting in northern Dévoluy was more or less continuous during deposition of the Pierroux Conglomerate Formation and the Nummulitic Conglomerate Member.

3.1.3. Depositional setting and provenance

The sedimentary characteristics of the Nummulitic Conglomerate Member are consistent with a shallow marine environment with variable energy, such as the upper shoreface, the foreshore, or

the flanks of shallow tidal bars (cf. McCubbin, 1982; Inden & Moore, 1983). These sediments were deposited in an environment characterized by syndepositional topography and tectonic activity. Fabre & Pairis (1984) suggest that the Dévoluy Nummulitic Limestone Formation was deposited in an internal "infralittoral" setting, based on the presence of encrusting algae and *Nummulites garnieri*, and the rarity of *Nummulites fabianii*.

This interpretation is supported by the fact that lithofacies association LN-III culminates an overall upsection transition from conglomerate-dominated deposition in the lower part of the Nummulitic Conglomerate Member (lithofacies association LN-I) to slightly deeper water, non-conglomeratic deposition in the upper part of the member. Lithofacies association LN-II occupies the intermediate position in this transition.

A spectacular modern analogue for the Nummulitic Conglomerate, however without syndepositional faults, exists at La Tilleul on the coast of Normandy in northwestern France. La Tilleul is a modern high-energy shoreface. Sediments there include clast-supported conglomerates deposited as beach fans, well-rounded, matrix-supported conglomerates with non-bored clasts deposited in a beach and shallow shoreface setting, and sands containing few or no clasts (personal observation). The locality is especially analogous because the sediments are carbonate- and chert-dominated and occur at the base of chalk cliffs. These cliffs provide sediment and confine deposition in the same way that the Lucles and Pierre Baisse fault scarps may have done.

3.2. The Nummulitic Calcarenite Member

The Nummulitic Calcarenite Member is present everywhere in the basin except in southwesternmost Dévoluy. It is always transitional with the Nummulitic Conglomerate Member below it. The lower boundary is taken at the upper surface of the last bed of the Nummulitic Conglomerate Member with $\geq 5\%$ pebble-sized clasts (lithofacies LN-3). The member is considered to be transitional with the Queyras Marlstone Formation above it, although the boundary has not been observed in the field. The upper boundary is taken at the top of the last bed containing visible *Nummulites*. In northwestern Dévoluy, where the member is overlain by the St. Disdier Arenite Formation, the boundary is an unconformity (Fig. 3.1).

The member is 1 - 15 m thick where present. The median grain size of the Nummulitic Calcarenite Member decreases upsection from medium-grained to fine-grained calcareous sand. The member is distinguished from the Nummulitic Conglomerate Member by (1) a lack of pebble-sized Senonian limestone and chert clasts and (2) a visible increase in the amount of *Nummulites* present (Fig. 3.2). It is distinguished from the Queyras Marlstone Formation by (1) its relatively coarser grain size, (2) its lack of *Zoophycos* ichnofacies trace fossils, and (3) its tendency to weather a dark grey rather than a light grey to yellow color, as with the Queyras Marlstone Formation.

The Nummulitic Calcarenite Member has two constituent lithofacies (Table 3-I; Figs. 3.11a, b): fossiliferous grainstone (lithofacies UN-1); and lime mudstone (lithofacies UN-2).

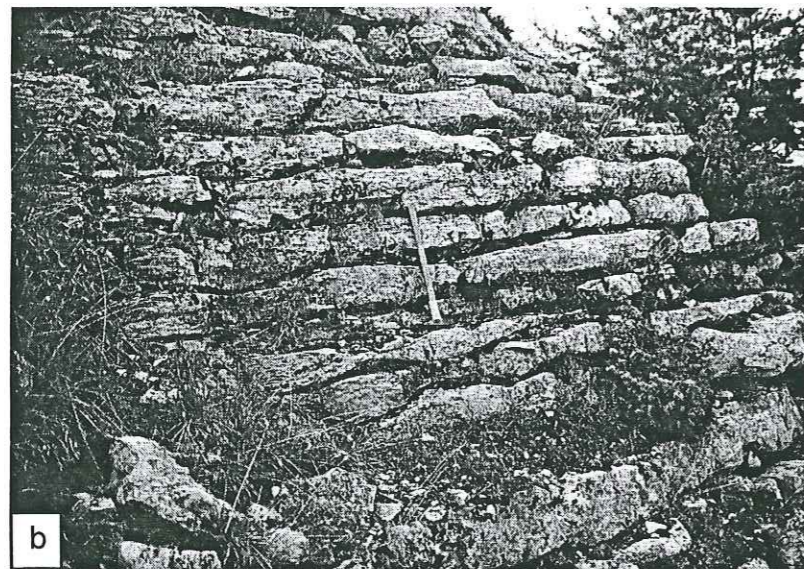
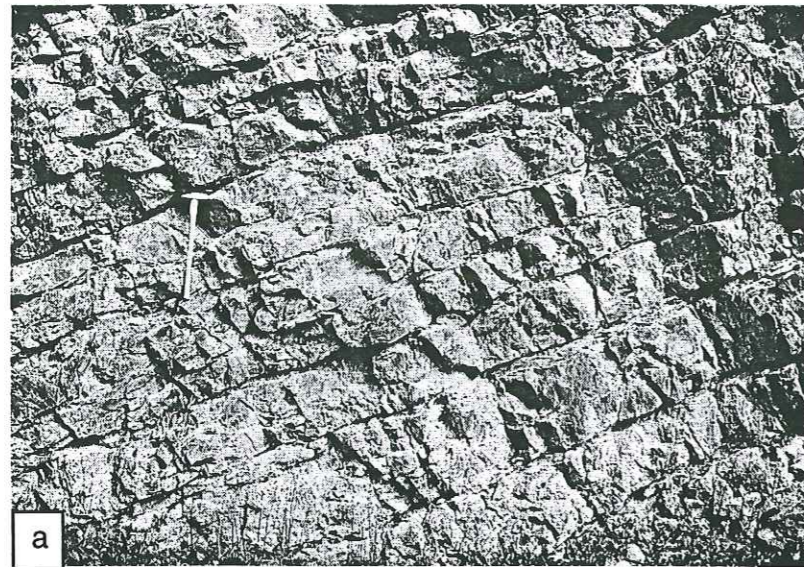


Fig. 3.11. (a, b) Photographs of interbedded facies UN-1 and UN-2. The photographs were taken in southern Dévoluy, south of Superdévoluy.

3.2.1. Lithofacies analysis and stratigraphy

Lithofacies UN-1: Fossiliferous grainstone

Lithofacies UN-1 is a well-sorted, well-bedded grainstone with well-rounded to subangular grains. It is medium- to fine-grained and grey in color, and resembles lithofacies LN-4 in many aspects.

Beds of this lithofacies have variable thickness, from 2 - 300 cm (Fig. 3.2). The average thickness is 10 - 75 cm (Figs. 3.11a, b). The beds are internally structureless and typically have very gently undular upper and lower surfaces (Figs. 3.11a, b). Beds of lithofacies UN-1 have tabular external geometries (Figs. 3.11a, b) and are continuous over the length of a given outcrop.

In the field, occasional *Nummulites* and single bivalve shells are visible in beds of this lithofacies (e.g., Fig. 3.2). There is also infrequent evidence of burrowing by unidentified ichnofauna. The burrows are usually identified as darker or lighter elongate traces oriented subperpendicular to bedding. They are 0.5-1cm in width and a few centimeters long, and may be infilled with coarser

sediment or *Nummulites*.

This lithofacies is interpreted as representing sedimentation on a moderately deep (20-40m), relatively calm carbonate ramp (cf. Enos, 1983; Wilson & Jordan, 1983). Coarser-grained fossil fragments and carbonate debris are transported by bottom currents or storm currents in such settings (Enos, 1983). There are no distinctive sedimentary structures or bathymetrically significant fauna to aid in a more conclusive interpretation.

Lithofacies UN-2: Lime mudstone

The second lithofacies of the Nummulitic Calcarenite Member (lithofacies UN-2) is a marly lime mudstone. It is finer-grained and darker grey than lithofacies UN-1. Beds of lithofacies UN-2 are typically less than 1 cm thick and occur between beds of lithofacies UN-1 (Figs. 3.11a, b).

Occasional grains, usually fossil and/or carbonate lithic fragments, are uniformly sized and moderately-rounded. These are supported by a mud-sized to micritic matrix.

Beds of Lithofacies UN-2 usually have mm-thick planar laminations. Upper and lower bounding surfaces are subplanar, with no evidence of erosion into underlying beds or by overlying beds. The beds are sheetlike, and may pinch out locally along strike (Figs. 3.11a, b).

This lithofacies is interpreted as deposits of weaker ramp currents, or alternately, as non-event "background" settling of finer-grained sediment in a moderately deep-water setting (e.g., Enos, 1983; Wilson & Jordan, 1983).

LITHOFACIES ASSOCIATION

Lithofacies UN-1 (> 90% of the association) is interbedded in a regular manner with lithofacies UN-2 (< 10% of the association) (Figs. 3.11a, b). This interbedded occurrence of the two lithofacies comprises lithofacies association UN-I. The most common vertical arrangement of the lithofacies is for a bed of lithofacies UN-2 to occur at the top of a bed or several stacked beds of Lithofacies UN-1 (Figs. 3.11a, b).

The interbedding is interpreted as representing periods of fluctuating energy on the carbonate shelf. It is probable that this lithofacies association represents a deeper water equivalent of lithofacies association LN-III in association with continued transgression. The lack of significant amounts of mm- to cm-scale chert clasts reflects the calmer water conditions.

3.2.2. Depositional setting

The Nummulitic Calcarenite Member is interpreted to have been deposited in a medium-energy ramp-type shelf environment (cf. Wilson & Jordan, 1983; Tucker & Wright, 1988). Currents sweeping over the ramp would occasionally bring in coarser sediment (Lithofacies UN-1), and the deposits of these currents dominates the sedimentary record of the member. The thinner beds of Lithofacies UN-2 represent periods of relative calm on the shelf.

CHAPTER 4

The Queyras Marlstone Formation

The Queyras Marlstone Formation is the uppermost formation of the Queyras Group. The formation has previously been called the "marno-calcaires priaboniens" (BRGM, 1980d), the "marnes nummulitiques" (Pairis *et al.*, 1983), the "calcaires intermediares" (Fabre *et al.*, 1986), the "argillites noires/marnes à foraminifères/marno-calcaires priaboniens" (Pairis, 1988, p. 236), and the "marnes à foraminifères et calcaires intermediares" (Pairis, 1988, p. 241) (Table 1.I). This formation can be lithologically correlated with the Globigerina Marls and Tertiary "Marnes Bleues" elsewhere in south-eastern France.

The lower boundary of this formation is considered to be gradational with the Dévoluy Nummulitic Limestone Formation, and is taken in the field at the top of the last bed containing visible *Nummulites*. The formation grades upsection into the siliciclastic Souloise Greywacke Formation through a 25-50m thick, black mud- to siltstone. The upper surface of the Queyras Marlstone Formation is taken at the bottom of the first siliciclastic sandstone bed above this mudstone unit.

The formation is dated as late Priabonian (planktonic foraminifera biochronozone P16-17, nannofossil biochronozone NP 19-20) by foraminiferal and nannofossil assemblages. The foraminiferal assemblages include the benthic foraminiferal genera *Lenticulina*, *Nodosaria*, *Baggina*, *Cibicides*, *Heterolepa*, *Rotalia*, and *Pararotalia* and the planktonic foraminifers *Globigerina angiporoides*, *G. eoacena*, *G. senilis*, and *G. tripartita*, and *Globigerinita dissimilis*, *G. martini scandretti*, and *G. pera*, (BRGM, 1980; Pairis *et al.*, 1983, 1984a; Fabre *et al.*, 1986; Pairis, 1988). The nannofossil assemblage contains *Discoaster barbadiensis*, *Discoaster saipanensis*, and *Isthmolithus recurvus* (Fabre *et al.*, 1986).

The Queyras Marlstone Formation is predominantly present in the hangingwall of the Median Dévoluy Thrust, but also occurs in its footwall in northern Dévoluy (Fig. 4.1). The type section of the formation (Fig. 4.2) is located at the Ravine de Charbournasse, approximately 2km west of the Montagne de Faraud in eastern Dévoluy. The formation is named after its most abundant occurrence, in the valley of the Queyras River in northeastern Dévoluy.

The Queyras Marlstone Formation consists of silty to very fine-grained marly limestones. The rocks weather a light grey or sulfurous yellow color, which distinguishes the formation from the underlying Nummulitic Calcarene Member of the Dévoluy Nummulitic Limestone Formation. Fresh surfaces are light grey. The formation is also distinguished by the abundant occurrence of trace fossils of the *Zoophycos* ichnofacies.

The formation is approximately 94 m thick in the type section (Fig. 4.2). In another measured section, southeast of the village of Haut Gicon, the formation is 192 m thick (Fig. 4.3). Although the type section is stratigraphically less complete than the GR 94 section (Fig. 4.1), it is considered to be more representative of the formation as it occurs throughout the Dévoluy Basin (e.g., Fig. 4.4). The

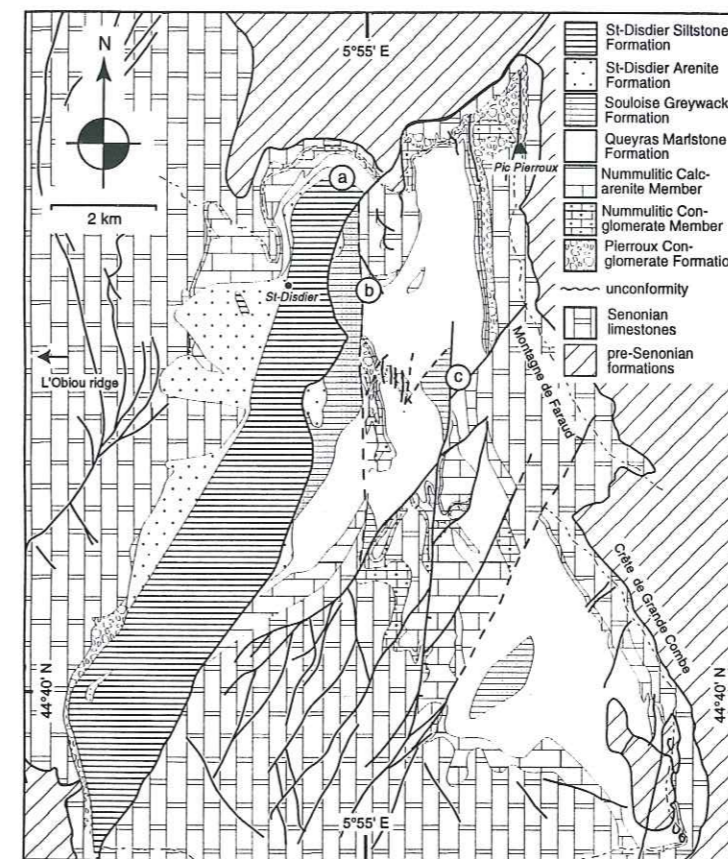


Fig. 4.1. Geologic map of Dévoluy, indicating locations of measured sections. a = Tête de la Tune section; b = GR94 section; c = Ravine de Charbournasse section (type section).

Lithofacies	Description	Interpretation
QM-1	Sparsely fossiliferous silty wackestone	hemipelagic; low-energy; deep shelf/upper continental slope
QM-2	Sparsely fossiliferous, very fine grained wackestone	intra-/extrabasinal sediment plumes deposited on deep shelf/upper slope
QM-3	Very fine- to medium-grained lenticular sandstone	sandy turbidites
QM-4	Carbonaceous mud- to siltstone	increased terrigenous influx on hemipelagic slope
Lithofacies association		
QM-I	Interbedded QM-1 and QM-2, with occasional beds of QM-3	hemipelagic shelf/slope with periodic fluxes in offshore currents

TABLE 4-I. Summary of lithofacies and lithofacies associations of the Queyras Marlstone Formation.

formation is poorly exposed elsewhere in the basin, so lateral variations in thickness can only be estimated. It is dominated by alternating beds of sparsely fossiliferous, silty lime wackestone (lithofacies QM-1) and very fine-grained, sparsely fossiliferous marly limestones (lithofacies QM-2). Very fine- to medium-grained lithic wacke beds (lithofacies QM-3) occur sporadically throughout the section. The fourth lithofacies of the Queyras Marlstone Formation, the carbonaceous mud- to siltstone at the top of the formation (lithofacies QM-4) occurs in the measured section on GR 94 (Fig. 4.3) and in southeastern Dévoluy. These facies are summarized in Table 4-I.

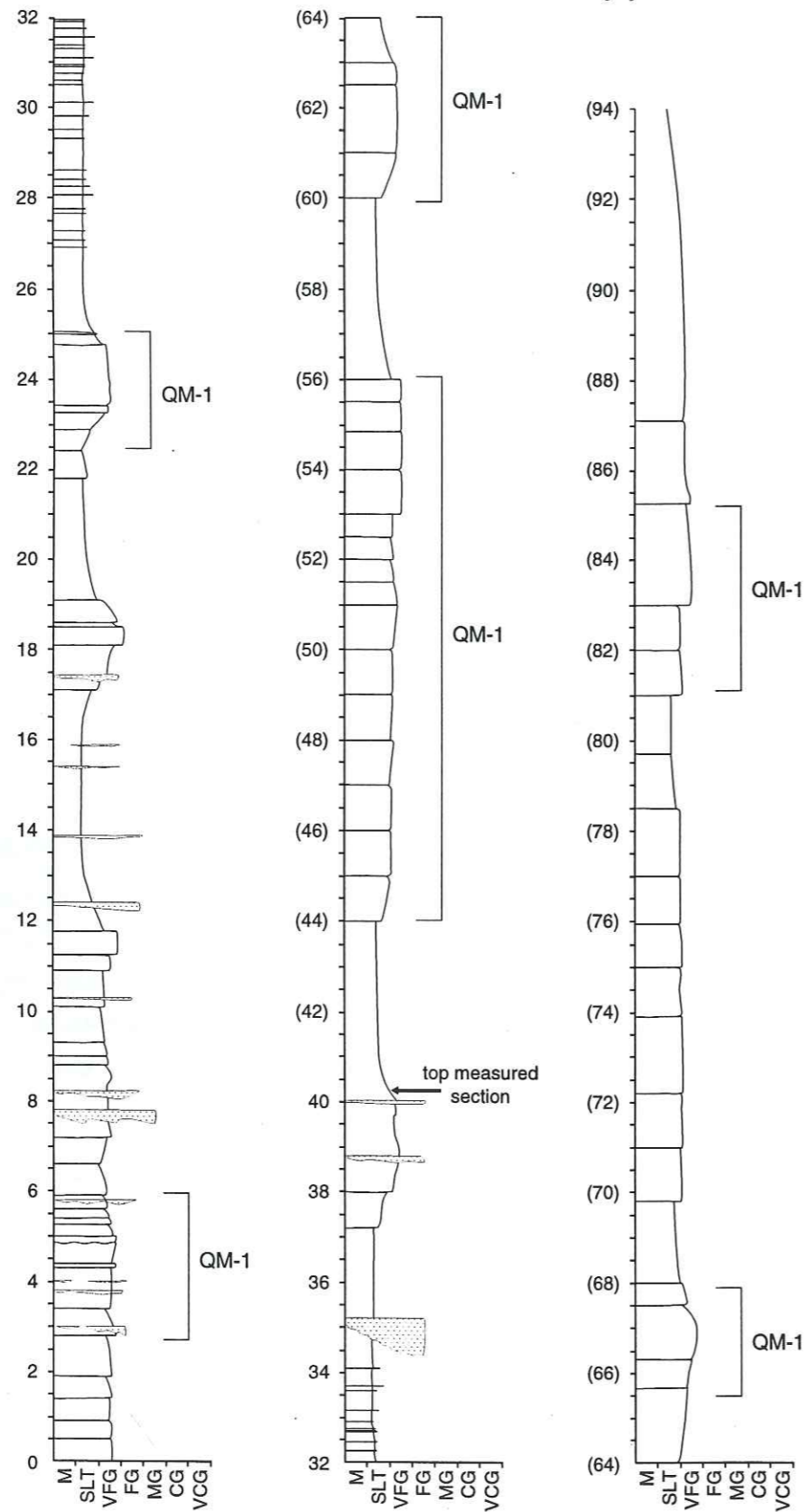


Fig. 4.2. Type section of the Queyras Marlstone Formation (scale in meters) at the Ravine de Charbournasse, showing lithofacies QM-1, QM-2, and QM-3. Section located in Fig. 4.1. Top part of the section (40 to approximately 94 m) was poorly exposed where accessible. Therefore, this part of the section is a composite of observations made in the poor exposures and through binoculars. Indicated intervals are beds of lithofacies QM-1; other unornamented intervals are lithofacies QM-2; stippled beds are lithofacies QM-3.

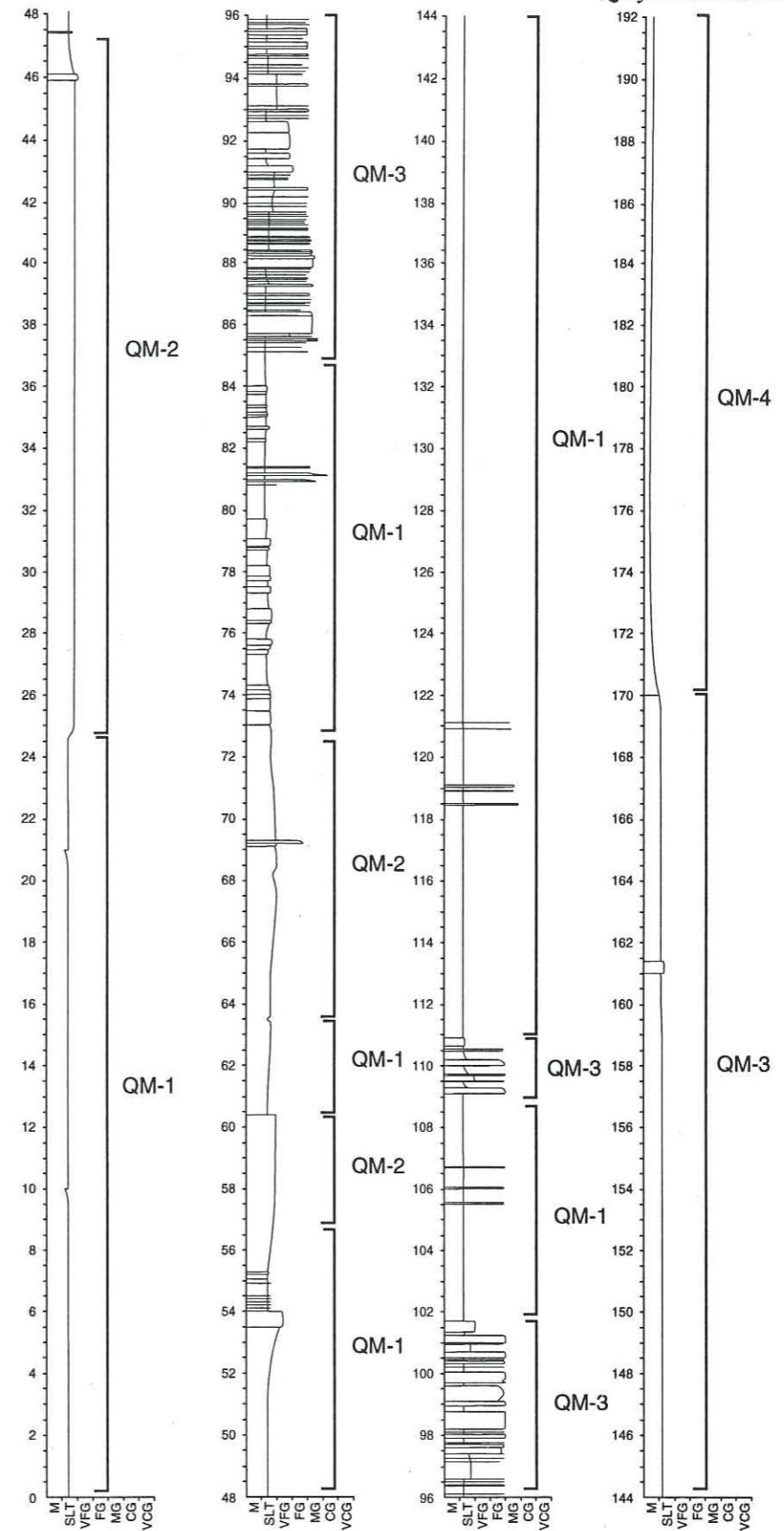


Fig. 4.3. Measured section of the Queyras Marlstone Formation on GR94 southeast of the village of Haut Gicon (scale in meters). Section located in Fig. 4.1. The section is highly cleaved, so lithofacies are not easily distinguished, except for lithofacies QM-3 and QM-4. Probable intervals of lithofacies QM-1 and QM-2 are indicated.



Fig. 4.4. View looking N at the Queyras Marlstone Formation at Sagne Brune, SE Dévoluy. This outcrop is similar in appearance to the type section, and typifies the formation. Note the interbedding of less resistant beds of lithofacies QM-1 and more resistant beds of lithofacies QM-2. Location of photograph indicated in Fig. 4.2.

4.1. Lithofacies analysis and stratigraphy

Lithofacies QM-1: Sparsely fossiliferous, marly lime wackestone

Lithofacies QM-1 is a marlstone (predominantly wackestone, grading locally into marly lime mudstone). Its primary constituents are micrite and silty to very fine sand-sized carbonate and quartz grains. It is light grey in color and is moderately to poorly indurated.

Beds are up to 70 cm thick, although they are typically 5 to 20 cm thick (Figs. 4.2, 4.3). No internal bedding is recognizable, which may be the result of intense bioturbation in this lithofacies. The beds have poorly defined planar upper and lower boundaries, giving layers tabular external geometries (Fig. 4.4). Individual beds are continuous, without significant thickness changes, over hundreds of meters (Fig. 4.4). Contacts between this lithofacies and lithofacies QM-2 (see description below) are gradational. This unit is less resistant to weathering than lithofacies QM-2.

Many burrows of *Planolites*, *Skolithos*, and *Chondrites* are present, as are abundant *Zoophycos* spreiten and grazing traces (Fig. 4.5a). These ichnofauna represent the *Zoophycos* ichnofacies (Pemberton *et al.*, 1992). Body fossils, which are rare, are incompletely preserved and strongly pyritized when present. They include gastropod shells and disarticulated bivalve shells of unknown species. Benthic and planktonic foraminifera and calcareous nannofossils are abundant (BRGM, 1980d; Pairis *et al.*, 1983, 1984a; Fabre *et al.*, 1986; Pairis, 1988) and document a relatively deep marine setting.

The extremely fine grain size, the high degree of bioturbation, and the presence of deep water fauna indicate that lithofacies QM-1 was deposited in a low-energy environment on the deep shelf or upper continental slope. The ichnofaunal assemblage implies a relatively deep paleobathymetry (≥ 200 m) with reduced oxygen levels and a high organic content in the sediment (Seilacher, 1978; Pemberton *et al.*, 1992). The lack of relatively coarse-grained material is consistent with such a setting. The presence of fine siliciclastic material indicates that this lithofacies is hemipelagic in

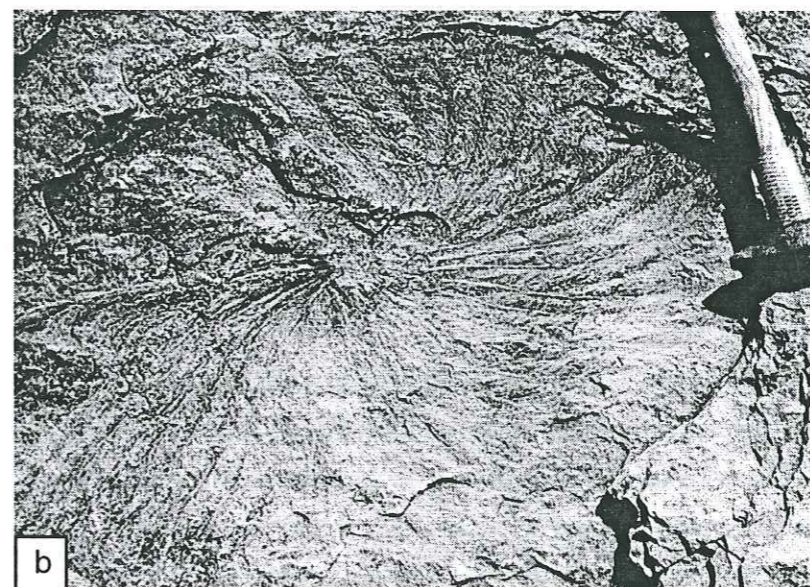


Fig. 4.5. Trace fossils in the Queyras Marlstone Formation. (a) *Skolithos* and *Planolites* burrows in lithofacies QM-1. (b) *Zoophycos* spreiten in lithofacies QM-2.

origin.

Lithofacies QM-2: Sparsely fossiliferous, very fine-grained wackestone

Lithofacies QM-2 is a very fine- to fine-grained silty lime wackestone. Its primary constituents are micrite, fine-grained carbonate debris, and 5-25% silt- and sand-sized quartz grains. This lithofacies is distinguished from lithofacies QM-1 by its greater resistance to weathering (possibly due to a higher carbonate content), its slightly coarser grain size, and its lighter grey color. Weathered surfaces appear massive, but fresh surfaces reveal either a highly bioturbated fabric, with no internal bedding preserved, or thin, non-bioturbated laminae.

Beds are 2 to 12 cm thick, with beds 2-4 cm and 10-12 cm thick being more common than beds 4-10 cm thick (Figs. 4.2, 4.3). The beds have poorly defined planar upper and lower boundaries, which are gradational with lithofacies QM-1. The beds have tabular geometries, and individual beds

Univ. J. Fourier - O.S.U.G.
MAISON DES GEOSCIENCES
DOCUMENTATION
B.P. 53
F. 38041 GRENOBLE CEDEX
Tél. 04 76 63 54 27 - Fax 04 76 51 40 58
Mail: ptalour@ujf-grenoble.fr

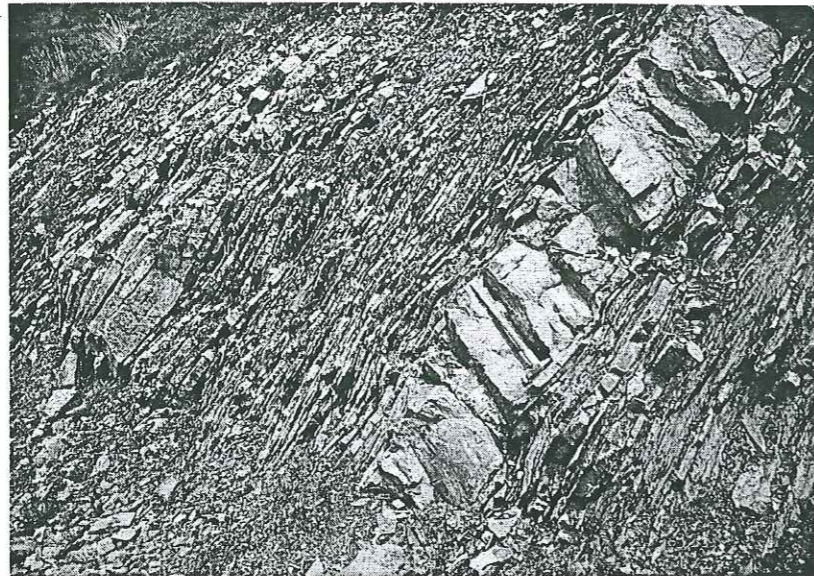


Fig. 4.6. Sandy turbidites of lithofacies QM-3 of the Queyras Marlstone Formation. Photograph corresponds to the section from 85 to 89 m in the measured section on GR 94 (Fig. 4.4). This interval is dominated by thick- and thin-bedded turbidites. Hammer is 50 cm long.

are continuous over hundreds of meters (Fig. 4.4).

Lithofacies QM-2 contains *Planolites*, *Skolithos*, *Chondrites*, and *Zoophycos* trace fossils. Although *Planolites* and *Skolithos* traces are less common than in lithofacies QM-1, *Chondrites* and *Zoophycos* traces are very abundant locally (Fig. 4.5b). Macrofossils such as pyritized gastropod shells are less common, but, when present, are more complete than in lithofacies QM-1. Benthic foraminifera and calcareous nannofossils documenting a hemipelagic setting are abundant (BRGM, 1980d; Pairis *et al.*, 1983, 1984a; Fabre *et al.*, 1986; Pairis, 1988).

Lithofacies QM-2, like lithofacies QM-1, is interpreted as having been deposited in a deep marine setting, based on the presence of deep water fauna. The trace fossil assemblage is consistent with a deep marine setting (Seilacher, 1978; Pemberton *et al.*, 1992). The increase in grain size, as well as the increased amount of terrigenous siliciclastic material relative to lithofacies QM-1, suggest that lithofacies QM-2 is not purely hemipelagic. Rather, these factors indicate that the deep shelf and upper slope were periodically subject to increases in continental- and/or shelf-derived material.

The most likely cause of such fluctuations in offshore flow are storm surges, seasonal or longer term variations in fluvial discharge into the marine system, and the shifting of deltaic lobes on the shelf (Coniglio & Dix, 1992). The sediment plumes associated with such currents can flow as far offshore as the deep slope or basin (Coniglio & Dix, 1992). Lithofacies QM-2 is not considered to be winnowed by bottom currents because of the high amount of micrite present.

Lithofacies QM-3: Very fine- to medium-grained lenticular sandstone

Lithofacies QM-3 occurs sporadically throughout the Queyras Marlstone Formation (e.g., Figs. 4.2, 4.3). The lithofacies is best developed at the Ravine de Charbournasse in eastern central Dévoluy (Fig. 4.2) and ESE of the village of Haut Gicon in northern Dévoluy (Fig. 4.3, 4.6). Most often, it forms lenticular beds within a sequence of beds of lithofacies QM-2, but can also occur within

sequences of lithofacies QM-1 (Figs. 4.2, 4.3).

Lithofacies QM-3 is a grey to orange lithic wacke (terminology of Williams *et al.*, 1954) with significant amounts of carbonate. The grains are monocrystalline quartz with straight and undulose extinction (60-70%), intra- and extrabasinal carbonate lithic fragments (usually micritic, 25-40%), and occasional chert, other lithic fragments, and feldspars (Table A-I). The grains are very fine- to medium sand sized, well-sorted, and angular to subrounded. The grains occur in a marly matrix which may comprise up to 50% of a given bed.

Beds of lithofacies QM-3 pinch out laterally over distances of up to 30 meters. Beds are 1 - 75 cm thick, with an average thickness of approximately 20 cm (Figs. 4.2, 4.3). Individual beds pinch out and reappear along strike at the same stratigraphic horizon over horizontal distances of up to 20m. The beds are either structureless or are crudely fining-up with some indication of planar bedding. Basal surfaces are planar to irregularly convex and are sharply discordant (Fig. 4.6). Scour marks and mud rip-up clasts on the base of some beds indicate that the basal surfaces are erosional. Upper surfaces are planar to gently undular and sharp.

At the base of one bed in the Ravine de Charbournasse section (38.60 - 36.80 m, Fig. 4.2), there are imbricated disc-shaped mud clasts which give corrected paleocurrent orientations to 270-292°. On the bases of two beds in the GR 94 section (Fig. 4.3), non-directional scour marks indicate corrected paleoflow in a NE-SW direction. Given the directional data from Ravine de Charbournasse, these data are interpreted to reflect flow from the northeast to the southwest, and not in two opposite directions.

Horizontal burrows (e.g., Fig. 4.5a), more prevalent at the bases of the beds, and vertical burrows, more prevalent towards the tops of beds, are filled with fine- to medium-grained sand from the bed itself, or with very fine- to fine-grained carbonate sediment from over- and/or underlying layers. This latter infill indicates that there was some degree of mixing, despite the sharp upper and lower boundaries of this lithofacies (see above). The horizontal burrows (ichnogenus *Planolites*?) are often, though not always, oval in cross section, with flattening parallel to bedding. The flattening is considered to be due to post-depositional compaction. Burrows average 1 to 4cm long and 0.5cm wide (long axis). The maximum measured diameter was 3 cm on a sample 7 cm long. The vertical burrows (ichnogenus *Skolithos*?) are up to 15 cm long and 1.25 to 1.5 cm wide. They are spherical in cross section.

Beds of lithofacies QM-3 are distinctively coarser-grained than the surrounding beds of lithofacies QM-1 or QM-2 (Figs. 4.2, 4.3). The erosional bases, the presence of sole marks and rip-up clasts, and the fining-up nature of the beds are equally distinctive. The beds are interpreted as sandy turbidites. They lack classic Bouma (1962) sequences, which is considered to be either the result of rapid deposition or, more likely, post-depositional bioturbation by *Planolites* and *Skolithos*(?) (cf. Coniglio & Dix, 1992). The paleocurrents indicate that the turbidity currents flowed to the west and southwest.

The presence of the shallow water coccolith species *Lanternithus minutus* reported in the Queyras

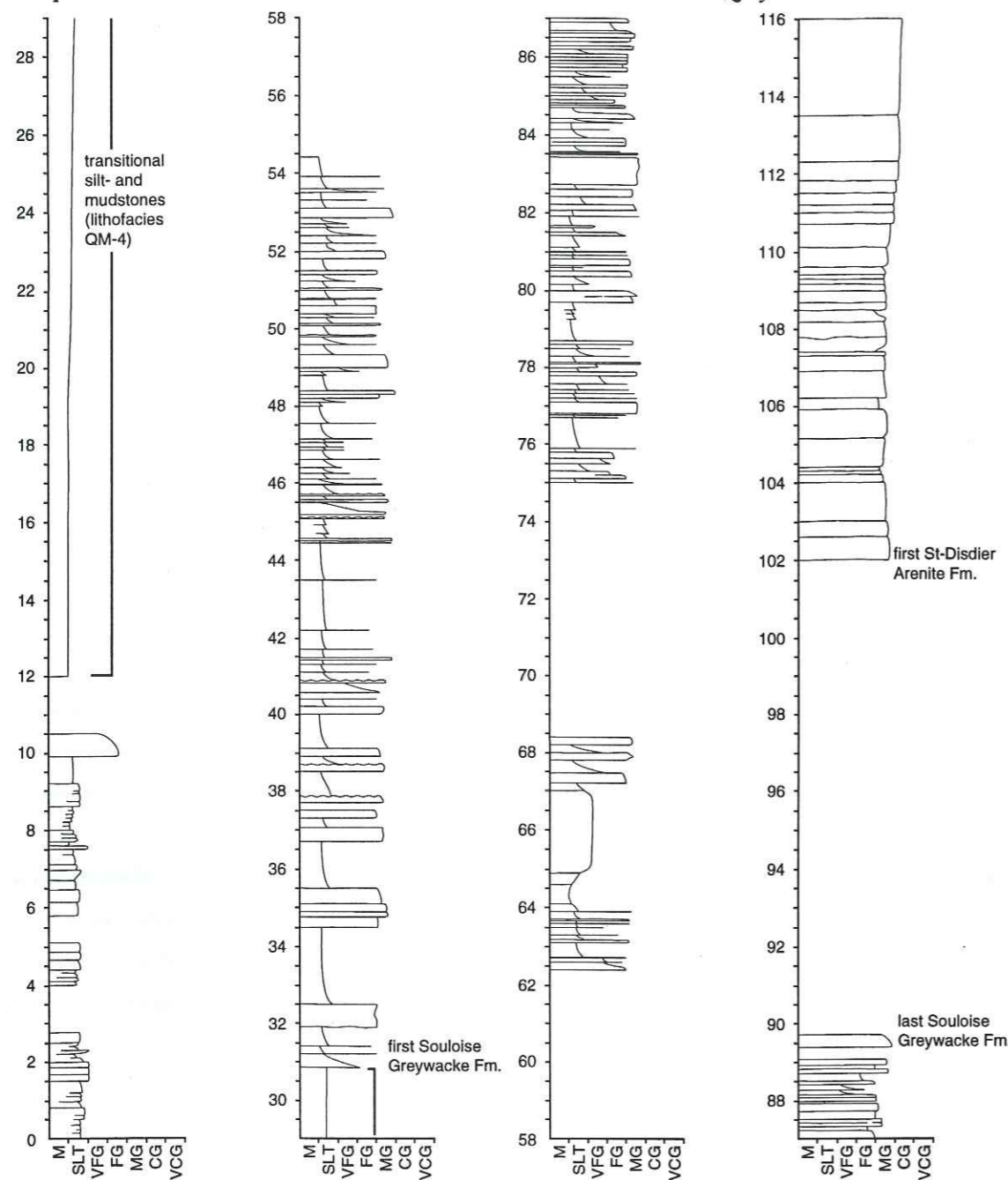


Fig. 4.7. Measured section from Tête de la Tune, northern Dévoluy (scale in meters), showing uppermost beds of lithofacies QM-1 and QM-2 (not indicated), and the 20m thick section of lithofacies QM-4 (12 - 30.80m). The transition to the overlying Souloise Greywacke Formation is also shown. Location of section indicated in Fig. 4.1.

Marlstone formation (Fabre *et al.*, 1986) is considered to be the result of redeposition in one of these turbidites, and not of shallow paleobathymetric conditions, as interpreted by Fabre *et al.* (1986).

Lithofacies QM-4: Carbonaceous mud- to siltstone

Lithofacies QM-4 occurs as a 20-50m thick deposit at the top of the Queyras Marlstone Formation (e.g., Figs. 4.3, 4.7). It occurs at all localities where the transition from the Queyras Marlstone Formation to the Souloise Greywacke Formation crops out and is therefore interpreted to be the

terminal deposit of the Queyras Marlstone Formation. Lithofacies QM-4 is a marly mud- to siltstone with abundant carbonaceous and siliciclastic material. It is distinguished from the other lithofacies of the Queyras Marlstone Formation by its black to dark grey color, extremely fine relative grain size (clay to silt), and well-bedded nature. This lithofacies is estimated to contain up to 50% silt and finer siliciclastic material.

The beds of lithofacies QM-4 are on the scale of millimeters to centimeters, and are monotonously stacked through the entire interval. They are laminated, but display mm-scale thickness changes along strike. The lower limit of the lithofacies is gradational with lithofacies QM-1 and QM-2. The upper limit is abrupt with the Souloise Greywacke Formation above (Fig. 4.7).

The abundant carbonaceous debris and the increase in siliciclastic debris relative to the lithofacies QM-1 and QM-2 of the Queyras Marlstone Formation indicates increased terrigenous influx. Similar influxes on hemipelagic slopes have been related to mild tectonic uplift and erosion or climate change on the continent (Wilson & Jordan, 1983). An alternative explanation is that the change in sedimentation reflects an autocyclic shifting of depositional systems on the shelf (H. Sinclair, personal communication).

LITHOFACIES ASSOCIATION

Lithofacies Association QM-I: Interbedded layers of lithofacies QM-1 and QM-2, with occasional beds of lithofacies QM-3

Lithofacies QM-1 and QM-2 are repetitively interbedded for most of the Queyras Marlstone Formation and crop out in approximately equal amounts (Figs. 4.2 - 4.4). Occasional beds of lithofacies QM-3 punctuate the sequence (Figs. 4.2, 4.3).

The gradational boundaries between the lithofacies QM-1 and QM-2 indicate that fine-grained sedimentation was continuous during deposition of the Queyras Marlstone Formation. There are no apparent internal hiatal surfaces. If such surfaces did exist, then they probably have been obliterated by bioturbation. The interbedding is thought to be the result of changes in sedimentation patterns on the shelf, resulting in periodic fluxes in offshore currents. The interbedding is not believed to be controlled by such allocyclic processes as orbital forcing because the beds do not thicken up or thin up, nor are they arranged in "bundles".

The occurrence of the turbidites of lithofacies QM-3 indicates that there were occasional sudden increases in erosion, which may have been caused by: (1) an increase in sediment supply; (2) progradation of shallower marine depositional systems; or (3) an increase in depositional gradient on the slope or shelf due to a fall in relative sea level. The preferential occurrence of lithofacies QM-3 within bedsets of lithofacies QM-2 indicates increased currents on the shelf may also have been associated with the turbidity currents.

Lithofacies QM-4, which only occurs at the top of the formation (Fig. 4.2), is not considered to be part of the lithofacies association. It is interpreted as recording increased terrigenous input, and

anticipates a transition from carbonate-dominated deposition in the Queyras Group to siliciclastic-dominated deposition in the Souloise Group.

4.2. Depositional setting

The Queyras Marlstone Formation is interpreted to have been deposited in deeper, calmer water than the Dévoluy Nummulitic Limestone Formation. Overall, the four lithofacies of the Queyras Marlstone are interpreted as having been deposited on the hemipelagic outer slope of the Alpine foreland basin in a low energy environment that was periodically subject to periods of coarse sediment input.

CHAPTER 5

The Souloise Greywacke Formation

The Souloise Greywacke Formation, the lowermost formation in the siliciclastic-dominated Souloise Group, occurs stratigraphically above the Queyras Marlstone Formation and below the St-Disdier Arenite Formation. The Souloise Greywacke Formation is dated as late Eocene to early Oligocene based on the presence of foraminiferal and dinofloral assemblages (Gidon *et al.*, 1980; Fabre *et al.*, 1986).

The formation is present primarily in northern and central Dévoluy, but is also present in a single outcrop in southeastern Dévoluy (location e in Fig. 5.1). It is approximately 70 m thick at Tête de la Tune in northern Dévoluy, which is the only nearly complete exposure of the formation (Fig. 5.2). Elsewhere, the formation lies in the immediate hanging wall of the Median Dévoluy Thrust, or the top of the formation does not crop out. The formation is more than 28 m thick near the village of Haut Gicon in northern Dévoluy (Figs. 5.3, 5.4), more than 31 m thick at Puy de Rioupes in central Dévoluy (Fig. 5.5), and at least 0.8 m thick northeast of the village of L'Enclus in southeastern Dévoluy (Fig. 5.6). Because of the incomplete exposures, lateral thickness variations cannot be constrained.

The lower boundary of the unit is defined as the base of the first sandstone bed above the black silt- and mudstone lithofacies at the top of the Queyras Marlstone Formation (Fig. 5.2). The silt- and mudstone lithofacies reflects a gradual transition from carbonate-dominated deposition to siliciclastic-dominated deposition, and the Souloise Greywacke Formation documents the first significant input of terrigenous clastic material into the basin.

The upper boundary of the Souloise Greywacke Formation is defined as the top of the last mud- to siltstone bed below the overlying coarser grained sandstone beds of the Lower St-Disdier Arenite (Fig. 5.5). This conformable boundary, seen in central Dévoluy, is laterally equivalent with an unconformity in western Dévoluy.

The type section of the Souloise Greywacke Formation is located at Tête de la Tune in northern Dévoluy (Figs. 5.1, 5.2). As seen in the type section, the formation is well-bedded, with alternating beds of fine- through medium-grained sandstones and silt- and mudstones.

Four lithofacies have been determined for the Souloise Greywacke Formation. These are: well-bedded, fine-grained graded sandstone and siltstone and finely laminated silt- to mudstone (lithofacies SG-1); fine-grained, hummocky cross stratified sandstone and finely laminated silt- to mudstone (lithofacies SG-2); heterolithic, very fine-grained sand-, silt-, and mudstone (Lithofacies SG-3); and well-bedded, graded sandstones with symmetrical ripples and finely laminated siltstones (lithofacies SG-4) (Table 5-I).

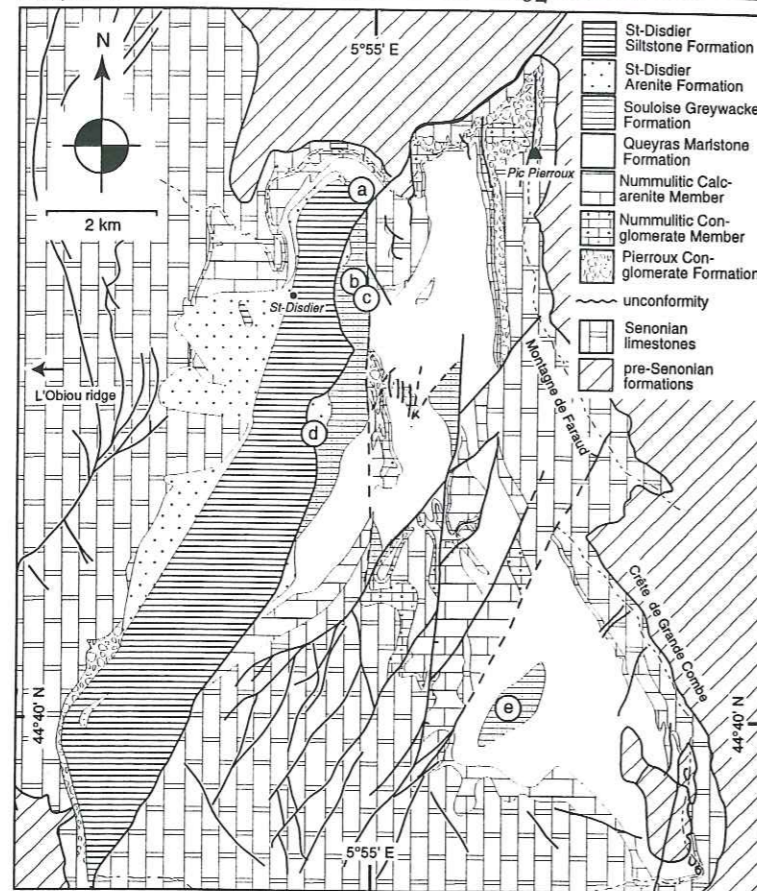


Fig. 5.1. Geologic map of Dévoluy, indicating measured sections of the Souloise Greywacke Formation. **a** = Tête de la Tune section (type section); **b** = Haut Gicon section; **c** = Radio Tower section; **d** = Puy de Rioupes section; **e** = L'Enclus sections. Outcrop at **a** too small to be distinguished (refer to Fig. 1.6).

Lithofacies	Description	Interpretation
SG-1	Well-bedded, fine-grained, graded sandstone, siltstone, and finely laminated silt- to mudstone beds	distal turbidites, occasionally reworked by bottom currents
SG-2	Fine-grained hummocky cross stratified sandstone and finely laminated silt- to mudstone	Tempestites and distal turbidites deposited in water 10s-100s of m deep
SG-3	Heterolithic, very fine-grained sand-, silt-, and mudstone	hemipelagic silts, muds interbedded with very thin, very fine-grained sandy "microturbidites" or contourites
SG-4	Well-bedded, fining-up sandstones with symmetrical ripples and finely laminated siltstones	shallow marine, distal turbidites reworked by bidirectional currents
Lithofacies Association		
SG-I	Interbedded SG-1, SG-2, and SG-3	distal fan/distal delta turbidites, shallowing from below to above storm wave base
SG-II	SG-1, SG-2, SG-3, and SG-4	shallow marine turbidites, above fair-weather wave base

TABLE 5-I. Summary of lithofacies and lithofacies associations of the Souloise Greywacke Formation

5.1. Lithofacies analysis and stratigraphy

Lithofacies SG-1: Well-bedded, fine-grained, graded sandstone and siltstone and finely laminated silt- to mudstone

Beds of lithofacies SG-1 fine up from very fine- to medium-grained sandstone at their bases to extremely fine siltstone and silty mudstone at their tops. There is typically an abrupt grain size shift from the sandstone to the silt- and mudstone (Figs. 5.2 - 5.6). The sandier parts of the beds are rusty brown to grey, while the finer-grained fraction is grey. Abundant micas and carbonaceous debris are visible in sandy hand specimens, especially on bedding surfaces. The sediment of this lithofacies is well-sorted and well-rounded.

The bases of the graded beds are usually planar, but occasionally they have flute casts (Fig. 5.6b), tool marks, load casts (e.g., middle bed, Fig. 5.6b; upper bed, Fig. 5.7a), and/or horizontal grazing traces of an unidentified fauna. Rare vertical to subvertical burrows in the sandier parts of the beds are approximately 1cm wide and are smooth-walled. The ichnofauna has not been identified.

The lowermost parts of the sandy intervals can be structureless (Fig. 5.6; upper bed, Fig. 5.7a), or can begin with parallel laminations (lower beds, Figs. 5.7a, b; Fig. 5.7c). If the beds are massive at their bases, then they typically abruptly become parallel laminated (upper bed, Fig. 5.7a), although occasionally the sandy parts of beds show little or no planar lamination (Figs. 5.4, 5.6). Most often, the sandy intervals begin with parallel laminations that are generally less than 1cm thick, and are identified by darker carbonaceous material at their tops. The upper parts of the sandy intervals have unidirectional current ripples and, sometimes, disturbed bedding (e.g., upper sandy bed, Fig. 5.7b; Fig. 5.7c). Types of disturbed bedding include discontinuous, disrupted, or convolute bedding. The disturbed bedding may grade laterally into undisturbed bedding, or the disruption may be continuous along strike. The upper part of the sandy interval may be missing, in which case the sandy part of the bed is characterized only by parallel lamination (e.g., Fig. 5.7a; lower bed, Fig. 5.7b). If the upper part of the sandy interval is present, then there is generally a return to parallel lamination at the top (Fig. 5.7c). The uppermost part of the sandy interval may also be characterized by a bed of medium-grained sand that is either massive or has unidirectional ripple structures (e.g., Figs. 5.7c, d). When present, such beds have undular tops.

The finer-grained layers above the sandy intervals, which are not always present (Figs. 5.7a, b), have sub-millimeter to millimeter scale parallel laminations. These layers usually fine up from silt to muddy silt, although the muddier parts of the beds are commonly absent.

Upper surfaces of this lithofacies are sharp when overlain by beds of lithofacies SG-1, SG-2, or SG-4 (see Table 5-I for summary of the other facies). These surfaces may be planar, loaded, or eroded. The upper surface is less sharp when lithofacies SG-1 is overlain by lithofacies SG-3. The upper surface of a given bed is taken at the base of the overlying sandstone bed when the silt- or mudstone part of the bed is present, or otherwise at a discernible break in grain size (Figs. 5.7a, b).

Beds of this lithofacies are continuous over 100s of meters. The beds are 5 cm to 2 m thick; the sandy parts of the beds are 1 to 100 cm thick. Thinner beds are more common than thick ones.

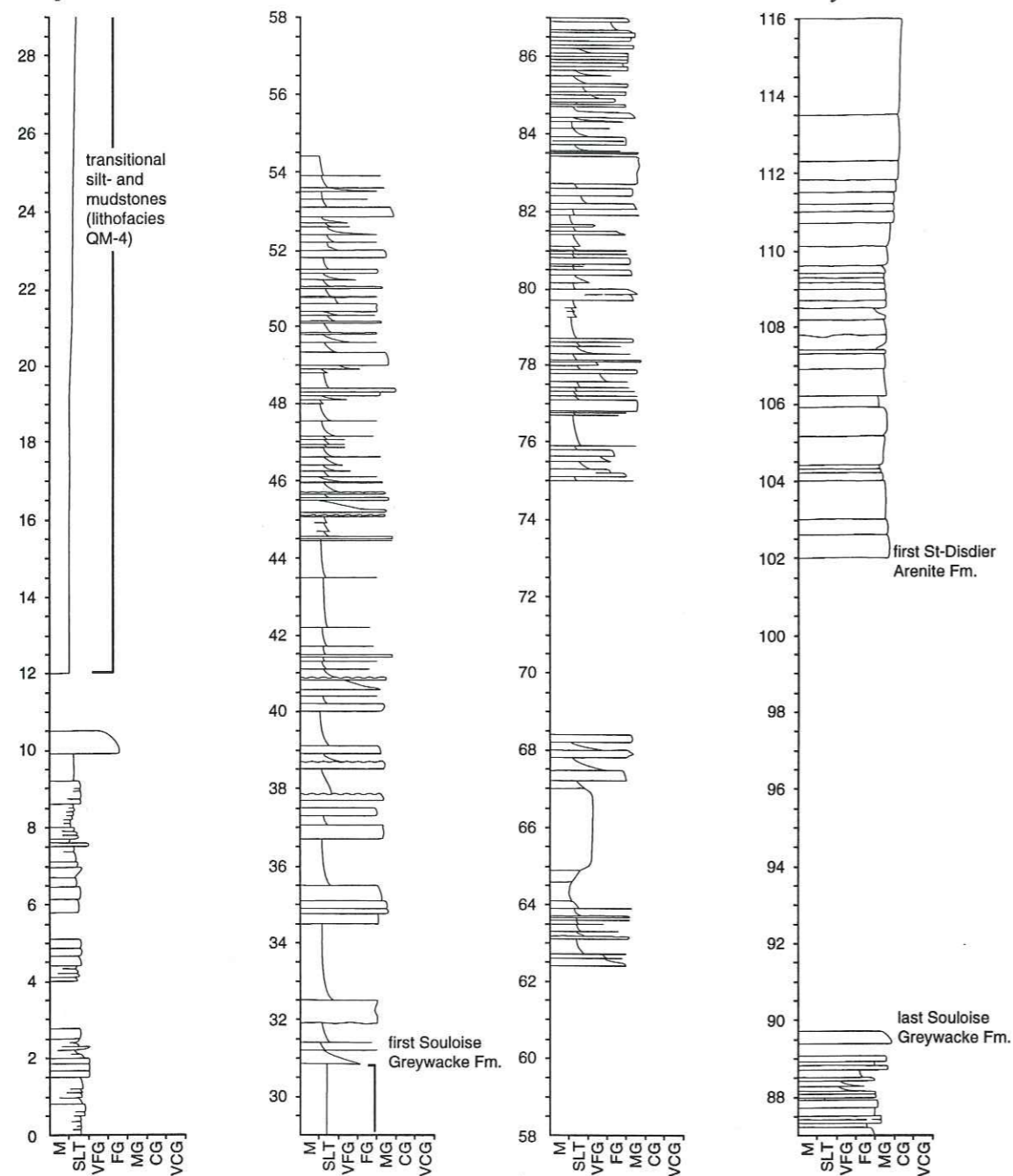


Fig. 5.2. Type section of the Souloise Greywacke Formation at Tête de la Tune, northern Dévoluy (scale in meters), showing the lower contact of the formation with the underlying Queyras Marlstone Formation (30.80m). The upper part, with the St-Disdier Arenite Formation, does not crop out. Location indicated in Fig. 5.1. Lithofacies are not indicated.

Their external geometry is tabular, with no evidence of channelization. However, the sole marks on the bases of some beds, and the amalgamation of certain beds, indicate that some erosion occurred in association with deposition.

Corrected directional data on the bases of beds (usually prod marks or flute casts) show flow to the NNW at Tête de la Tune in northern Dévoluy (Fig. 5.9a), to the N and NE at Haut Gicon in north-central Dévoluy (Fig. 5.9b), and to the NNW, NE, and E at L'Enclus in southeastern Dévoluy

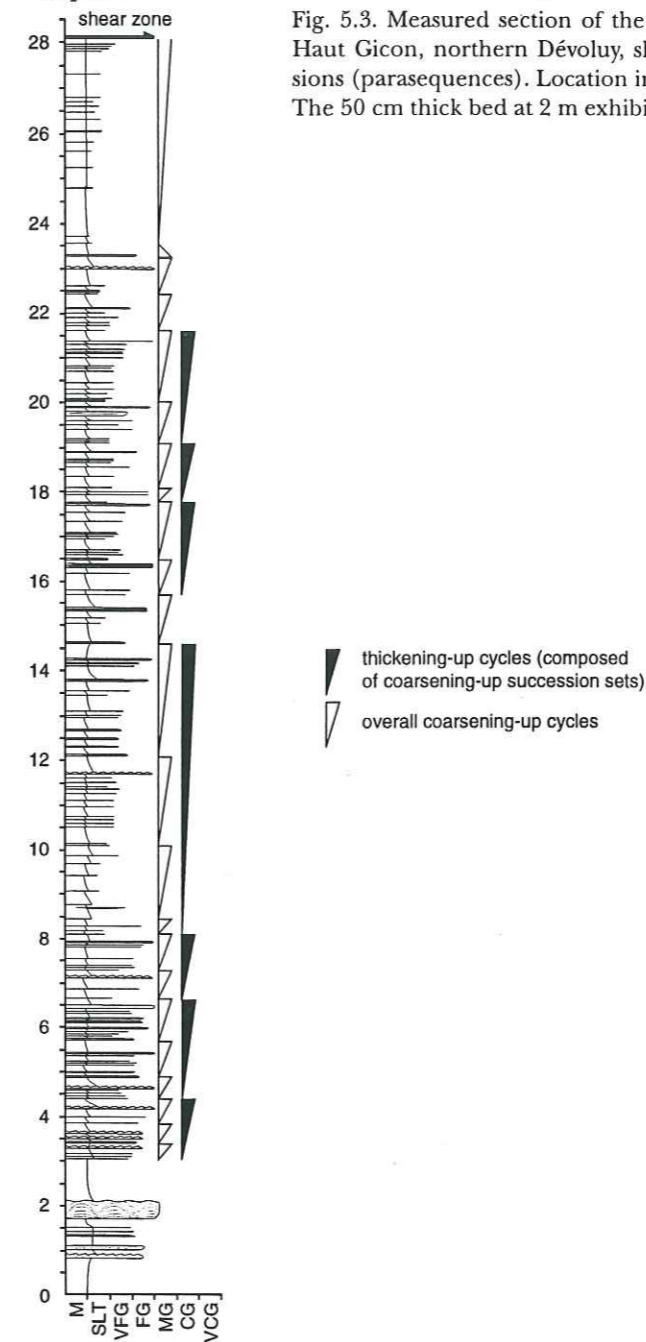


Fig. 5.3. Measured section of the Souloise Greywacke Formation at the village of Haut Gicon, northern Dévoluy, showing coarsening-up and thickening-up successions (parasequences). Location indicated in Fig. 5.1. Lithofacies are not indicated. The 50 cm thick bed at 2 m exhibits hummocky cross-stratification (see Fig. 5.10a).

(Fig. 5.9d). These data indicate northward flow, with variation to the west and east. Non-directional data are therefore interpreted as being northwest- and northeast-directed, in keeping with the bulk of directional data. The currents probably flowed parallel to a topographic feature such as the axis of a sub-basin or a lateral bounding slope. Local variations in the paleocurrents may reflect topographic irregularities on the basin floor. Paleocurrents derived from current ripples at the tops of beds (not differentiated in Figs. 5.9a, b, and d) are always directed to the northeast. Their semi-orthogonal orientation with respect to the predominantly northward-directed flow at the base of the turbidites is considered to be related to offshore-directed reflection by a lateral bounding slope (cf. Kneller *et al.*, 1991; King, 1994), and would indicate that the basin geometry deepened to the

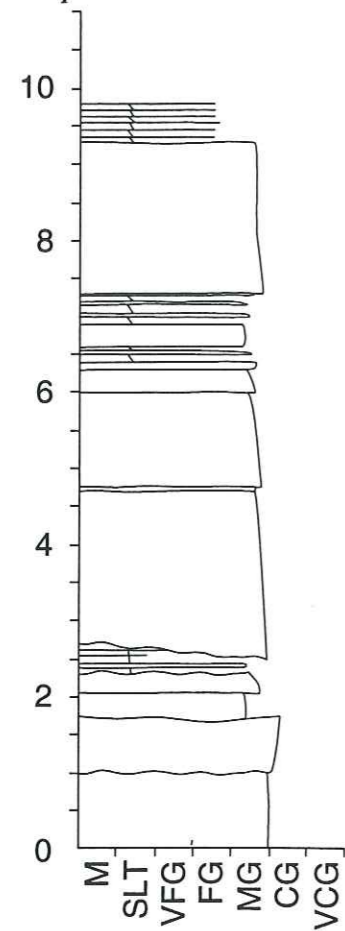


Fig. 5.4. Radio Tower measured section of the Souloise Greywacke Formation, southeast of the village of Haut Gicon, northern Dévoluy (scale in meters). The sandstone beds (lithofacies SG-1) are uncharacteristically thick in this section. Location indicated in Fig. 5.1.

northeast.

The upsection arrangement of internal sedimentary structures in beds of lithofacies SG-1 are consistent with those observed in Bouma sequences (Bouma, 1962). A complete Bouma sequence consists of a structureless or graded interval at the base (Ta), overlain by a parallel laminated interval (Tb) that grades upwards into rippled or distorted sediment (Tc), an upper interval of parallel laminated sandstone (Td), and parallel laminated to homogeneous siltstones and mudstones (Te). Beds of lithofacies SG-1 contain multiple variants on the Bouma sequence (Fig. 5.8).

Bouma sequences are generally considered to be diagnostic of turbidites. The overall fine-grained nature of the beds, as well as the common lack of scour structures and the lateral continuity of beds, suggests that lithofacies SG-1 is best interpreted as the deposits of dilute turbidity currents, or as distal turbidites. The presence of burrows in this lithofacies implies that bottom waters were relatively well-oxygenated (Seilacher, 1978).

In most of the beds, there is no evidence of reworking by waves or other bottom currents. These beds are therefore considered to have been deposited in relatively deep water, below storm wave base. In contrast, beds with undular surfaces at the top of the sandy interval (e.g., Figs. 5.7c, d) appear to have been reworked by marine currents prior to the deposition of the siltier part of the bed. These bottom currents could be related to storm waves, tsunamis, deep tidal currents, or contour or geostrophic currents.

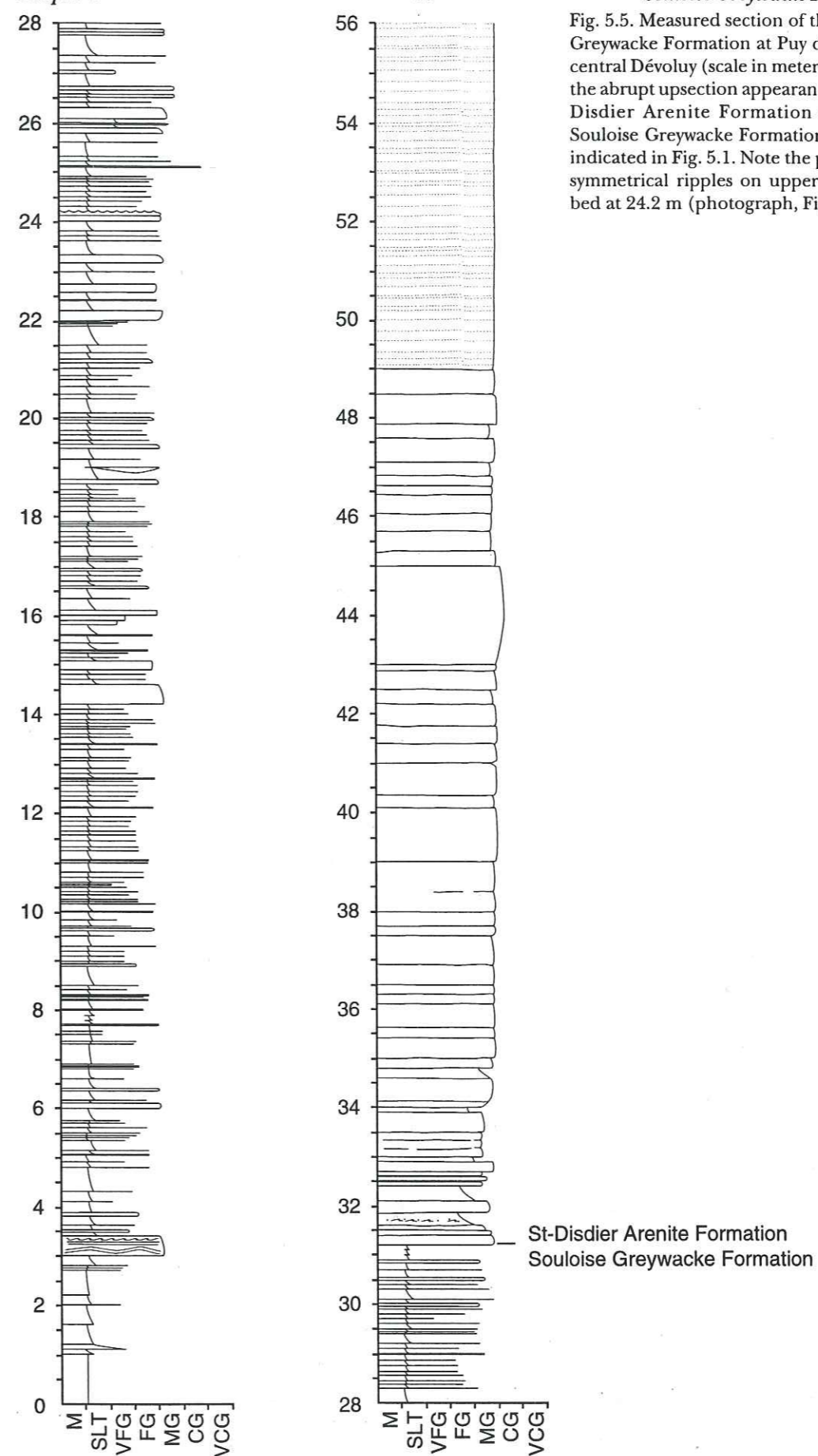


Fig. 5.5. Measured section of the Souloise Greywacke Formation at Puy de Rioupes, central Dévoluy (scale in meters), showing the abrupt upsection appearance of the St-Disdier Arenite Formation above the Souloise Greywacke Formation. Location indicated in Fig. 5.1. Note the presence of symmetrical ripples on upper surface of bed at 24.2 m (photograph, Fig. 5.11).

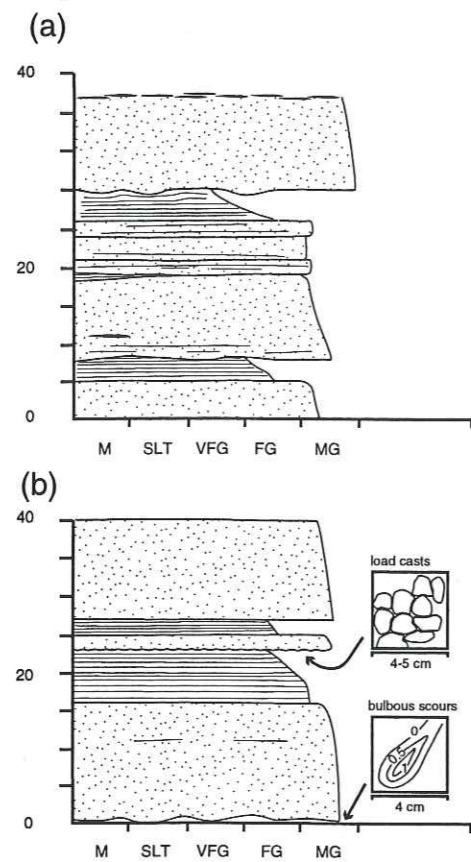


Fig. 5.6. Detailed sections of lithofacies SG-1 of the Souloise Greywacke Formation at L'Enclus, southern Dévoluy (scale in centimeters). Location indicated in Fig. 5.1.

swaley cross stratification, when present, occur in the middle and upper parts of the beds and are often coarser-grained than the sand of the same bed that occurs above and below them. Laminae may thicken into the swales or the hummocks. The hummocky cross-stratification is identified by a lack of unidirectional foresets on perpendicular outcrop faces. The tops of beds may have planar bedding or ripple cross-stratification.

The hummocky and swaley cross stratification, the more consistently medium-sand grain size (relative to lithofacies SG-1), and the lack of a prevalent muddy matrix in this lithofacies indicate that these beds were deposited by a different process than lithofacies SG-1. Hummocky cross-stratification is commonly interpreted as having been formed by storm waves, during oscillatory flow (Dott & Bourgeois, 1982; Duke, 1985; Pettijohn *et al.*, 1987; Brenchley, 1989; King, 1994). The upsection arrangement of sedimentary structures, from planar laminae at the base of the bed, to hummocky cross-stratified laminae in the middle, to planar or rippled laminae at the top, is consistent with those found in tempestites (Brenchley, 1989). Tempestites are deposited above storm wave base, in waters from a few tens to a few hundreds of meters deep (Brenchley, 1989). The tabular nature of beds of this lithofacies suggests deposition in deeper offshore waters (Brenchley, 1989).

The coarser average grain size relative to lithofacies SG-1 and the lack of muddy matrix probably

Lithofacies SG-2: Fine-grained, hummocky cross stratified sandstone and finely laminated silt- to mudstone

This lithofacies first appears in the middle half of the Souloise Greywacke Formation. It consists of medium- to fine-grained sandstone beds 0.2 - 0.5 m thick that have a more uniform, slightly coarser grain size than beds of lithofacies SG-1. The beds fine up in the last few centimeters. The sandstone is well-sorted and the grains are well-rounded. It does not have as much mud in the matrix, and mica and carbonaceous debris are not as common as in lithofacies SG-1. The beds weather brown to brownish grey.

The lower bounding surfaces of beds of this lithofacies are planar, with no evidence of bottom marks. Upper bounding surfaces are typically undular, but may also be planar. The beds have tabular geometries that extend over the length of a given outcrop.

The most common sedimentary structures in the beds are hummocky and swaley cross stratification (Fig. 5.10) overlain by planar beds. The bases of the beds may be structureless or have planar laminae. Hummocky and

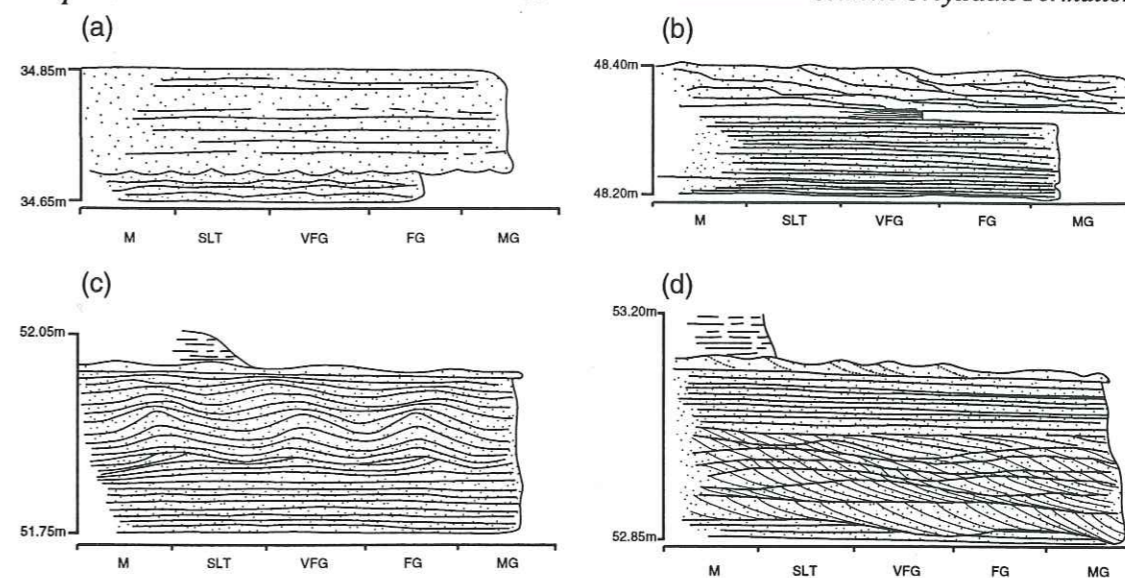


Fig. 5.7. Sedimentary structures in lithofacies SG-1, as observed at Tete de la Tune, northern Dévoluy. Measured thicknesses refer to locations in the Tete de la Tune measured section (Fig. 5.2). (a) Load casts on the base of a parallel-laminated sandstone bed. (b) Two sandstone beds separated by a finer-grained sandstone bed. The lower bed has planar bedding while the upper displays disrupted foresets. (c) Gradation from laminar bedding to undular bedding, back into planar bedding. Although the base of the undular bedding is erosive, the laminae themselves are not internally erosive and thicken over the highs, possibly indicative of hummocky cross stratification. (d) Upsection transitions from planar to rippled to planar bedding. The uppermost sandy bed is reworked. This "bed" may actually be two amalgamated beds.

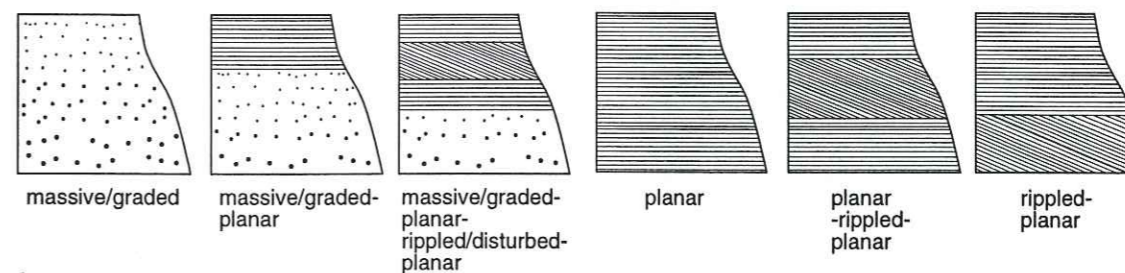


Fig 5.8. Common variants of the Bouma sequence observed in beds of lithofacies SG-1. Only the sandy parts (Ta-Td) of the beds are shown, although either the silty (Te) or muddy (Tf) parts of the beds, or both, may also be present. The total range of possibilities is therefore eighteen. Foreset angles (22.5°) are somewhat exaggerated in terms of the angle of repose.

indicate that originally more poorly-sorted sediments (possibly beds of lithofacies SG-1) were probably winnowed by the high-energy storm currents. The ripple cross-stratification and finer grain size at the tops of beds indicates waning flow, probably in an offshore direction, towards the end of deposition (Brenchley, 1989). The greater amount of muddy matrix in the upper laminae indicates that these particular sediments were not winnowed.

Lithofacies SG-3: Heterolithic, very fine-grained sand-, silt-, and mudstone

This lithofacies is composed of poorly cemented, dark grey to light brown, very fine-grained sand, silt, and mud. Beds are characteristically silty, with occasional muddier or slightly sandier lenses occurring throughout. The beds do not have internal grading. The siltier fraction has discon-

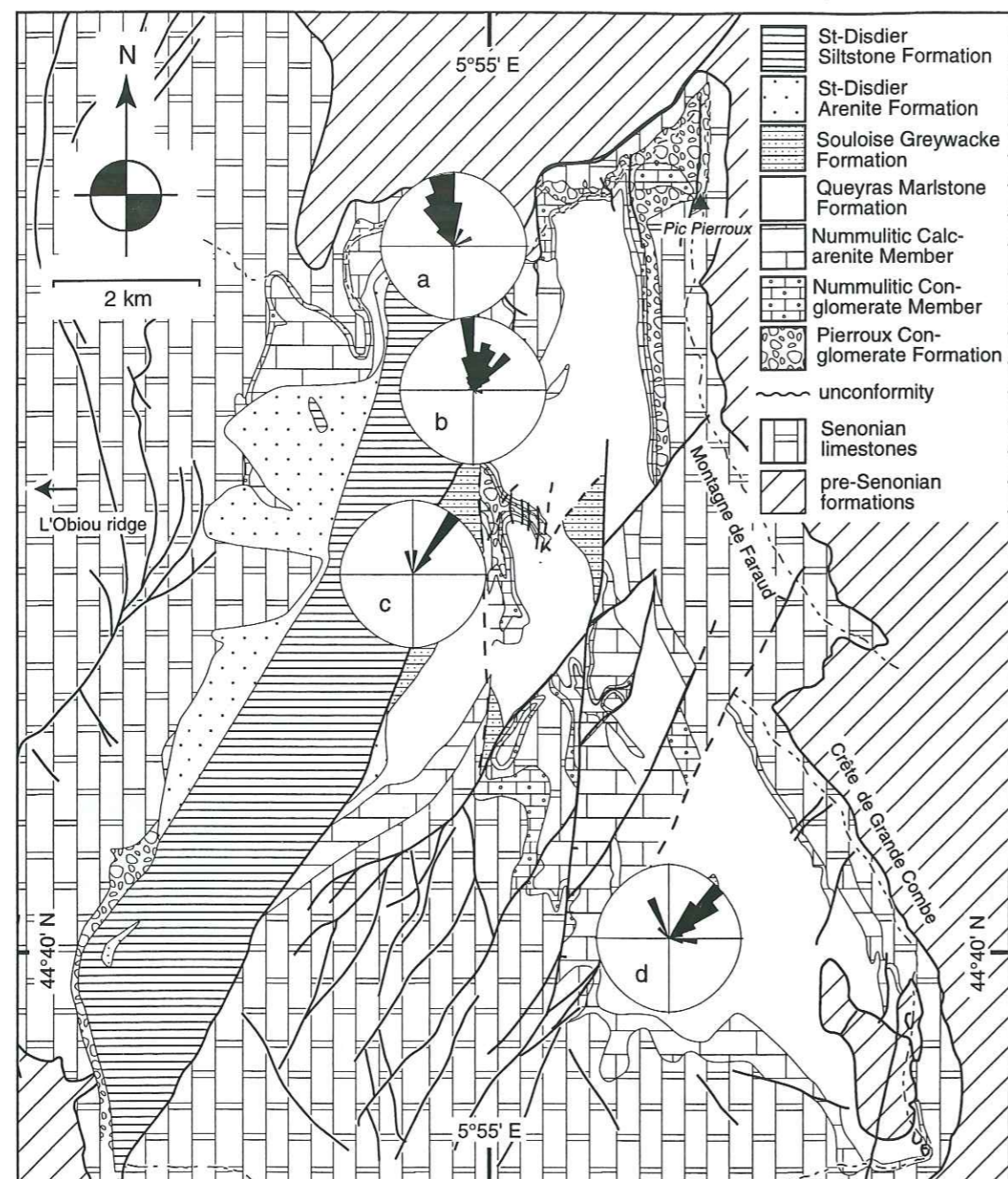


Fig. 5.9. Equal area rose diagrams indicating flow directions in the Souloise Greywacke Formation. (a) Tête de la Tune, where data include prod marks, tool marks, ripple crest orientations, and ripple foresets (121 data; circle = 19%); (b) Haut Gicon, north-central Dévoluy, where directional data include ripple trough axes, ripple foresets, ripple crest orientations, and tool marks (83 data; circle = 18%); (c) Puy de Rioupes, where directional data include ripple crest orientations and ripple foreset orientations (6 data; circle = 50%); (d) L'Enclus, where directional data include flute casts and non-directional scour marks, which are interpreted to be northward directed in the rose diagram (22 data; circle = 23%). Data in (a), (b), and (d) are taken from the bases of lithofacies SG-1, interpreted as turbidites deposited below storm wave base, while the data in (b) are taken from lithofacies SG-4, interpreted as turbidites deposited above fair weather wave base.

tinuous laminar bedding, or is massive. Sandy lenses are moderately- to poorly-sorted, have well-rounded particles, and fine up.

Lithofacies SG-3 occurs above beds of lithofacies SG-1, SG-2, or SG-4 (see Table 5-I for descrip-

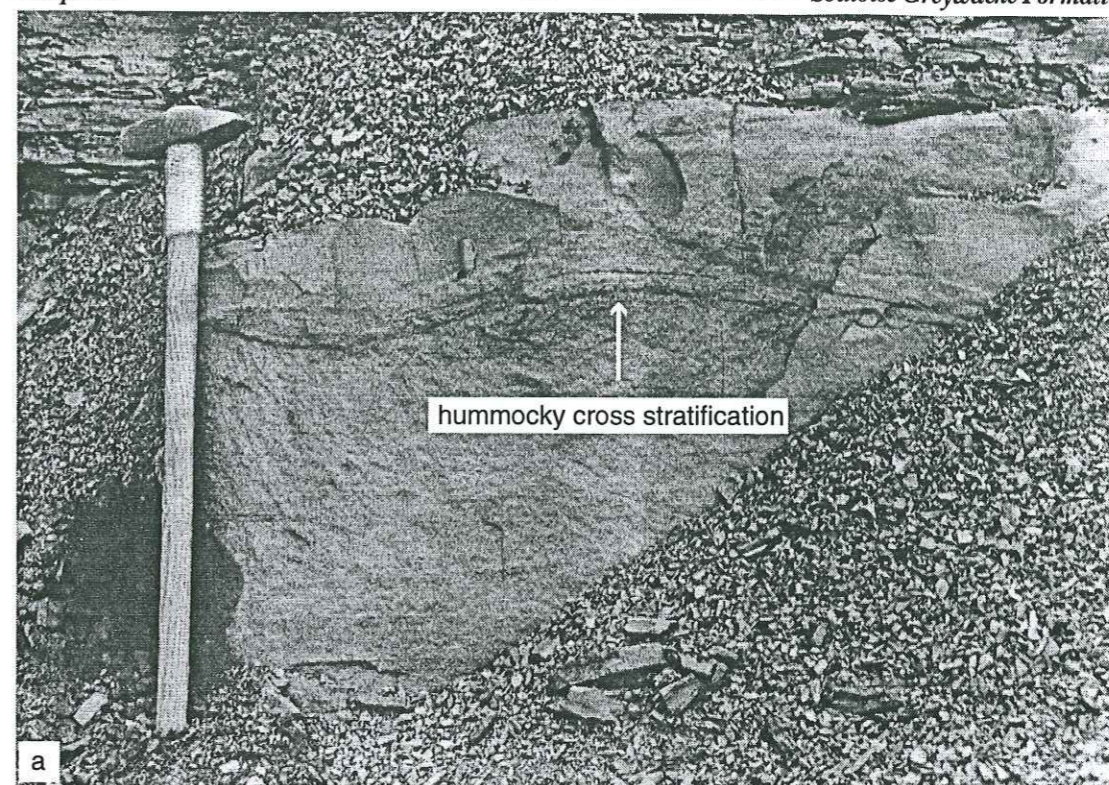


Fig. 5.10. Field photographs of hummocky cross-stratification in lithofacies SG-2 of the Souloise Greywacke Formation. Photographs taken at Haut Gicon, northern Dévoluy (located in Fig. 5.1). Hammer is 50cm long.

tions of these other lithofacies), and is present throughout the Souloise Greywacke Formation. Lower bounding surfaces of beds of this lithofacies are abrupt, and may be planar to undular depending on the characteristics of the underlying bed. Upper bounding surfaces are typically planar or eroded. The external geometry of the beds is laminar to tabular, depending on the thickness, which varies from 0.01 - 1.2 m.

Indistinct tube-like stains on some weathered surfaces may be burrows. Poorly-sorted textures in thin section tend to support this hypothesis, although no clear bioturbation structures were discerned.

The silts and muds are interpreted as hemipelagic deposits. The thin sandy lenses within the silts and muds represent sporadic influxes of slightly coarser grained sediment, and may be "microturbidites" or contourites (cf. Stow & Shanmugam, 1980; Pettijohn *et al.*, 1987) deposited by bottom currents. Overall, this lithofacies represents periods of relative calm deposition in the Dévoluy area, when larger turbidity currents (represented by lithofacies SG-1) and storms (represented as lithofacies SG-2) were not prevalent.

Lithofacies SG-4: Well-bedded, graded sandstones with symmetrical ripples and finely laminated siltstones

Lithofacies SG-4 is found only in the uppermost part of the Souloise Greywacke Formation (Figs. 5.2, 5.5). The lithofacies is composed of sandstones similar in appearance to the sandier part of lithofacies SG-1. The sandstones are moderately-sorted and the grains are well-rounded. Beds of this lithofacies fine up from medium- to fine-grained sandstone at their bases to very fine-grained sandstone or silty sandstone at their tops. Abundant micas and carbonaceous debris are visible in hand specimens.

The bases of the graded intervals are planar, with no sole marks or bioturbation present. The lowermost parts of the sandy intervals often contain parallel lamination (Tb of Bouma, 1962), but may also be massive (Ta of Bouma, 1962). Unidirectional current ripples appear upsection (Tc of Bouma, 1962). These ripples become more symmetrical towards the top of a given bed, and the upper surfaces of these beds have symmetrical ripple marks with both unidirectional and bidirectional foresets (e.g., Fig. 5.11). The ripples have average crest-to-crest wavelengths of 10 to 20 cm and amplitudes of 0.5 to 2.5 cm. The upper surfaces are sharp, and are overlain by beds of lithofacies SG-1, SG-2, or SG-3 (see Table 5-I for descriptions of these facies). Beds are 1 to 10cm thick, tabular in outcrop, and continuous over distances of 100s of meters.

At Puy de Rioupes, in central Dévoluy, unidirectional ripple foresets and the crests of these ripples show corrected flow to the northeast, with subsidiary flow to the N (Fig. 5.9c). Symmetrical ripple crests on the upper surfaces of beds at Puy de Rioupes are oriented NW-SE. Currents associated with symmetrical ripple crests are generally oriented perpendicular to the crests (cf. Pettijohn *et al.*, 1987). Therefore, these paleocurrents were oriented NE-SW. Thus, the paleocurrents in this facies show NE-directed unidirectional flow and bidirectional NE-SW directed flow, in keeping with a deepening direction to the NE, as determined for lithofacies SG-1.

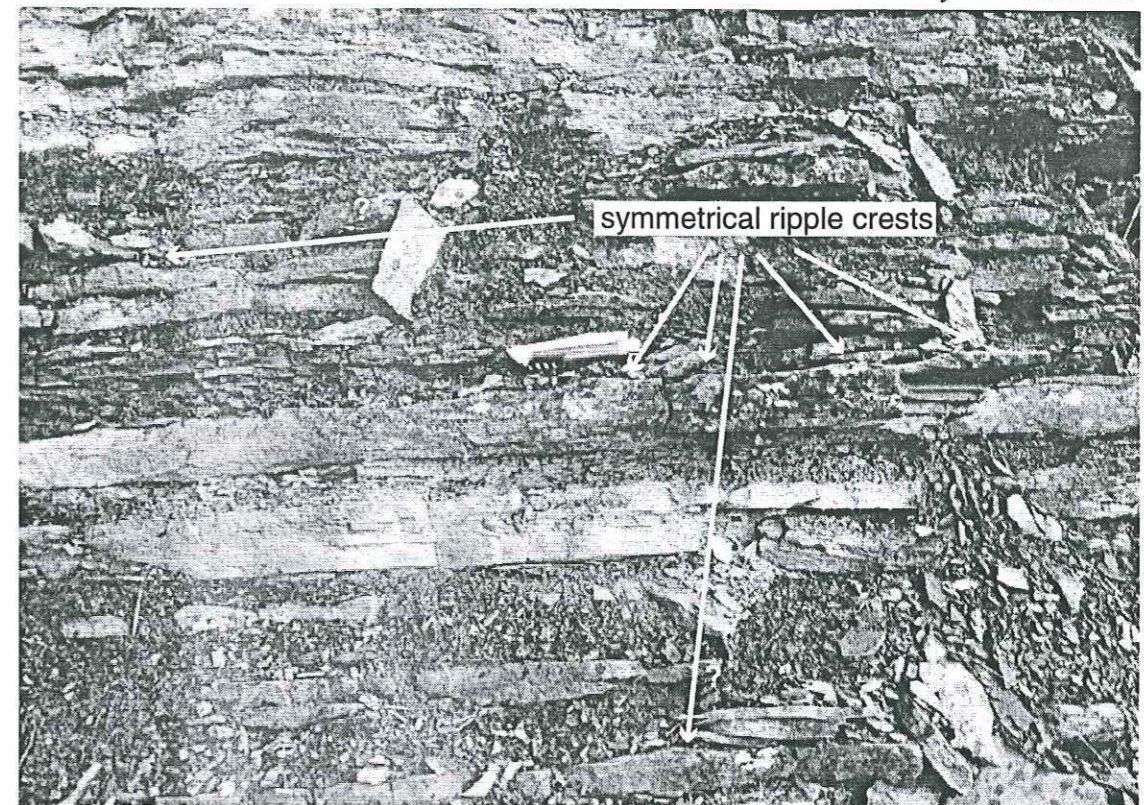


Fig. 5.11. Field photograph of symmetrical ripple marks on the tops of bed of lithofacies SG-4 at Puy de Rioupes, central Dévoluy (located in Fig. 5.1). Knife is 7.5cm long. See Fig. 5.5 for location.

The symmetrical ripples at the top of this facies indicate that it was deposited above fair weather wave base, where bidirectional currents reworked the tops of ripple crests. The relatively short wavelength of the ripples indicates that the depth to wave base was shallow, based on the theory that the radius of orbital water flow patterns which create bidirectional currents on the sea floor is a function of water depth (e.g., Boggs, 1995). Symmetrical ripples are most common in shallow marine settings, where currents are both onshore- and offshore-directed and there is no net transport of sediment (Pettijohn *et al.*, 1987). The beds of this lithofacies are therefore interpreted as relatively shallow marine deposits - possibly the deposits of dilute turbidity currents - that were subsequently reworked by bidirectional currents. Silty and muddy parts of the turbidites were probably originally present, but were removed by currents.

LITHOFACIES ASSOCIATIONS

Two lithofacies associations occur in the Souloise Greywacke Formation. These are interbedded layers of lithofacies SG-1, SG-2, and SG-3 (lithofacies association SG-I) and interbedded layers of lithofacies SG-1, SG-2, SG-3, and SG-4 (lithofacies association SG-II).

Lithofacies association SG-I: Interbedded SG-1, SG-2, and SG-3

Lithofacies association SG-I is comprised of lithofacies SG-1, SG-2, and SG-3 (Figs. 5.2 - 5.4). The

association occurs in the lower half of the Souloise Greywacke Formation (Fig. 5.2). The three lithofacies do not display a predictable vertical arrangement, except that lithofacies SG-2 becomes more common upsection. Lithofacies SG-1 is the most volumetrically significant of the three lithofacies (ca. 80%). Lithofacies SG-2 is the next most common (ca. 15%), and lithofacies SG-3 occurs sporadically (ca. 5%) (Figs. 5.2, 5.4).

Within this association, lithofacies SG-1 commonly occurs in coarsening-up cycles defined by an increase in grain size of the sandy part of the turbidite (e.g., Fig. 5.3). These coarsening-up cycles are arranged into thickening-up cycles, in which each successive coarsening-up cycle is thicker than the previous one (e.g., Fig. 5.3). A coarsening-up cycle typically consists of 2 to 15 beds, while a thickening-up cycle consists of 2 to 4 coarsening-up cycles.

These two hierarchies of cycles imply an overall progradation of the turbidites, although this implication cannot be borne out by three-dimensional geometries due to lack of outcrop. The two sets of cycles additionally imply a systematic control on turbidite deposition, such as autocyclic sediment input (lobe switching of a delta or turbidite fan, for instance) or repetitive allocyclic processes such as relative sea level or climatic changes, or tectonic pulses.

Storm deposits of lithofacies SG-2 punctuate lithofacies association SG-I. These beds do not appear to be related to the coarsening- or thickening-up cycles. This non-cyclicality thus apparently reflects non-rhythmic control on deposition. Similarly, sand-rich examples of the lithofacies association do not display any clear cyclic patterns. In these cases, a more arbitrary pattern of fining- and coarsening-up cycles with no thickening trends is developed (e.g., Figs. 5.2, 5.4).

The preceding arguments lead to the following interpretation of lithofacies association SG-I: organized autocyclic deposition of turbidites and background sediments in moderately deep water was occasionally disrupted by extraordinary non-cyclic events which led to periods of non-predictable deposition. The fine-grained nature of this lithofacies association suggests that it was deposited away from the sedimentary depocenter, in a distal fan or pro-delta setting. The lack of reworking by symmetrical ripples indicates that the association was probably deposited below fair-weather wave base. The more frequent upsection occurrence of lithofacies SG-3 is thought to reflect shallowing conditions from approximately storm wave base to above it.

Lithofacies association SG-II: SG-1, SG-2, SG-3, and SG-4

Lithofacies association SG-II comprises lithofacies SG-1, SG-2, SG-3, and SG-4 (Figs. 5.2, 5.5). It characterizes the upper half of the Souloise Greywacke Formation (Fig. 5.2). This association is in all ways the same as lithofacies association SG-I, except that lithofacies SG-4, which is interpreted as having been deposited above fair-weather wave base, occurs in it (e.g., Fig. 5.4). Thus, whereas lithofacies association SG-I was deposited above storm-wave base, but below fair-weather wave base, lithofacies association SG-II was deposited above fair-weather wave base.

There is no clear consensus of how deep fair-weather wave base extends, but the occurrence of lithofacies SG-4 is considered diagnostic of the change from deeper water to shallower water condi-

tions during deposition of the Souloise Greywacke Formation. The shallowing may be connected with a fall in eustatic sea level, as suggested by Homewood *et al.* (1985, 1986) for a similar succession in time-equivalent deposits in the Swiss Molasse Basin (the Lower Freshwater Molasse). In contrast, Meckel (1995) has suggested that tectonic activity in the external domain may have caused local uplift in Dévoluy that would have outstripped eustatic changes in sea level, and would have resulted in the same succession. Regardless of the cause, a fall in relative sea level leading to an overall shallowing of the depositional systems of the formation is probable.

5.2. Petrography and provenance

The siliciclastic material of the Souloise Greywacke Formation includes significant quantities ($\geq 10\%$ avg.) of monocrystalline and polycrystalline quartz, metamorphic lithic fragments, and metaigneous fragments (almost completely serpentinite) (Table A-I). Subordinate amounts ($\geq 5\%$ avg.) of carbonate lithic fragments are also present (Table A-I). The increase in siliciclastic material relative to the Queyras Marlstone Formation, which is dominated by monocrystalline quartz and carbonate lithic fragments, indicates that a new source area became active and/or was exposed. The presence of significant amounts of serpentinite, which must have been sourced from an ophiolitic domain, indicates an internal Alpine source area (Fig. 1.1).

Plotting the petrographic data on ternary plots developed by Dickinson & Suczek (1979) to determine provenance of sandstones reveals that the Souloise Greywacke Formation was sourced from a recycled collision/arc orogen and an uplifting foreland source (Figs. 5.12a, b, c). The slight input of arc orogen sediments (Fig. 5.12c) may have come from a volcanic arc in the Alps which developed during the latest Eocene and earliest Oligocene (see Chapter 9). The presence of serpentinite in the Souloise Greywacke Formation is reflected in the increased ratio of oceanic to continental components within the recycled orogen field (Fig. 5.12a). As discussed above, the source of the serpentinite was most likely a Mesozoic ophiolite of Tethys. Monocrystalline framework components (quartz, plagioclase, and orthoclase) plot consistently near the quartz pole (Fig. 5.12d). This clustering indicates that the Souloise Greywacke Formation is composed of relatively mature sediments, despite the presence of serpentinite and rock fragments.

5.3. Depositional Setting

During deposition of the Souloise Greywacke Formation, internal Alpine units had been thrust to a position less than 50km east of Dévoluy (Fig. 9.5). The load created by the internal units created a NW-trending basin, deeper in the east near the load, and shallowing to the west (Fig. 9.5; Sinclair, 1996).

If the primary depocenter of the southern sub-Alpine foreland basin were located southeast of Dévoluy, then turbidity currents may have been deflected parallel to the basin axis, leading to N- and NW-directed primary flow in Dévoluy (Fig. 5.9). NE-directed unidirectional ripple foresets in the upper parts of the turbidites probably indicate that the currents banked back towards the deeper

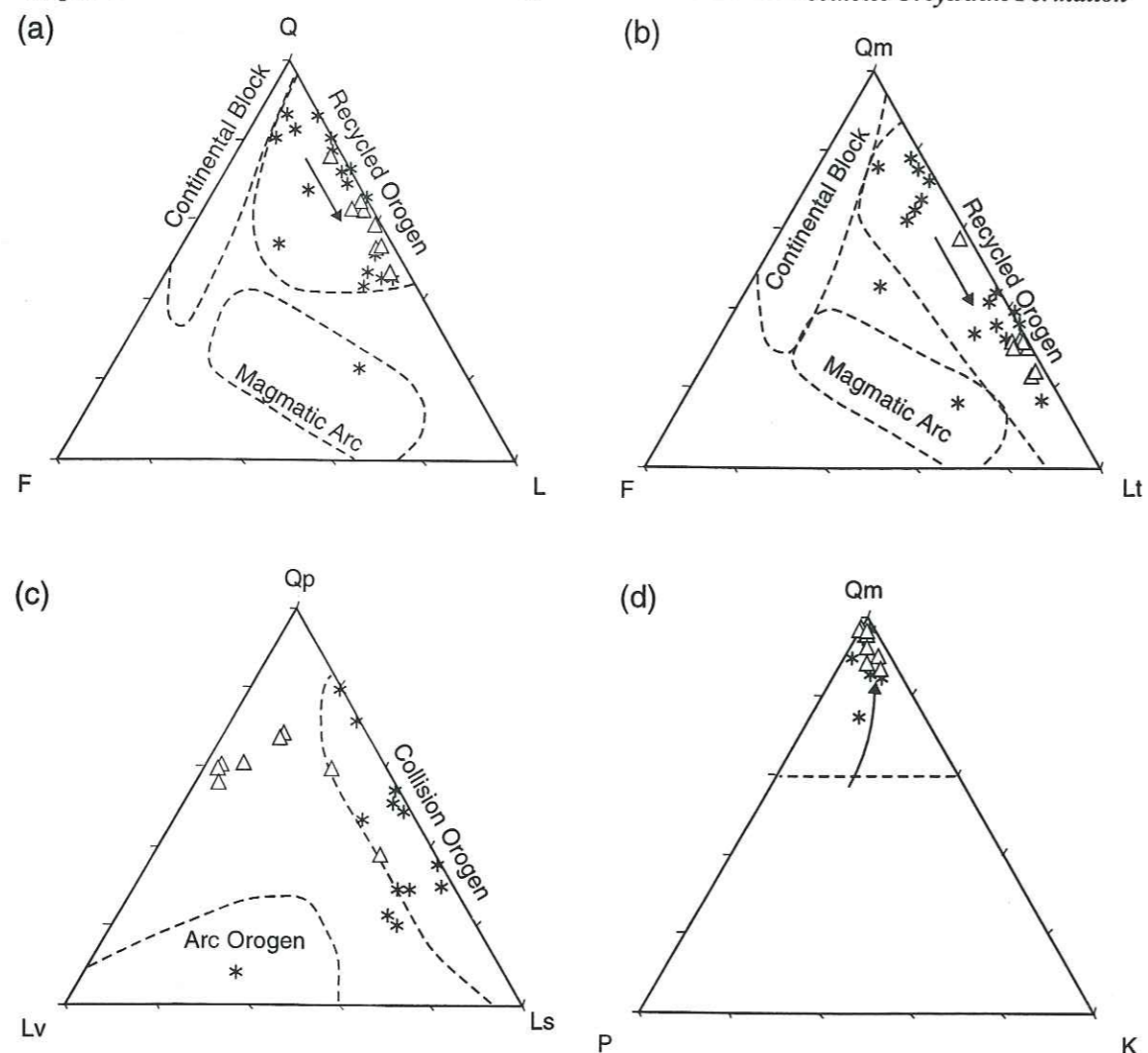


Fig. 5.12. Ternary diagrams illustrating the petrographic composition of the Souloise Greywacke Formation. Data shown as open triangles. (a) Q-F-L plot. Arrow indicates an increasing ratio of oceanic to continental components. (b) Qm-F-Lt plot. Arrow indicates an increasing ratio of chert to quartz. (c) Qp-Lv-Ls plot. (d) Qm-P-K plot. Arrow indicates increasing maturity. Dashed line indicates 60% monocrystalline quartz. All poles are Gazzi-Dickinson combined categories (see Appendix A-1). Provenance fields, asterisks (data points from modern foreland basin and collision orogen sediments), and arrows after Dickinson & Suczek (1979). See text for more detailed discussion of plots.

part of the basin axis during waning flow. In this hypothesis, the internal Alpine debris in the Souloise Greywacke Formation was transported from the south, and not the east, as might otherwise be expected.

The fine-grained nature of the turbidites in Dévoluy probably reflect its position on the distal edge of the Alpine foreland basin (Fig. 9.5), in that coarser-grained sediments would presumably have been preferentially trapped in the more proximal part of the basin, and only the dilute tails of the turbidity currents would have reached Dévoluy.

The upsection succession from lithofacies association SG-I to lithofacies association SG-II documents shallowing conditions at the distal edge of the basin, from above storm wave base, but below fair weather wave base, to above it. The Queyras Marlstone Formation beneath the Souloise Greywacke Formation is interpreted to have been deposited in a shelf to slope setting. The turbid-

ites of the Souloise Greywacke Formation are therefore interpreted as having been deposited in a shallowing basin (Meckel *et al.*, 1996), possibly in a delta-front environment, as suggested for the time-equivalent distal turbidites of the Lower Marine Molasse of central Switzerland (Homewood *et al.*, 1985; Sinclair *et al.*, 1991). The turbidites of the Lower Marine Molasse have alternately been interpreted as the deposits of a prograding "Normark-type" turbidite fan (Diem, 1986), but there is not enough three-dimensional outcrop control in Dévoluy to ascertain whether the Souloise Greywacke Formation was deposited as part of a similar fan system.

The change from deepening-up conditions documented in the Queyras Group to shallowing-up conditions in the Souloise Greywacke Formation coincides with a change from carbonate-dominated to siliciclastic-dominated deposition. This fundamental reorganization of depositional systems is discussed in Chapter 9.

CHAPTER 6

The St-Disdier Arenite Formation

The St-Disdier Arenite Formation occurs above the Souloise Greywacke Formation and below the St-Disdier Siltstone Formation in the Souloise Group. The St-Disdier Arenite Formation has previously been interpreted as the lateral equivalent of the Priabonian Queyras Marlstone and Eocene-Oligocene Souloise Greywacke Formations on the *St-Bonnet* geologic map (BRGM, 1980d), and also by Paris *et al.* (1983, 1984a). Alternatively, it has been correlated with the deep marine turbidite deposits of the uppermost Eocene Champsaur Sandstone and similar deposits around the Alpine foreland basin (Paris, 1988; Waibel, 1990). Finally, on the *Gap* geologic map, Gidon *et al.* (BRGM 1971) postulated that, south of Dévoluy, the St-Disdier Arenite Formation ("molasse verte") is the lateral equivalent of the St-Disdier Siltstone Formation ("marnes et molasse rouge") and Montmaur Conglomerate Formation ("poudingues exotiques [Nagelfluh]"). Each of these correlations is considered problematic because of differences in petrography, lithofacies, and/or age.

The formation does not contain biostratigraphically significant fossils (BRGM, 1980d), but is considered to be early Oligocene (Rupelian) in age because of its stratigraphic position between the uppermost Priabonian - lowermost Oligocene Souloise Greywacke Formation and the upper Oligocene (Chattian) St-Disdier Siltstone Formation.

The St-Disdier Arenite Formation crops out predominantly west of the Median Dévoluy Thrust and also in two northern localities east of it (Fig. 6.1). It is at least 14 m thick in the Tête de la Tune section in northern Dévoluy (Fig. 6.2), more than 25 m in the Puy de Rioupes section in central Dévoluy (Fig. 6.3), approximately 105 m in its most complete outcrop, at the Torrent des Pertusets section in western Dévoluy (Fig. 6.4), more than 5 m at the Château Roland section in southwestern Dévoluy (Fig. 6.5), and at least 46 m at the La Cluse section in southwesternmost Dévoluy (Fig. 6.6). Because there is no complete outcrop of the formation, lateral variations in its depositional thickness are not known. However, based on outcrop restraints, it is probably no more than 110 m thick.

The lower bounding surface of the St-Disdier Arenite Formation is a progressive unconformity. The erosional hiatus of the unconformity decreases from west to east, and the contact with the Souloise Greywacke Formation in central Dévoluy is conformable (see Section 6.2). The upper boundary of the St-Disdier Arenite crops out in the La Cluse measured section (Fig. 6.6). It is defined at the first appearance of red or yellow mud- and siltstones in the section.

The type section of the St-Disdier Arenite Formation is located at Torrent des Pertusets in western Dévoluy (Fig. 6.4). The section is characterized by fine- to medium-grained sandstones that grade upsection into coarsening-up parasequences of finer-grained material.

Five lithofacies are present in the St-Disdier Arenite Formation (Table 6-I): cross-bedded and rippled sandstone (lithofacies SDA-1); chaotically-bedded medium- and coarse-grained sandstone

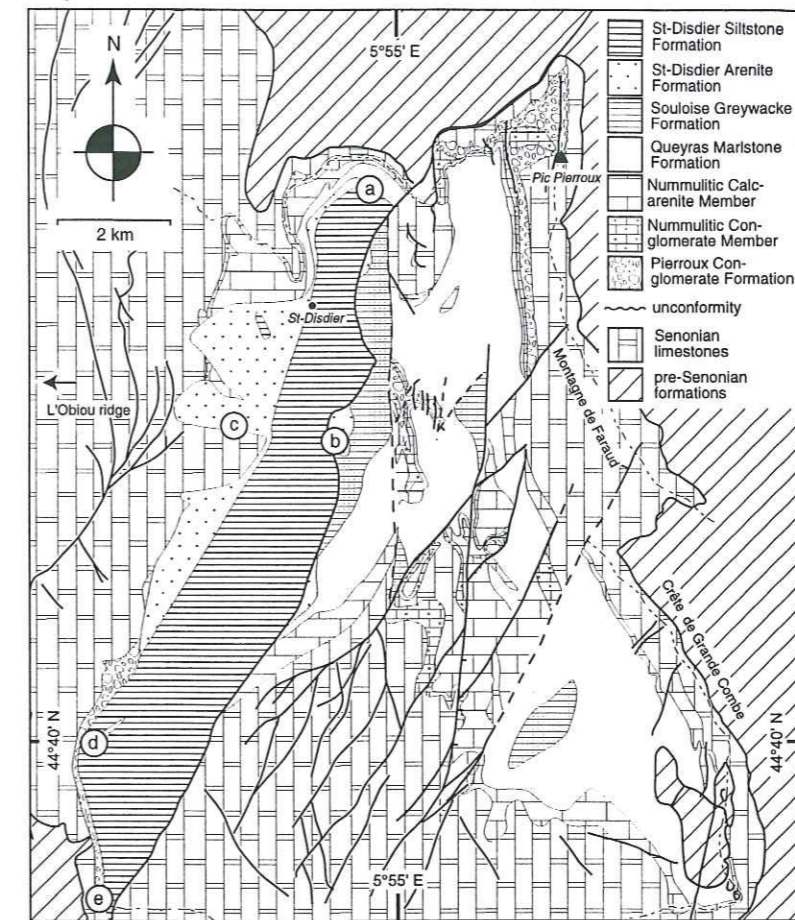


Fig. 6.1. Geologic map of Dévoluy, indicating measured sections of the St-Disdier Arenite Formation. a = Tête de la Tune section; b = Puy de Rioupes section; c = Torrent des Pertusets section (type section); d = Château Roland section (outcrops smaller than map resolution); e = La Cluse section.

Lithofacies	Description	Interpretation
LSD-1	Cross-bedded and rippled sandstone	upper to middle shoreface
LSD-2	Chaotically-bedded medium- and coarse-grained sandstone	soft-sediment deformation, upper to middle shoreface
LSD-3	Heterolithic mud-, silt- and very fine-grained sandstone	fluvially-sourced flood-surge sediments
LSD-4	Coarsening-up, very fine- to medium grained sandstone	crevasse splay/interdistributary bay deposits; delta-plain environment
LSD-5	Graded gravel	progradation of fluvial systems
Lithofacies association		
LSD-I	Interbedded LSD-1, LSD-2, and LSD-3, and LSD-5	prograding wave-dominated delta/barrier bar system/strandplain

Table 6-I. Summary of lithofacies and lithofacies associations of the St-Disdier Arenite Formation.

(lithofacies SDA-2); heterolithic mud-, silt-, and very fine-grained sandstone (lithofacies SDA-3); coarsening-up very fine- to medium grained sandstone (lithofacies SDA-4); and graded gravel (lithofacies SDA-5).

6.1. Lithofacies analysis and stratigraphy

Lithofacies SDA-1: Cross-bedded and rippled sandstone

Lithofacies SDA-1, the diagnostic lithofacies of the formation, is a coarse- to fine-grained, green to grey-green sandstone with very little interstitial mud. Most beds of this lithofacies are medium-

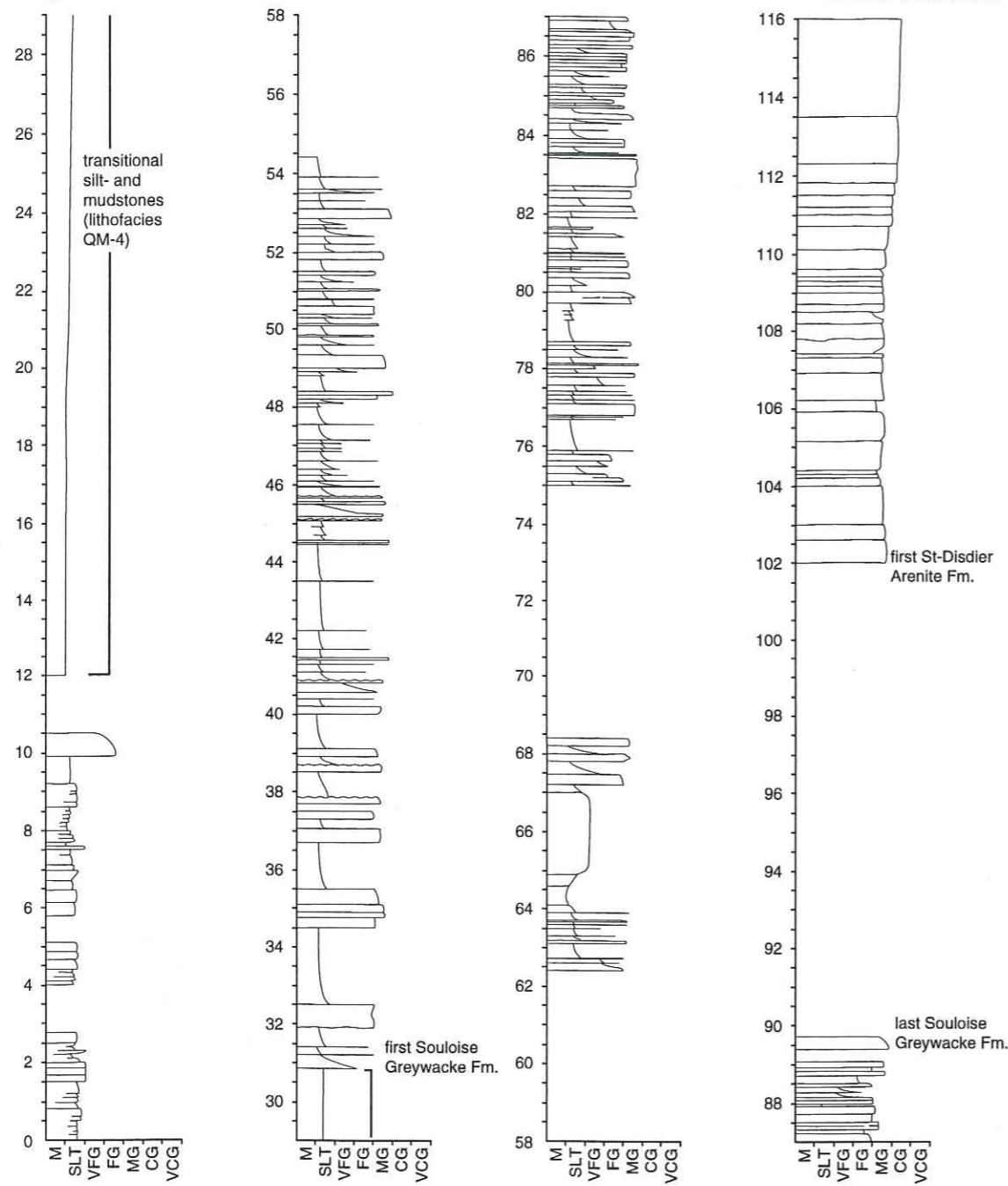


Fig. 6.2. Measured section of the Queyras Marlstone, Souloise Greywacke, and St-Disdier Arenite formations at Tête de la Tune, northern Dévoluy (scale in meters). All beds of the St-Disdier Arenite Formation are lithofacies SDA-1. Location indicated in Fig. 6.1.

grained (Figs. 6.3 - 6.6). The lithofacies has moderately- to well-sorted grains that are subangular to well-rounded.

The sandstone occurs in 5 to 250 cm thick beds that display massive bedding, planar, tabular, and trough cross bedding, asymmetrical, symmetrical, and climbing ripples. One or two of these structures typically dominates a given bed. Massive or planar bedding and low-angle trough cross-bedding, the most common sedimentary structures, are best-developed in the medium grained sandstones, although they occur in beds of all grain sizes. Unidirectional ripples are fairly common

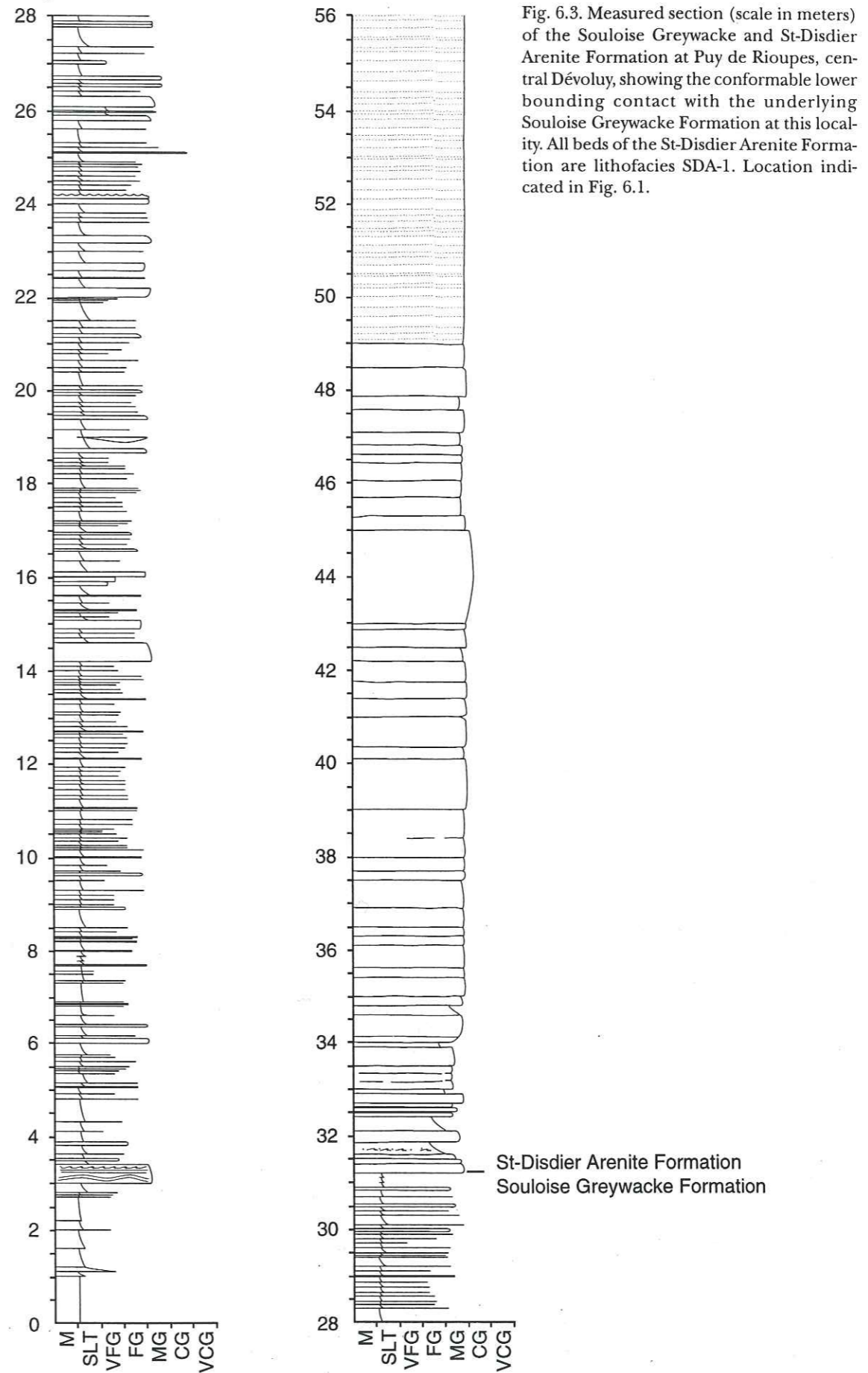


Fig. 6.3. Measured section (scale in meters) of the Souloise Greywacke and St-Disdier Arenite Formation at Puy de Rioupes, central Dévoluy, showing the conformable lower bounding contact with the underlying Souloise Greywacke Formation at this locality. All beds of the St-Disdier Arenite Formation are lithofacies SDA-1. Location indicated in Fig. 6.1.

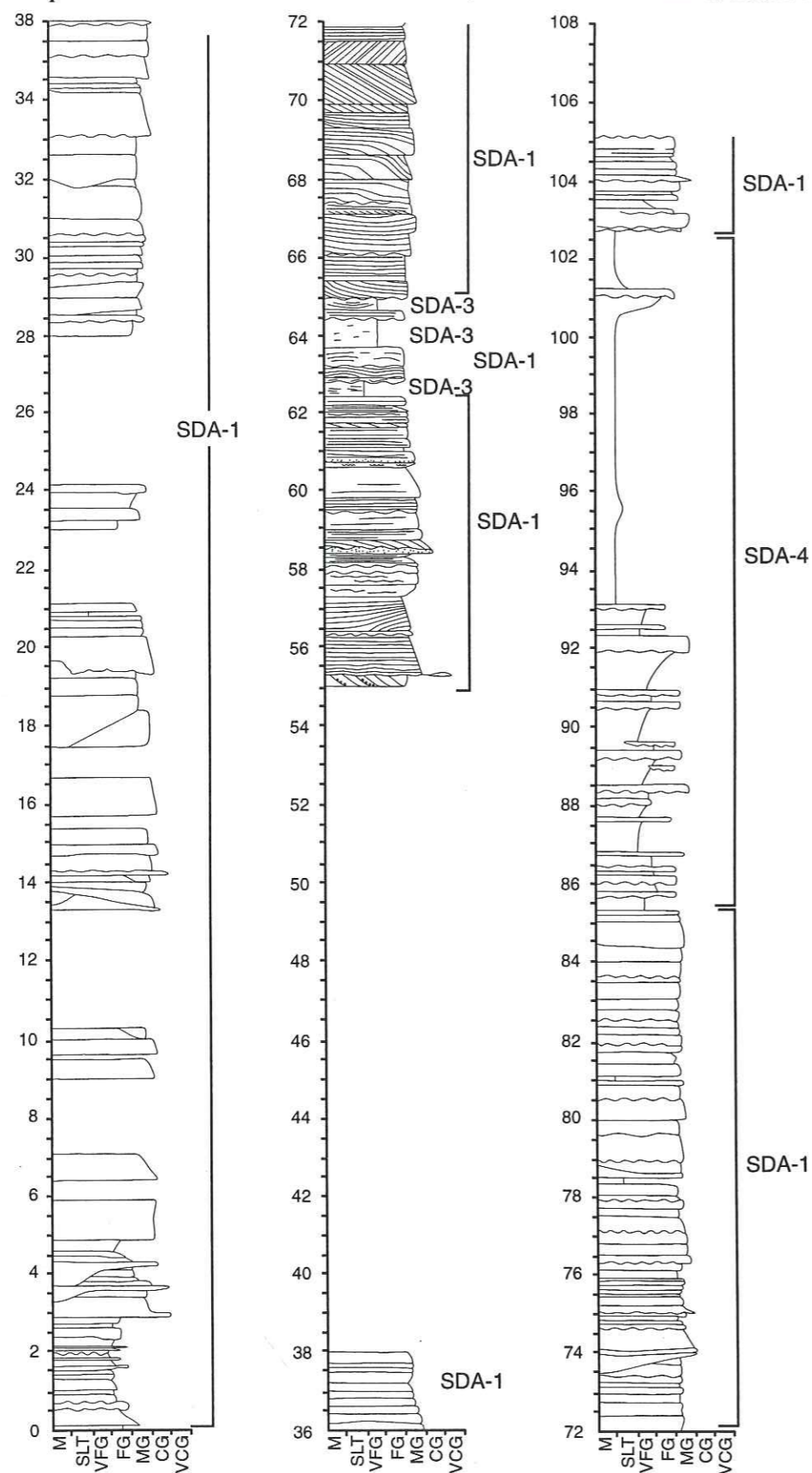


Fig. 6.4. Type section of the St-Disdier Arenite Formation at Torrent des Pertusets, western Dévoluy (scale in meters). Lithofacies indicated beside section. This is the only nearly complete section of the formation. Location indicated in Fig. 6.1. Detailed sedimentary structures from 55 - 72 m are typical of the section.

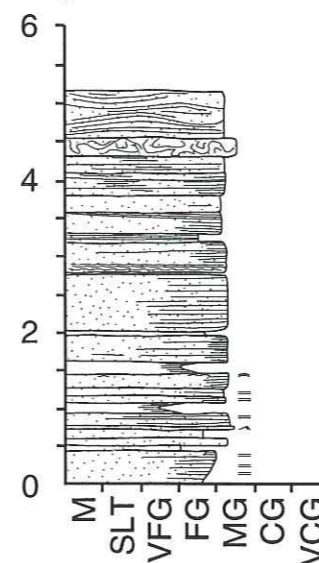


Fig. 6.5. Measured section of the St-Disdier Arenite Formation at Chateau Roland, southwestern Dévoluy (scale in meters). Very fine grained sandstones are lithofacies SDA-3. The bed from 4.30 - 4.55 m is lithofacies SDA-2. All other beds are lithofacies SDA-1. Location indicated in Fig. 6.1.

and occur in beds of all grain sizes except coarse-grained sandstone. Climbing ripples either occur on trough foresets, in which case they show paleocurrents in the opposite direction of the trough foresets, or are unrelated to other sedimentary structures. Tabular cross beds, which occur in medium- and coarse-grained sandstones, and symmetrical ripples, which occur in finer-grained beds, are the least common structures.

The lower bounding surfaces of beds of this facies are undular to planar, as are the upper surfaces. Beds are distinguished by changes in grain size, changes in sedimentary structures across bedset surfaces, erosional contacts between beds, or by well-delineated bedding planes. Undular lower surfaces are erosive. Planar surfaces may also be erosional, in which case sedimentary structures of the underlying bed are truncated, or may be apparently conformable, as when beds with planar laminations overlie each other. Beds have tabular to lenticular external geometries, depending on the amount of erosion present. Most beds are discontinuous over the length of an outcrop.

Paleocurrents were measured using trough foreset and trough axis orientations, and also tabular foreset orientations, ripple crest orientations, and ripple foreset orientations. No sole marks or other erosional features were found on the lower surfaces of beds. Current data are strongly bidirectional, with a strong component of NE-SW flow and a secondary component of NW-SE flow (Fig. 6.7). Scatter in the data (Fig. 6.7) is primarily due to a wide spread of orientations of foresets. Trough axis orientations are less variable (cf. Meckel, 1967) and show preferential flow to the southwest in northern Dévoluy.

There are few organic remains preserved in the sediments, the most common of which are carbonaceous plant debris. There is also occasional bioturbation in finer-grained beds (e.g., Fig. 6.4, 102.75 - 105 m), which occurs as poorly-defined subvertical burrows up to 2cm wide and 5cm long (ichnogenus *Ophiomorpha*?). In other fine-grained beds towards the top of the section, the uppermost few centimeters of the beds have root traces (e.g., Fig. 6.6, 30.50 - 32.00 m and 43.20 m). The root traces are distinguished from the burrows by being thinner and longer (usually $\ll 0.05$ cm wide, and up to 8 cm long), by their bifurcating-downward structure, and by the buff aureoles that surround them.

Lithofacies SDA-1 is characterized by relatively uniform, medium-grained sandstone with well-sorted and -rounded grains. Sedimentary structures show two opposing current directions, interpreted as reflecting the back-and-forth action of waves in a shallow marine (tidal?) setting. The oscillatory flow led to deposition of well-sorted, well-rounded sandstones, and to the removal of the finer-grained components. The scarcity of bioturbation indicates a relatively high-energy environment where the substratum was constantly being shifted, such that marine plants and burrowing

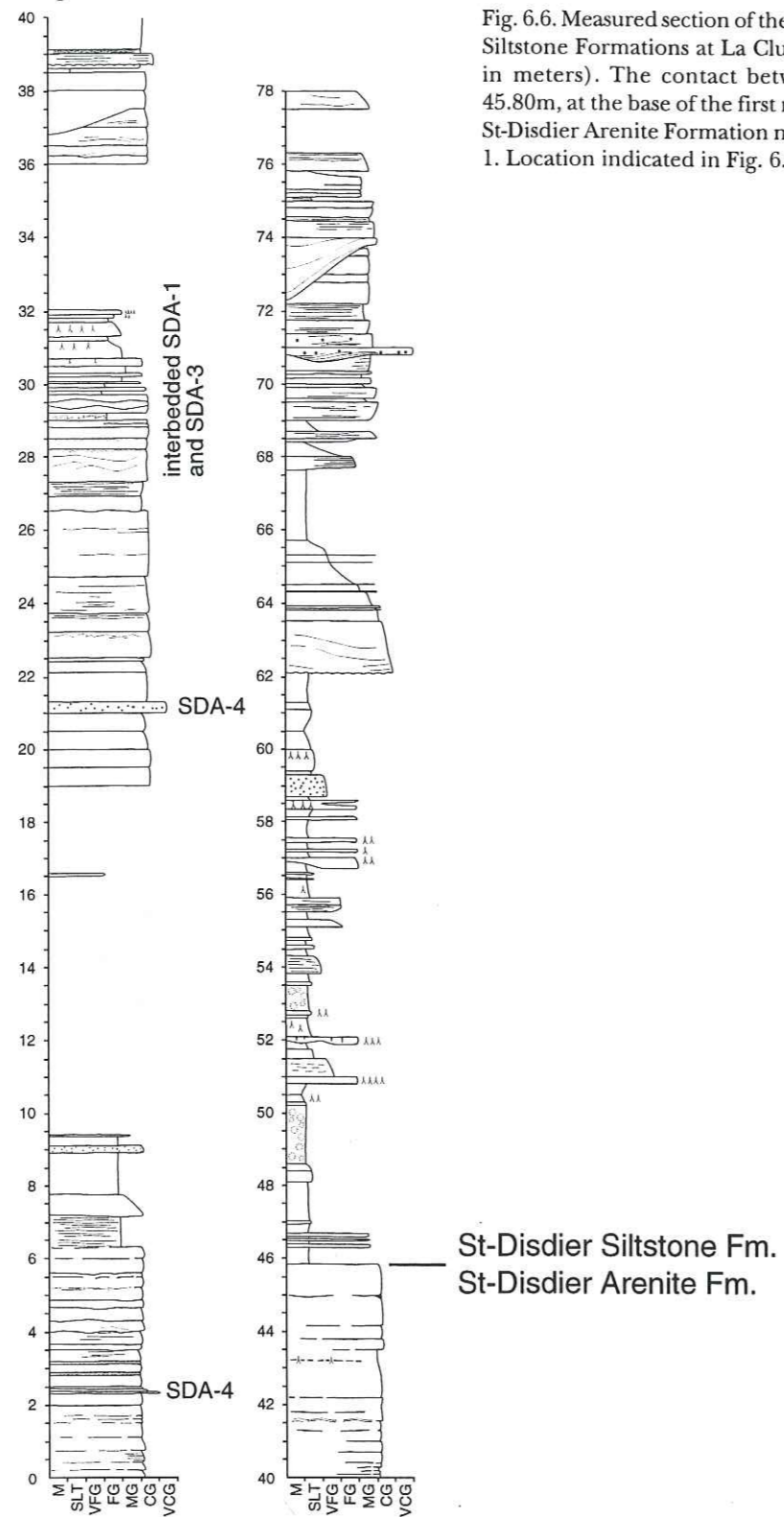


Fig. 6.6. Measured section of the St-Disdier Arenite and St-Disdier Siltstone Formations at La Cluse, southwestern Dévoluy (scale in meters). The contact between the formations occurs at 45.80m, at the base of the first red siltstone layer. All beds of the St-Disdier Arenite Formation not indicated are lithofacies SDA-1. Location indicated in Fig. 6.1.

animals could only rarely establish themselves. The beds are relatively discontinuous, but are not typically channelized, which indicates that bedform migration dominated over incisional erosion. The bedforms probably had primarily sinuous crests, based on the preferential preservation of trough cross-bedding over tabular foresets. These characteristics are consistent with a shorezone

setting where on- and offshore directed waves were dominant over channelized deposition and longshore currents.

The general lack of diagnostic subaerial features (cement textures, dehydration structures) indicates that the environment was probably marine. However, there may have been periodic exposure or shallower water conditions, such that plants could become established in the upper part of the formation. Such conditions would tend to occur in the shallow shoreface. The lack of significant amounts of mud- and silt-sized material precludes a lower shoreface setting. Therefore, this lithofacies is thought to represent deposition in the upper to middle shoreface.

Lithofacies SDA-2: Chaotically-bedded medium- and coarse-grained sandstone

Lithofacies SDA-2 occurs seldomly in the St-Disdier Arenite Formation. The lithofacies is composed of medium- to coarse-grained, moderately-sorted sandstone with well-rounded grains. The sandstones are green.

The internal bedding of the lithofacies is chaotic and discontinuous (e.g., Fig. 6.5, 4.25 - 4.5m). There is no preferred orientation of fold structures within a bed, and original bedding is completely distorted, so no fold orientations and paleocurrent directions could be measured.

The lower bounding surfaces of this lithofacies are planar. Upper bounding surfaces are planar to slightly undular. Beds are continuous over the length of an outcrop. Beds of this lithofacies are 0.25 - 0.50 m thick.

No fossils or trace fossils were found in this lithofacies. However, carbonaceous debris is common.

The chaotic internal structures in this lithofacies are indicative of soft sediment deformation, in which the sand became unstable soon after deposition and bedding was disrupted. Possible causes for such instabilities include an excess of pore water because of rapid deposition of the bed and subsequent deposition of the next sandstone bed, storm-induced wave activity, minor tectonic perturbances, or oversteepening of the depositional slope by sedimentary processes.

Lithofacies SDA-3: Heterolithic mud-, silt- and very fine-grained sandstone

Lithofacies SDA-3 is composed of beds consisting of unsorted, brown to brownish-green mud, silt, and very fine-grained sand. The silt- and sand-sized particles are well-rounded. Silt or sand-sized particles are dominant. Occasionally, inverse grading is observed. Beds, 0.2 - 7.5 m thick, are sometimes characterized by mm-scale lamination. The lithofacies does not occur in the lower part of the formation (Figs. 6.3, 6.4), but tends to occur towards its top (e.g., Figs. 6.5).

Lower bounding surfaces of beds are sharp, and delineate an abrupt change from the underlying lithofacies to lithofacies SDA-3. Upper bounding surfaces are almost always eroded and are generally concave up. Thinner beds often have lenticular external geometries that are discontinuous over a few meters. Thicker beds may be continuous over the length of a given outcrop.

There is abundant carbonaceous debris in many of the layers. This material is fine-grained and

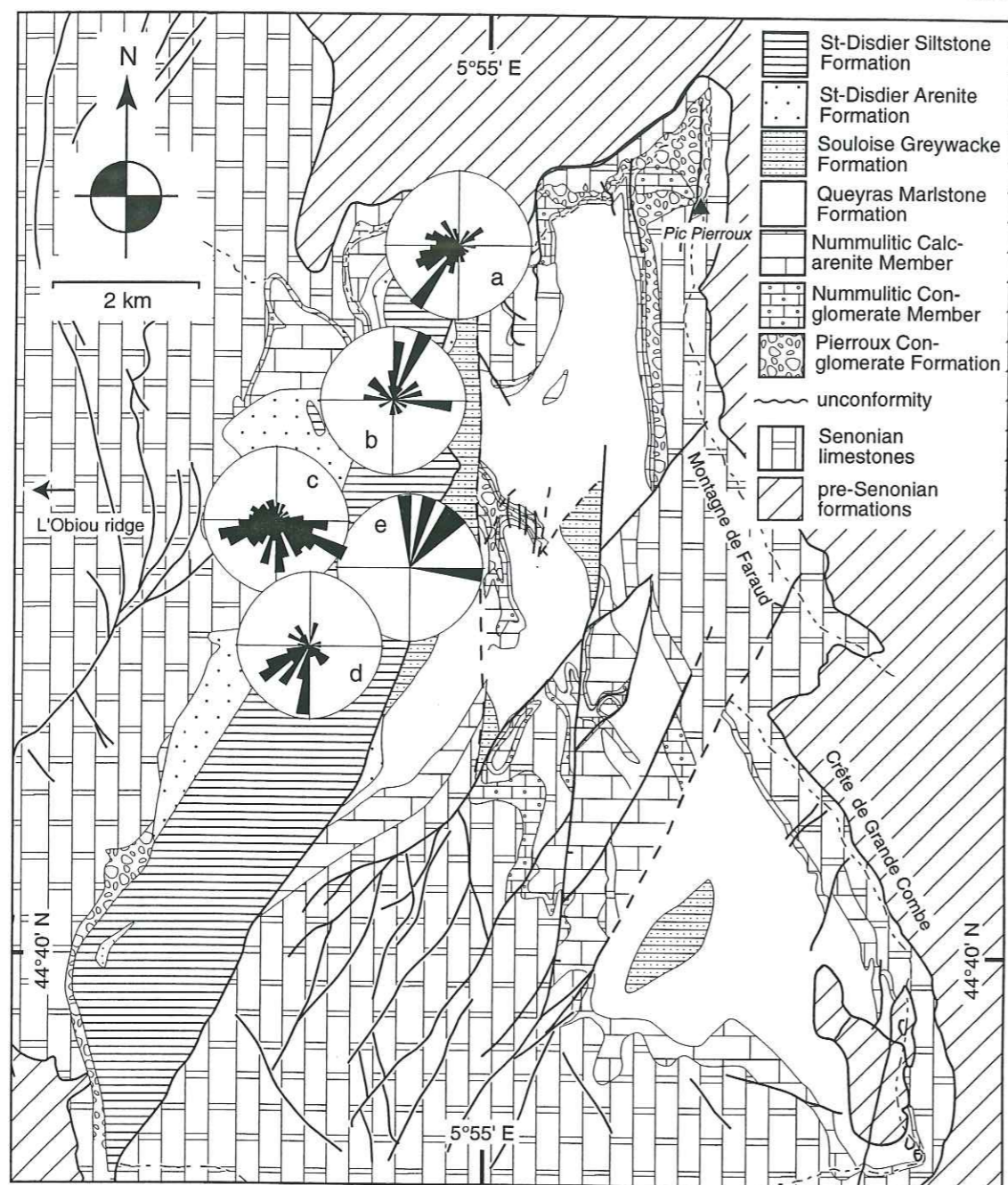


Fig. 6.7. Paleocurrent analysis of the St-Disdier Arenite Formation, corrected for post-depositional tectonism. Localities as in Fig. 6.1. (a) Tête de la Tune (116 data; circle = 11%). (b) Approximately 500m E of the village of St-Disdier (35 data; circle = 14%). (c) Torrent des Pertusets (320 data; circle = 7%). (d) Grand Villard, located 1km south of the Torrent des Pertusets section (48 data; circle = 13%). (e) Puy de Rioupes (5 data; circle = 20%). All data include ripple, trough, and tabular foreset orientations, trough axis orientations, ripple crest orientations, and orientations of strongly erosional surfaces.

occurs preferentially at the tops or bottoms of beds. The common lack of internal sedimentary structures may be due to bioturbation, although there is a lack of trace fossils.

The relatively fine-grained nature of these beds relative to the other lithofacies of the St-Disdier Arenite Formation indicates a calmer environment. The reason for these periods of relative calm is enigmatic. The lack of macrofossils indicates that the depositional environment was not protected,

such as in a lagoon, where fauna would presumably have thrived. These sediments may alternatively represent flood-surge muds, deposited on the shelf from an unidentified fluvial plume.

Lithofacies SDA-4: Coarsening-up, very fine- to medium grained sandstone

Lithofacies SDA-4 is composed of (1) inversely graded silty sandstone and (2) well-sorted, well-rounded, fine- to medium-grained, lenticular sandstone beds. Beds are brownish green, becoming greener upsection, which reflects decreasing mud content upsection. The lithofacies occurs only in the Tête de la Tune section, from 86.70 to 101.25 m (Fig. 6.4).

The lower part of this lithofacies is characterized by planar stratification. Upsection, where the lithofacies is sand-rich, there are no internal structures. Lower and upper bounding surfaces of the lithofacies are sharp and planar, with no evidence of erosion. However, there is usually an internal, concave-up erosion surface between the finer- and coarser-grained fractions of the lithofacies. Above the erosion surface, the sandstones appear to fill channels. The lithofacies ranges in thickness from 0.5 - 1.25 m; the medium-grained sandstones at the tops range from 0.1 - 0.4 m.

The sedimentology of this lithofacies in the lower part of the formation is similar to that of lithofacies SDA-3, which is interpreted as the fine-grained deposits of a flood-surge sediment plume. However, lithofacies SDA-4 is distinguished from lithofacies SDA-3 by its inverse grading, the presence of structureless, channelized sandstones at the top of lithofacies SDA-4, and the repetitive, stacked occurrence of lithofacies SDA-4 in only one part of the St-Disdier Arenite Formation, all of which suggest that these beds are not storm surge deposits, but probably crevasse splay or interdistributary bay sediments deposited in a delta-plain environment (e.g., Pettijohn *et al.*, 1987). Such deposits are coarsening-up and occur above progradational prodelta and delta-front sediments (Pettijohn *et al.*, 1987). If the beds were storm surge deposits, then their stacked nature would indicate the unlikely occurrence at least 15 such surges occurring without the preservation of intervening sediments.

Lithofacies SDA-5: Graded, very coarse sandstone and gravel

Facies SDA-5 is represented by light green to whitish green, crudely graded beds composed of moderately- to poorly-sorted coarse sand and gravel with angular to well-rounded grains. Very little interstitial mud is present, and the grains are poorly cemented. This lithofacies does not occur often in outcrop, but is instead found as float on hillsides where the St-Disdier Arenite Formation crops out. The sands appear to have the same composition as the other lithofacies, although this has not been confirmed by petrographic inspection.

Lower bounding surfaces are sharp or undular; when undular, they are erosional. Upper bounding surfaces are planar to undular, and are most often, though not always, eroded to some extent. They are recognized by sharp grain-size variations between these and overlying beds. The beds have tabular to lenticular external geometries and are 0.25 - 1 m thick.

Lithofacies SDA-5 contains the coarsest sediment in the St-Disdier Arenite Formation. Its infre-

quent occurrence therefore appears to be associated with short, sudden pulses of coarse sedimentation. The most likely explanation for such pulses is increased terrigenous input into the basin. Storm deposits are generally finer-grained (Brenchley, 1989), so this particular interpretation is considered unlikely. Rather, the sediment was probably brought into the system by momentary progradation of more proximal fluvial sources. Such progradation may have been associated with increased sediment input into the fluvial system.

LITHOFACIES ASSOCIATION

Only one lithofacies association has been determined for the St-Disdier Arenite Formation. It occurs throughout the St-Disdier Arenite Formation, and is composed of interbedded layers of lithofacies SDA-1, SDA-2, SDA-3, and SDA-5. The unique occurrence of lithofacies SDA-4 at the Torrent des Pertusets outcrop precludes its inclusion in the lithofacies association.

Lithofacies Association SDA-I: Interbedded SDA-1, SDA-2, SDA-3, and SDA-5

Lithofacies association SDA-I is primarily made up of beds of lithofacies SDA-1 (ca. 85% of the association). Beds of lithofacies SDA-2 (ca. 5%), SDA-3 (ca. 5%), and SDA-5 (ca. 5%) occur sporadically (Figs. 6.2, 6.3, 6.5). There is no predictable upsection arrangement of the four lithofacies, except that lithofacies SDA-3 has not been found in the lowermost part of the formation (Figs. 6.3, 6.5; gaps in the section could represent beds of lithofacies SDA-3).

The dominance of lithofacies SDA-1 in the association implies that shoreface sedimentation was the dominant process, and occurred more or less continuously during deposition of the St-Disdier Arenite Formation. Periods of soft-sediment deformation (lithofacies SDA-2), relatively fine-grained deposition (lithofacies SDA-3), and relatively coarse-grained deposition (lithofacies SDA-5), all of which are consistent with the interpreted shoreface setting (Galloway & Hobday, 1983; Pettijohn *et al.*, 1987), punctuated overall deposition of the medium-grained sand (Figs. 6.4 - 6.6). Because the subordinate lithofacies occur infrequently, it seems that these periods of less-characteristic deposition are not related to significant variations in shoreface deposition.

However, the unique occurrence of 17.5 m of beds of lithofacies SDA-4 at the top of the Torrent des Pertusets section (Fig. 6.3) may represent a longer-term change in the depositional environment of the St-Disdier Arenite Formation. If these beds represent interdistributary bay or crevasse splay deposits, then this lithofacies represents a transition from medium-grained clastic shoreface deposition to finer-grained delta-plain deposition. Such transitions represent a change from deltaic submarine progradation to subaerial aggradation (e.g., Galloway & Hobday, 1983; Pettijohn *et al.*, 1987, their Fig. 10-33).

The depositional system responsible for the deposition of lithofacies association SDA-I could have been a wave-dominated delta, a barrier bar system, or a strandplain, but better three-dimensional control on geometries and lateral facies variations is necessary to discriminate between these

6.2. Rupelian thrusting and uplift: the development of the western Dévoluy unconformity

A local unconformity occurs at the base of the St-Disdier Arenite Formation (Fig. 6.9). At Puy de Rioupes in central Dévoluy, in the hanging wall of the Median Dévoluy Thrust (Fig. 6.1), the St-Disdier Arenite Formation appears abruptly above the Souloise Greywacke Formation (Fig. 6.3). The beds of the two formations are parallel and there is no evidence of erosion, so the two formations are interpreted to be conformable. There may, however, be a disconformity between them. At Tête de la Tune in northern Dévoluy (Fig. 6.1), the same relationship is inferred in the foot wall of the Median Dévoluy Thrust (Fig. 6.2). Two kilometers to the west of Tête de la Tune, the Souloise Greywacke Formation is absent and the St-Disdier Arenite Formation lies with an erosive contact upon the Queyras Marlstone Formation (Fig. 6.8). To the west, the St-Disdier Arenite Formation unconformably overlies first the Dévoluy Nummulitic Limestone Formation and then the Senonian limestones (Fig. 6.1). These relationships are schematically illustrated in Figure 6.9.

This lower bounding unconformity suggests that the western border of Dévoluy was tilted and eroded before or during deposition of the St-Disdier Arenite Formation, which overlapped the eroded western flank of the basin, but was deposited in an apparent continuum in central Dévoluy. This previously unrecognized unconformity is significant because it reflects tectonism in Dévoluy which may be related to the shallowing documented from the Souloise Greywacke Formation to the St-Disdier Arenite Formation.

The cause of the uplift is unknown. It is possible that a blind thrust exists at depth that would have caused local uplift in Dévoluy (Fig. 6.9). Another possibility is that the uplift reflects forebulge uplift associated with more internal orogenic loading.

6.3. Petrography and Provenance

The St-Disdier Arenite Formation is composed of significant amounts ($\geq 10\%$ avg.) of monocrySTALLINE and polycrystalline quartz, carbonate lithic fragments, and meta-volcanic lithic fragments (about half of which is serpentinite) (Table A-I). Orthoclase, plagioclase, and siliciclastic and metamorphic lithic fragments are present in subordinate amounts ($\geq 5\%$ avg.) (Table A-I). The percentages of quartz and metamorphic lithic fragments decrease with respect to the Souloise Greywacke Formation, whereas the percentages of feldspar, volcanic, carbonate, and siliciclastic lithic clasts increase. The serpentinite content remains approximately the same (Table A-I). These changes in the composition of the siliciclastic input into the Dévoluy area indicate that the source area of the sediments was more complex: both locally-sourced carbonate and distantly-sourced "exotic" material increase at the expense of quartz (a 16% decrease). The increase in complexity is possibly related to, on the one hand, the uplift of western Dévoluy, which would have introduced a new source of carbonate clasts, and, on the other hand, the emplacement of the Embrunnais-Ubaye



Fig. 6.8. Erosional contact between the St-Disdier Arenite Formation (above) and the Queyras Marlstone Formation (below). This outcrop occurs approximately 2km west of the Tête de la Tune measured section. 35mm lens cap for scale.

internal nappes to the east. Thermoluminescence characteristics of sand-sized quartz grains is consistent with a Penninic (Embrunnais-Ubaye) source (Ivaldi, 1989).

Plots of sandstone provenance indicate that the St-Disdier Arenite Formation is less mature than the Souloise Greywacke Formation, in that all plots indicate increased amounts of lithic fragments or monocrystalline feldspar (compare Fig. 6.10 with Fig. 5.12).

Although the Q-F-L (Fig. 6.10a) and Qm-F-Lt (Fig. 6.10b) plots still indicate that this formation is sourced from a recycled orogen, the data are less grouped along the Q-L and Qm-Lt joins. Moreover, a significant amount of the data falls outside the boundaries of a recycled orogen as defined by Dickinson & Suczek (1979). These two factors are interpreted as reflecting the complex influence of the two source areas east and west of the basin.

Additionally, the type of orogen that sourced the sediments is very poorly-defined in terms of Dickinson & Suczek's (1979) categories: the data plot between the collision and arc orogen fields, with a few data falling in the arc orogen field (Fig. 6.10c). This mixed influence is probably due to siliciclastic material derived from both the Embrunnais-Ubaye nappes (Kerckhove, 1969) and the volcanic arc that provided detritus to the Champsaur Sandstone to the east of Dévoluy (Waibel, 1990).

Finally, the Qm-P-K plot (Fig. 6.10d) documents very clearly the decreased maturity of the St-Disdier Arenite Formation relative to the Souloise Greywacke Formation (compare with Fig. 5.12d).

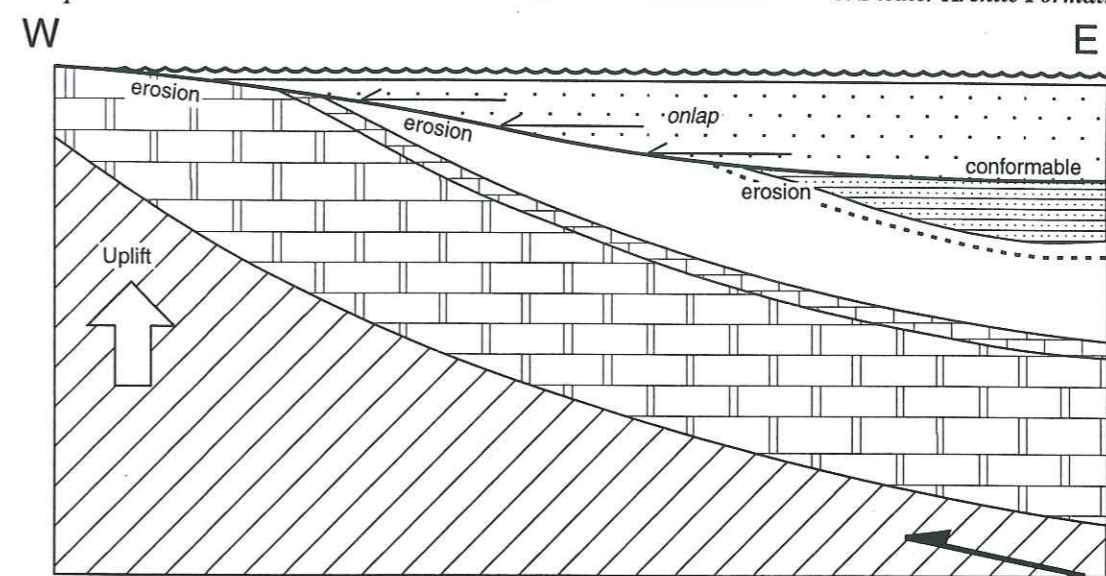


Fig. 6.9. Schematic cross section illustrating the unconformity at the base of the St-Disdier Arenite Formation, and showing the onlap of the St-Disdier Arenite Formation onto increasingly older formations to the west. Horizontal scale approximately 3 km. Vertical scale approximately 750 m. Patterns as in Fig. 6.1.

The samples all plot away from the quartz pole, and exhibit a spread towards both the plagioclase and orthoclase poles.

6.4. Depositional Setting

The transition from the shallowing-up Souloise Greywacke Formation to the St-Disdier Arenite Formation suggests that they were deposited in a successively shallower marine setting. This hypothesis is supported by the presence of bidirectional currents, which suggest that the unit was deposited by marine currents. The high percentage of relatively clean, well-sorted sand in the lower part of the formation suggests that it was deposited in a medium- to high-energy, perhaps in an upper to middle shoreface setting (cf. McCubbin, 1982). A wave-dominated deltaic setting is likely, but cannot be conclusively demonstrated.

The decrease in mineralogical maturity relative to the Souloise Greywacke Formation reflects a new and nearby metamorphic source area. The abundant serpentinite indicates that this source area had to lie to the east of Dévoluy, in the more internal Alpine nappes, where there are ophiolites. Although the location of this source area cannot be conclusively established, two lines of evidence give a qualitative assessment: (i) the sediments were deposited in a medium to high energy setting, yet are relatively immature, indicating that they were not subject to significant reworking before being deposited; (ii) serpentinite, an extremely non-durable mineral, is present in abundance, and so could not have been transported a long distance. The nearest ophiolite source exposed today is over 100km away (Fig. 1.1), which is quite far for serpentinite to have been transported in abundance. Therefore, ophiolites may have been closer to Dévoluy in the Oligocene than they are in their presently eroded position.

The St-Disdier Arenite was deposited on the distal western margin of the Alpine foreland basin

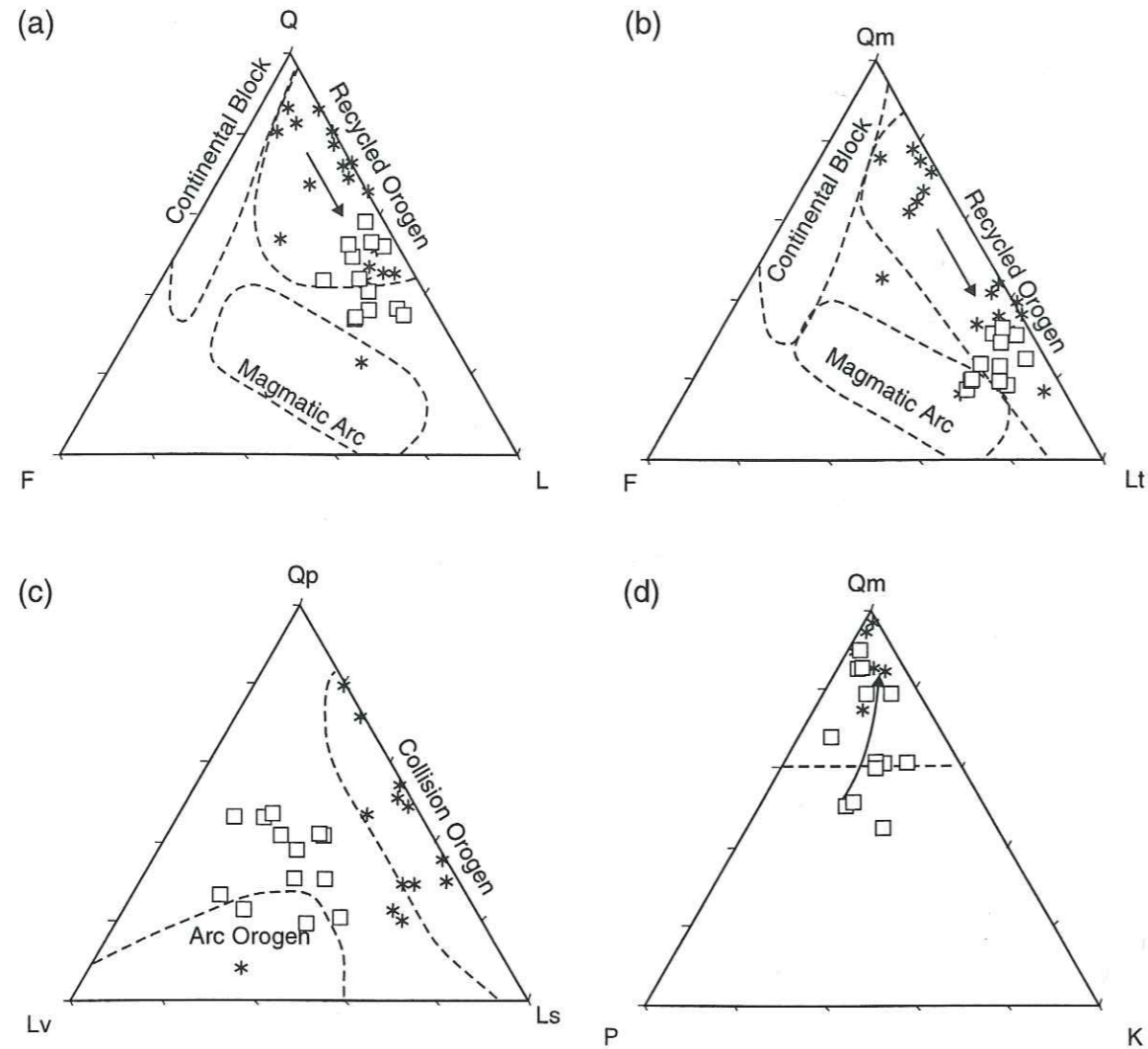


Fig. 6.10. Ternary diagrams illustrating the petrographic composition of the St-Disdier Arenite Formation (open boxes). (a) Q-F-L plot. Arrow indicates an increasing ratio of oceanic to continental components. (b) Qm-F-Lt plot. Arrow indicates an increasing ratio of chert to quartz. (c) Qp-Lv-Ls plot. (d) Qm-P-K plot. Arrow indicates increasing mineralogical maturity. Dashed line indicates 60% monocrystalline quartz. All poles are Gazzi-Dickinson combined categories (see Appendix A-1). Provenance fields, asterixes (data points from modern foreland basin and collision orogen sediments), and arrows (petrographic trends) after Dickinson & Suczek (1979). Note that the St-Disdier Arenite Formation, a foreland basin sediment, plots consistently away from the classic foreland basin samples (asterixes) of Dickinson & Suczek (1979).

(Fig. 9.6). However, based on the above arguments, the basin could not have been very wide locally, as the source area and depositional area were not separated by a large distance. Furthermore, there are no Oligocene marine deposits of the same age as the St-Disdier Arenite Formation in Champsaur, now 15 km to the east of Dévoluy (Fig. 9.6). During the Oligocene, the sediments in Champsaur were buried a minimum of 4 km (Waibel, 1990), probably beneath internal Alpine thrust sheets. These thrust sheets may have contained the ophiolitic source area of the serpentinite in the St-Disdier Arenite Formation.

Local syndepositional uplift of the western margin of Dévoluy, reflected in the basal unconformity of the formation, may have been related to the emplacement of such nappes. The uplift, which could have been caused by a blind thrust at depth, is reflected in the increase in carbonate lithic

fragments relative to the Souloise Greywacke Formation.

Thus, the marine western Alpine foreland basin decreased in width during the Oligocene as a result of tectonic uplift to the east and west. Interestingly, the foreland basin did not experience subsidence-related deepening due to the emplacement of the internal nappes to the east. Although the load of the nappes no doubt depressed the crust (e.g., the burial of Champsaur), the uplift of western Dévoluy and, possibly, a concomitant increase in sediment supply due to erosion of the nappes allowed the basin to maintain overall shallowing conditions in the Oligocene. This unexpected relationship is discussed in detail in Chapter 9.

CHAPTER 7

The St-Disdier Siltstone Formation

In Dévoluy, the St-Disdier Siltstone Formation occurs stratigraphically above the St-Disdier Arenite Formation and is the youngest preserved Tertiary formation. South of Dévoluy, the St-Disdier Siltstone Formation is consistently mapped as occurring below the Montmaur Conglomerate Formation (BRGM, 1971). Therefore, the formation is considered to lie stratigraphically below the Montmaur Conglomerate Formation.

The age of the formation is taken as late Oligocene (Chattian) based on the presence of the diagnostic charophytes *Rhabdochara kraeuseli* and *Sphaerochara hirmeri* (Pairis *et al.*, 1983, 1984; Fabre *et al.*, 1986).

The St-Disdier Siltstone Formation crops out only in western Dévoluy, in the foot wall of the Median Dévoluy Thrust (Fig. 7.1). It is not known how thick the formation was, because its top is eroded or removed by thrusting. However, it is at least 63 m thick in its type section, southeast of the village of Bas Gicon in northern Dévoluy (Fig. 7.2), and more than 32 m thick at La Cluse in southwesternmost Dévoluy (Fig. 7.3).

The type section (Fig. 7.2) shows that the formation is dominated by fine-grained silt- and mudstone. Occasional erosion-based lenticular sandstones and tabular coarse siltstones also occur.

The lower boundary of the formation has only been observed in southwesternmost Dévoluy, where the contact is abrupt with the St-Disdier Arenite Formation (Fig. 7.3). In southwestern Dévoluy and possibly also in northern Dévoluy (Fig. 7.1), the St-Disdier Arenite Formation does not occur below the St-Disdier Siltstone Formation. The lower contacts of the St-Disdier Siltstone Formation are not exposed at these localities, but are inferred to be unconformable. An upper bounding surface, possibly with the younger Montmaur Conglomerate Formation, was not observed and is not described in the literature.

The formation is characterized by four lithofacies (Table 7-I): red and greenish-red mud- and siltstones (lithofacies SDS-1); lenticular, fining-up sand- and siltstone (lithofacies SDS-2); graded medium-grained sandstones to siltstones (lithofacies SDS-3); and calichified silt- and fine-grained sandstones (lithofacies SDS-4).

7.1. Lithofacies analysis and stratigraphy

Lithofacies SDS-1: Red and greenish-red mud- and siltstones

Lithofacies SDS-1 consists of very thinly-bedded to massive mud- and/or siltstone (Fig. 7.4). It is the most volumetrically significant lithofacies of the St-Disdier Siltstone Formation, and is present in all outcrops.

Silt-sized grains are well-rounded. Typically, the silt grains float in a muddy calcareous matrix,

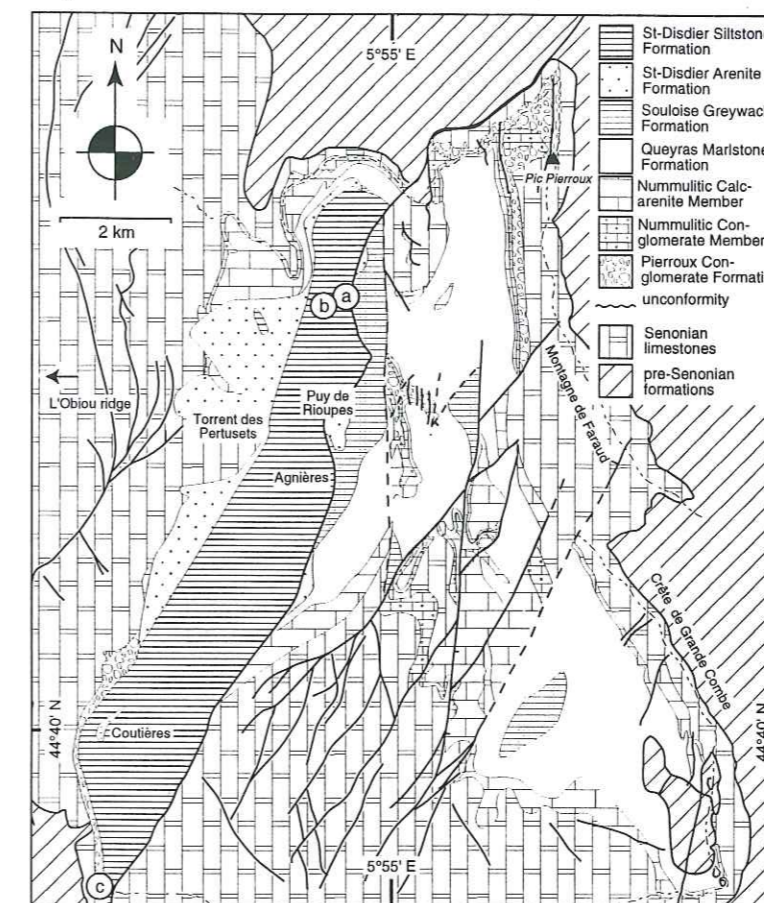


Fig. 7.1. Geologic map of Dévoluy, showing locations of measured sections of the St-Disdier Siltstone Formation. a = Bas Gicon section (type section); b = La Mère Eglise measured section; c = La Cluse section.

Lithofacies	Description	Interpretation
USD-1	Red and greenish-red mud- and siltstones	alluvial floodplain mud-/siltstones
USD-2	Lenticular, fining-up sand- and siltstone	mixed-load fluvial channels
USD-3	Graded siltstones to medium-grained sandstones	probably crevasse splays
USD-4	Calichified silt- and fine-grained sandstones	paleosols; calichified overbank, crevasse splay, or levee deposits
Lithofacies association		
USD-I	Lithofacies USD-1, USD-2, USD-3, and USD-4	distal alluvial floodplain

Table 7-I. Summary of lithofacies and lithofacies associations of the St-Disdier Siltstone Formation

although some samples show grain-to-grain contacts of silt-sized material. Silt-sized grains are predomina variable amounts of quartz, feldspar, and lithic fragments. Beds may have nodular horizons (e.g., Fig. 7.3, 48.60 - 50.25 m and 52.75 - 53.50 m), which appear to be diagenetic features.

Lower bounding surfaces are gradational to sharp. Upper bounding surfaces are sharp or eroded. Beds, which vary in thickness from 0.5 - 14 m, are continuous over the extent of an outcrop.

The lithofacies is often replete with root casts (e.g., Fig. 7.2, 55.70 - 63.05 m). These casts are thin (≤ 1 mm wide) and occur in all orientations. They commonly have white to buff coronas.

One of the most characteristic, and diagnostic, features of this lithofacies is its color. Beds are red, greenish red, or yellow. These colors distinguish lithofacies SDS-1 from the other fine-grained lithofacies of the Souloise Group. The transition between layers of different colors occurs over a few

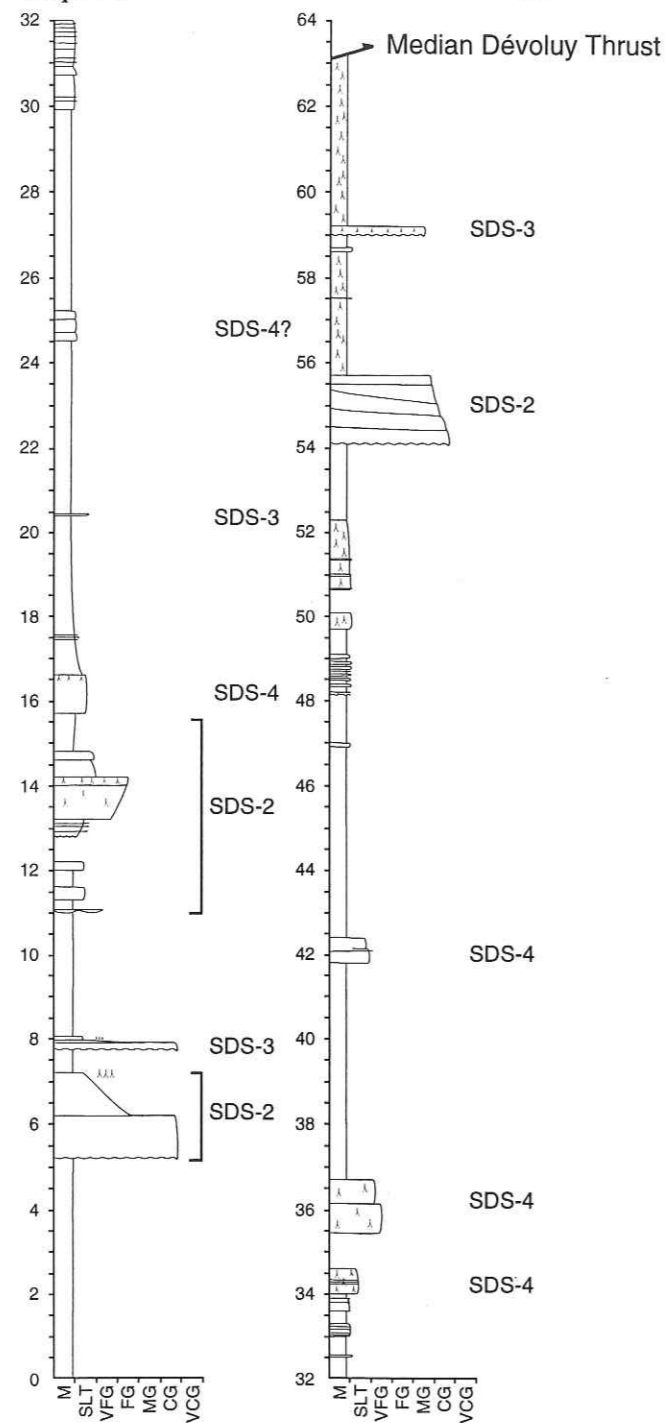


Fig. 7.2. Type section of the St-Disdier Siltstone Formation at Bas Gicon, northern Dévoluy (scale in meters). Beds of lithofacies SDS-1, 2, and 3 indicated. All other sediments are lithofacies SDS-1. Location indicated in Fig. 7.2.

Beds of lithofacies SDS-2 are composed of siltstones and medium- to coarse-grained sandstone with moderately-sorted, moderately-rounded grains. Sorting, roundness, and the amount of fine-grained matrix increase towards the tops of beds. The beds are typically fining-up (e.g., Fig. 7.2, 5.20 - 7.20 m; Fig. 7.3, 62.10 - 65.70 m), but may also be heterogeneously mixed. Fresh and weathered surfaces are deep green to green-

centimeters.

The distinctive red and yellow color, the root casts, and the nodular character of certain beds of this lithofacies, as well as the total lack of marine bioturbation, indicate that it was probably deposited in a subaerial environment (cf. Cant, 1982). Certainly, deposition occurred under oxidizing conditions, as evidenced by the red color of some beds. The abrupt occurrence of this lithofacies above the St-Disdier Arenite Formation at La Cluse (Fig. 7.3, 45.80m) thus documents a change from marine to continental conditions. This change in conditions may be represented at Torrent des Pertusets (Fig. 6.4) by the delta-plain deposits (lithofacies SDA-4) of the St-Disdier Arenite Formation.

Lithofacies SDS-1 is interpreted as alluvial floodplain mudstones and siltstones. The abundance of root casts, the oxidized nature of the sediments, and the lack of dehydration structures (e.g., desiccation cracks) suggests that the floodplain was highly vegetated and was above the regional water table, such that the area was not subject to significant periods of wetting and drying (Galloway & Hobday, 1996).

Lithofacies SDS-2: Lenticular, fining-up sand- and siltstone

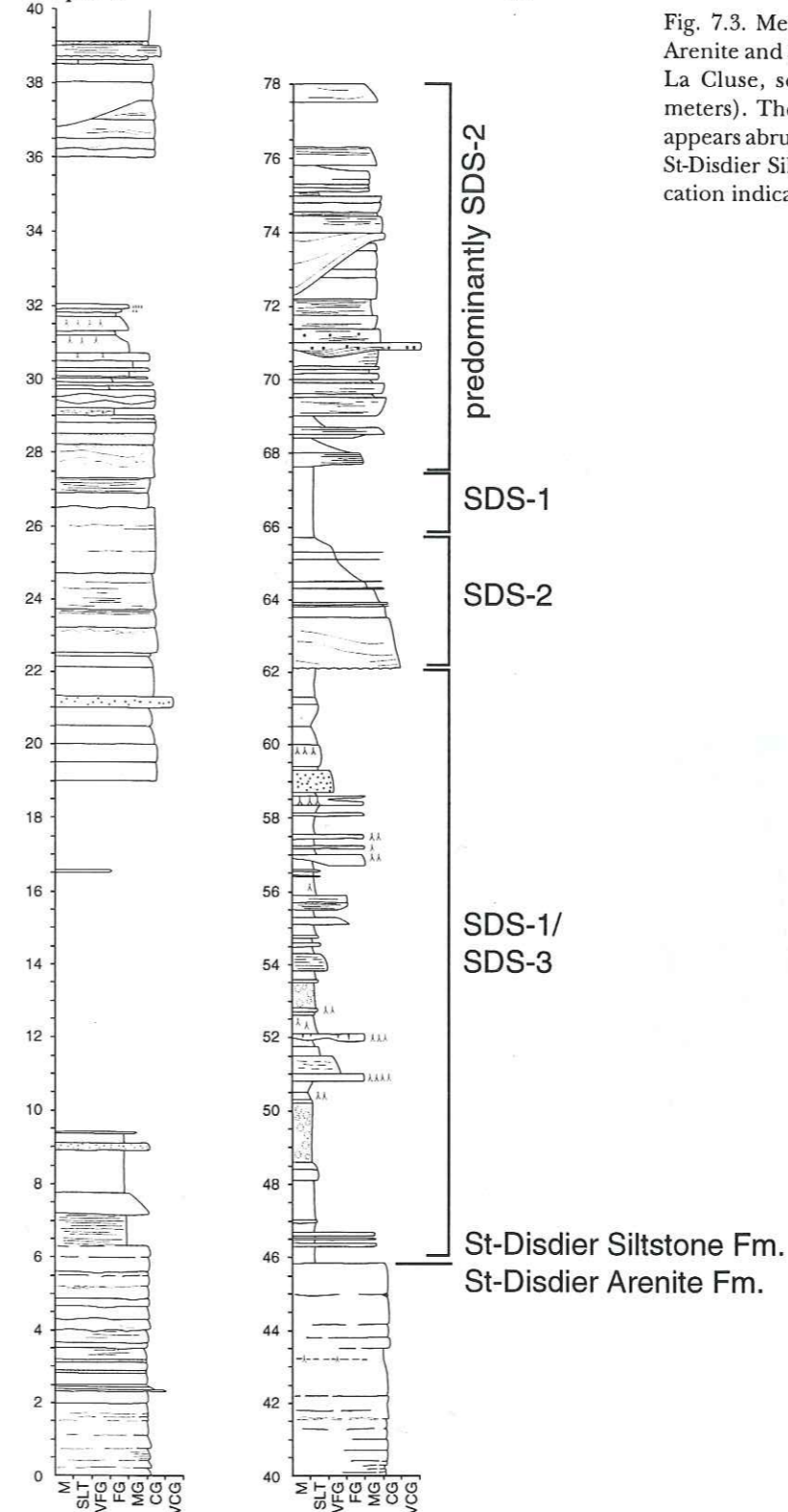


Fig. 7.3. Measured section of the St-Disdier Arenite and St-Disdier Siltstone formations at La Cluse, southwestern Dévoluy (scale in meters). The St-Disdier Siltstone Formation appears abruptly at 45.80 m. Lithofacies of the St-Disdier Siltstone Formation indicated. Location indicated in Fig. 7.1.

ish-brown due to an unusually large volume of serpentinite in the sandstones (see section 7.2).

Lower bounding surfaces are broadly concave up and incise into lithofacies SDS-1 as a series of channels (Fig. 7.6). The channels often contain rounded to angular clay rip-up clasts at their bases. Upper bounding surfaces are planar or gently undular. The channels are overlain by mud- and

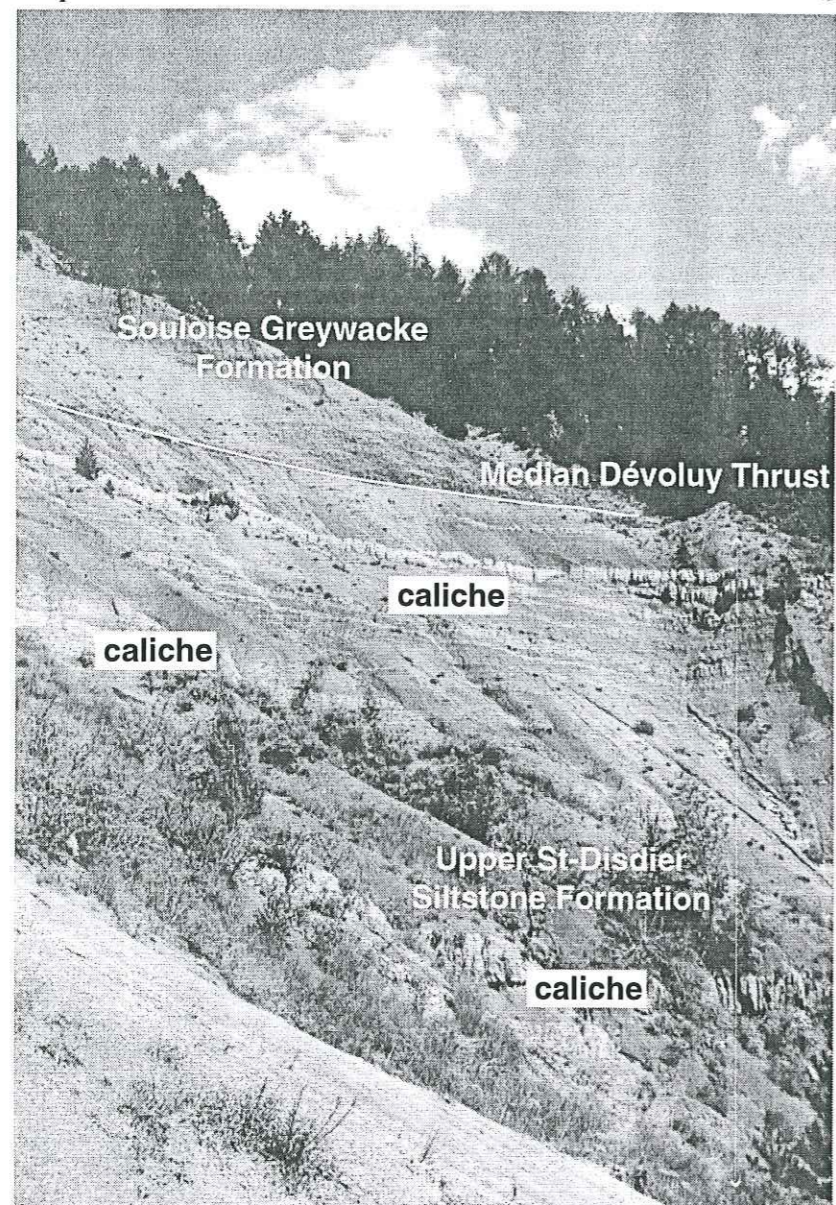


Fig. 7.4. The St-Disdier Siltstone Formation at Bas Gicon, looking west. Lithofacies SDS-1 is dominant. Section is approximately 50 m thick

siltstone that may or may not be calichified.

The channels have broadly symmetrical two-dimensional geometries (Figs. 7.6) that display internal asymmetry. Deposition occurred on both the channel margin and channel base (Fig. 7.6). Channels have moderate width-to-depth ratios (100+ m wide, 1 - 10 m deep).

Common internal structures in the channels include large-scale, laterally-accreted sigmoidal cross beds, tabular and trough cross beds, planar beds, and unidirectional and climbing current ripples (Figs. 7.6 - 7.7). The paleocurrents preserved in these sedimentary structures show a wide spread of flow directions (Fig. 7.8). One or two predominant flow directions exist at each outcrop—NE at Bas Gicon (Fig. 7.8a), N and NE at Puy de Rioupes (Fig. 7.8b), W at Agnières (Fig. 7.8c), N and NW at Coutières (Fig. 7.8d), and NW and SW at La Cluse (Fig. 7.8e)—but individual paleocurrent readings vary by as much as 180°. Unidirectional current ripples (e.g., Fig. 7.7) show slightly or-

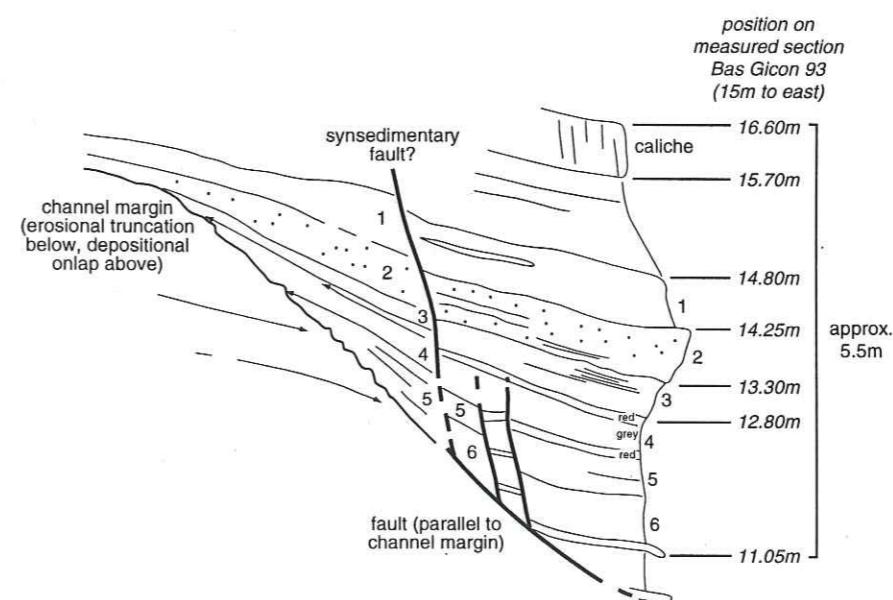
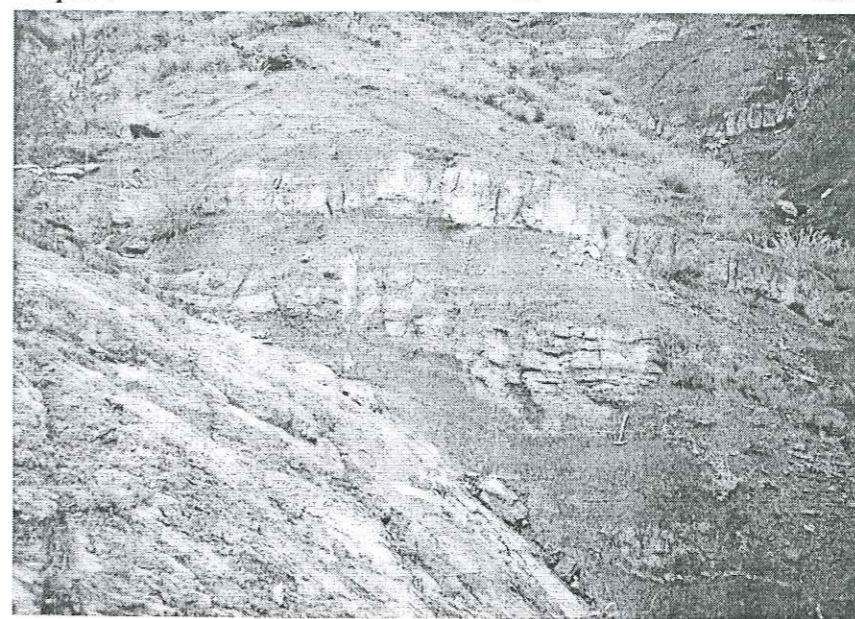


Fig. 7.5. Detailed depiction of a fine-grained channel in the St-Disdier Siltstone Formation (compare lithologies with Fig. 7.2, 11.05 - 16.60 m). (a) Field photograph, looking NE. 50 cm hammer for scale. (b) Line drawing of (a). (c) Idealized flow-perpendicular (NNE-SSW) field sketch of the channel. Note the presence of intrachannel faults, possibly due to differential compaction, and the heterogeneous nature of the fill.

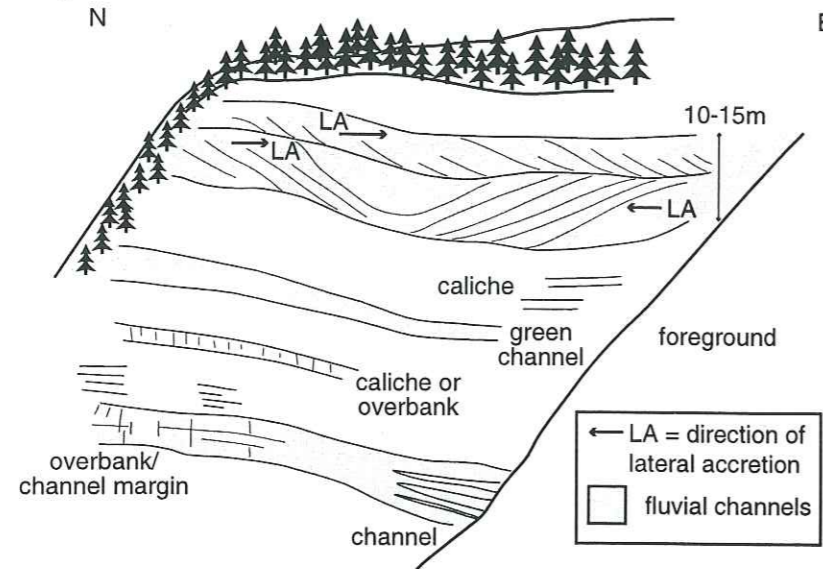


Fig. 7.6. Field sketch of an oblique view of stacked and isolated channels in the St-Disdier Siltstone Formation at Puy de Rioupes, central Dévoluy. Note the large-scale sigmoidal bedding that records lateral accretion. The third channel from the bottom shows lateral accretion from both sides of the channel towards the center.

thogonal transport directions to larger-scale cross beds (e.g., Fig. 7.8e).

This lithofacies is interpreted as channelized fluvial deposits with mixed-load fills. Such channels are characterized by width-to-depth ratios of 10:1 to 40:1, contain relatively low (5 to > 20%) amounts of mud, and tend to deposit on both the channel margin and the channel base (Galloway, 1977; Schumm, 1977), all of which are consistent with observations of this lithofacies. Mixed-load channels have sinuous map patterns (Galloway, 1977), so the wide spread of paleocurrent data probably reflects the natural meanders of the channels and different hierarchies of bedforms within them.

Lithofacies SDS-3: Graded medium-grained sandstones to siltstones

Lithofacies SDS-3 is composed of thin (≤ 30 cm thick) beds of green or reddish-green medium-grained sandstone grading up into siltstone. The constituent grains are well-sorted and moderately rounded. A single grain size tends to predominate in a given bed. The beds are recurrent within certain intervals (e.g., Fig. 7.2, 48.20 - 49.10 m; Fig. 7.3, 46.00 - 59.00 m), but are not generally common throughout the section.

Lower bounding surfaces incise underlying layers only a few centimeters deep. Upper bounding surfaces are sub-planar. The overall external geometry of these beds is lenticular. They are encased within the finer-grained sediments of lithofacies SDS-1, and commonly disappear and reappear along strike, giving them an aspect of channelization.

Root casts are prevalent in this lithofacies. These root casts are poorly- to well-developed, and are more commonly developed in medium-grained, rather than fine-grained sandstones or siltstones.

This lithofacies is interpreted as probable crevasse splay deposits because (1) the channels are

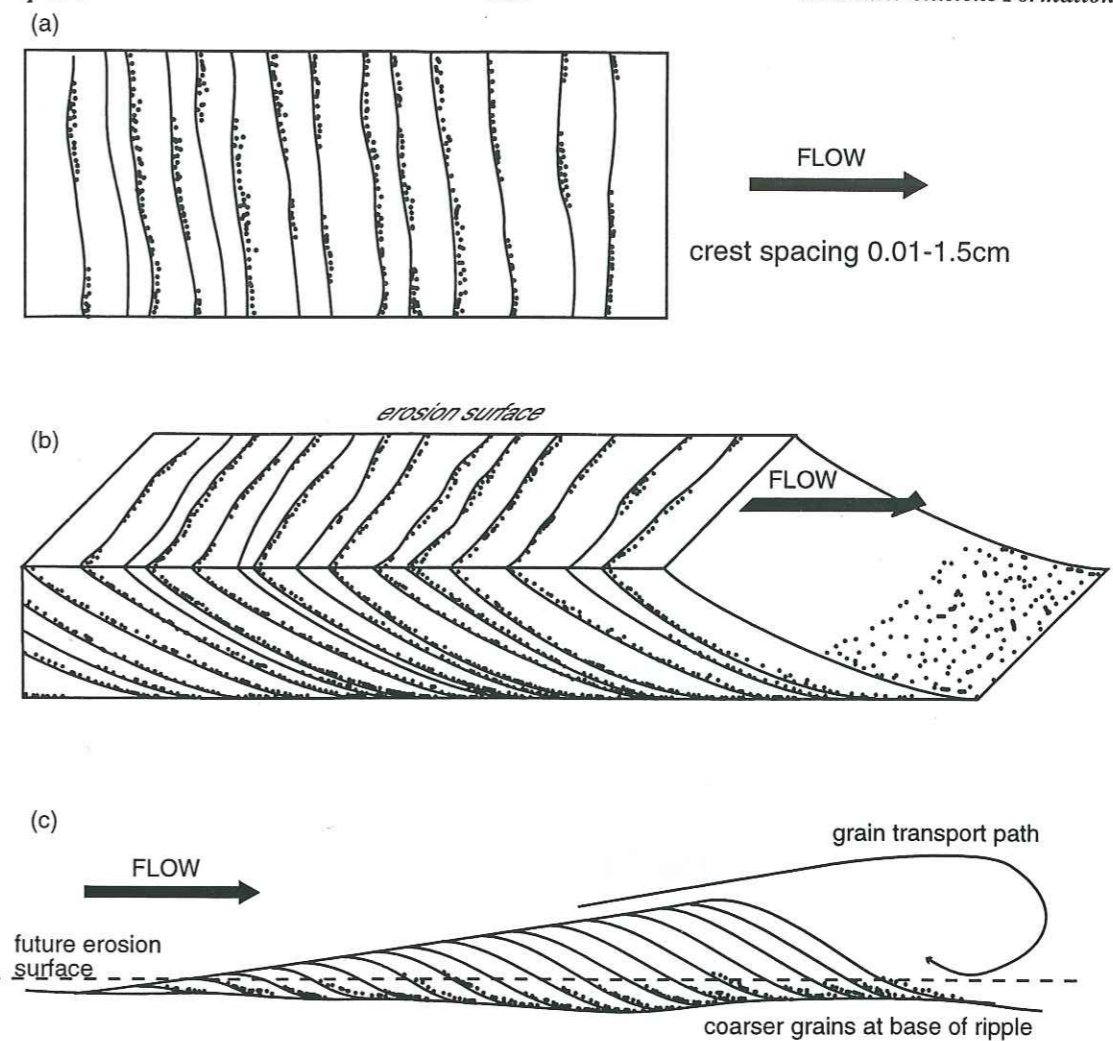


Fig. 7.7. Unidirectional current ripples at La Cluse, SW Dévoluy (63.50 - 63.90 m, Fig. 7.4). Coarser grains (dots) occur on downcurrent sides of ripple crests. (a) Irregular crest lines (average orientation was measured) looking down on erosional surface; coarse grains are observed to accumulate on the lee side (to right) of ripple crests. Flow (arrow) is interpreted to be perpendicular to the ripple crests. Scale indicated. (b) Observed three-dimensional relationship between foresets and crest lines of ripples and coarser grains. Arrow shows interpreted flow direction. Same scale as (a). (c) Flow-parallel cross section through an idealized current ripple. Dashed line shows future erosion surface as preserved (Figs. 9.9a, b). Approximately same scale as (a) and (b).

thinner and not so well-developed as those of lithofacies SDS-2, and (2) the lithofacies tends to occur sporadically throughout the section, such as would happen when a channel levee is breached. However, because the three-dimensional geometries of beds of this lithofacies cannot be constrained, this interpretation is equivocal. The lithofacies could also be interpreted as subsidiary channels to the distributary channels of lithofacies SDS-2.

Lithofacies SDS-4: Calichified silt- and fine-grained sandstones

Lithofacies SDS-4 is composed of light pink, nodular to massive, carbonate-cemented silt- and sandstone. It is moderately sorted, and silt-sized grains are well-rounded. Overall, this lithofacies is slightly coarser-grained than lithofacies SDS-1.

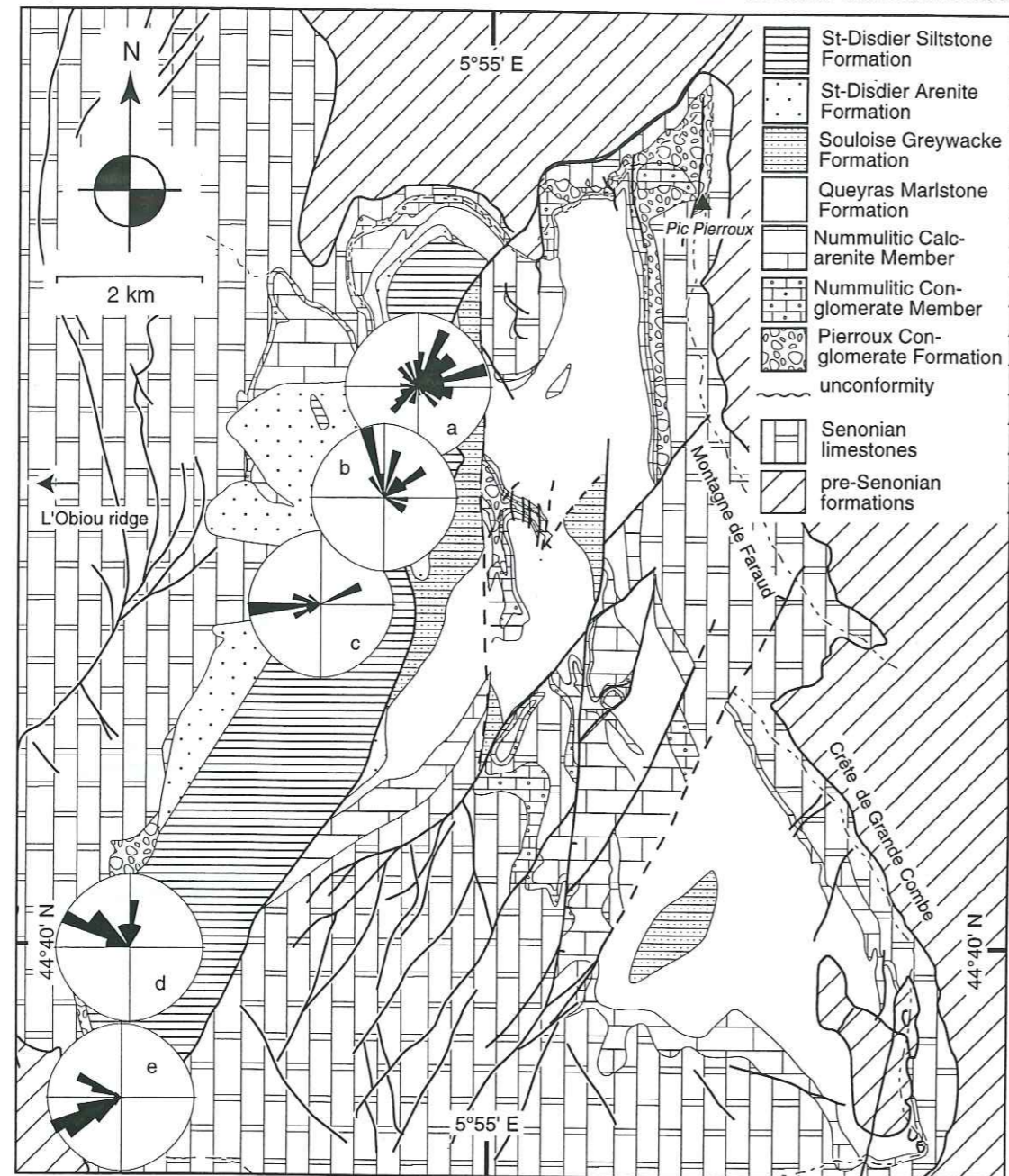


Fig. 7.8. Rose diagrams of current data in channels of the St-Disdier Siltstone Formation. Localities as in Fig. 7.1. (a) Bas Gicon (91 data; circle = 9%). (b) Puy de Rioupes (15 data; circle = 20%). (c) Agniers (16 data; circle = 31%). (d) Coutières (16 data; circle = 19%). (e) La Cluse (98 data; circle = 22%). Data (not distinguished) include ripple crests (perpendicular to flow direction), lateral accretion surfaces (strike parallel to flow direction), and trough axes.

Upper and lower surfaces are subplanar and display gradational grain-size trends with under- and overlying sediments. These surfaces are therefore transitional in nature. The beds have tabular geometries. They are 10 - 100 cm thick and display crude fining-up trends. The beds are continuous over the length of a given outcrop. Beds of lithofacies SDS-4 may occur at the top of beds of lithofacies SDS-2 (e.g., Fig. 7.2, 15.70 - 16.60 m; Fig. 7.5) or may occur in apparent stratigraphic isolation in the section (e.g., Fig. 7.2, 35.50 - 36.70 m and 41.80 - 42.40 m; Fig. 7.6).

Internally, beds display parallel bedding, which may or may not be discontinuous, carbonate

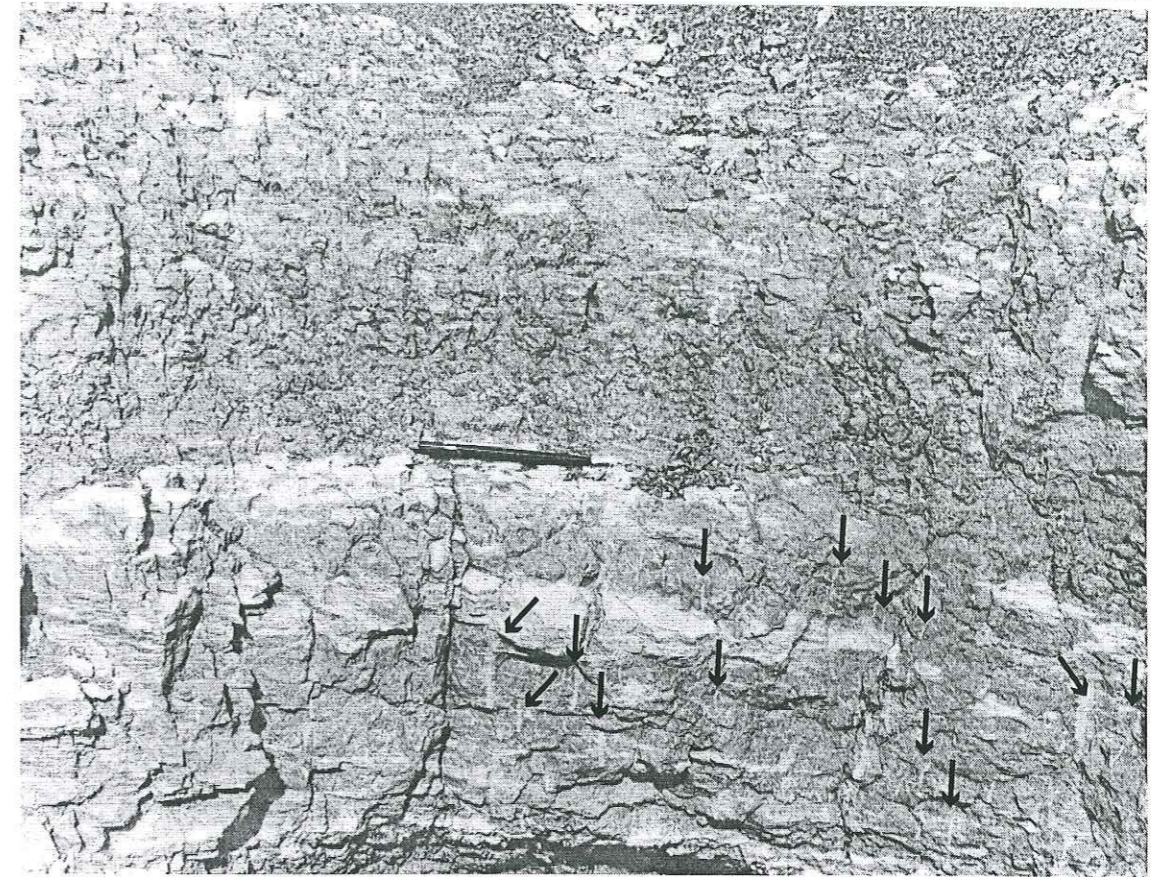


Fig. 7.9. Root casts in lithofacies SDS-3. Pencil lies at the top of the bed. Arrows indicate particularly well-developed root casts. Photo taken at Bas Gicons, north central Dévoluy

nodules, and inverted flame-like structures at their tops that are interpreted as mud cracks. The nodules are associated with local concentrations of calcite.

This lithofacies commonly has vertical root casts that are particularly well-developed towards the tops of beds (Fig. 7.9). These root casts are identical to those of lithofacies SDS-1, but are better-developed.

The lithofacies is interpreted as calichified floodplain deposits based on the presence of root casts, calcite nodules, and mud-cracks (cf. Esteban & Klappa, 1983). Some samples of this lithofacies additionally display floating and embayed grains, which are considered to be characteristic of caliche horizons (Esteban & Klappa, 1983). Caliche (or calcrete) is considered to be indicative of sub-aerial environments (Esteban & Klappa, 1983; Tucker & Wright, 1988). The root traces indicate that the environment of deposition was relatively stable and that these sediments were inundated only infrequently, such that suberial plants were able to thrive (Esteban & Klappa, 1983). Similar horizons have been interpreted as paleosols in other systems (Esteban & Klappa, 1983, and references therein). The coarser grain size relative to lithofacies SDS-1 probably indicates that the original sediments were overbank, crevasse splay, or levee deposits that were subsequently calichified during paleosol formation. The calcite cement may have preferentially lithified these coarser-grained

deposits.

LITHOFACIES ASSOCIATION

One lithofacies association has been determined for the St-Disdier Siltstone Formation. This association is composed of all of the lithofacies.

Lithofacies association SDS-I: Lithofacies SDS-1, SDS-2, SDS-3, and SDS-4

Lithofacies association SDS-I consists of (1) thick floodplain deposits (lithofacies SDS-1), which can locally comprise up to 90% of the outcrop, (2) isolated to stacked mixed-load fluvial channels (lithofacies SDS-2), (3) occasional occurrences of crevasse splay or overbank deposits (lithofacies SDS-3), and (4) calichified paleosols (lithofacies SDS-4).

This association is characteristic of distal alluvial floodplains (Cant, 1982; Galloway & Hobday, 1996; Platt & Keller, 1992). Distal alluvial floodplains are distinguished from proximal floodplains by the absence of alluvial fan conglomerates in the former (e.g., Platt & Keller, 1992). The floodplain of the St-Disdier Siltstone Formation may have been located in a delta-plain setting, if the St-Disdier Arenite Formation was deposited in a wave-dominated delta system. Alternatively, if the St-Disdier Arenite Formation was deposited in a strandplain system, the floodplain of the St-Disdier Siltstone Formation can be interpreted as a prograding continental depositional system.

7.2. Petrography and provenance

The petrography of the St-Disdier Siltstone continues the trends seen from the Souloise Greywacke Formation to the St-Disdier Arenite Formation. Monocrystalline and polycrystalline quartz and carbonate and volcanic lithic fragments (including serpentinite) are present in significant ($\geq 10\%$) amounts, while feldspars remain a subordinate ($\geq 5\%$ avg.) component (Table A-I). While the amounts of monocrystalline quartz (41% vs. 38%), carbonate lithic fragments (12% in both cases), and volcanic lithic fragments including serpentinite (20% vs. 22%) do not change relative to the St-Disdier Arenite Formation, the amount of metamorphic lithic clasts increases (from 6% to 13%), and the amount of siliciclastic material becomes relatively insignificant (1%) (Table A-I). Overall, the composition of the St-Disdier Siltstone Formation is similar to that of the St-Disdier Arenite Formation, except that serpentinite makes up a larger percentage of the volcanic material. The predominance of metamorphic and carbonate lithic fragments as components indicates that, like the St-Disdier Arenite Formation, the St-Disdier Siltstone Formation was sourced from both internal Alpine units and local carbonate rocks. Sand-sized quartz grains have thermoluminescent properties similar to those of the Penninic nappes (Ivaldi, 1989).

Ternary plots of major components (based on Dickinson & Suczek, 1979) reflect the immaturity of the sediments and also the complexity of the source area (Fig. 7.10). Q-F-L and Qm-F-Lt plots (Figs. 7.10a, b) show that the sediments of the formation were primarily sourced from a recycled

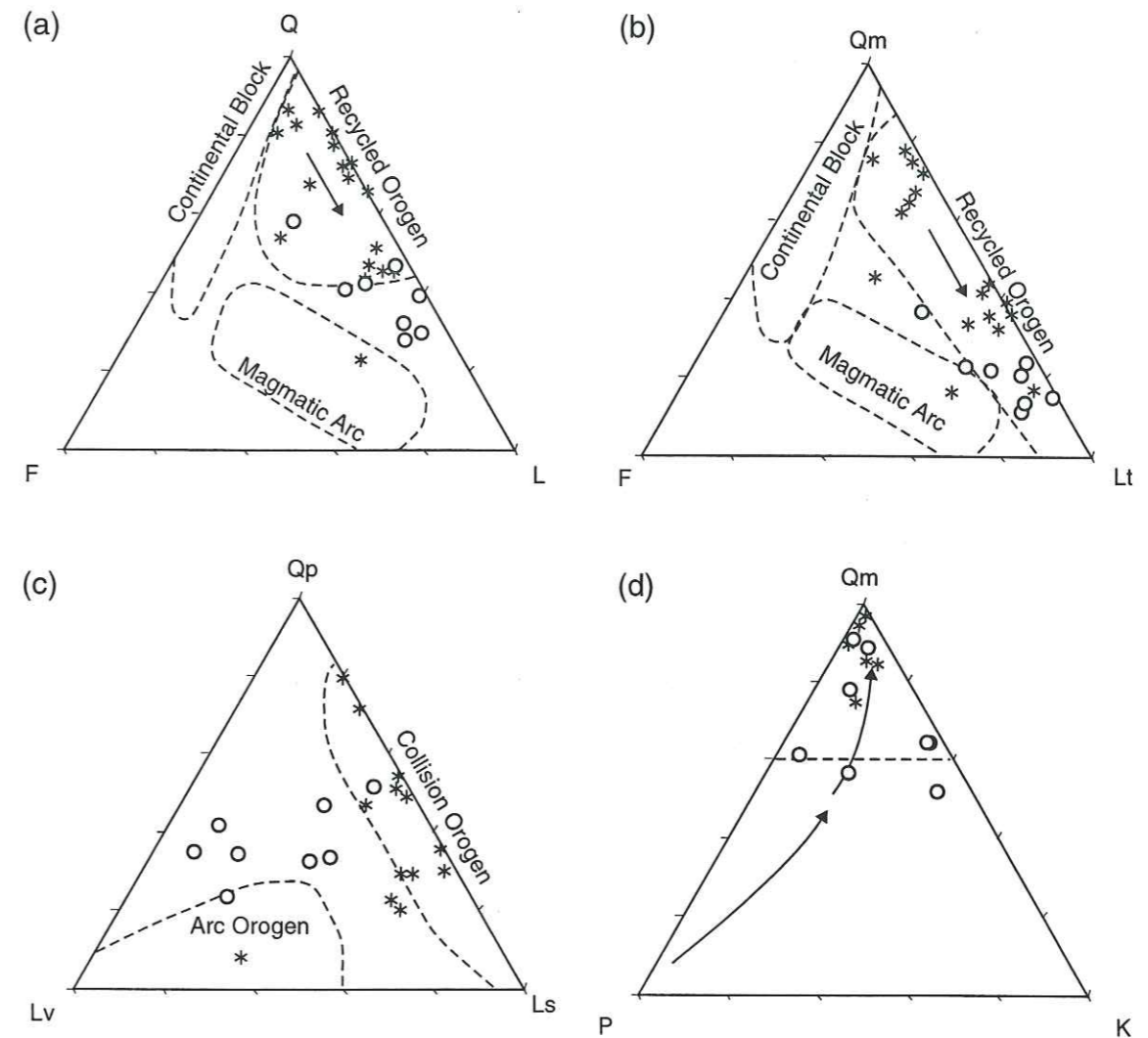


Fig. 7.10. Ternary diagrams illustrating the petrographic composition of the St-Disdier Siltstone Formation. Data shown as asterisks. (a) Q-F-L plot. Arrow indicates an increasing ratio of oceanic to continental components. (b) Qm-F-Lt plot. Arrow indicates an increasing ratio of chert to quartz. (c) Qp-Lv-Ls plot. (d) Qm-P-K plot. Arrow indicates increasing maturity. Dashed line indicates 60% monocrystalline quartz. All poles are Gazzi-Dickinson combined categories (see Appendix A-1). Provenance fields, asterisks (data points from modern foreland basin and collision orogen sediments), and arrows (petrographic trends) after Dickinson & Suczek (1979). Open circles represent data from this study. See text for more detailed discussion of plots.

orogen, but that lithic fragments comprise an even more significant component of the sediments than for the St-Disdier Arenite Formation (compare Figs. 6.11a, b and 7.10a, b). The type of orogen that sourced the sediments was predominantly collisional, but also displayed arc affinities (Fig. 7.10c). These three diagrams (Figs. 7.10a-c) clearly show the increase in lithic fragments noted in the previous paragraph, in that most of the samples plot closer to the lithic pole than the quartz pole.

The Qm-P-K ternary diagram (Fig. 7.10d) shows a scatter similar to that for the St-Disdier Arenite Formation (Fig. 6.11d). The scatter reflects the immaturity of the sediments relative to the Souloise Greywacke Formation (Fig. 5.12d).

7.3. Depositional setting

The St-Disdier Siltstone Formation is composed of alluvial floodplain deposits of a mixed-load fluvial system. Floodplain muds and silts dominate the system; channels are vertically stacked or isolated; overbank (crevasse) splays and paleosols are subsidiary.

The significantly larger percentage of serpentinite (16%) and other metamorphic lithic fragments (15%) relative to carbonate lithic fragments (12%) indicates that the primary source area of the sediments was the internal Alpine nappe stack with ophiolites, and that relatively minor tributaries were sourced in local carbonates. The internal Alpine nappes are today situated to the east of Dévoluy; therefore, the fluvial system should have flowed generally east to west. The wide range of paleocurrent directions in the fluvial sandstones (lithofacies SDS-2) probably reflects deposition in a meandering stream system.

A significant percentage of the metamorphic lithic fragments are not broken down into their constituent monocrystalline components, which indicates that the sediments were not subject to large amounts of reworking prior to deposition. This fact implies a relatively adjacent source area. As with the St-Disdier Arenite Formation, the absolute proximity of the source area cannot be determined. However, the increase in the abundance of serpentinite probably indicates that the source area was more proximal to this depositional system than that of the St-Disdier Arenite Formation.

Given that Dévoluy occupied the western edge of the marine foreland basin (Fig. 9.7), the presence of the St-Disdier alluvial deposits in western Dévoluy indicates that by the late Oligocene (Chattian), the western Alpine foreland basin had been completely infilled at this locality. The infilling marks a significant change in the evolution of the Alpine foreland basin, from marine to continental deposition. Dévoluy occupies the documented eastern limit of late Oligocene continental deposition (Fig. 9.7).

CHAPTER 8

The Montmaur Conglomerate Formation

The Montmaur Conglomerate Formation was not studied or mapped in detail as part of this thesis, as it only occurs south of the study area. However, significant sedimentologic aspects of the formation are presented here because it represents the uppermost deposits of the Tertiary succession in the vicinity of Dévoluy.

The formation is considered to be Upper Oligocene (Chattian) based on its interpreted stratigraphic position above the Chattian St-Disdier Siltstone Formation. A lack of biostratigraphic data precludes a more precise age determination, and the formation could also be Miocene in age. The *Gap* geologic map (BRGM, 1971) shows the St-Disdier Arenite, St-Disdier Siltstone, and Montmaur Conglomerate Formations as being Stampian (late early Oligocene) in age. However, their ages are based on correlations with data from Dévoluy, where the formations have more recently been dated more precisely (Pairis *et al.*, 1983, 1984; Fabre *et al.*, 1986).

The type section (Fig. 8.1) of the Montmaur Conglomerate Formation is located approximately 650m east of the village of Montmaur. The formation is superbly exposed at this outcrop, and all basic characteristics of the formation can be seen here. The formation is predominantly a crudely-bedded, poorly stratified and sorted conglomerate with well-rounded clasts and a sandy matrix. Occasional sandy lenses occur within or between conglomeratic beds. The maximum clast size varies from 10 - 25 cm (Fig. 8.1).

The lower boundary of the unit has not been observed in the field. East of the village of La Montagne (BRGM, 1971), the Montmaur Conglomerate Formation occurs stratigraphically above, and within a few meters of, the Nummulitic Limestone Formation. The contact here is inferred to be an unconformity. Contacts between the Montmaur Conglomerate Formation and the St-Disdier Arenite and St-Disdier Siltstone Formations were not observed, although the Montmaur Conglomerate Formation is mapped as occurring above the St-Disdier Siltstone Formation (BRGM, 1971). The original upper stratigraphic boundary of the Montmaur Conglomerate Formation is not known because it is overlain by Quaternary sediments or is overthrust by the Median Dévoluy Thrust sheet (BRGM, 1971).

Two lithofacies have been determined in the field (Table 8-I). These are a conglomerate with well-rounded clasts (lithofacies MC-1); and graded to massive, medium-grained sandstone (lithofacies MC-2).

8.1. Lithofacies analysis and stratigraphy

Lithofacies MC-1: Conglomerate with well-rounded clasts

Lithofacies MC-1 is a poorly-sorted clast- to matrix-supported conglomerate with a medium-

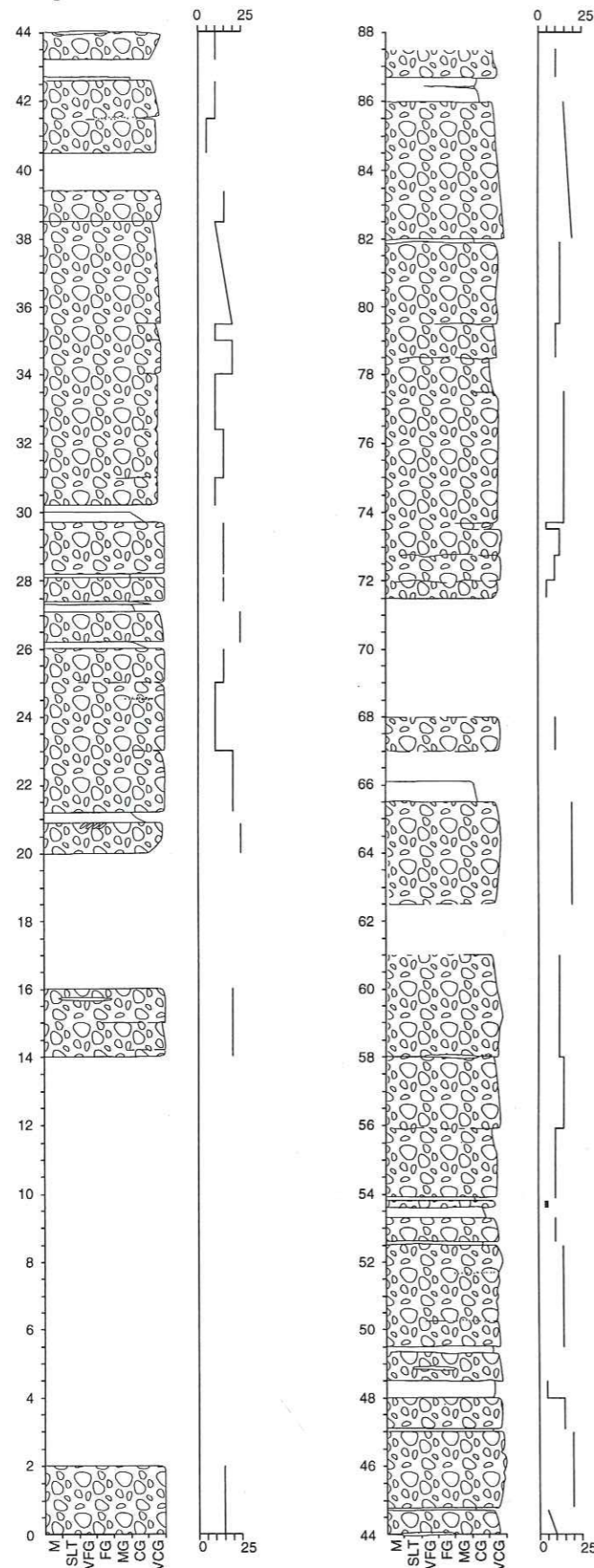


Fig. 8.1. Type section (scale in meters) of the Montmaur Conglomerate Formation, 650m east of the village of Montmaur (see BRGM, 1971 for location of Montmaur). Lithofacies MC-1 (conglomerate pattern) is the dominant lithofacies. Lithofacies MC-2 is the remainder of the section. Spaces in the section indicate area of no outcrop. Scale bars to the right of the columns indicate maximum observed clast size in each bed.

Lithofacies	Description	Interpretation
MC-1	Conglomerate with well-rounded clasts	broad, relatively shallow braided stream channels, alluvial fan deposits, or fan-delta deposits
MC-2	Graded sandstone	inter-channel sandstones or interbedded finer-grained fan deposits
Lithofacies association		
MC-1	Interbedded MC-1 and MC-2	proximal alluvial plain or alluvial fan deposition

Table 8-I. Summary of lithofacies and lithofacies associations of the Montmaur Conglomerate Formation.

grained sand matrix. The sand is green-colored, whereas the clasts have many different colors. The clasts are 1 to 25 cm in diameter (Fig. 8.1) and are very well-rounded (sub-spherical to disc-shaped) (Fig. 8.2). The clasts include locally sourced Senonian chert and limestone and rocks derived from the internal Alps, such as radiolarian chert, fragments of pillow lavas, albite porphyry, "Verrucano-facies" sandstones and microconglomerates, quartzite, fine-grained micaceous sandstone, migmatite, quartz, calcite, and chlorite (Ivaldi, 1989).

Most often, beds are massive. However, they may also be crudely stratified or graded (Fig. 8.2). Lower bounding surface are planar to concave up, and are distinguished by either a sandstone interbed or a change in the average maximum clast size (Fig. 8.1). Upper bounding surfaces are eroded or subplanar. The external geometry of beds is more often tabular than broadly lenticular. Beds are more often tabular than lenticular; the beds are between 0.2 and 4 m thick (Fig. 8.1).

The disc-shaped clasts are often imbricated (e.g., Fig. 8.2a). The long axes of the clasts are always oriented parallel to the direction of imbrication. Therefore, the orientations of the long axes were measured as a proxy for flow direction. These long axes are consistent in their orientation: at five localities, they show partially corrected* paleoflow to the NW.

The interpretation of this lithofacies is problematic because three-dimensional control is poor and distinctive sedimentary structures do not exist. The incisional bases of many beds suggests that the conglomerates may have been deposited in channels, although, if so, the channels must have been poorly-developed, based on the lack of well-defined channel margins. Alternatively, the channels may have been so broad that the channel margins do not outcrop. The well-rounded nature of the clasts and the poorly stratified nature of the beds suggests a high-energy environment, where such large clasts could be transported and rounded, and where bedding structures would not be so well-developed. Reasonable interpretations therefore include broad, relatively shallow braided stream

* The paleocurrent measurements were corrected in the field for local strike and dip, but structural considerations (e.g., plunging folds) were not considered because the sediments were not mapped in detail. The paleocurrent measurements thus contain a degree of error that cannot be calculated.

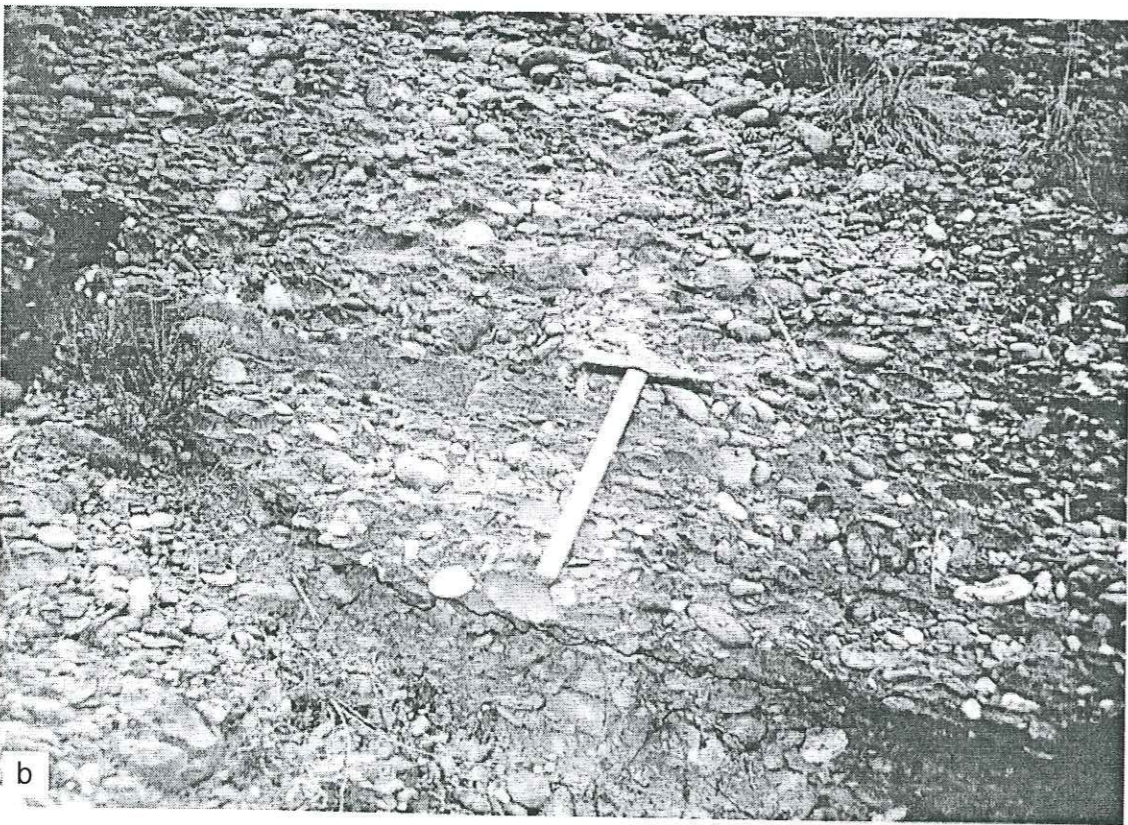


Fig. 8.2. The Montmaur Conglomerate Formation. (a) Predominantly lithofacies MC-1, with well-rounded, imbricated clasts (indicated by pencil). (b) Predominantly lithofacies MC-1, with interbeds and lenses of lithofacies MC-2 (e.g., beneath hammer head). Hammer is 65cm long. Note erosive base of conglomerate bed at base of hammer. Both photographs were taken at the type section, 650 m east of the village of Montmaur.

channels, alluvial fan deposits, or fan-delta deposits (Galloway, 1977; Galloway & Hobday, 1996).

Lithofacies MC-2: Graded Sandstone

This lithofacies consists of green to greenish-brown, coarse- to medium-grained sandstone. The grains are well-sorted and well-rounded. No significant amounts of clay-sized particles are present. Beds are crudely fining-up or massive.

Lower bounding surfaces are sub-planar, and infill minor topography on the tops of beds of lithofacies MC-1. Upper bounding surfaces are eroded and, therefore, the resulting external geometry of the lithofacies is lenticular (e.g., Fig. 8.2b). Beds are 0.01 - 1 m thick (Fig. 8.1).

The sandstones of lithofacies MC-2 strongly resemble the sandy lithofacies of the St-Disdier Arenite and the St-Disdier Siltstone formations in color and appearance (lithofacies LSD-1, LSD-2, and USD-2). However, they lack sedimentary structures and bioturbation and are therefore difficult to interpret. They may represent inter-channel sandstones, if lithofacies MC-1 is interpreted as channel deposits, or interbedded finer-grained fan deposits, if lithofacies MC-1 is interpreted as fan deposits.

LITHOFACIES ASSOCIATION

One lithofacies association has been determined for the Montmaur Conglomerate Formation. This association comprises lithofacies MC-1 and MC-2.

Lithofacies association MC-I: Interbedded MC-1 and MC-2

Lithofacies MC-1 dominates lithofacies association MC-I (Fig. 8.2). This lithofacies locally makes up more than 95% of the formation. Lithofacies MC-2 occurs only subsidiarily in the lithofacies association (Fig. 8.1).

As discussed above, the interpretations of the two lithofacies are problematic because of a lack of well-documented three-dimensional geometries. Lithofacies MC-1 was probably deposited in poorly constrained channels with large width to depth ratios. The coarse grain-size and lack of lateral accretionary sedimentary structures indicates that, if this lithofacies does indeed represent channel deposits, then they were bedload-dominated (cf. Galloway, 1977; Schumm, 1977). The relatively finer-grained deposits of lithofacies MC-2 were probably deposited as inter-channel sandstones.

The presence of the conglomerates of lithofacies MC-1 indicates that lithofacies association MC-I probably represents proximal alluvial plain or alluvial fan deposition, as documented in the proximal Lower Freshwater Molasse of the Swiss Molasse Basin (e.g., Platt & Keller, 1992). The well-rounded nature of the clasts indicates a significant amount of reworking prior to deposition. The lithofacies association may therefore represent braided stream or alluvial fan deposits, which typically have such rounded clasts (cf. Cant, 1982). If so, then lithofacies association MC-I represents progradation of the alluvial system relative to the more distal alluvial plain deposits of the St-Disdier Siltstone Formation.

There is no conclusive evidence to support subaerial deposition, and the association could also be a Gilbert delta (fan-delta) deposit, as interpreted for similar conglomerates (the La Poste member of the Marnes Bleues) in the Barrême basin 50 km south of Dévoluy (Evans, 1987; Evans & Mange-Rajetzky, 1991). However, those interpretations are based on the occurrence of the La Poste Member within the marine sediments of the Marnes Bleues, and are therefore not exactly analogous with the Montmaur Conglomerate Formation, which was deposited after the continental St-Disdier Siltstone Formation (see Chapter 9). Therefore, the hypothesis of continental deposition is preferred.

8.2. Provenance

Ivaldi (1989) conducted a thermoluminescence study of 50 pebble-sized quartz clasts from the Montmaur Conglomerate Formation. His findings show that 50% of the clasts are sourced from the "Schistes lustrés"; 14% are sourced from granites, gneisses, and migmatites of the Pelvoux/Belledone massifs and from the Permo-Carbiniferous substratum of the Briançonnais domain; 10% are sourced from anchi- to epimetamorphic grade Lower Tertiary marine sediments and the Briançonnais, Subbriançonnais, Dauphinois, and Ultradauphinois units; and 2% are sourced from the volcanoclastic Vieux Chaillol region of southwesternmost Pelvoux. Sand-sized quartz grains have thermoluminescent properties similar to those of the South Penninic Embrunnais-Ubaye nappes (Ivaldi, 1989). These data indicate that the most significant source of sediment for the Montmaur Conglomerate Formation were the internal Alpine units east and east-southeast of Dévoluy.

8.3. Depositional setting

The Montmaur Conglomerate Formation is interpreted as an alluvial fan/braidplain deposit. Similar deposits in the Swiss Molasse Basin have been interpreted as fan-delta or braidplain deposits (Platt & Keller, 1992). The Montmaur Conglomerate Formation therefore probably represents a younger upstream analog of the St-Disdier Siltstone Formation, which is interpreted as an alluvial floodplain and associated mixed-load channel system. In fact, the complete vertical arrangement of the Souloise Group, from (1) shallow marine (shelfal?) turbidites (the Souloise Greywacke Formation) at the base to (2) delta/shorezone deposits (the St-Disdier Arenite Formation) to (3) fluvial deposits (the St-Disdier Siltstone) to (4) fan/braidplain deposits (the Montmaur Conglomerate Formation) is consistent with a laterally contiguous, westward prograding, terrigenous clastic basin system. The Montmaur Conglomerate Formation would logically be the most source-proximal of the depositional systems in such a basin.

The Montmaur Conglomerate Formation was sourced from SE to NW, as indicated by imbricated pebbles. This paleocurrent direction is consistent with the present-day location of the Embrunnais-Ubaye nappes, east and east-southeast of Dévoluy, which were the major source of siliciclastic debris. The paleocurrent direction suggests that the absence of the Montmaur Conglomerate Formation in Dévoluy may represent a paleo-depositional limit of the fan/braidplain

system. That is, the fan/braidplain system may have prograded as far northwest as southern Dévoluy.

CHAPTER 9

The sedimentary evolution of the Dévoluy basin within the framework
of the western Alpine foreland basin

The purpose of this chapter is to compare the Eocene - Oligocene sedimentary evolution of Dévoluy (Chapters 2-8) to that of other remnants of the Tertiary western Alpine foreland basin, and to synthesize these observations into a generalized evolution of the foreland basin. The comparisons will focus on the well studied remnants in the southern Chaînes Subalpines, and will conclude with a larger scale comparison of the southern Chaînes Subalpines with the northern Chaînes Subalpines and the Swiss Molasse Basin.

The foreland basin remnants in the southern Chaînes Subalpines are divided here into proximal, central, and distal groups (Fig. 9.1). The stratigraphies of the groups are shown in Table 9-I.

(1) The proximal basin remnants consist predominantly of marine sediments that are generally Bartonian/Priabonian through earliest Oligocene in age (Fig. 9.2). The general stratigraphy (with common French synonyms in parentheses) of these remnants (Table 9-I) consists of:

- a local basal **continental conglomerate** ("Infrannummulitique") that is not present in all basin remnants; this conglomerate may be interbedded with or overlain by **Cerithium-rich marlstones**;
- the **transgressive marine Nummulitic limestone**;
- the **deeper marine Globigerina marls** (Marnes Bleues, Marnes à Foraminifères, Schistes à Melettes, etc.);
- usually coarse-grained, often thickly-bedded **siliciclastic turbidites** (Grès d'Annot, Grès de Champsaur) that, if present, occur above the marls;
- and locally a **melange** (Schistes à Blocs) underlying internal Alpine thrust sheets. This melange, which has a strong tectonic overprint, may have developed from olistostromes deposited ahead of the advancing thrust sheets.

The stratigraphy of the central basin remnants comprises aspects of both the proximal and distal remnants. The deposits are typically Priabonian through Oligocene in age (Fig. 9.2). The stratigraphy (Table 9-I) consists of:

- a local basal **continental conglomerate** (again, this unit is not present in all basin remnants);
- the **transgressive marine Nummulitic limestone**;
- the **deeper marine Globigerina marls**;
- fine-grained, thinly-bedded **siliciclastic turbidites**;
- **shallow marine siliciclastic deposits**;
- **continental siliciclastic deposits** (Molasse Rouge);
- and a coarse-grained siliciclastic **conglomerate** ("Nagelfluh"), not present in all remnants.

The distal basin remnants preserve the youngest (Oligocene through Mio-Pliocene, Fig. 9.2) deposits of the western Alpine foreland basin. This chapter will not address these remnants in detail, as they fall beyond the scope of this thesis. The remnants have an stratigraphy (Table 9-I) that consists of:

- **shallow marine siliciclastic deposits**, interbedded with and overlain by
- **continental siliciclastic deposits**.

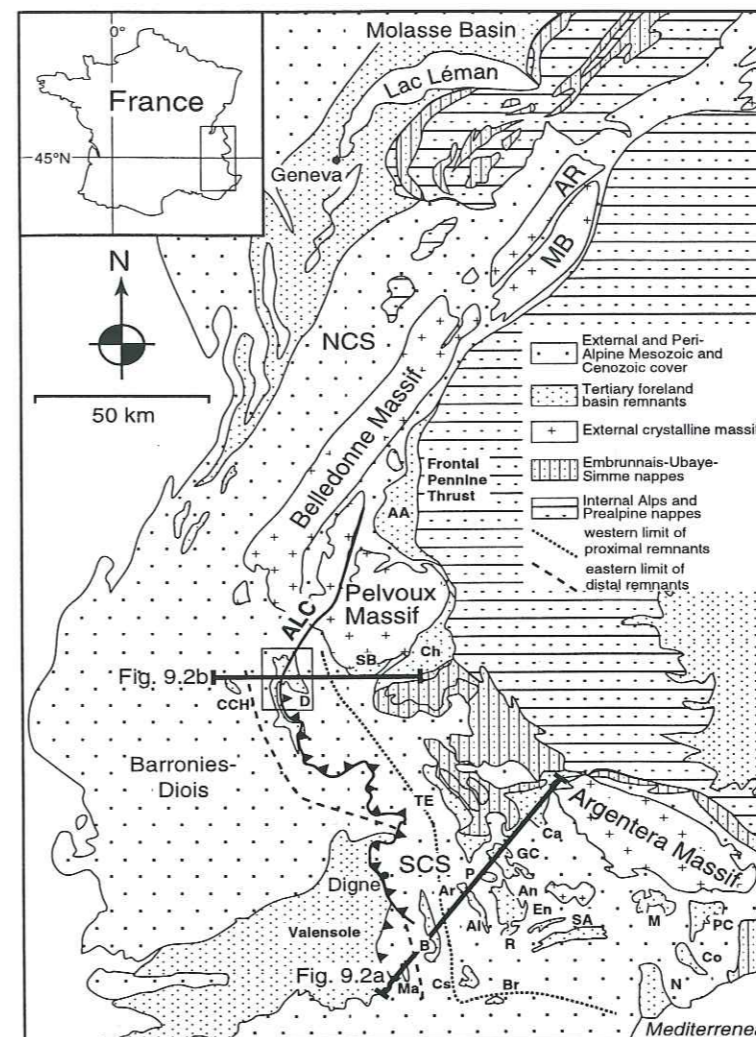


Fig. 9.1. Map of the proximal, central, and distal remnants of the external western Alpine foreland basin. Location of Figs. 9.2a, b indicated. A = Aar Massif; AA = Aiguilles d'Arves basin; Al = Allons basin; ALC = Aspres-lès-Corps Fault; An = Annot basin; AR = Aiguilles Rouges Massif; Ar = Argens basin; B = Barrême basin; Br = Bargême basin; Ca = Cayolle basin; CCH = Col de la Croix Haute basin; Ch = Champsaur basin; Co = Contes basin; Cs = Castellane basin; D = Dévoluy basin; En = Entrevaux basin; GC = Grand Coyer basin; M = Monoinas basin; Ma = Majestres basin; MB = Mont Blanc Massif; N = Nice basin; NCS = Northern Chaînes Subalpines; P = Peyresq basin; PC = Peira Cava basin; R = Rouaine basin; SA = St-Antonin basin; SB = Soleil Bouef; SCS = Southern Chaînes Subalpines; TE = Trois Evêches basin.

Tertiary succession separates Mesozoic sediments from either the basal continental conglomerate or the Nummulitic limestone. Along the southern and eastern borders of the Pelvoux Massif (Fig. 9.1), the Tertiary sediments overlie crystalline and metasedimentary Variscan basement. The unconformity developed during the Eocene, when folding in Provence and Dévoluy and extensional faulting throughout the southern Chaînes Subalpines (Parris *et al.*, 1986; Ravenne *et al.*, 1987) enhanced regional uplift associated with the development of the foreland bulge. The foreland bulge, which is connected with the early stages of the development of the western Alpine foreland basin, is well-documented in the northern Chaînes Subalpines (see Section 9.2), but has not been recognized in the southern Chaînes Subalpines because of the structural complexity of the substratum.

None of the basin remnants preserves the complete sedimentary succession of the western Alpine foreland basin (Fig. 9.2) because the basin depocenter migrated outward with time in response to the progressive emplacement of the Alpine thrust load (e.g., Karner & Watts, 1983, Allen *et al.*, 1986, 1991; Sinclair *et al.*, 1991; Sinclair & Allen, 1992). Given this migration, deposition is typically considered to be diachronous (e.g., Sinclair, in press, his Fig. 6). However, available biostratigraphic control does not allow fine distinctions in age to be made, and a given formation in two remnants is typically given the same age (e.g., the siliciclastic turbidites are considered to be uppermost Eocene/lowermost Oligocene, with no finer distinction being made).

9.1. The evolution of the southern Chaînes Subalpines

9.1.1. Initial stages of foreland basin development: Provençal-phase folding, extensional faulting, subaerial erosion, and development of the distal forebulge

In most basin remnants of the southern Chaînes Subalpines, an angular unconformity at the base of the

ALPINE FORELAND BASIN STRATIGRAPHY	Allons	Annot	Argens	Castellane	Cayolle	Champsaur	Contes	Entrevaux	Grand Coyer	Monoinas	Nice	Peira Cava	Peyresq	Rousains	Soleil Bouef	St-Antonin	From Evéches (Elliott et al., 1985)	Bargême	Barreme	Dévoluy (this study)	Col de la Croix Haute	Majestral	Valensole	COMPOSITION OF ALPINE FORELAND		
continental siliciclastics							Mio-Pliocene				Pli-Quaternary													Miocene marls, sandstones, and conglomerates	continental series/Valensole	
shallow marine siliciclastics "Nagelfluh" (and equivalents)																					Montaur				Miocene marine marls	
continental siliciclastics																			Stamplan continental sediments	Série Saumon/ Série Grise/ Grès	Siltstone Fm./ Montaur	Molasse Rouge		undifferentiated Oligocene	conglomerates, sandstones, and	
shallow marine siliciclastics																			Bruyère breccia!	Senez/St. Lions/ La Poste members (Marnes Bleues)	Lower St-Didier Arenite Formation					
tectonic melange					Schistes à Blocs	melange			Schistes à Blocs																	
siliciclastic turbidites		Annot Sandstone			Annot Sandstone	Champsaur Sandstone	Annot Sandstone		Annot Sandstone	Annot Sandstone/black		black flysch		Annot Sandstone	Champsaur Sandstone	detrital volcanic sediments										
Globigerina marls (and equivalents)	Marnes bleues		Marnes bleues	Marnes bleues	Marnes bleues	Marnes bleues	Marnes bleues/ Calcareous marls	Marnes bleues	Marnes bleues	yellow marls	undifferentiated marls	yellow marls		Marnes bleues	Globigerina marls	yellow marls	Marnes bleues	Präborean Marls	Marnes bleues							
Nummulitic limestone	basal limestone	basal/ intermediate limestones	basal limestone	Nummulitic sandstone/ Castellana	Nummulitic Limestone	Nummulitic limestone	Nummulitic limestone	basal limestones	Nummulitic Conglomerate	Nummulitic limestone	Nummulitic limestone	Nummulitic limestone	basal limestones	basal/ intermediate limestones	Nummulitic limestone	Nummulitic limestone	Nummulitic Limestone	Nummulitic Limestone	Nummulitic Limestone	Nummulitic Limestone	Nummulitic Limestone	Nummulitic Limestone	Nummulitic Limestone	Nummulitic Limestone	Devoluy Nummulitic Limestone Formation	
conglomerate ("infrannummulitic Conglomerate")	Argens Conglomerate		Argens Conglomerate	Cerithium marls	Argens Conglomerate	Infrannummulitic conglomerate/ Cerithium marls	"basal conglomerate"	Argens Conglomerate	Argens Conglomerate				Argens conglomerate	Argens Conglomerate	Argens conglomerate/ cerithium marls				Cerithium marls/ conglomerates and sands	Conglomerate/ Infrannummulitic	Pierroux Conglomerate Formation	continental sandstone				
Paleocene-L. Eocene continental deposits																									Luxedan limestone and marls	
geologic map (BRGM 1:50,000)/reference	Entrevaux	Entrevaux	Entrevaux	Castellane	Elliott et al. 1985	Orcières	Menton-Nice	Entrevaux	Allos	St-Martin-Vésubie/ Puget-Théniers	Menton-Nice	St-Martin-Vésubie	Entrevaux	Entrevaux		Puget-Théniers	Elliott et al. 1985	Fayence	Digne	this study	Mens			Digne/ La Javie		

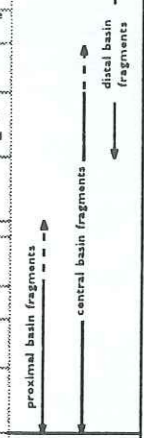


Table 9-1. Stratigraphies of the remnants of the western Alpine foreland basin found in the southern Chaînes Subalpines. Nomenclature from BRGM 1:50,000 geologic maps, Elliott et al. (1985), and this study.

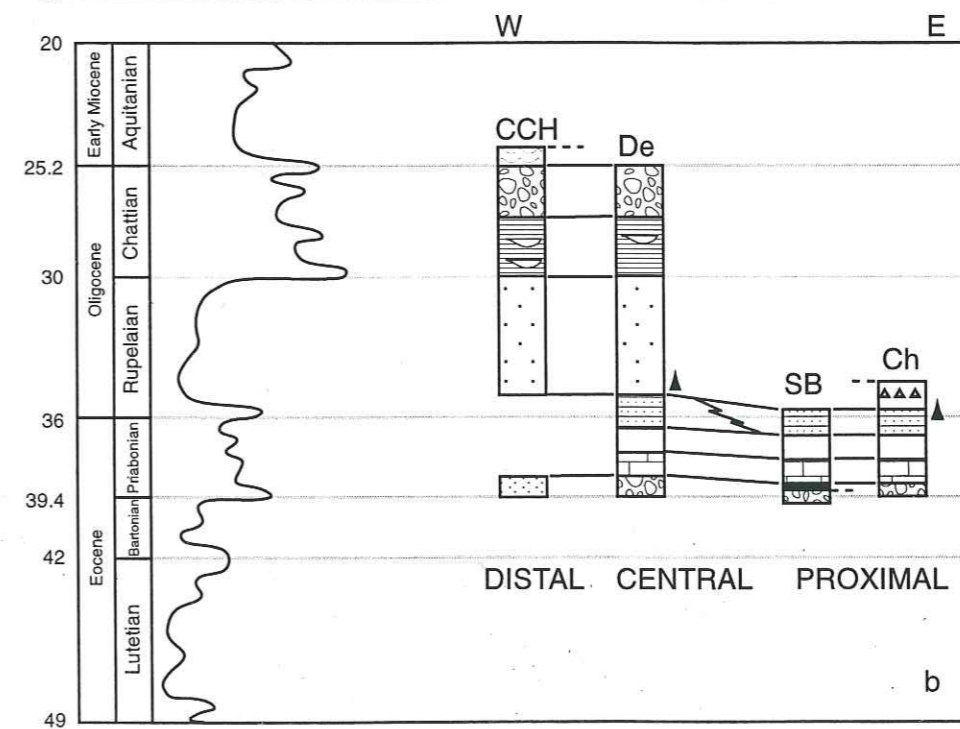
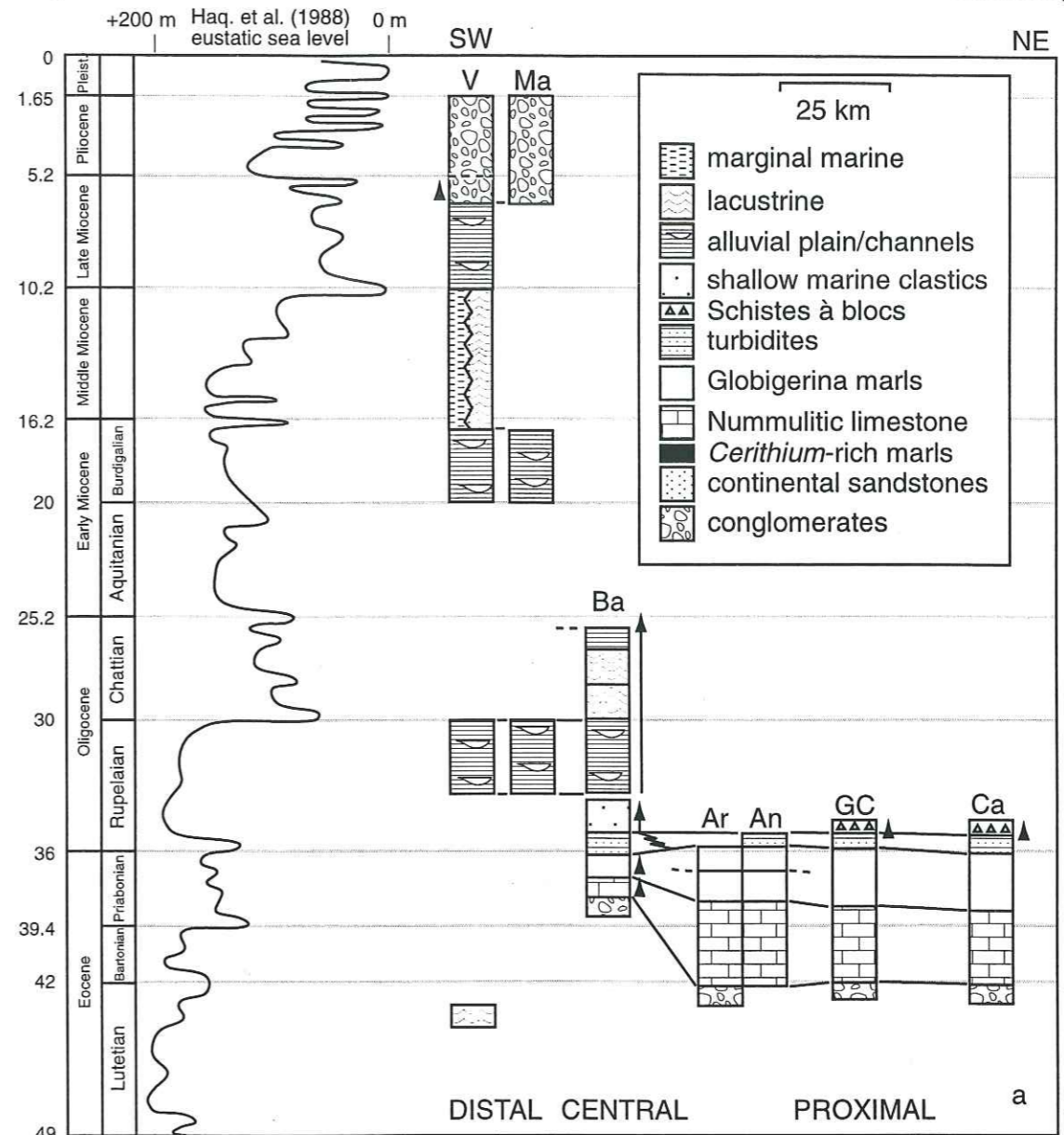


Fig. 9.2. Chronostratigraphic correlations through the southern Chaînes Subalpines. The different formations are probably time-transgressive, but biostratigraphic resolution does not allow this to be displayed. Arrows and arrow tips indicate tectonic activity. Note that the turbidites at Soleil Bouef are rich in volcanic detritus. Sections located in Fig. 9.1.

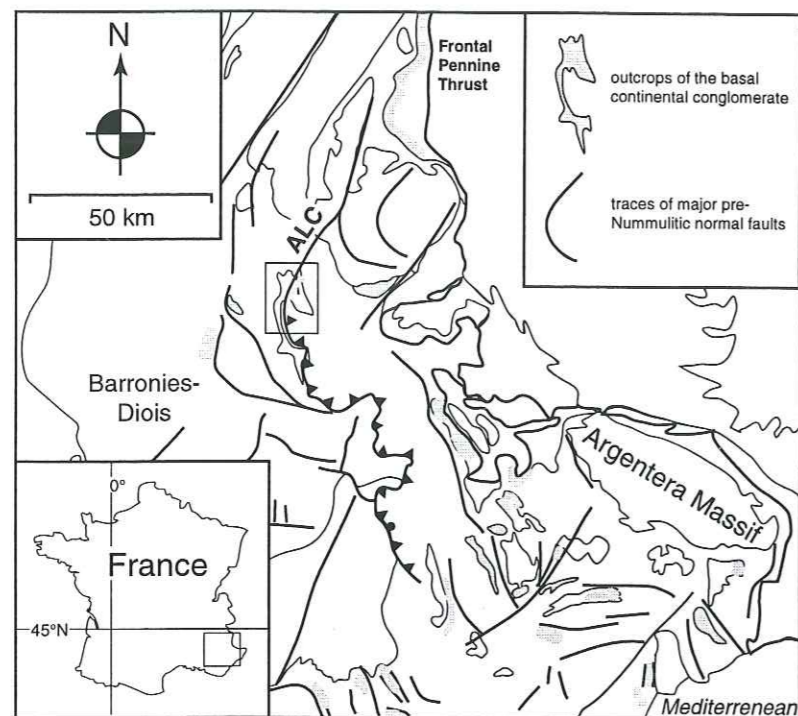


Fig. 9.3. Map of areas where there are isolated outcrops of the basal continental conglomerate in the southern Chaînes Subalpines. Modified in part after Kerckhove et al. (1980), Pairis et al. (1984b), Ravenne et al. (1987), and Pairis (1988).

If the unconformity developed in the earliest Eocene, it is potentially coeval with a eustatic sea-level fall at the Paleocene-Eocene boundary (Haq *et al.*, 1988). However, despite the obvious temptation to therefore ascribe a eustatic cause for the lower sequence boundary of the western Alpine foreland basin, two facts must be considered. (1) In the absence of a marine basin in the southern Chaînes Subalpines during the Paleocene, any erosion on the continent associated with this base-level fall would presumably have been subordinate to erosion of an already tectonically-uplifted topography. (2) The "Eocene" continental conglomerates are imprecisely dated (see below), and, therefore, potential correlations with the eustatic curve are, in this case, tenuous at best.

9.1.2. Eocene continental deposition

The oldest Tertiary deposits overlying the basal unconformity are the "infrannummulitic" conglomerates that occur in isolated outcrops throughout the southern Chaînes Subalpines (Fig. 9.3). A chronologic correlation of these conglomerates has not been established because the sediments are devoid of fossils. In figure 9.2, the conglomerates are shown as having been deposited immediately before the Nummulitic limestone, following Pairis (1988), Pairis *et al.* (1984), Evans & Mange-Rajetzky (1991), and Sinclair (1996).

The conglomerates are everywhere considered to be continental, and are assumed to have infilled pre-existing topography (e.g., Sinclair, 1996). The close spatial association of the conglomerates with normal faults (cf. Chapter 2; also, Ravenne *et al.*, 1987; Vially, 1994), which may or may not have been syndepositionally active, suggests that the occurrences of the conglomerates may have been tectonically controlled.

In some localities (Fig. 9.2; Table 9-I), *Cerithium*-rich marlstones are intercalated with or overlie the conglomerates towards the top of the succession. The presence of *Cerithium* typically indicates brackish water conditions, such as found in lagoonal environments. Therefore, the marlstones probably represent a gradual transition to marginal marine conditions before the onset of fully marine conditions during the late Eocene.

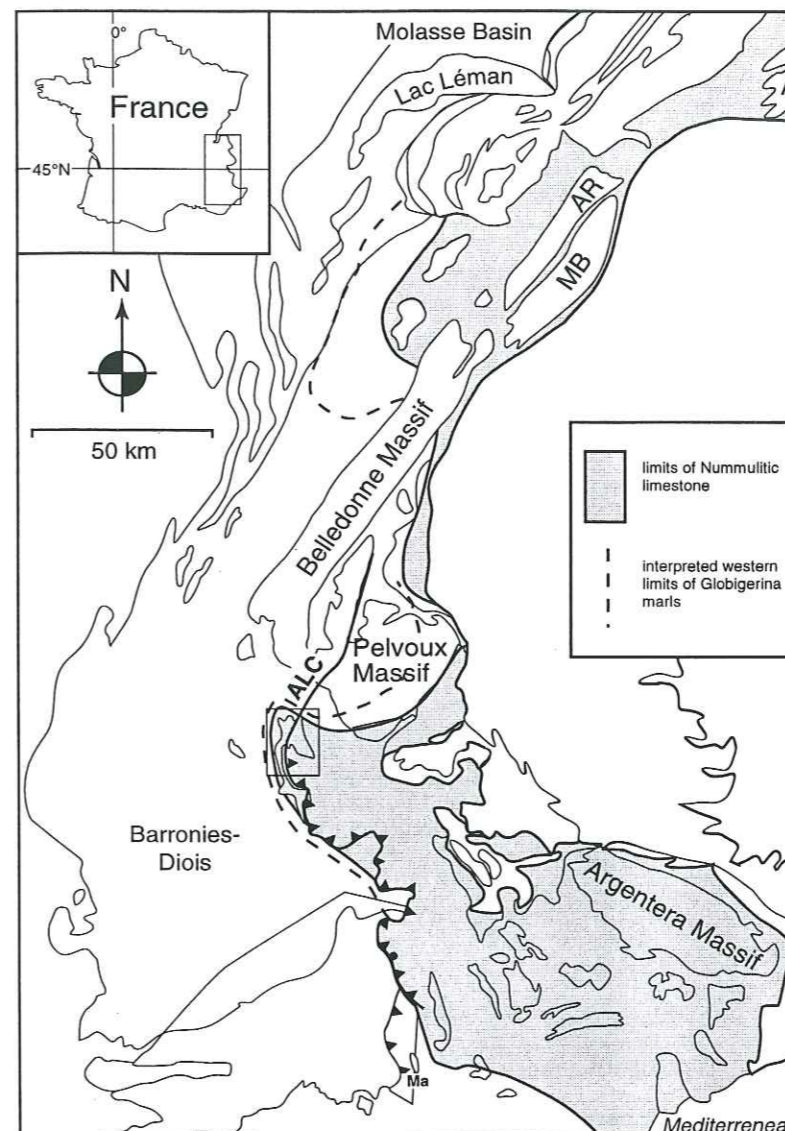


Fig. 9.4. Map of the interpreted depositional limits (below the Frontal Pennine Thrust) of the Nummulitic limestone and Globigerina marls throughout the external western Alps. Modified in part after Kerckhove et al. (1980), Pairis et

This interpretation supports the idea that the conglomerates were probably deposited immediately prior to the Nummulitic limestone.

9.1.3. The underfilled stage of foreland basin development: Deepening-up, carbonate-dominated deposition

The Alpine Nummulitic limestone was deposited throughout the southern Chaînes Subalpines (Table 9-I; Fig. 9.4) on the distal edge of the evolving marine Alpine foreland basin (Allen *et al.*, 1991; Crampton, 1992; Crampton & Allen, 1995). The Nummulitic limestone is diachronous (Fig. 9.2): older (Bartonian-Priabonian) deposits are located more internally, whereas younger (Priabonian) deposits occur more externally (Herb, 1988; Sinclair & Allen, 1992; Crampton & Allen, 1995).

The Nummulitic limestone was deposited in a transgressive marine environment, as seen, for instance, in Dévoluy, where the upsection transition from the shoreface setting of the Nummulitic Conglomerate Member to the shelf setting of the Nummulitic Calcarenite Member reflects gradual flooding. The limit of the Nummulitic sea at the end of the Eocene (Fig. 9.4) is based on the westernmost preserved deposits of the Nummulitic limestone in the southern Chaînes Subalpines. Sinclair (1996; in press) shows the temporal

Univ. J. Fourier - O.S.U.G.
MAISON DES GEOSCIENCES
DOCUMENTATION
F. 38041 B.P. 53
Tél. 04 76 63 54 27 - Fax 04 76 51 40 58
Mail: dialou@ujf-grenoble.fr

migration of this coastline from 49 - 40 Ma. The Nummulitic limestone is not present in external basin remnants (Table 9-I; Fig. 9.4).

The Queyras Marlstone Formation in Dévoluy and its Alpine equivalents (Table 9-I; Fig. 9.2), which overlie the Nummulitic limestone, are deeper marine deposits that reflect continued deepening in a still strongly carbonate-dominated basin. The deepening was largely the result of increased subsidence. For example, in Champsaur, at the edge of the Pelvoux Massif (Fig. 9.1), subsidence is estimated to have increased from 40 m/My during deposition of the Nummulitic Limestone to 80 m/My during deposition of the Globigerina marls (Crampton, 1992). At Trois Evéchés (Fig. 9.1), nearer to the interpreted basin center, subsidence is interpreted to have increased from 25 m/My during deposition of the Nummulitic Limestone to 825 m/My during deposition of the marls (Vially, 1994). The subsidence was probably enhanced by the local effects of syndepositionally active (Gidon & Pairis 1976; Fabre *et al.*, 1985a, b; Evans, 1987) normal faults, although movement on the faults cannot alone explain the deepening (Vially, 1994; Meckel *et al.*, 1996).

The deepest part of the basin is interpreted to have been northeast of Trois Evéchés based on condensed marl deposition or non-deposition here ("sedimentary vacuity area" of Ravenne *et al.*, 1987 and Vially, 1994). Blanc *et al.* (1987) suggested that this part of the basin was below the depth of carbonate compensation (CCD) during the Priabonian. The extent of this deepest part of the basin is unknown because most of the area in question presently lies beneath the Embrunais-Ubaye nappes (Fig. 9.4).

The deepening-up ("underfilled", Covey, 1986) conditions which characterize this early phase in the development of the southern Chaînes Subalpines indicate that the rate of creation of accommodation space was greater than the rate of sediment supply into the basin during the late Eocene.

9.1.4. Marine flooding

The deepest marine conditions in the external western Alpine foreland basin occurred in the late Priabonian, at the end of deposition of the Globigerina marls and equivalent sediments (Ravenne *et al.*, 1987; Vially, 1994, Sinclair, in press). Maximum depths have been estimated to vary in the proximal basin remnants from 900 m at Annot (Mougin, 1978 in Ravenne *et al.*, 1987; Kerckhove *et al.*, 1980), to between 2000 m (Vially, 1994) and 2300 m (Ravenne *et al.*, 1987) at Trois Evéchés, and approximately 3750 m east of Trois Evéchés in Sanguinière (Ravenne *et al.*, 1987). The maximum depth of the central basin remnants, at the western edge of the marine basin, has not been ascertained, but must have been less than that of the proximal remnants, given that the foreland basin shallowed towards the forebulge in the west.

The deep-water sediments record relatively stable and calm conditions in the basin. However, the upsection occurrence of carbonate turbidites, slumps, and, more significantly, terrigenous clastic material (Kerckhove *et al.*, 1980; Ravenne *et al.*, 1987) in the Globigerina marls indicates the onset of a fundamental change in depositional conditions in the foreland basin. The change is reflected by a transition from carbonate-dominated to siliciclastic-dominated deposition, and also by a transition from deepening-up (accommodation-dominated) to shallowing-up (supply-dominated) conditions at the Eocene-Oligocene boundary. The latter of these transitions indicates that maximum marine flooding occurred during the late stages of deposition of the Globigerina marls.

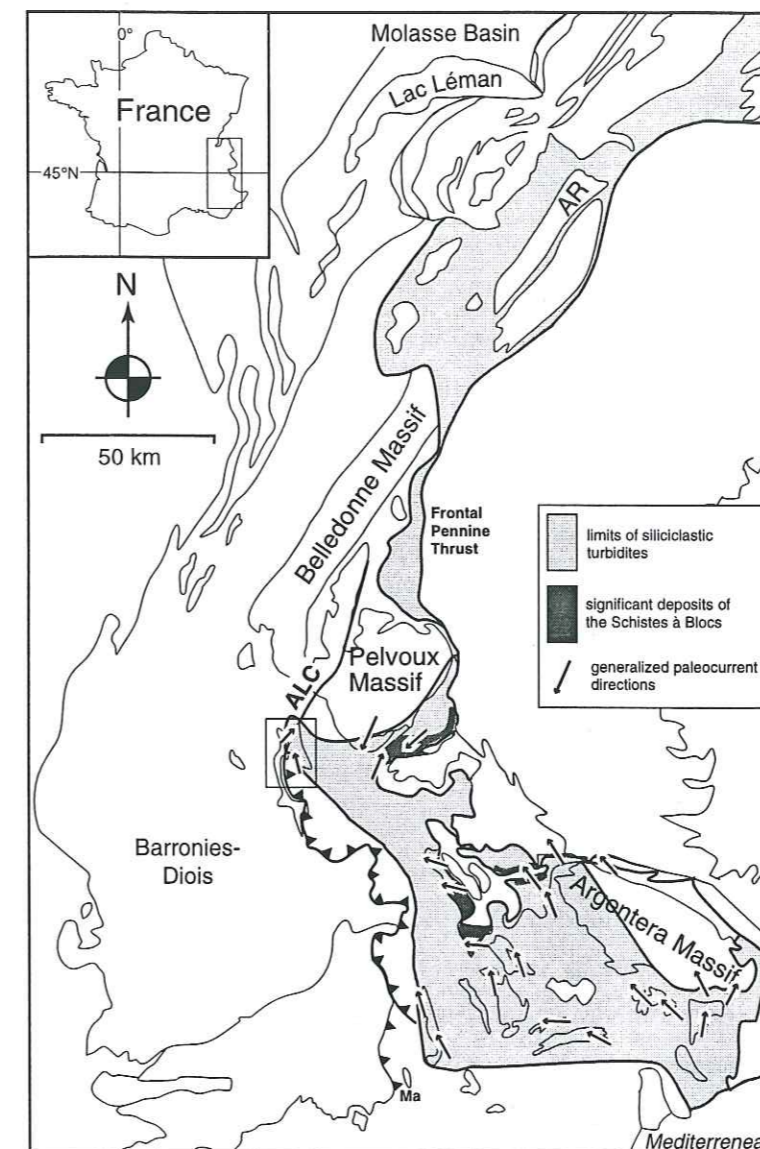


Fig. 9.5. Map of the interpreted depositional limits of the Eo-Oligocene turbidites below the Frontal Pennine Thrust. Paleocurrent indicators (arrows) show general NW-directed flow along the basin axis. Modified in part after Kerckhove *et al.* (1980), Pairis *et al.* (1984b), Ravenne *et al.* (1987), and Pairis (1988).

9.1.5. The transition from underfilled to overfilled conditions: shallowing-up, siliciclastic marine sedimentation and syndepositional deformation

The initial siliciclastic sediments in the southern Chaînes Subalpines were deposited in proximal and central basin remnants at around the Eo-Oligocene boundary (e.g. BRGM, 1957, 1968, 1970b, 1978a, 1978b, 1980a, 1980b, 1981). The change to predominantly siliciclastic sedimentation may have been tectonically controlled (e.g., Meckel, 1995), as the Embrunais-Ubaye nappes had been transported to a position bordering the foreland basin by the early Oligocene (Kerckhove *et al.*, 1980; Waibel, 1990) and the Maures-Esterel Massif to the south was actively uplifting (e.g., Ravenne *et al.*, 1987; Vially, 1994). However, more sophisticated geohistory analysis is necessary to document the exact cause of the transition.

The first siliciclastic deposits are a series of turbidites that include the Annot Sandstone in Annot and other internal basin remnants of southeastern France, the Champsaur Sandstone in Champsaur, the Grès de Ville Sandstone in Barrême, and the Souloise Greywacke Formation in Dévoluy (Table 9-I; Fig. 9.2). The Annot and Champsaur Sandstones have traditionally been interpreted as deep-water submarine fan turbid-

ites deposited along the internal side of the western Alpine foreland basin (e.g., Bouma, 1962; Stanley, 1975; Elliott *et al.*, 1985; Ravenne *et al.*, 1987). Sinclair (1993) reports evidence for shallow marine, fluviially-fed source systems for these turbidites in easternmost Annot. The turbidites in the central basin remnants (Table 9-I) have been interpreted as having been deposited in a distal delta/pro-delta setting (the Grès de Ville, Evans, 1987; Evans & Mange-Rajetzky, 1991; the Souloise Greywacke Formation, this report) or, more generally, in a shallow marine setting (Kerckhove *et al.*, 1980; Meckel *et al.*, 1996).

The various turbidite deposits have differing petrographies (e.g., Ivaldi, 1989), and so cannot be lithologically correlated although they are of the same age (Fig. 9.2). The sediments of the southernmost basin remnants in the southern Chaînes Subalpines were primarily derived from the Corso-Sardinian Massif and the internal Alpine nappes (Kerckhove *et al.*, 1980; Ravenne *et al.*, 1987; Ivaldi, 1989; Vially, 1994), whereas basin remnants to the north were sourced only from the internal Alpine nappes (Bodelle, 1971; Fontignie, 1981; Fontignie *et al.*, 1987; Ivaldi, 1989; Waibel, 1990). Internal basins, with the exception of southeastern Champsaur, contain a characteristic volcanoclastic (andesitic) component, whereas central basin remnants and northwestern Champsaur have a predominantly metamorphic (notably, ophiolitic) petrology (Kerckhove *et al.*, 1980; Waibel, 1990). The abundant volcanic detritus present in proximal basin remnants is enigmatic, because no andesitic source areas are presently exposed. However, Pairis (1988) and Sinclair (in press) indicate possible paleo-locations of these volcanoes (Fig. 9.5) based on petrologic considerations.

The distribution of these differing petrographies may be attributed to the deposition of turbidites from different source areas in tectonically-compartmentalized depositional sub-basins (e.g., Elliott *et al.*, 1985; Vially, 1994). However, at least some of the sediment from the different source areas was mixed in certain sub-basins, as seen for instance in the Barrême basin remnant, where the Grès de Ville turbidites contain both volcanic and ophiolitic material (Kerckhove *et al.*, 1980; Evans, 1987; Evans & Mange-Rajetzky, 1991).

At a regional scale, the turbidites of the southern Chaînes Subalpines have NW-directed flow indicators, reflecting basin-axial flow from the southeast (Fig. 9.5). Local variations in the paleocurrent directions that exist in several of the basin fragments may have been caused reflection of the currents by local sea-floor topography (cf. Chapter 5). These local variations probably also reflect input from internal Alpine sources.

Overall, the turbidites record progressively shallower water conditions upsection, which reflects the onset of supply-dominated conditions in the southern Chaînes Subalpines. The shallowing is best documented in the central basin remnants, where a decrease in water depth from below wave base to above fair weather wave base occurs (Evans, 1987; this report). In the proximal basin remnants, where the sea was deeper, the shallowing is not as well established because of a lack of precise bathymetric control, and because the internal Alpine nappes were subaqueously emplaced onto the turbidites (e.g., BRGM, 1967a; BRGM, 1980c). The shallowing seen in the turbidites may have been the result of (1) an increase in sediment supply, (2) tectonic uplift of the basin, (3) a fall in global sea level, or (4) some combination of these factors.

(1) In the basin remnants where the Annot sandstones *sensu lato* are preserved, the turbidites onlap the basin floor from east to west (Elliott *et al.*, 1985; Ravenne *et al.*, 1987; Vially, 1994). This onlap reflects a dramatic increase in sediment supply, as follows. The onlap was contemporaneous with ongoing Alpine orogenesis (Arnaud *et al.*, 1977; Trümpy, 1980; Karner & Watts, 1983; Dewey *et al.*, 1989; Fry, 1989a; Vially, 1994). The associated load should have caused subsidence and deepening in the external domain, as happened in the north Alpine foreland basin (Lemcke, 1974; Homewood, 1986; Homewood *et al.*, 1985, 1986). However,

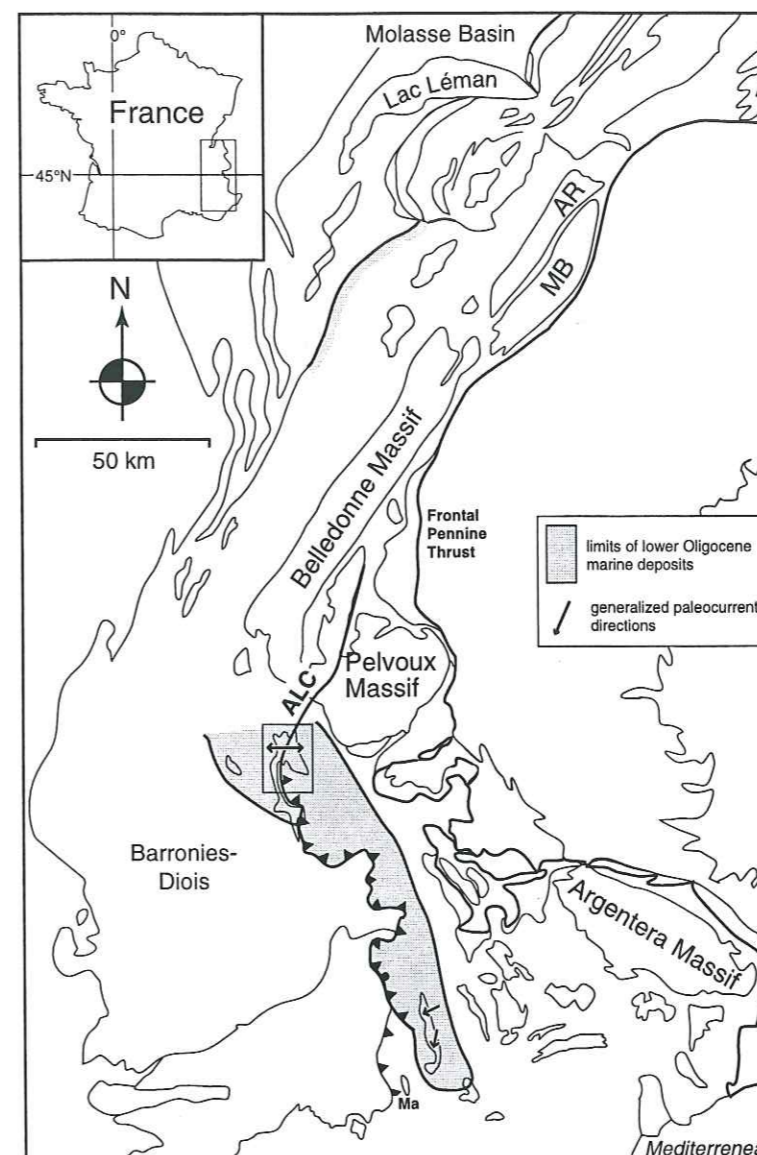


Fig. 9.6. Map of the interpreted depositional limits of the lower Oligocene shallow marine siliciclastics throughout the external western Alps. Modified in part after Kerckhove *et al.* (1980), Pairis *et al.* (1984b), Ravenne *et al.* (1987), and Pairis (1988).

in the southern Chaînes Subalpines, sediments prograded towards the west, which implies that sediment supply had to have increased at a greater rate than the creation of accommodation space.

(2) Overall subsidence may also have been partially countered by more localized tectonic uplift ahead of the advancing internal nappes, caused by the transportation of parts of the basin as "piggyback" basins (Ori & Friend, 1984; Evans, 1987; Lateltin, 1988; Sinclair, 1989; Vially, 1994). For instance, Vially (1994) estimates from subsidence models that the Trois Evéchés area (Fig. 9.1) was tectonically uplifted approximately 250 m during deposition of the Annot Sandstone.

(3) A significant eustatic influence in the southern Chaînes Subalpines is doubtful because the eustatic sea level rise in the early Oligocene (Haq *et al.*, 1988) is not reflected in the sedimentary record. One possible explanation is that the eustatic fall at the Eocene-Oligocene boundary complimented the uplift in the southern Chaînes Subalpines, resulting in shallowing at the Eocene-Oligocene boundary. In this hypothesis, the ensuing eustatic rise did not outstrip the effects of uplift and increased sediment supply in the southern Chaînes Subalpines, and deep marine conditions werer not re-established.

During and following deposition of the turbidites, the most internal of the proximal basin remnants of the southern Chaînes Subalpines were overthrust by the internal nappes, burying them to depths of 6-8 km (prehnite-pumpellyite metamorphic facies) in the case of Champsaur (Waibel, 1990). In the Cayolle, Champsaur, Grand Coyer, and Trois Evéchés basin remnants, the Schistes à Blocs (Fig. 9.5) are the last sediments found (Table 9-I). These rocks underlie the Embrunnais-Ubaye nappes.

Stratigraphy in the central basin remnants shows that shallow marine deposition continued (e.g., the St-Disdier Arenite Formation in Dévoluy and the Grès de Senez/St-Lions/La Poste Members in Barrême; Table 9-I; Fig. 9.2). This deposition, which is associated with a reduction in the width of the foreland basin (compare Figs. 9.5 and 9.6), records the late stage of infilling of the marine foreland basin.

The infilling was rapid enough that, as with the deposition of the preceding turbidites, any overall regional subsidence associated with the emplacement of the nappes was outstripped by sedimentation, whereby the basin was completely filled. The high rate of sediment supply was enhanced in Dévoluy by local uplift of the western margin of the basin, which resulted in the formation of a progressive unconformity at the base of the St-Disdier Arenite Formation (see Chapter 6). The uplift was probably due to a blind, foreland-propagating thrust beneath Dévoluy.

9.1.6. The "overfilled" stage of foreland basin development: Re-establishment of continental conditions and terminal sub-aerial erosion

The upper Oligocene St-Disdier Siltstone and Montmaur Conglomerate Formations in Dévoluy, their equivalents in the central and distal basin remnants of the southern Chaînes Subalpines, and the later Mio-Pliocene deposits of the distal basin remnants (Table 9-I) are continental deposits that reflect the "overfilling" (Covey, 1986) of the western Alpine foreland basin late in its history. Although the shift from marine to continental deposition occurred at the same time as a significant fall in eustatic sea level that lasted from the middle of the early Oligocene through the end of the early Oligocene (Haq *et al.*, 1988), the transition cannot only have been eustatically forced for two reasons. (1) The overall sedimentary succession in the Oligocene is shallowing-up, which does not correspond with the third-order eustatic highstand (Haq *et al.*, 1988) at this time (Fig. 9.2). (2) The shift from marine to continental deposition occurs at the same time as a progressive westward shift of the sedimentary depocenter that continued through the Mio-Pliocene (Figs. 9.2, 9.7); such a geographic shift cannot be explained by a purely eustatic cause. If the transition was not eustatically forced, then, as with other transitions in the southern Chaînes Subalpines, this change must have been associated with an advance of the internal thrust sheets. An advance of the internal nappes may have been responsible, for instance, for the depositional hiatus during the Aquitanian in the Majestres and Valensole basin remnants (Fig. 9.2a; Evans, 1987). Finally, the upper Oligocene continental deposits consist primarily of internal Alpine components (e.g., Ivaldi, 1989), which further documents their genetic association with the nappes.

9.2. Correlation with the Swiss Molasse Basin

The evolution of the northern Chaînes Subalpines and Swiss Molasse Basin (hereafter referred to collectively as the northwestern Alpine foreland basin) is in many regards similar to that of the southern Chaînes Subalpines. In particular, the stratigraphy consists of comparable units that are approximately time-equivalent with those in the southern Chaînes Subalpines: a basal continental formation, a deepening-up carbonate succession comprising the Nummulitic limestone and Globigerina marls, and a shallowing-up succession

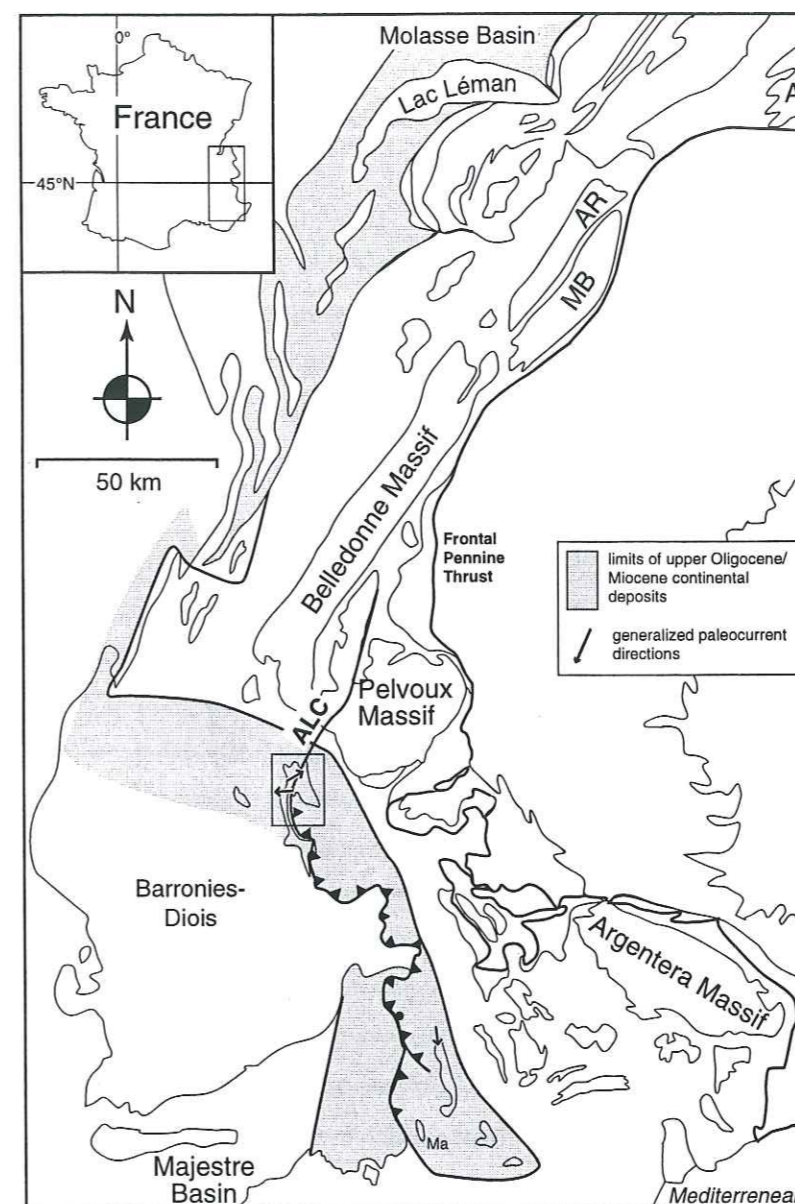


Fig. 9.7. Map of the interpreted depositional limits of the upper Oligocene and Mio-Pliocene continental deposits throughout the external western Alps. Modified in part after Kerckhove *et al.* (1980), Pairis *et al.* (1984b), Ravenne *et al.* (1987), and Pairis (1988).

comprising siliciclastic turbidites (the "North Helvetic flysch") and shallow marine and continental clastics ("Lower Marine Molasse", "Lower Freshwater Molasse") (e.g., Trümpy, 1980; Homewood *et al.*, 1985, 1986; Sinclair *et al.*, 1993; Sinclair, 1996, in press). In addition, the northwestern Alpine foreland basin has an upper shallow marine and continental succession ("Upper Marine Molasse", "Upper Freshwater Molasse") not found in the southern Chaînes Subalpines.

The following discussion treats comparable units from the northern and southern Chaînes Subalpines as equivalents; however, detailed correlations of the units from the two areas have not been established, and to do so here is beyond the scope of this work. The primary differences between the two areas are tectonic, as summarized below.

A basal subaerial unconformity that bounds the sedimentary sequence of the northwestern Alpine foreland basin - as in the southern Chaînes Subalpines - has been identified as a probable forebulge unconformity associated with the early stages of crustal loading by the internal Alpine units (Allen *et al.*, 1991; Sinclair *et al.*, 1991; Crampton & Allen, 1995). This feature is more prominent than in the southern Chaînes Subalpines because the subcrop in the northwestern Alpine foreland basin is less faulted and folded. The beginning of

forebulge erosion in the northwestern Alpine foreland basin is taken as Paleocene (Allen *et al.*, 1991).

The oldest deposits overlying the unconformity in the northwestern Alpine foreland basin (the "siderolithique" laterites and residual quartzarenites and glauconite-rich shallow marine sandstones) infill a karstified topography (Herb, 1988) on the forebulge (Crampton & Allen, 1995). This style of localized infilling of minor erosional topography (Allen *et al.*, 1991) contrasts with the coarse, fault-controlled continental conglomerates in the southern Chaînes Subalpines, which can be as thick as 200 m (e.g., the Argens Conglomerate south of Barrême, Evans, 1987; this study, Chapter 2).

The continental deposits in the northwestern Alpine foreland basin are overlain by the Nummulitic limestone, which is interpreted as having been deposited on the forebulge of the incipient Alpine foreland basin (Fig. 5.19; Herb, 1988; Crampton, 1992; Crampton & Allen, 1995). Large-scale crustal relaxation (e.g., Quinlan & Beaumont, 1984; Jordan, 1995) or foreland migration of the orogenic load led to the outward migration of the forebulge with time (Sinclair & Allen, 1992). The Nummulitic limestone tracked this migration (Allen *et al.*, 1991; Sinclair, 1996) and is thus diachronous (older in the southeast and younger in the northwest) (Herb, 1988). Tectonic subsidence associated with the migration is generally accepted to have been less in the north than in the south (e.g., Homewood *et al.*, 1985, 1986; Crampton, 1992), but relative sea level rose nonetheless in the northwestern basin, such that there was a rapid flooding and Globigerina marls were deposited in the late Eocene (Allen *et al.*, 1991). The cause of the different rates of subsidence is still enigmatic. Sinclair (1996) suggests that it may reflect local variations in the structural rigidity (effective elastic thickness) of the European crust in the two areas.

A rapid influx of siliciclastic turbidites (the lower part of the Lower Marine Molasse, and the Taveyennaz and Val d'Illez Sandstones in eastern France and western Switzerland) in the late Eocene and early Oligocene followed the deposition of the Globigerina marls in the northwestern Alpine foreland basin (Homewood & Caron, 1982; Homewood *et al.*, 1985, 1986). These turbidites preserve the same proximal to distal relationships seen in the southern Chaînes Subalpines: (1) coarse-grained, thick-bedded turbidites in a more internal setting, the deposition of which was terminated by the emplacement of thrust sheets, and (2) shallowing of more distal, thinly-bedded turbidites from moderate through relatively shallow water depths (Homewood *et al.*, 1985, 1986; Sinclair, 1991). These latter turbidites have been interpreted as distal delta deposits (Homewood *et al.*, 1985).

A eustatic sea level fall at the Eocene-Oligocene boundary (Haq *et al.*, 1988) has been invoked as a mechanism for the observed shallowing in the Swiss Molasse Basin (Homewood *et al.*, 1985, 1986). However, as with the similar situation in the southern Chaînes Subalpines, this interpretation is problematic because the preceding late Eocene and subsequent Oligocene deposits are not consistent with the eustatic respective fall and rise in eustatic sea level (see sea level curve, Fig. 9.2). Moreover, Sinclair (1991) suggests that a blind "front-runner" thrust ahead of the internal Alpine thrust sheet may have caused the onset of the turbidite sedimentation, and Homewood *et al.* (1986) state that tectonically-related "wildflysch" deposits are interbedded with turbidite beds in the upper Val d'Illez Sandstone. This syndepositional tectonism could have led to uplift and/or increased sediment supply, which would have caused a shallowing unrelated to the eustatic event.

The turbidites of the Lower Marine Molasse are overlain by middle Oligocene shallow marine, shoreface, and marginal marine siliciclastics, which are themselves overlain by upper Oligocene - lower Miocene fluvial and alluvial clastics of the Lower Freshwater Molasse (Homewood *et al.*, 1985, 1986). The sedimentary struc-

tures and interpreted depositional environment of the marine deposits (Homewood *et al.*, 1986) are similar to the St-Disdier Arenite Formation in Dévoluy, while the Lower Freshwater Molasse deposits (Platt & Keller, 1992) are similar to the St-Disdier Siltstone and Montmaur Conglomerate Formations in Dévoluy and the Molasse Rouge elsewhere in the southern Chaînes Subalpines. Thus, it seems that similar sedimentological conditions were present throughout the external western Alpine foreland. However, one significant difference between the two areas is that, because deposition of the Lower Freshwater Molasse began synchronously with the onset of a phase of rapid subsidence in the Molasse Basin (Homewood *et al.*, 1985, 1986; Burbank *et al.*, 1992), the preserved Lower Freshwater Molasse deposits are significantly thicker (up to 4 km, Homewood *et al.*, 1986) than the Molasse Rouge (approximately 360 m in Barrême, Evans & Mange-Rajetzky, 1991). The cause of the differential loading is unknown.

9.3. Summary

The upper Eocene through Oligocene sediments of the western Alpine foreland basin have a relatively consistent stratigraphy that can be divided into deepening-up, carbonate-dominated deposits and shallowing-up, siliciclastic-dominated deposits. The sedimentary sequence is bounded at its base by a subaerial unconformity that is interpreted to be associated with flexural uplift at the forebulge. Continental "infrannummulitic" conglomerates overlying the unconformity appear to have a tectonically-controlled distribution in the southern Chaînes Subalpines. A marine transgressive surface separates these sediments from the overlying shallow marine Nummulitic limestone, which is interpreted to have been deposited at the edge of the forebulge. Tectonically-induced deepening in the latest Eocene led to maximum marine flooding during deposition of the Globigerina marls, after which the deposits of the foreland basin became siliciclastic. These deposits, Oligocene in age, include turbidites, shallow marine sandstones, and fluvial/alluvial siltstones, sandstones, and conglomerates. These units represent a period during which sedimentary infilling of the basin occurred at a faster rate than the creation of accommodation space, in particular tectonic subsidence associated with the emplacement of the internal Alpine nappes. The outward migration of these nappes with time caused a synchronous shift in the sedimentary depocenters of the basin, most notably during the late Oligocene and Miocene.

The evolution of the northern and southern branches of the external Alpine foreland basin are similar, but significant differences exist because of variable responses of the two areas to large-scale tectonic forces.

PART II
NEOGENE STRUCTURAL GEOLOGY OF THE DÉVOLUY BASIN

Chapter 10
LATE ALPINE STRUCTURES

Late Alpine (post-Oligocene) structures in Dévoluy include a locally developed pressure solution cleavage, large-scale folds, thrust faults, and sub-vertical N-S and NNE-SSW striking faults that cut through central Dévoluy (Fig. 10.1). The following analysis expands on a previously published description and interpretation of these structures (Meckel *et al.*, 1996).

10.1. Folds in northern Dévoluy

Large-scale folds in northern Dévoluy are open, N-S to NNW-SSE trending, W-verging, and shallowly to moderately plunging (Figs. 10.1, 10.2, 10.3). They have long western limbs and short eastern ones, and are thus asymmetric to the west. The folds, which include the Tête de la Tune, Rourebean, Puy de Rioupes, and the Col de l'Aup Synclines, and the Combette and Gicon Anticlines, are cut by the Median Dévoluy Thrust and the Lucles, Les Bourrettes and Malmort Faults (Figs. 10.1, 10.3). These folds are described below from west to east.

The Tête de la Tune Syncline (fold axis = 25-171; Fig. 10.2a), the foot wall syncline of the Median Dévoluy Thrust, has a half-wavelength of approximately 4 km and an amplitude of 500 m (Fig. 10.3a). It is only completely visible at the northern end of Dévoluy, as its eastern limb is overthrust south of the village of Haut Gicon (Figs. 10.1, 10.3). At Puy de Rioupes (Fig. 10.1), a minor fold pair occurs in the western limb of the fold (Fig. 10.3d).

The locally defined Rourebean, Puy de Rioupes, and Malmort Synclines and Combette Anticline occur in the hanging wall the Median Dévoluy Thrust, west of the Malmort Fault (Figs. 10.1, 10.3c, d). These folds, which trend NNE-SSW to NNW-SSE, have 1 km half wavelengths and 100-200 m amplitudes.

The Gicon Anticline (fold axis = 20-177; Fig. 10.2b) occurs in the hanging wall of the Median Dévoluy Thrust. It has a 1 km half wavelength and a 200 m amplitude. It is cut in central Dévoluy by N-S and NNE-SSW faults (Figs. 10.3c, d), but may be laterally equivalent to the south to the Auroze Anticline in southern Dévoluy (Fig. 10.1).

The Col de l'Aup Syncline (fold axis = 14-181; Fig. 10.2c) lies east of the Gicon Anticline (Fig. 10.1). It has a half wavelength of at least 2 km, and an amplitude of at least 500 m (Fig. 10.3a). The northern hinge zone contains small, meter-scale synthetic folds that plunge to the SSE in the west and to the SSW in the east (Fig. 3.7). Its hinge is cut by the Les Bourrettes Fault in central Dévoluy (Figs. 10.1, 10.3d), but the fold is considered to be laterally equivalent to the St-Etienne Syncline in southeastern Dévoluy (Gidon & Pairis, 1976).

The folds are all oriented approximately perpendicular to the W-directed transport recorded on

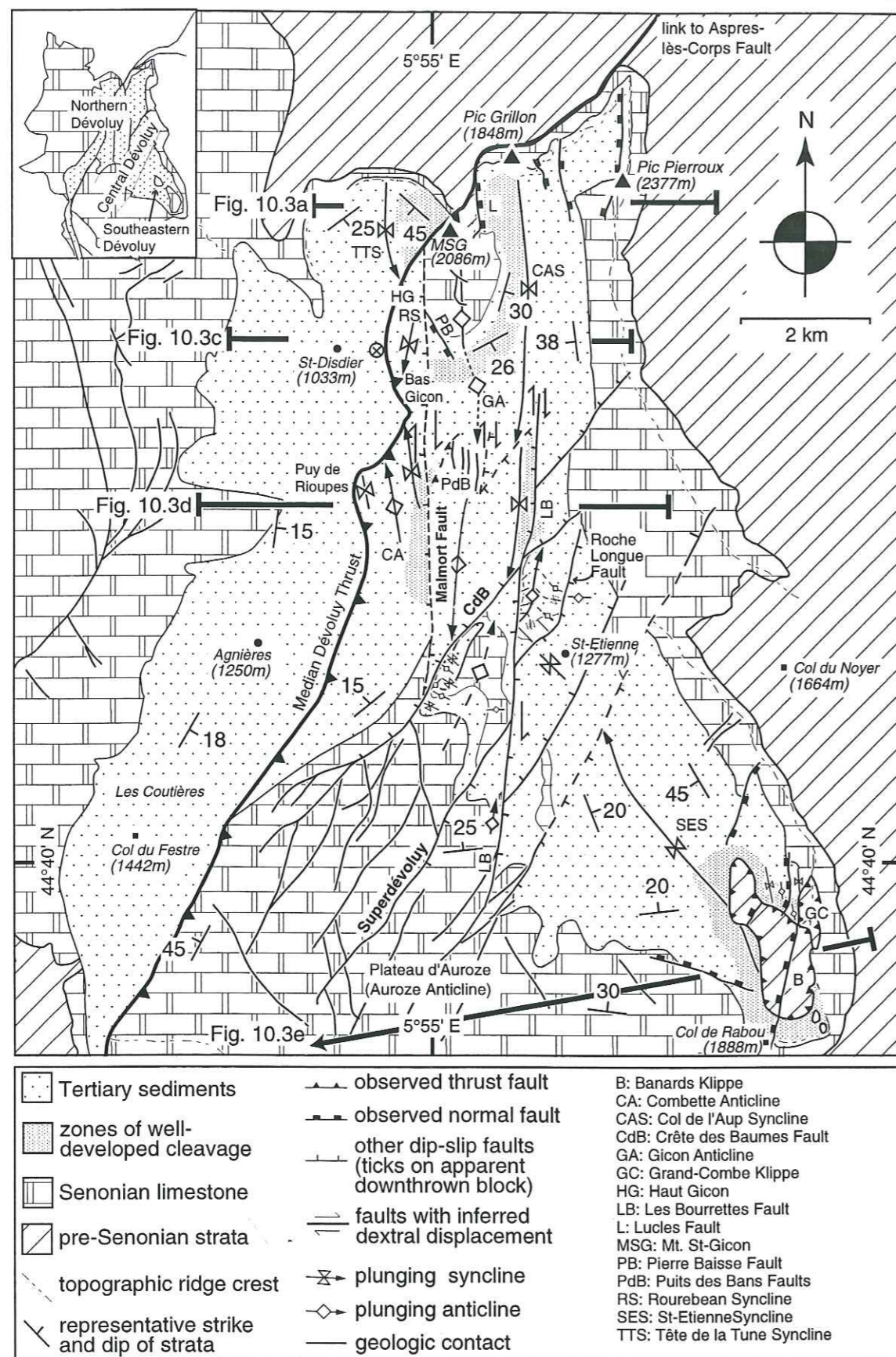


Fig. 10.1. Simplified map of Tertiary structures in Dévoluy. The St-Etienne Fault Zone occurs between the northwesternmost and southeasternmost NNE-SSW oriented faults in central Dévoluy (see inset). Location of fission track sample (part 10.6) indicated by circled x east of St-Disdier.

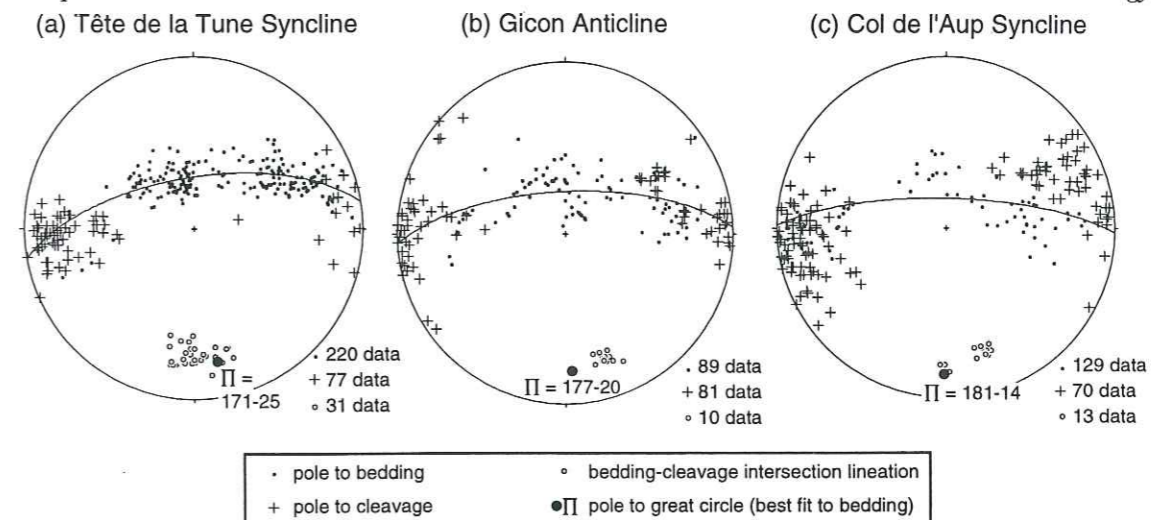


Fig. 10.2. Lower hemisphere, equal area projections of poles to bedding, poles to cleavage, and bedding-cleavage intersection lineation data associated with (a) the Tête de la Tune Syncline, (b) the Gicon Anticline, and (c) the Col de l'Aup Syncline. Folds located in Fig. 10.1.

the Median Dévoluy Thrust (see next section). Their orientations, W-vergence, and asymmetry to the west are consistent with W-directed compression.

10.2. The Median Dévoluy Thrust and the Lucles Fault

10.2.1. The Median Dévoluy Thrust

The Median Dévoluy Thrust (average orientation 000-20E) places Senonian rocks over Upper Eocene and Oligocene rocks in northern and southern Dévoluy and Upper Eocene and Oligocene rocks over Upper Oligocene rocks in central Dévoluy (Figs. 10.1, 10.3). South of the study area, Jurassic rocks are thrust over upper Oligocene rocks. Therefore, movement on the fault postdates the late Oligocene. Further constraints on the age of thrusting are presented in Part 10.6.

Although stratigraphic cutoff points for the Median Dévoluy Thrust are difficult to constrain, cross sectional models (Fig. 10.3) indicate that horizontal displacement is on the order of 2 to 3 km in central and southern Dévoluy. Estimates of thrust sheet advance rates during the late Eocene through Oligocene in the western Alps vary from 0.2 - 4 mm/yr (Pfiffner, 1986; Sinclair *et al.*, 1991); assuming that the Median Dévoluy thrust moved at a comparable rate (2.5 mm/yr), the displacement took place in approximately 1 My. The thrust steepens to the north and cuts upsection (Figs. 10.3a, c). At the same time, horizontal displacement decreases to less than 100 m where the fault exits the valley (Fig. 10.3a). Here, a zone of well-developed pressure solution cleavage occurs in the Queyras Marlstone Formation in the immediate foot wall, within a few hundreds of meters of the fault (Fig. 10.1). Its average orientation (355-74E; Fig. 10.4a) indicates E-W compression on the fault, and its orientation immediately adjacent to the fault (360-56E) is considered to be sub-parallel to the thrust plane, as suggested by Gidon & Pairis (1976).

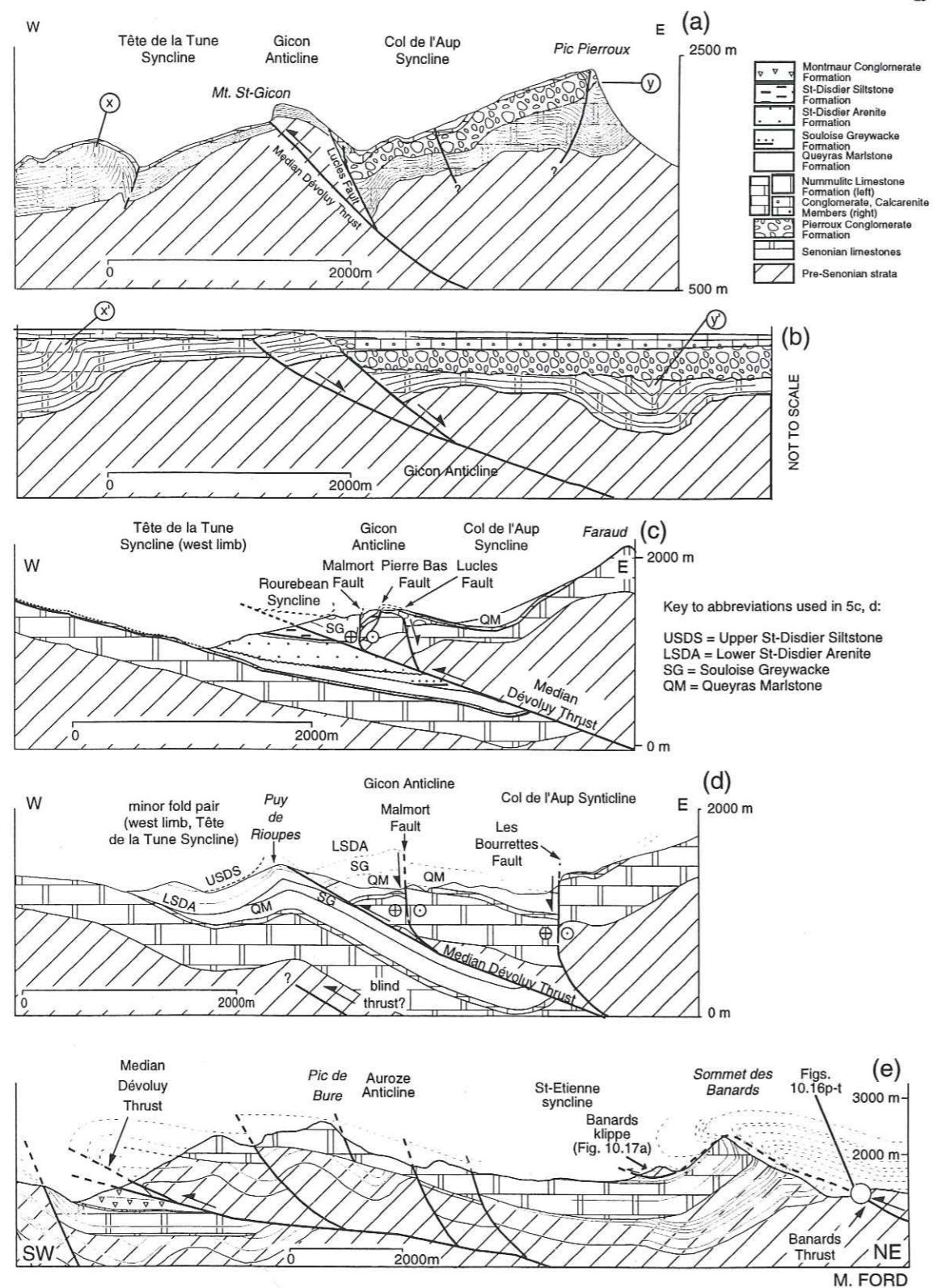


Fig. 10.3. W-E oriented cross sections across Dévoluy. Locations indicated in Fig. 10.1. Note that the scale in Fig. 10.3e is different than that in Figs. 10.3a-d. The Median Dévoluy Thrust steepens to the north, the hanging wall stratigraphy thins, and horizontal shortening decreases. Subvertical normal faults in its hanging wall in northern Dévoluy (Fig. 10.3a-c) are Eocene normal faults (Sections 2.2, 3.1.2); subvertical faults in its hanging wall in central and southern Dévoluy (Figs. 10.3d, e) are interpreted to sole into the thrust as high-angle reverse faults (Section 10.5). An Oligocene blind thrust in the foot wall of the Median Dévoluy Thrust (Fig. 10.3d) may have caused folding and uplift in western Dévoluy (Section 6.2).

At Bas Gicon (Fig. 10.1), the Median Dévoluy Thrust emplaces the Souloise Greywacke Formation on the St-Disdier Siltstone Formation. Slickenfiber and fault plane orientation data on the basal thrust surface at this locality show displacement to 278° (Figs. 10.4b, c). A 2-5 m thick shear zone overlying the fault surface is characterized by small (< 5 cm thick) stacked synthetic duplexes comprising folded and faulted sandstone, siltstone, and mudstone beds of the Souloise Greywacke Formation. Minor faults in the shear zone and in the foot wall of the thrust show displacement to 254° (Fig. 10.4d, e). Minor fold axes in the shear zone plunge to the NE and SE (Fig. 10.4f). Axial planes of these folds have an average orientation of $358-55^\circ\text{E}$ (Fig. 10.4f). Poorly developed, spaced pressure solution cleavage in caliche layers in the immediate foot wall has an average orientation of $167-88^\circ\text{W}$ (Fig. 10.4f).

Higher in the hanging wall, at Haut Gicon (Fig. 10.1), minor folds in the Souloise Greywacke Formation have axes that plunge to the SSE ($28-171^\circ$ average) and axial planes that have an average orientation of $356-82^\circ\text{E}$ (Fig. 10.4g). Intraformational faults in 1-2 m thick shear zones show displacement to 261° (Fig. 10.4h, i).

At Puy de Rioupes (Figs. 10.1, 10.3d), the Median Dévoluy Thrust crops out as a discrete plane emplacing the St-Disdier Arenite Formation upon the St-Disdier Siltstone Formation. Slickenfibers on the basal thrust surface show displacement to 258° (Figs. 10.4j, k). Subsidiary strike slip and thrust faults show W-directed displacement (Figs. 10.4l, m). Elsewhere at this locality, the Souloise Greywacke is emplaced over the St-Disdier Siltstone Formation. The contact does not crop out. However, sandy layers of the Souloise Greywacke Formation are occasionally folded in centimeter-to meter-scale folds that have NE-plunging axes and axial planes with an average orientation of $002-42^\circ\text{E}$, and poorly-developed cleavage in caliche layers of the St-Disdier Siltstone Formation has an average orientation of $196-90^\circ$ (Fig. 10.4n).

Occasional intraformational reverse faults with minor displacement occur in the St-Disdier Siltstone Formation in the foot wall of the Median Dévoluy Thrust at Les Coutières (Fig. 10.1). The faults show displacement to 255° (Fig. 10.4o, p).

At Source des Granges (Fig. 10.4), the Median Dévoluy Thrust is a discrete plane placing Senonian limestones over the Montmaur Conglomerate Formation. The fault plane and slickenfiber data show compression to 281° (Figs. 10.4q, r). Minor faults in the hanging wall of the thrust show compression to 289° (Fig. 10.4s, t).

In summary, displacement on the Median Dévoluy Thrust varies from $258^\circ-281^\circ$ (average to 270°), with tightly grouped slickenfiber orientations (Figs. 10.5a, b). Slickenfibers on synthetic faults provide a wider spread of displacement directions, with an average compression to 257° (Figs. 10.5c, d). The east-dipping axial planes of minor folds (Figs. 10.4f, g, n) and the N-S oriented cleavage (Figs. 10.4a, f, n) associated with the Median Dévoluy Thrust are consistent with the top-to-the-west displacement recorded by the fault kinematic data.

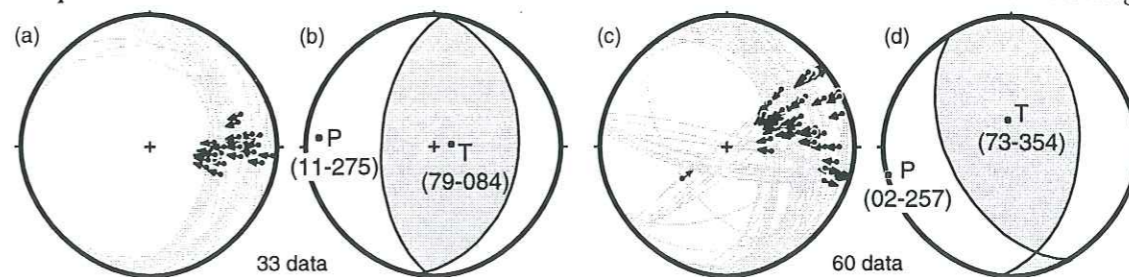
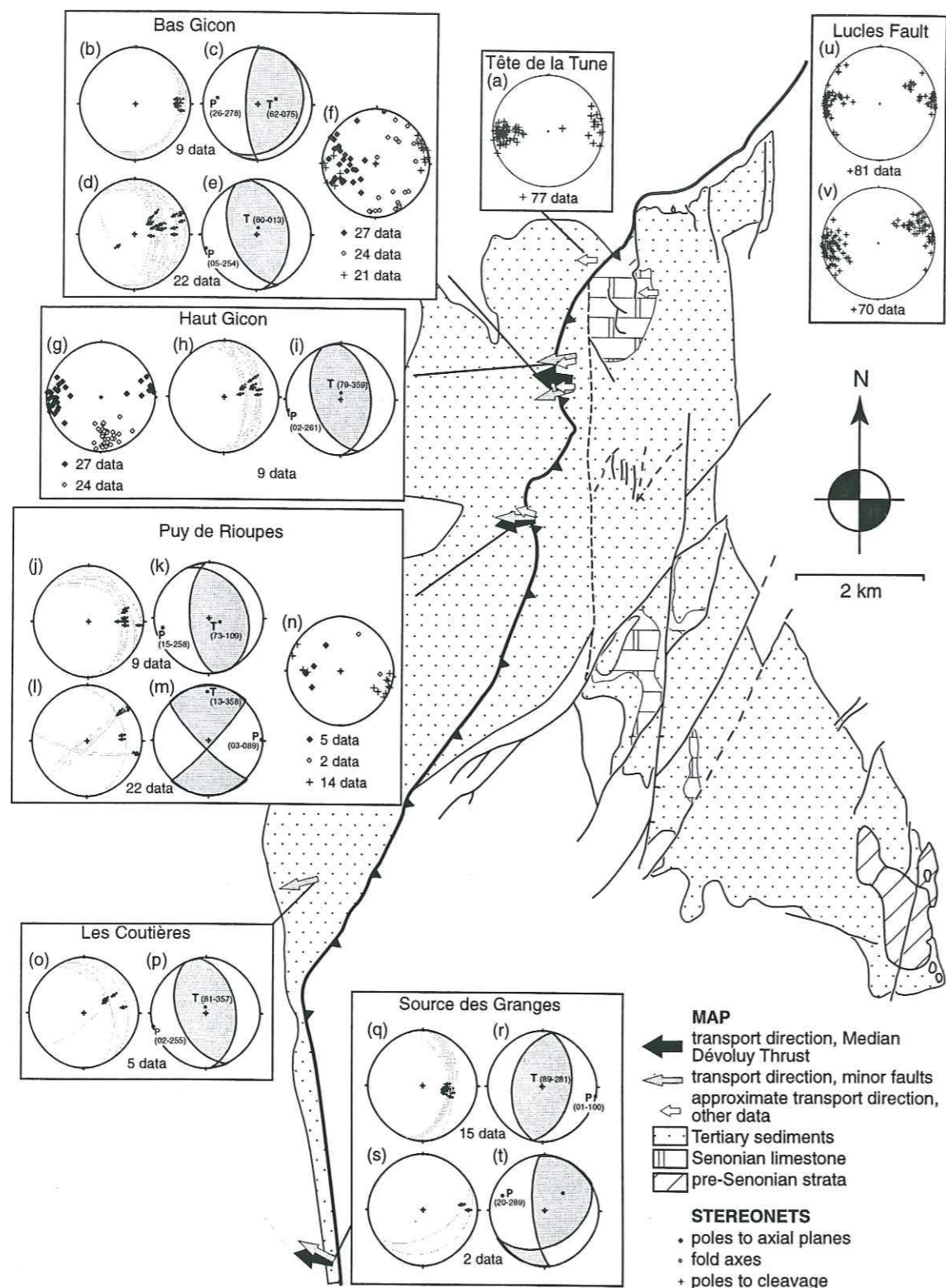


Fig. 10.5. Combined data for the Median Dévoluy Thrust. (a) All fault plane and slickenfiber orientations measured on the Median Dévoluy Thrust; (b) linked Bingham axis solution for data presented in (a); (c) all fault plane and slickenfiber orientations measured on minor faults in the hanging- and foot-walls of the Median Dévoluy Thrust; (d) linked Bingham axis solution for data presented in (c).

10.2.2. The Lucles Fault

The Lucles Fault (Fig. 10.1), an Eocene normal fault (see Section 3.1.2), has been interpreted to have been reactivated as a thrust fault later in its history (Gidon & Pairis, 1976). No slickenfiber data were found to document the kinematics of later displacement history. However, a well developed pressure solution cleavage in the the Queyras Marlstone Formation in the hanging wall of the fault (average orientation 349-88E, Fig. 10.4u) and at its southern termination (average orientation 177-87W, Fig. 10.4v) may be related to its reactivation, in which case the compression was E-W to ENE-WSW.

10.3. Structures in central Dévoluy

Two sets of subvertical faults, oriented N-S and NNE-SSW, affect the Tertiary strata in the hanging wall of the Median Dévoluy Thrust in central Dévoluy (Fig. 10.1). The timing of movement on these faults is not known, but appears to have occurred at the same time as movement on the Median Dévoluy Thrust, as discussed below. Where the two fault sets intersect, they divide the hanging wall into lozenge-shaped blocks (Fig 10.1). In two of these blocks, NNE-SSW trending open folds refold smaller-scale NW-SE trending folds.

Fig. 10.4 (facing page). Lower hemisphere, equal area projections of structural data associated with the Median Dévoluy Thrust. (a) Poles to cleavage, Tête de la Tune. (b) Fault plane and slickenfiber orientations measured on the Median Dévoluy Thrust at Bas Gicon; (c) linked Bingham axis solution of data in (b); (d) fault plane and slickenfiber orientations measured on minor faults at Bas Gicon; (e) linked Bingham axis solution of data presented in (d); (f) minor fold axis, fold axial plane, and cleavage orientations near Bas Gicon; (g) minor fold axis and fold axial plane orientations near Haut Gicon; (h) fault plane and slickenfiber orientations measured on minor faults at Haut Gicon; (i) linked Bingham axis solution of data in (g); (j) structural data associated with the Median Dévoluy Thrust at Puy de Rioupes; (k) linked Bingham axis solution of data presented in (j); (l) fault plane and slickenfiber orientations measured on minor faults, Puy de Rioupes; (m) linked Bingham axis solution of data presented in (l); (n) minor fold axis, fold axial plane, and cleavage orientations at Puy de Rioupes; (o) fault plane and slickenfiber orientations measured on minor faults at Les Coutières; (p) linked Bingham axis solution of data presented in (o). (q) Fault plane and slickenfiber orientations measured on the Median Dévoluy Thrust at Sources des Granges; (r) linked Bingham axis solution of data presented in (q); (s) fault plane and slickenfiber orientations measured on minor fault planes at Source des Granges; (t) linked Bingham axis solution of data presented in (s); (u) poles to cleavage, Col de l'Aup Syncline, interpreted to be associated with the Lucles Fault; (v) poles to cleavage, Gicon Anticline, interpreted to be associated with the Lucles Fault.

10.3.1. North-south oriented faults

The two principal subvertical N-S trending faults are the Les Bourrettes and Malmort Faults (Fig. 10.1). The trace of each fault is approximately 7 km long. The Puit des Bans Faults occur between the Malmort and Les Bourrettes Faults (Fig. 10.1).

The Les Bourrettes Fault

The Les Bourrettes Fault can be traced from southeast of Mt. St-Gicon into the Auroze Plateau, where it bends to the SW (Fig. 10.1). The fault plane crops out in a single inaccessible locality (star, Fig. 10.6a), where it can be seen to be subvertical. Its N-S trace is marked by the juxtaposition of different Tertiary formations (Fig. 10.6a). Small-scale kinematic indicators near the Les Bourrettes Fault provide information on its displacement.

(1) NNW-SSE striking, subvertical minor faults (locality 1, Fig. 10.6a; P in Fig. 10.7a) have calcite slickenfibers that show oblique to pure dextral displacement (Fig. 10.6b). Shallowly dipping, NW-SE to WNW-ESE striking faults (locality 1, Fig. 10.6a; X in Fig. 10.7a) show top-to-the-SW and top-to-the-NE displacement (Fig. 10.6b). The two fault sets have an oblique dextral strike-slip solution (Fig. 10.6c).

(2) A moderately- to well-developed planar to anastomosing pressure solution cleavage (localities 1-3, Fig. 10.6a; C in Fig. 10.7a) is developed in the Queyras Marlstone Formation within 500 m of the Les Bourrettes Fault and dies out away from it. The cleavage has an average orientation of 325-79E, indicating WSW-ENE compression (Fig. 10.6d).

(3) ENE-WSW oriented fractures (localities 1, 3, Fig. 10.6a; T in Fig. 10.7a) filled with massive calcite and exhibiting no slip are interpreted to indicate NNW-SSE extension (Fig. 10.6d). These fractures are arranged in a right-stepping en-echelon fashion. The "tails" of the fractures (R in Fig. 10.7a) are oriented parallel to a set of NNE-SSW oriented, calcite-filled fractures (T_2 in Fig. 10.7a).

(4) NNE-SSW trending faults (locality 3, Fig. 10.6a; R_L in Fig. 10.7a) show up to 2 cm of down-to-the-east dip-slip displacement. No slickenfibers were found on the fault surfaces.

The observed orientations and kinematics of the P and X faults, cleavage (C), and the T fractures (Fig. 10.7a) are consistent with theoretical and experimental orientations and kinematics in a N-S oriented dextral transpressional zone (Fig. 10.7b). Similarly, the orientations of T_2 fractures and R_L faults (Fig. 10.7a) are consistent, respectively, with Riedel shears and low-angle synthetic Riedel shears (Figs. 10.7b). Therefore, the Les Bourrettes Fault (Y in Fig. 10.7a), which is oriented parallel to theoretical Y shears (Fig. 10.7b), is interpreted to have accommodated dextral strike-slip in a transpressional system.

The amount of lateral displacement on the Les Bourrettes Fault cannot be estimated reliably, as there are no clear cutoff points. The sense of vertical offset varies along the strike of the fault (Fig. 10.1). For instance, at the Les Bourrettes locality (Fig. 10.6a), the fault has a down-to-the-west displacement of several hundred meters (Fig. 10.3d). South of the village of St-Etienne (Fig. 10.1), the relative displacement is down-to-the-east. This change in sense of displacement may reflect lateral

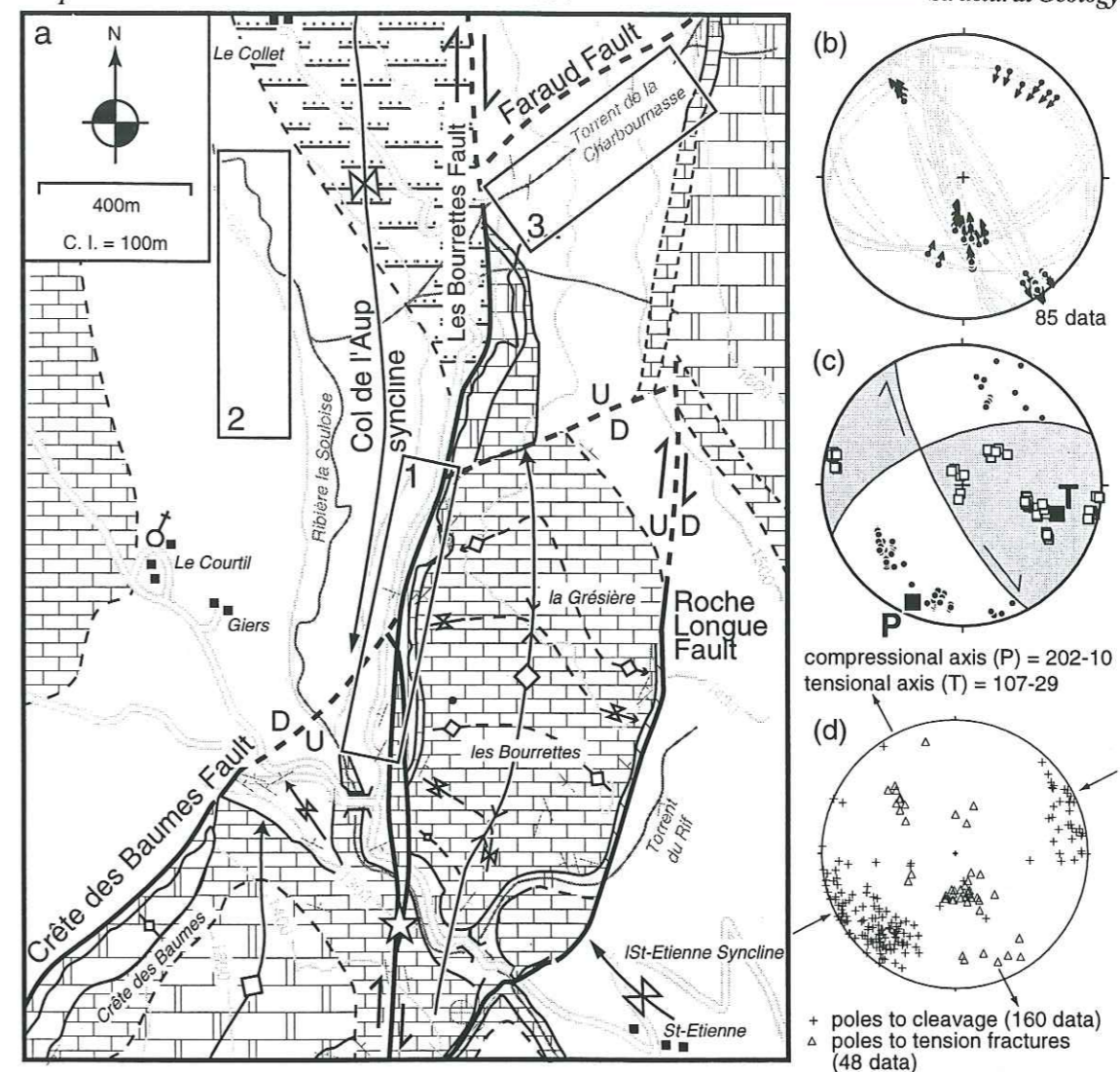


Fig. 10.6. (a) Map of the Les Bourrettes area, showing subareas where structural data were collected. (b-d) Lower hemisphere, equal area projections of (b) slickenfiber and minor fault plane orientations, (c) linked Bingham axis for data in (b), (d) cleavage and tension fracture data. Arrows in (d) show interpreted compression and extension directions. Patterns as in Fig. 1.3.

offset of folded sediments, scissor-like dip-slip movement on the fault, or differential amounts of vertical displacement on the intersecting NNE-SSW faults.

The Malmort Fault

The Malmort Fault can be traced from the north, where it is interpreted to terminate against the Median Dévoluy Thrust, to the south, where it is interpreted to terminate against the NNE-SSW trending Crête des Baumes Fault (Fig. 10.1). The fault plane crops out at a single locality 400 m south of the village of Malmort (locality 1, Fig. 10.8a), where it has an average orientation of 183-82W (Fig. 10.8b). Elsewhere, its presence is inferred from the juxtaposition of either different Tertiary formations or the Souloise Greywacke Formation against Senonian limestones (Figs. 10.1, 10.8a). No fiber data were found on the fault surface. However, as with the Les Bourrettes Fault, minor

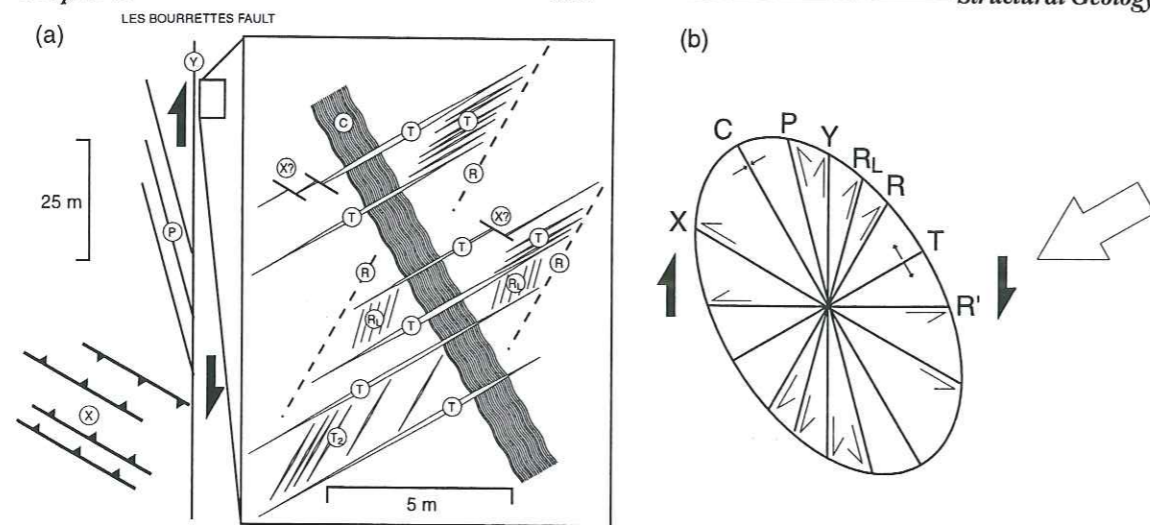


Fig. 10.7. (a) Schematic sketch of theoretical and structural orientations in a N-S oriented dextral transpressional regime (after Woodcock & Schubert, 1994). (b) Plan view of structural features observed in association with the Les Bourrettes Fault. The features are shown as developing in a dextral shear zone. X = X shears; C = cleavage; P = P shears; Y = Y shear; R_L = low angle synthetic Riedel shears; R = Riedel shears; T = tension

structures provide information on its probable kinematics.

(1) Within a few meters of the fault outcrop (locality 1, Fig. 10.8a), an intensely developed pressure solution cleavage (average orientation 329-88E; Fig. 10.8b) is associated with shear bands that record N-S oriented dextral strike-slip (Fig. 10.9).

(2) South of the village of Malmort (locality 2, Fig. 10.8a), subvertical cleavage in the Queyras Marlstone Formation (average orientation 328-88E, Fig. 10.8c) occurs in the eastern limb of the Malmort Syncline (fold axis = 08-342, Fig. 10.8c), but dies out into the hinge. The counter-clockwise orientation of cleavage relative to the Malmort Fault indicates a dextral shear regime.

(3) 300 m north of the village of Malmort (locality 3, Fig. 10.8a), a minor thrust fault oriented 330-35E (Fig. 10.8d; NNE-SSW surface trace) branches eastward from the Malmort Fault. The thrust places the Pierroux Conglomerate Formation over the Queyras Marlstone, Nummulitic Limestone, and Pierroux Conglomerate Formations. No fibers were found on the fault surface; however, cleavage developed within 5 m of the fault has an average orientation of 335-80E, indicating SW-directed compression (Fig. 10.8d).

(4) Slickenfibers on minor fault planes between the thrust and the Malmort Fault (locality 3, Fig. 10.8a) show strike-slip, thrust, and oblique dip-slip displacement (Fig. 10.8e). These data give a poorly constrained kinematic solution with a SW-directed compressional axis and a subvertical tensional axis (Fig. 10.8f). Shallowly-dipping tension fractures (Fig. 10.8c) at locality 2 (Fig. 10.8a) are consistent with this tensional axis.

Thus, the dextral strike-slip on the Malmort Fault, recorded by cleavage and shear bands at localities 1 and 2, is obscured at locality 3 by SW-directed thrusting. At Puy de Rioupes, 1.3 km west of the village of Malmort (locality 4, Fig. 10.8a), the Median Dévoluy Thrust shows WSW- to W-directed compression (Figs. 10.4k, m). These facts suggest that the SW-directed compression re-

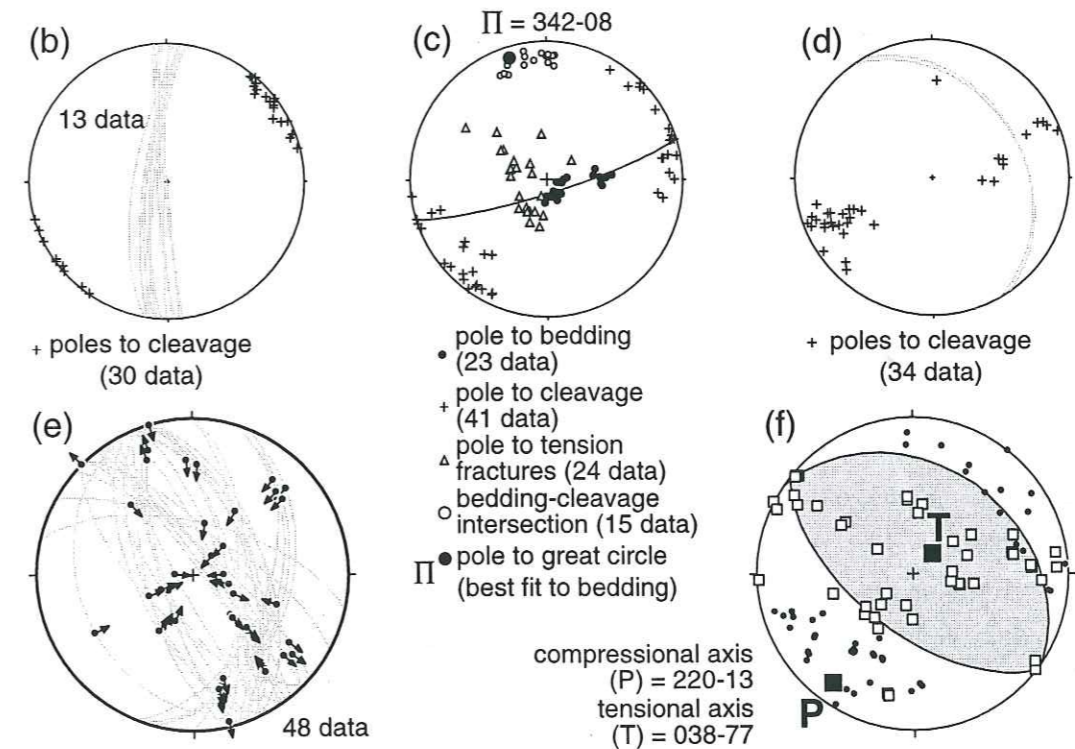
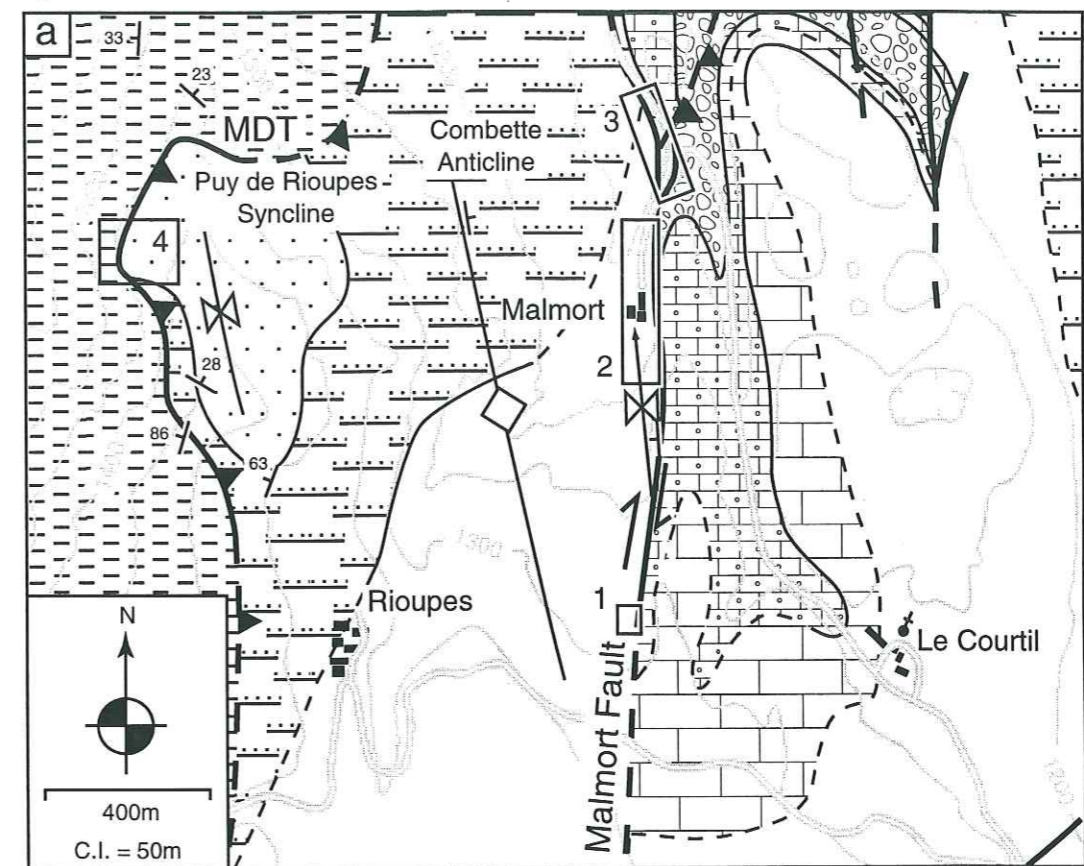


Fig. 10.8. (a) Map of the Malmort area, showing subareas where structural data were collected. (b-f) Lower hemisphere, equal area projections of (b) the Malmort Fault plane and associated shear bands, (c) bedding, cleavage, bedding-cleavage intersection lineation, and tension fracture data, (d) thrust fault and cleavage orientations, and (e) other fault plane and slickenfiber data, and (f) the linked Bingham axis solution for the fault data shown in (e). Patterns as in Fig. 1.6.

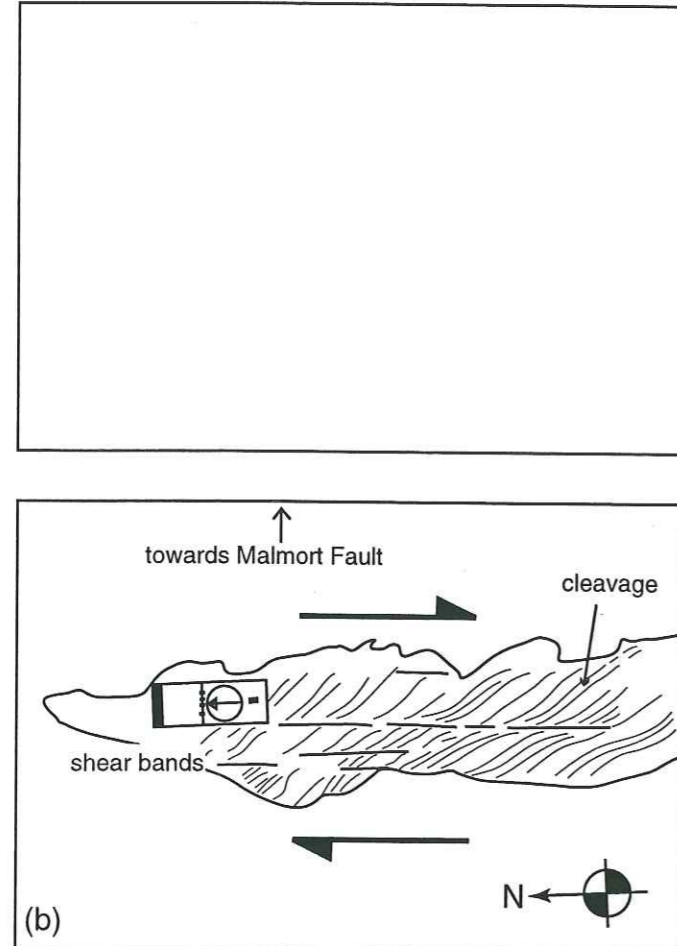


Fig. 10.9. (a) Field photograph and (b) line drawing of dextral shear bands developed in cleavage in the Queyras Marlstone Formation near the Malmort Fault.

Thrust as a series of high angle oblique dip-slip faults (e.g., Fig. 10.3c, d).

Strain analysis at Malmort

At locality 3 (Fig. 10.8a), small, flat, black ellipses of unknown organic composition are visible on bedding surfaces between pressure solution seams (i.e., on microlithons) in strongly cleaved layers of the Queyras Marlstone Formation (Fig. 10.11a). These elliptical plates allow two-dimensional, cleavage-related strain to be estimated on the bedding plane.

When viewed with a hand lens, the plates show tension fractures parallel to the short axis and micro-folds parallel to the long axes (Fig. 10.11a). Therefore, shortening is considered to have been perpendicular to the long axis and stretching, perpendicular to the short axis (Fig. 10.11a). Recognizing that, in 97% (29 of 30) of observed cases, the long axes of the ellipses are visibly parallel to the bedding-cleavage intersection lineation (e.g., Fig. 10.11a; Table 10-1), the deformation of the strain markers was probably contemporaneous with cleavage development, and the short axis corresponds to the cleavage shortening axis. The other two strain axes cannot be constrained.

The axes of thirty ellipses (Fig. 10.11b) were measured in the field. The long axes ($1 + e_1$) vary

corded at locality 3 may have been partitioned into components of N-S dextral shear on the Malmort Fault and WSW-to W-directed thrusting on the Median Dévoluy Thrust (Fig. 10.10).

The amount of lateral displacement on the Malmort Fault is not known. However, the fault accommodated at least 30 m of downthrow to the west at the village of Malmort (Fig. 10.3d) and approximately 150 m of downthrow to the east at its southern termination. As with the Les Bourrettes Fault, the change in sense of vertical offset may reflect lateral offset of folded sediments, scissor-like dip-slip movement on the fault, or differential amounts of vertical displacement on the intersecting NNE-SSW

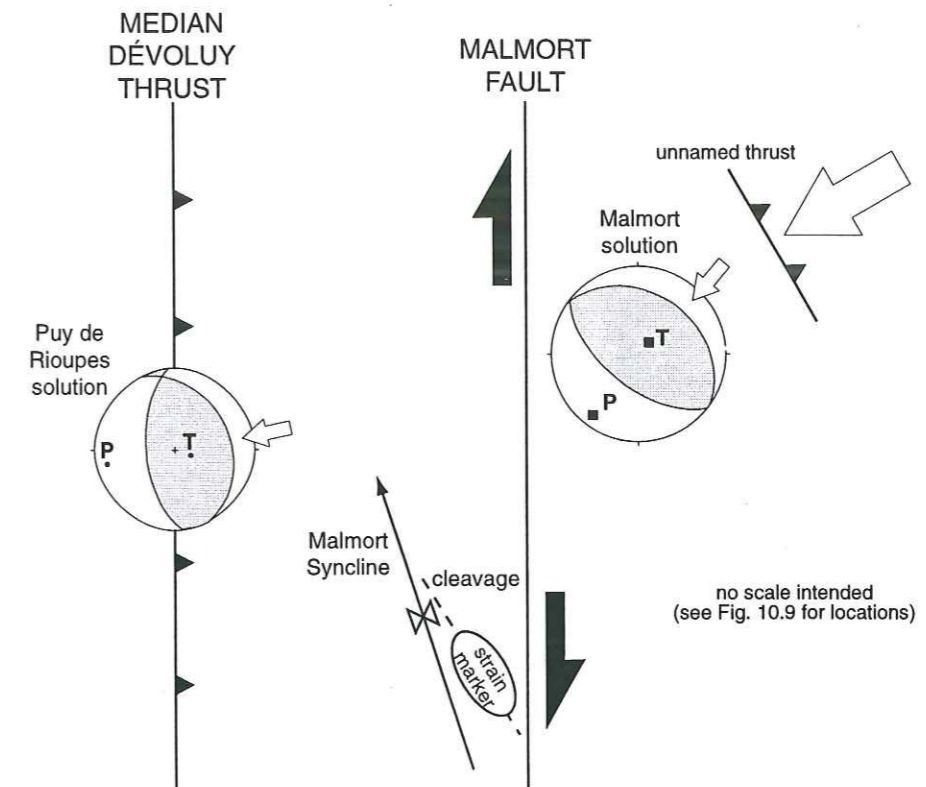


Fig. 10.10. Schematic representation of structural data associated with the Malmort Fault, showing how overall SW-directed compression in the east is partitioned into N-S oriented dextral shear on the Malmort Fault and WSW-directed thrusting on the Median Dévoluy Thrust at Puy de Rioupes.

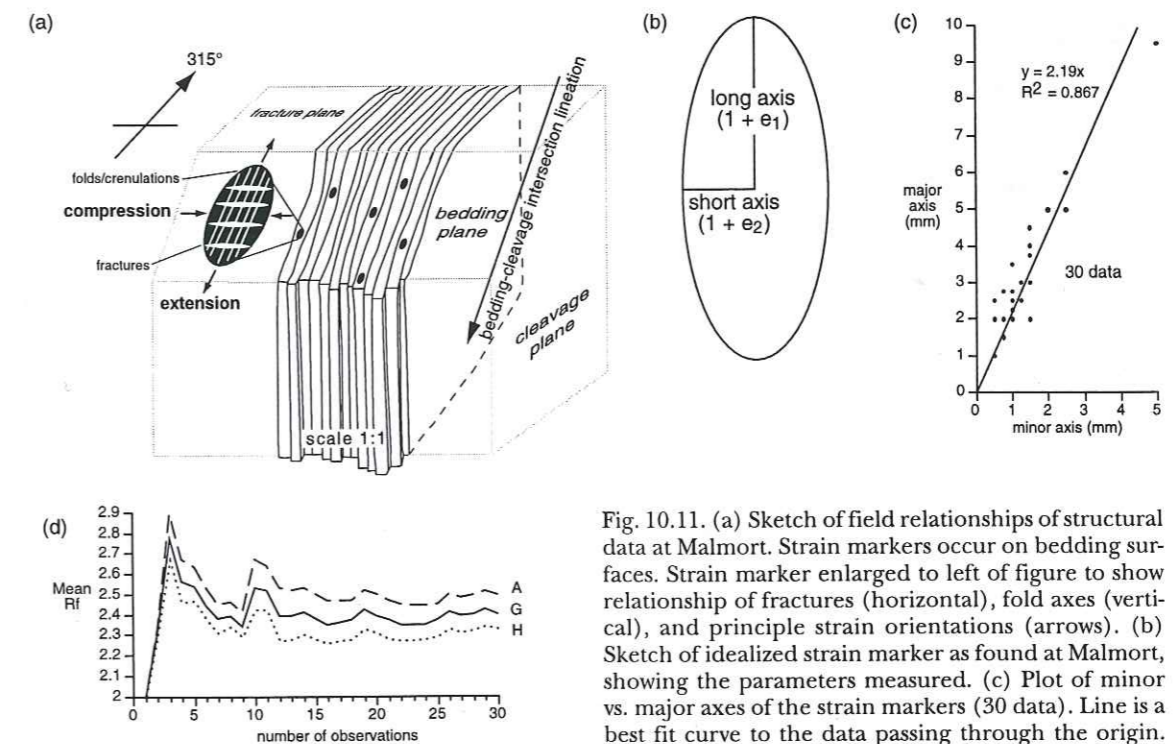


Fig. 10.11. (a) Sketch of field relationships of structural data at Malmort. Strain markers occur on bedding surfaces. Strain marker enlarged to left of figure to show relationship of fractures (horizontal), fold axes (vertical), and principle strain orientations (arrows). (b) Sketch of idealized strain marker as found at Malmort, showing the parameters measured. (c) Plot of minor vs. major axes of the strain markers (30 data). Line is a best fit curve to the data passing through the origin. (d) Plots of cumulative averages of ellipticity (R_f) of Malmort strain markers. Curves show that R_f is relatively constant after approximately 15 observations. A = arithmetic mean ($A_{30} = 2.49$); G = geometric mean ($G_{30} = 2.4$); H = harmonic mean ($H_{30} = 2.33$).

data ID numbe r	long axis (L) in mm	short axis (S) in mm	major axis (1 + e1)	minor axis (1 + e2)	ellipticity of strain ellipse (Rf) = (1 + e1)/(1 + e2)	Strain markers, Malmort cumulative arithmetic mean	cumulative geometric mean	cumulative harmonic mean	long axis oriented with pencil?
1	5	2.5	2.5	1.25	2.00	2.00	2.00	2.00	yes
2	8	3	4	1.5	2.67	2.33	2.31	2.29	yes
3	4	1	2	0.5	4.00	2.89	2.77	2.67	yes
4	3	1.5	1.5	0.75	2.00	2.67	2.56	2.46	yes
5	5	2	2.5	1	2.50	2.63	2.54	2.47	yes
6	4	2	2	1	2.00	2.53	2.44	2.38	yes
7	10	5	5	2.5	2.00	2.45	2.38	2.31	yes
8	5	2	2.5	1	2.50	2.46	2.39	2.34	yes
9	2	1	1	0.5	2.00	2.41	2.34	2.29	yes
10	5	1	2.5	0.5	5.00	2.67	2.53	2.42	yes
11	6	2.5	3	1.25	2.40	2.64	2.52	2.42	no
12	4	3	2	1.5	1.33	2.53	2.39	2.27	yes
13	12	5	6	2.5	2.40	2.52	2.39	2.28	yes
14	4	1.5	2	0.75	2.67	2.53	2.41	2.30	yes
15	3	1.5	1.5	0.75	2.00	2.50	2.38	2.28	yes
16	6	3	3	1.5	2.00	2.47	2.35	2.26	yes
17	5	2	2.5	1	2.50	2.47	2.36	2.27	yes
18	10	4	5	2	2.50	2.47	2.37	2.28	yes
19	7	2	3.5	1	3.50	2.52	2.42	2.33	yes
20	6	3	3	1.5	2.00	2.50	2.39	2.31	yes
21	19	10	9.5	5	1.90	2.47	2.37	2.28	yes
22	3	1.5	1.5	0.75	2.00	2.45	2.35	2.27	yes
23	4.5	2	2.25	1	2.25	2.44	2.35	2.27	yes
24	7.5	3	3.75	1.5	2.50	2.44	2.35	2.28	yes
25	5.5	2	2.75	1	2.75	2.45	2.37	2.29	yes
26	5.5	1.5	2.75	0.75	3.67	2.50	2.41	2.33	yes
27	4	2	2	1	2.00	2.48	2.39	2.31	yes
28	8	3	4	1.5	2.67	2.49	2.40	2.32	yes
29	9	3	4.5	1.5	3.00	2.51	2.42	2.34	yes
30	2	1	1	0.5	2.00	2.49	2.40	2.33	yes
6.07		2.58				2.49	2.40	2.33	29 of 30 aligned

Table 10-I. Data from strain markers at Malmort locality (see Fig. 10.11).

in length from 1.5 to 9 mm, while the short axes (1 + e₂) vary in length from 0.5 to 5 mm (Table 10-1). The ratio of the axes (1 + e₁/1 + e₂, Table 10-1) defines the final ellipticity (R_f) of the deformed marker, which represents tectonic strain (R_s) in originally circular markers (Ramsay & Huber, 1983). To prove that the markers were originally circular in the bedding plane, the orientation of the long axis must be known (Ramsay & Huber, 1983). However, these orientations were not measured in the field because of the small sizes of the ellipses. Although original circularity can therefore not be proven at Malmort, its assumption is justified because (1) the long axis is visibly parallel to the bedding-cleavage intersection lineation (e.g., Fig. 10.11a, Table 10-1), and (2) the ellipticity of the markers is relatively constant (R² (correlation coefficient) = 0.87; Fig. 10.11c).

When the lengths of the two axes are plotted against each other (Fig. 10.11c), R_f is determined by the slope of the best fit line to the data passing through the origin (Ramsay & Huber, 1983). The slope is 2.19 (Fig. 10.11c); therefore, R_f (≈ R_s) = 2.19. A plot of the arithmetic (A), geometric (G), and harmonic (H) means of R_f versus the number of observations (Fig. 10.11d) corroborates this value. Figure 10.11d shows that mean R_f is relatively constant after 15 observations in all cases, with values after 30 measurements of A = 2.49, G = 2.4, and H = 2.33. These values are all higher than the true tectonic strain (Ramsay & Huber, 1983). Therefore, R_s < 2.33*. The estimates of strain (2.19 ≈ R_s < 2.33) indicate that cleavage-related, bedding-parallel shortening at Malmort was 50% in the microlithons.

* The similarity between the approximate (R_s ≈ 2.19) and maximum (R_s < 2.33) strain values (6% difference) provides further support that the markers were probably initially circular.

The Puits des Bans Faults

The Puits des Bans Faults are subvertical, N-S oriented faults that occur between the Les Bourrettes and Malmort Faults (Fig. 10.1). They offset the Queyras Marlstone Formation and older rocks and are assumed to be part of the same system as the Les Bourrettes and Malmort Faults. No kinematic data were recorded for these faults. However, dip-slip displacement of up to 40 m is visible in cliff outcrops (e.g., Fig. 2.5).

10.3.2. North-northeast—south-southwest faults: the St-Etienne Fault Zone

A series of subvertical, NNE-SSW oriented faults in the hanging wall of the Median Dévoluy Thrust form the 2 km wide St-Etienne Fault Zone in central Dévoluy. The fault zone is uplifted relative to both northern and southeastern Dévoluy (Fig. 10.1 inset). Overall, northern Dévoluy is downthrown relative to southeastern Dévoluy across the fault zone. The faults accommodated both dextral and reverse movement, as discussed below.

At locality 1 (Fig. 10.12a), two overlapping sets of slickenfibers on the Superdévoluy Fault (Fig. 10.12b) give an overall oblique reverse dextral solution (Fig. 10.12c). Drag folds here (Fig. 10.12a) also indicate that the fault accommodated dextral shear. At locality 2 (Fig. 10.12a), slickenfibers on minor faults associated with the Crête des Baumes Fault (Fig. 10.12d) also give an oblique reverse dextral solution (Fig. 10.12e).

The amount of strike-slip movement on the faults cannot be calculated. Dip-slip displacement is greatest where the faults cut major Tertiary fold axes and dies out to the northeast and southwest. For instance, the Roche Longue Fault (Fig. 10.6a) has approximately 50 m of down-to-the-SW offset where it cuts the St-Etienne Syncline, and the Crête des Baumes Fault (Fig. 10.12a) has more than 150 m of down-to-the-NW offset where it cuts the Gicon Anticline and Col de l'Aup Syncline (Fig. 10.1). This displacement pattern suggests that the faults developed during large-scale folding of the Tertiary strata.

The downthrow across the Crête des Baumes Fault is associated with a thinning of the hanging wall stratigraphy of the Median Dévoluy Thrust, which cuts abruptly upsection from south to north across the St-Etienne Fault Zone. Thus, the zone can be described as a "hanging wall drop fault" zone (Butler, 1982). The fault zone may coincide with an older feature.

The faults of the St-Etienne Fault Zone either terminate the Les Bourrettes and Malmort Faults or are terminated by them (Fig. 10.1), indicating that the two fault systems were active contemporaneously. Differences in the amounts of displacement on the faults of the St-Etienne Fault Zone may have led, in part, to the differential senses of relative offset along the N-S oriented Les Bourrettes and Malmort Faults.

10.3.3. Folds

In two fault-bounded blocks of the St-Etienne Fault Zone, Senonian and Tertiary strata are affected by superposed, semi-orthogonal folds (Figs. 10.6a, 10.12a). The folds are considered to be

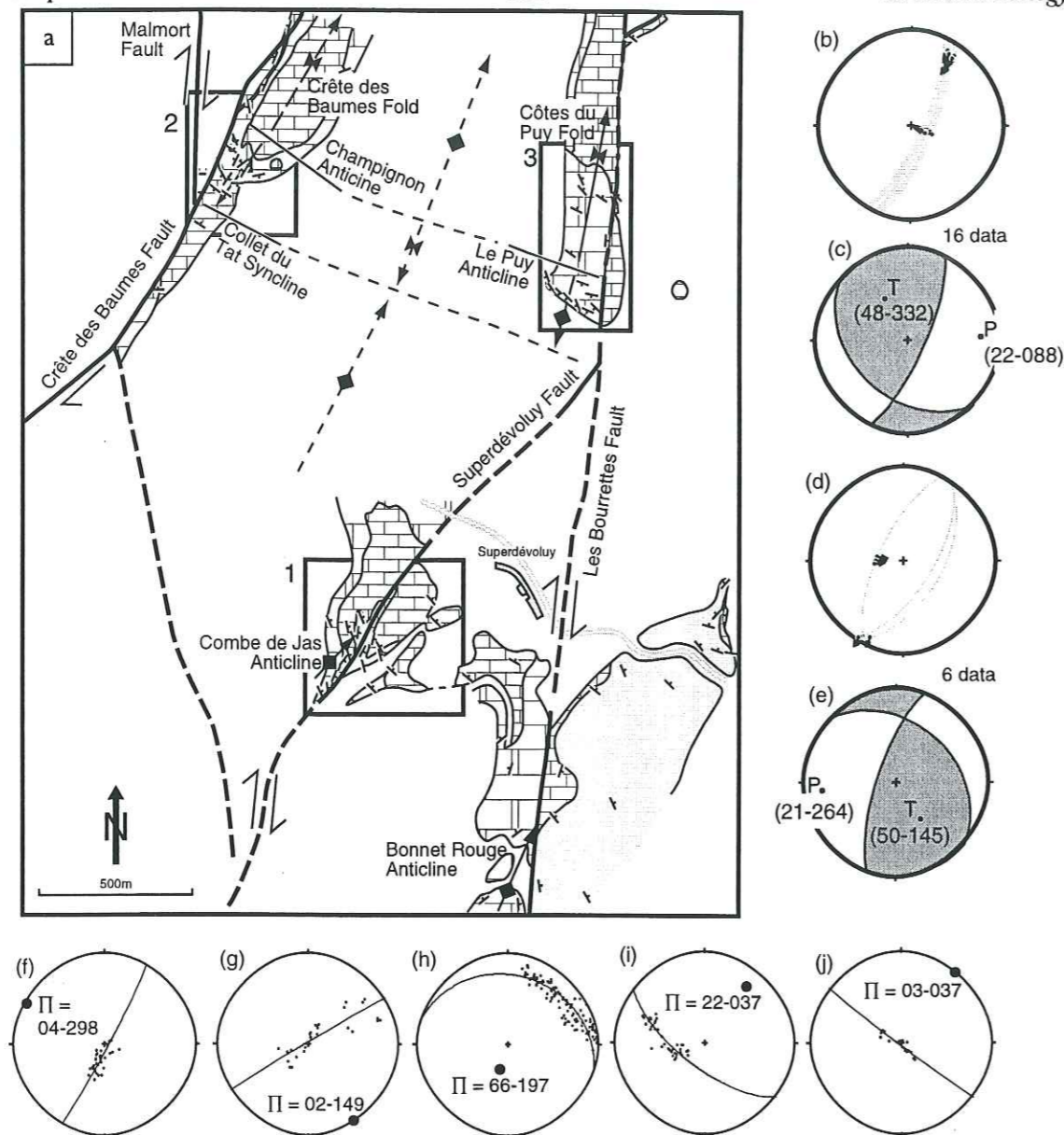


Fig. 10.12. (a) Detailed map of the Crête des Baumes, Cotes du Puy, and Superdévouly localities. (b-e) Lower hemisphere, equal area projections of fault plane and slickenfiber orientations of the (b) Superdévouly and (d) Crête des Baumes Faults, and the linked Bingham axis solutions (c and e) of the data presented in (b) and (d), respectively. (f-j) Lower hemisphere, equal area projections of bedding plane orientations of the (f) Collet du Tat Syncline, (g) Le Puy Anticline, (h) Crête des Baumes Fold between Collet du Tat and Champignon folds, (i) Combe de Jas Anticline, and (j) Bonnet Rouge Anticline. Solid circles = poles to bedding; great circle = best fit to data; large filled circle = pole to best fit great circle (Π (fold) axis). Patterns as in Fig. 10.6, except no pattern indicates Quaternary cover and grey indicates the Queyras Marlstone Formation.

related to movement on the faults bounding the blocks. Thus, they are considered to be small-scale "wrench folds" (e.g., Little, 1992).

The first set of folds, with 100 m half wavelengths and 25 m amplitudes, trends approximately NW-SE and has subhorizontal axes (Figs 10.6a, 10.12a, f, g). The axial plane of one of these folds, the Champignon Anticline (Fig. 10.12a), is SW-facing (305-45N). The sense of plunge of these folds changes across the axes of the second set of folds.

The second set of folds, which have 0.5-1 km half-wavelengths and 50-100 m amplitudes, trends

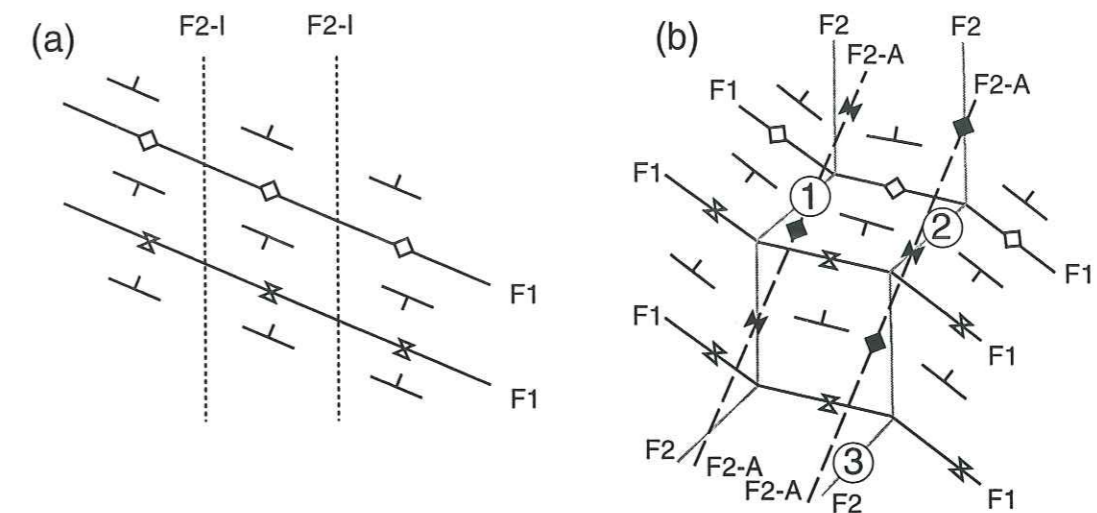


Fig. 10.13. Schematic drawing of the apparent deflection to a NNE-SSW trend of a N-S oriented fold axis that is superposed on a pre-existing WNW-ESE trending fold set. Abbreviations explained in text. 1, 2, and 3 refer, respectively, to the positions of the Crête des Baumes Fold at the south end of Crête des Baumes, and the Combe de Jas and Bonnet Rouge Anticlines (located in Fig. 10.13).

approximately NNE-SSW (Figs. 10.6a, 10.12a, h-j). In one of the fault-bounded blocks (Fig. 10.12a), these folds change from anticlines to synclines, and also change their senses of plunge, across the axes of the first fold set. The geometric relationships between the two fold sets indicate that the NNE-SSW folds are superimposed on the NW-SE folds.

The approximate NW-SE orientation of the earlier folds is consistent with the dextral shear recorded on the N-S Les Bourrettes and Malmort faults. The orientation of the NNE-SSW folds, which are subparallel to the faults of the St-Etienne Fault Zone, is more enigmatic. One possible hypothesis to explain the orientation of these folds is that they formed in response to a WNW-ESE directed compression. However, no such regional compression is recorded in Dévoluy. A more satisfactory hypothesis (Fig. 10.13) utilizes the observations that (1) the kinematic solutions of the Superdévouly and Crête des Baumes Faults show W-E directed compression (Figs. 10.12b, d), and (2) that the NNE-SSW folds are superposed on the NW-SE folds. In this hypothesis, a W-E compression (F2-I, Fig. 10.13a) was imposed on the early NW-SE trending structures (F1, Fig. 10.13a), resulting in apparent NNE-SSW fold axes (F2-A, Fig. 10.13b) that are oblique to the actual F2 fold axes (F2, Fig. 10.13b). The hypothetical folds at points 1-3 (Fig. 10.13b) correspond in the field to (1) the anticline on the southern end of the Crête des Baumes (Figs. 10.12a, h), (2) the Combe de Jas Anticline (Fig. 10.12a, i), and (3) the Bonnet Rouge Anticline (Figs. 10.12a, j). The N-S trending segments of the Crête des Baumes and Cotes de Puy Folds shown in Figure 10.13b have not been observed in the field.

Because the NW-SE folds are interpreted to have formed before the NNE-SSW ones (Fig. 10.13), the N-S oriented faults with which the former are associated are considered to have formed before the NE-SW oriented faults, with which the latter are associated. This order of development is supported by the fact that the later NE-SW faults often terminate against the earlier N-S faults (Fig.

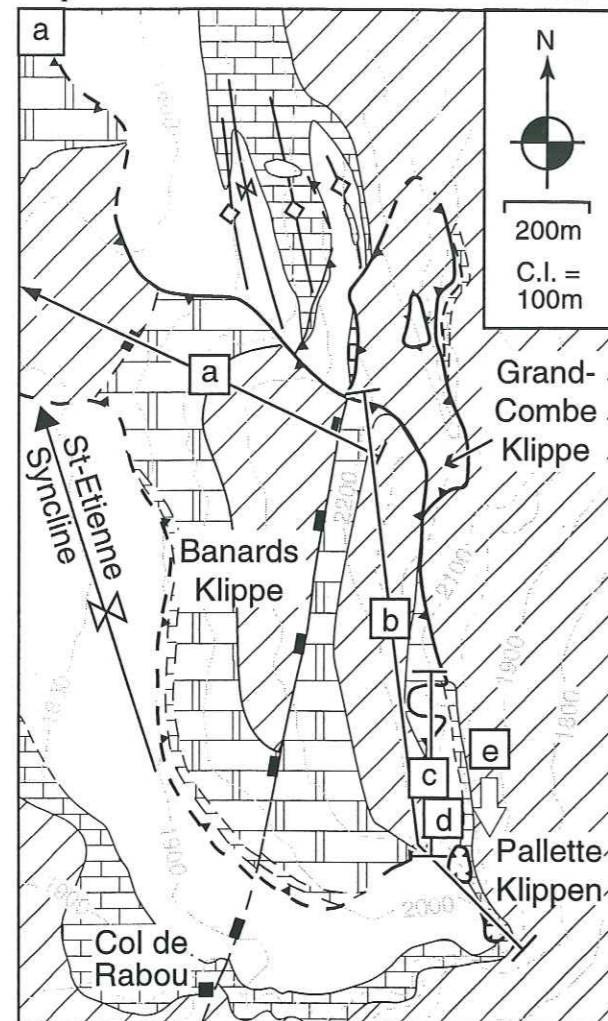


Fig. 10.14. Detailed map of the southeastern corner of the Dévoluy Basin. (a)-(e) indicate locations of Figs. 10.17a-e. Patterns as in Fig. 1.6.

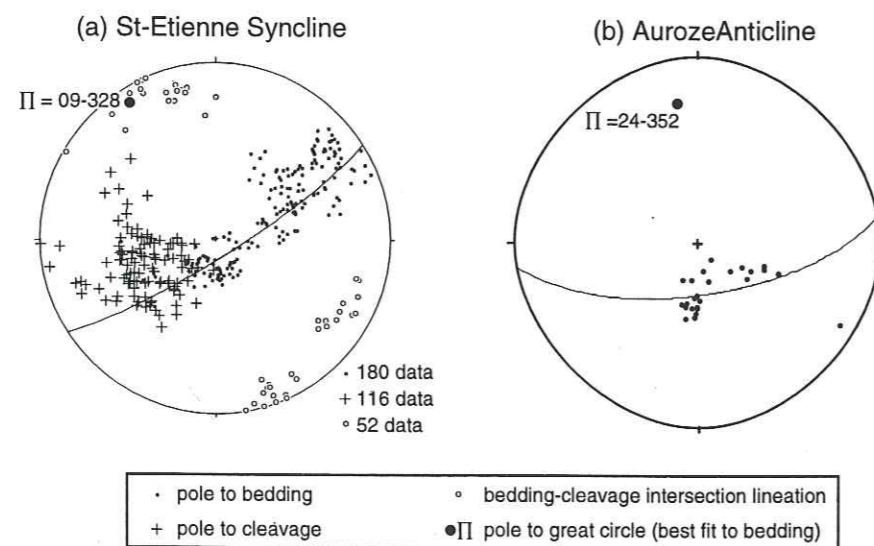


Fig. 10.15. Lower hemisphere, equal area projections of (a) bedding, cleavage, and bedding-cleavage intersection lineation data associated with the St-Etienne Syncline, and bedding data associated with (b) the Auroze Anticline.

10.1). The southern terminations of the N-S faults against NE-SW oriented faults (Fig. 10.1) probably reflects interference between the two fault sets after the NE-SW faults formed.

10.4. Structures in southeastern Dévoluy

The major structures in southeastern Dévoluy are the St-Etienne Syncline, the Auroze Anticline, and four klippen that occur near Col de Rabou in southeasternmost Dévoluy (Figs. 10.1, 10.14).

The open, west-facing St-Etienne syncline plunges shallowly to the northwest (fold axis = 09-328, Fig. 10.15a). It has a half-wavelength of 4 km, and an approximate amplitude of 1 km (Fig. 10.3e). Small synthetic folds in Tertiary sediments in its eastern limb (northwest of the Grand-Combe Klippe, Fig. 10.14) have NNW-SSE orientations.

The Auroze Anticline is a broad, open fold affecting Senonian and Tertiary sediments in the hanging wall of the Median Dévoluy

Thrust. It has a 6 km half-wavelength and a 1 km amplitude (Fig. 10.3e). It plunges moderately to the north (fold axis = 24-352, Fig. 10.15b).

The four klippen are the Grand-Combe, Banards, and the two Palette Klippen (Fig. 10.14). The four klippen lie on W-dipping beds of the Nummulitic Limestone and Queyras Marlstone Formations in the eastern limb of the St-Etienne Syncline (Fig. 10.14). This geometry indicates that the klippen were thrust over the Tertiary sediments and were subsequently rotated during the formation of the St-Etienne Syncline (Fig. 10.3e). Therefore, the rotational effects of the St-Etienne Syncline have been removed from the fault data.

The Grand-Combe Klippe, bounded by the Grand-Combe Thrust, consists of overturned Albian-Cenomanian, Turonian, and Senonian strata. It is overlain by the Banards Klippe at its southern end (Fig. 10.14), indicating that the Grand-Combe Thrust sheet was an imbricate in the foot wall of the Banards Thrust sheet. Slickenfibers on the Grand-Combe Thrust show top-to-the-west and top-to-the-south movement (Fig. 10.16a; n.b.: the apparent normal displacement on some slickenfibers is a relict of the FaultKin program and cannot be corrected; the fibers all show thrust displacement). Because the Grand-Combe Thrust surface is gently crenulated, the top-to-the-south fibers appear to show normal displacement. However, the stratigraphic offset indicates that the fault is a thrust. The corrected kinematic solution of the Grand-Combe Thrust shows that the fault accommodated SW-directed compression (Fig. 10.16b).

The Banards Thrust has accommodated approximately 2 km displacement (Fig. 10.3e). Some blocks of the overturned, E-dipping Cretaceous and Tertiary strata in the hanging wall have been displaced to the west on approximately N-S oriented, W-dipping normal faults (Figs. 10.16c, d, 10.17a). The normal faults sole into the underlying thrust plane, which also dips to the west (Fig. 10.17a).

When kinematic data from the Banards Thrust are corrected, the restored thrust plane has an average NW-SE strike and NE dip (Fig. 10.16e). Variations from this orientation occur because the fault plane is folded in both N-S and E-W directions (Figs. 10.17a-c; note that the mid-Cretaceous unconformity shown in the figs is an angular unconformity). Slickenfibers show compression varying from S- to W-directed (Fig. 10.16e; n.b.: the apparent normal displacement on some slickenfibers is a relict of the FaultKin program and cannot be corrected; the fibers all show thrust displacement). The corrected compressional axis of these fibers is SW-directed (Fig. 10.16f).

Beneath the Banards Klippe, an intense pressure solution cleavage is developed in the Queyras Marlstone Formation (Fig. 10.1). It dies out away from the klippe and is considered to be fault-related. Its corrected average orientation is 162-81E (Fig. 10.16g), comparable to the cleavage orientations in northern Dévoluy (compare Figs. 10.6 and 10.16g). Moreover, calcite slickenfibers on the cleavage surfaces (e.g., Fig. 10.17d) show overall W-directed displacement (Figs. 10.16h, i). These orientations are significantly oblique to the SW-directed compression recorded on the Banards Thrust (Fig. 10.16f), and indicate that overall displacement was probably to the WSW.

The northern Palette Klippe is composed of south-dipping beds of the Queyras Marlstone For-

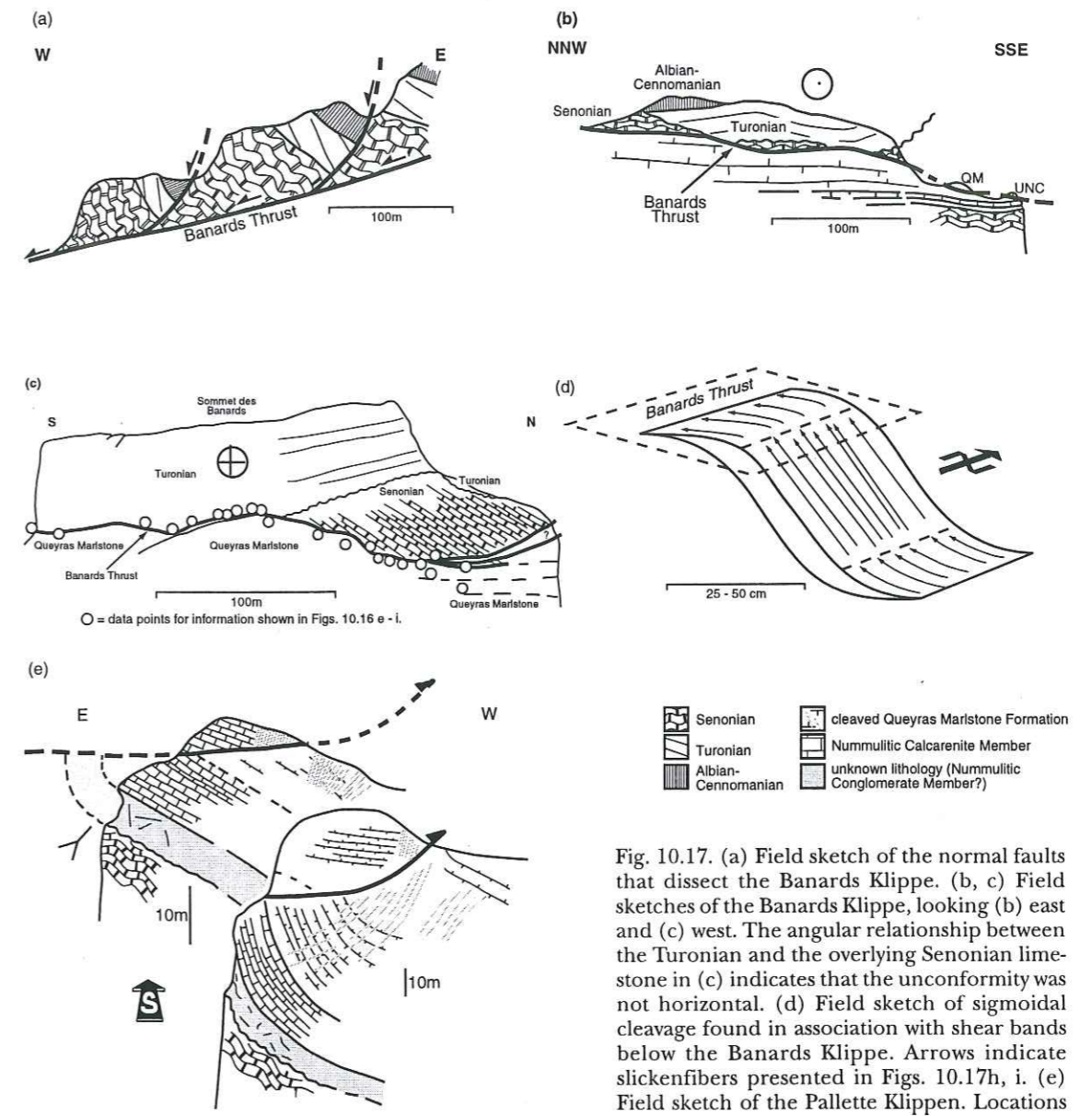
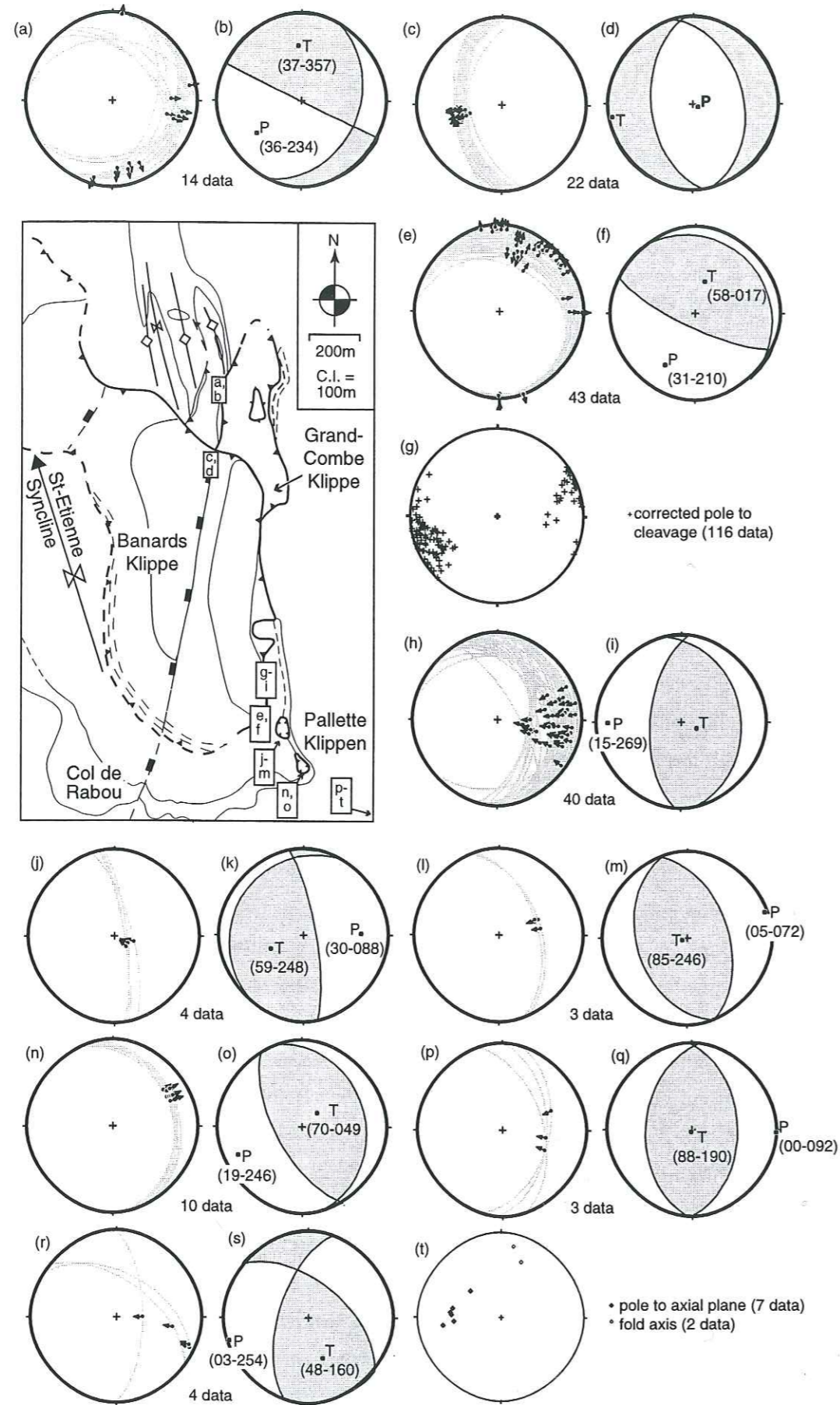


Fig. 10.17. (a) Field sketch of the normal faults that dissect the Banards Klippe. (b, c) Field sketches of the Banards Klippe, looking (b) east and (c) west. The angular relationship between the Turonian and the overlying Senonian limestone in (c) indicates that the unconformity was not horizontal. (d) Field sketch of sigmoidal cleavage found in association with shear bands below the Banards Klippe. Arrows indicate slickenfibers presented in Figs. 10.17h, i. (e) Field sketch of the Palette Klippen. Locations indicated in Fig. 10.15.

Fig. 10.16 (previous page). Lower hemisphere, equal area projections of structural data in southeastern Dévoluy. The apparent normal displacement in Figs. 10.16a, e, and n is a relict of the FaultKin program that could not be corrected. (a) Corrected fault plane and slickenfiber data associated with the Grand-Combe Thrust; (b) linked Bingham axis solution of the data presented in (a); (c) fault plane and slickenfiber data associated with the normal faults that dissect the Banards Klippe; (d) linked Bingham axis solution of the data presented in (c); (e) corrected fault plane and slickenfiber data associated with the Banards Thrust; (f) linked Bingham axis solution of the data presented in (e); (g) corrected orientation of cleavage beneath the Banards Klippe; (h) slickenfiber data from shear bands beneath the Banards Thrust; (i) linked Bingham axis solution of the data presented in (h); (j) fault plane and slickenfiber data on a minor fault beneath the northern Palette Klippe; (k) linked Bingham axis solution of the data presented in (j); (l) fault plane and slickenfiber data associated with the basal fault surface of the southern Palette Klippe; (m) linked Bingham axis solution of the data presented in (l); (n) fault plane and slickenfiber data associated with a bedding-plane parallel fault in the hanging wall of the southern Palette Klippe; (o) linked Bingham axis solution of the data presented in (n); (p) fault plane and slickenfiber data associated with the thrust plane east of the Palette Klippen (located in Fig. 10.3e); (q) linked Bingham axis solution of the data presented in (p); (r) fault plane and slickenfiber data associated with minor faults at the same locality as (p); (s) the linked Bingham axis solution of the data presented in (r); (t) axial plane orientations of minor folds at the same locality as (p).

mation (Fig. 10.17e), while the southern Palette Klippe is composed of SE-dipping beds of the Dévoluy Nummulitic Limestone Formation (Fig. 10.17e). It cannot be ascertained if the beds of these klippen are overturned. The relationship of the Palette Klippen to the Banards Klippe is not well established: they may be an imbricate thrust slice in the foot wall of the Banards Thrust or, alternatively, they may belong to the Banards Thrust sheet itself.

Slickenfibers preserved on a small fault 20 cm below the main fault surface of the northern klippe show corrected oblique dextral thrust displacement to the W (Figs. 10.16j, k). The basal fault surface of the southern klippe has corrected slickenfiber orientations to the WSW (Figs. 10.16l, m). Slickenfibers on a bedding-subparallel slip plane in the hanging wall of the southern klippe have corrected orientations that show compression to 246° (Figs. 10.16n, o; n.b.: the apparent normal displacement on some slickenfibers is a relict of the FaultKin program and cannot be corrected; the fibers all show thrust displacement).

A thrust plane that can be correlated with the thrusts at Col de Rabou crops out in Mesozoic sediments approximately 1.15 km ESE from Col de Rabou (Fig. 10.3e). The plane strikes approximately N-S, and has slickenfibers showing WSW- to WNW-directed displacement (Fig. 10.16p). The data have a kinematic solution showing W-directed displacement (Fig. 10.16q). Minor faults at this locality have W-directed fibers that show compression to 254° (Figs. 10.16r, s). Folds near the fault have N-S to NE-SW striking, E-dipping axial planes and N-plunging axes (Fig. 10.16t), consistent with the W-directed displacement recorded on the underlying thrust surface. This displacement is consistent with the data recorded beneath the Banards Klippe and northern Palette Klippe (Figs. 10.16g-k).

In summary, the kinematic data in southeastern Dévoluy show predominantly SW- and W-directed displacement. The orientation of the St-Etienne Syncline is consistent with the SW-directed thrusting. The W-directed displacement reflects either a differential response of the structures to the later folding of the St-Etienne Syncline or partitioning of the SW-directed thrusting, as interpreted in central Dévoluy. These two displacement directions, and their relationship to the dextral strike-slip faults in central Dévoluy are discussed below.

10.5. Cleavage

Cleavage in Dévoluy is best developed in the Queyras Marlstone Formation. It is not distributed throughout folds, but rather occurs in linear zones within a few tens of meters of faults such as the Median Dévoluy Thrust, the Lucles, Les Bourrettes, and Malmort Faults, and the Banards and Grand-Combe Klippen (Fig. 10.1). Its orientation is strongly dependent on the sense of displacement on the faults (sections 10.2 - 10.4). This distribution, and the fact that cleavage transects local fold axes (compare bedding-cleavage intersection lineations to fold axis orientations, Figs. 10.2, 10.8c, 10.15a), suggests that cleavage and folding do not have a direct relationship, but rather that cleavage developed in zones of distributed strain around thrusts and strike-slip faults ("ductile beads" of Cooper &

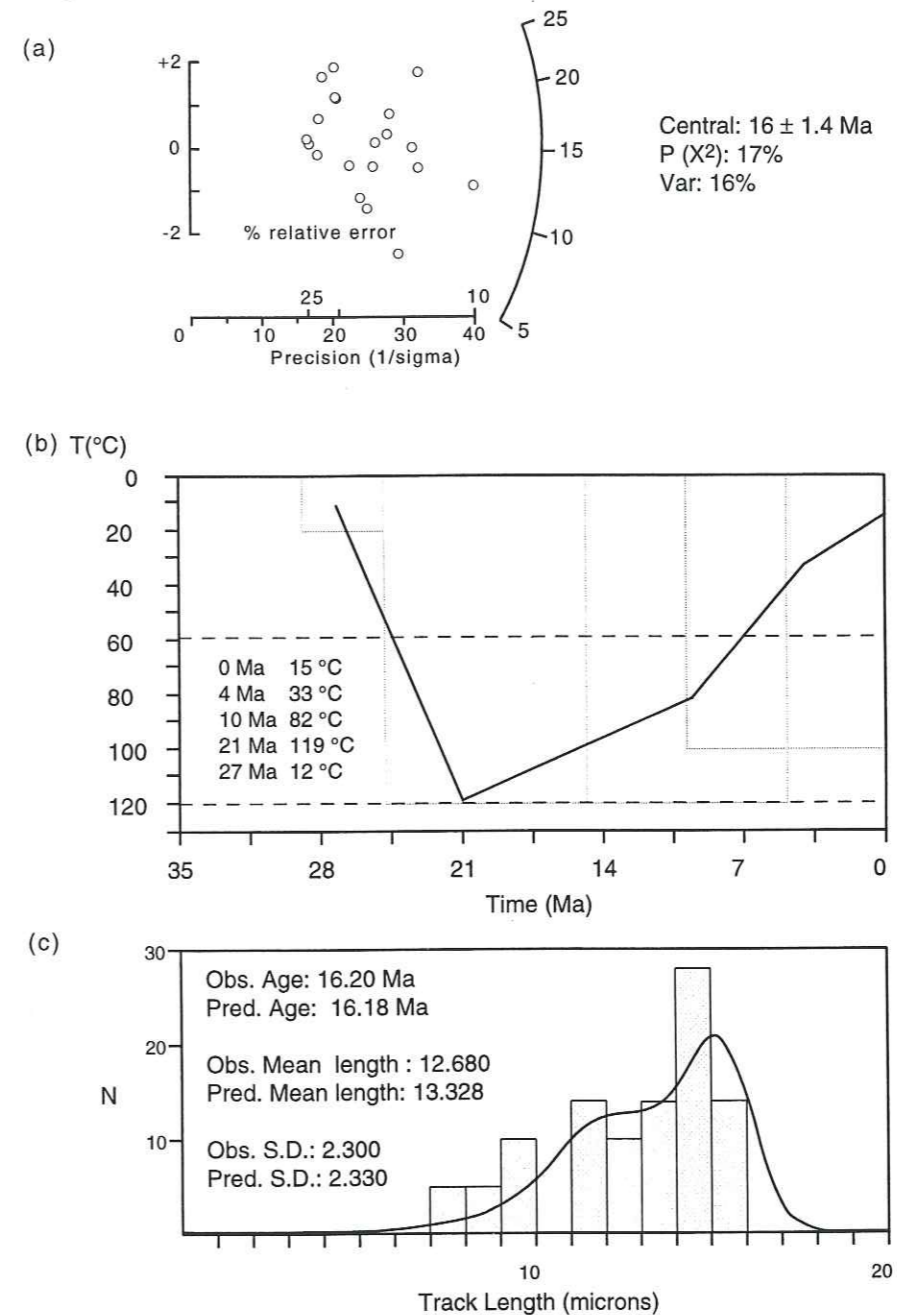


Fig. 10.18. (a) Radial plot of an apatite fission track age of a sample in the St-Disdier Siltstone Formation. (b) Temperature-depth model of the burial and exhumation history of the sample. (c) Histogram of track lengths.

Trayner, 1986). However, because cleavage in northern and southeastern Dévoluy strikes sub-parallel to large-scale fold axes, faulting and folding are interpreted to have had a close temporal relationship.

10.6. Fission track evidence for early Miocene tectonic burial of Dévoluy

Fission track analysis was performed by Dr. D. Seward of ETH on a sample taken from a medium-grained channel sandstone within the St-Disdier Siltstone Formation in the immediate foot wall of

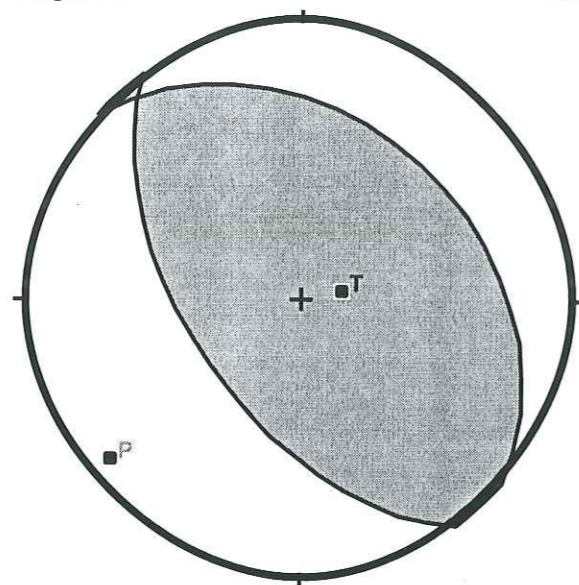


Fig. 10.19. Lower hemisphere, equal area projection of the linked Bingham axis solution of all the data associated with the Median Dévoluy Thrust and the St-Etienne Fault Zone (248 data).

Burial history

Assuming a geothermal gradient of 25°C/km, the sample was buried to slightly more than 4 km by 21 Ma. This depth is consistent with the observation that the sediments in Dévoluy have not experienced metamorphism at a higher grade than diagenesis (e.g., Niggli *et al.*, 1973).

Only 40 m of the St-Disdier Siltstone Formation occur above the sample in the foot wall of the thrust. Therefore, if the burial were caused only by sedimentation, 4 km of sediments, now eroded, were deposited from 27 to 21 Ma. Although the Chattian-Aquitainian Lower Freshwater Molasse in the North Alpine Foreland Basin is this thick (Homewood *et al.*, 1985, 1986; Burbank *et al.*, 1992; Platt & Keller, 1992), the sediments of this age in the southern Chaînes Subalpines are never more than 2 km thick (Evans, 1987). Therefore, sediment-related burial is considered unlikely. Rather, burial is considered to be tectonically-related, as the timing of burial is equivalent with a period of prolonged tectonism in the southern Chaînes Subalpines (Evans, 1987). This consideration is supported by the fact that, according to the model, the minimum time-averaged burial rate is 0.71 mm/yr over 6 Ma (27 - 21 Ma). This rate is significantly higher than typical sediment-related burial rates: Schwab (1986) estimates that foreland basins have an average sedimentation rate of 0.2 mm/yr, and that marine "flysch" basins have an average sedimentation rate of 0.4 mm/yr.

Thus, the burial may be related to either (1) emplacement of the Median Dévoluy Thrust sheet; or (2) emplacement of a thrust sheet or sheets (perhaps the Embrunnais-Ubaye nappes) that were eroded prior to subsequent emplacement of the Median Dévoluy Thrust sheet.

The first hypothesis requires that the hanging wall of the Median Dévoluy Thrust was 4 km thick. However, at this locality, the oldest sediments in the hanging wall belong to the Souloise Greywacke

the Median Dévoluy Thrust, 40 m below the thrust surface (1220 m, 44°43.73' N 5°54.42' E, Fig. 10.1; 55.0 m, Fig. 6.2). The object of the investigation was to determine the burial history of the Dévoluy area. The sample gives an apatite fission track age of 16.2±1.4 Ma (Fig. 10.18a), which indicates that the sample was between 60 - 120°C at this time.

A time-temperature model of the burial and exhumation history of the sample (Figs. 10.18b, c) was developed assuming that the sample was at the surface (i.e., depositional conditions; 12°C) at 27±2 Ma (late Oligocene). The model shows that the sample reached 119°C at 21 Ma by burial, and was subsequently exhumed to 82°C at 10 Ma and 33°C at 4 Ma.

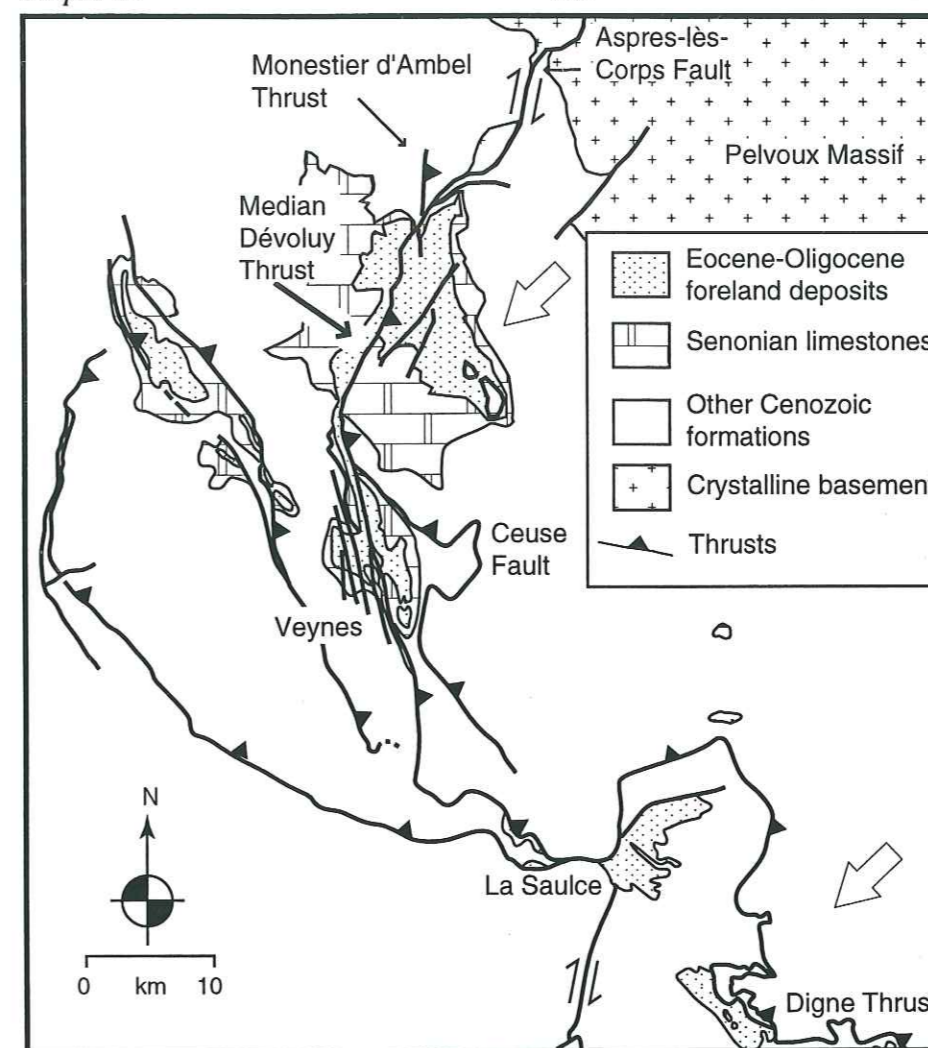


Fig. 10.20. Regional structures associated with the northward and southward continuations of the Median Dévoluy Thrust.

Formation. Because the maximum known thickness in Dévoluy of the sedimentary column above and including this formation is approximately 450 m, one must suppose either (1) that at least 3.5 km of Aquitanian sediments were present in the hanging wall at the time of emplacement and have since been eroded, or (2) that the Median Dévoluy Thrust was overlain by at least one "piggyback" thrust sheet. As discussed above, Aquitanian sediments in Dévoluy were not 3.5 km thick; therefore, in this hypothesis, the Median Dévoluy Thrust must have carried other thrust sheets, such as the Banards Thrust sheet (Fig. 10.3) and/or more internal thrust sheets.

The second hypothesis implies that 4 km of nappes were emplaced over the Dévoluy area by 21 Ma, burying the sample to its maximum depth. In this hypothesis, erosion of the overburden brought the sample out of the partial annealing zone, and subsequent thrusting on the Median Dévoluy Thrust emplaced a significantly smaller load which did not bury the sample to within the annealing zone.

Additional fission track samples from the hanging wall of the Median Dévoluy Thrust would aid in proving one of the hypotheses. If the hanging wall sediments were also buried to depths of 4 km, the first hypothesis would be more likely, whereas if the hanging wall samples have not been deeply

buried, the second hypothesis would be more likely.

Exhumation history

The fission track model (Fig. 10.18b) suggests that the sample was exhumed at very similar rates from 21 - 10 Ma (0.14 mm/yr) and from 4 Ma to present (0.18 mm/yr). From 10 - 4 Ma, however, the sample was exhumed at a noticeably higher rate (0.33 mm/yr). The increase in exhumation rate in Dévoluy is consistent with time-equivalent uplift of the Pelvoux basement massif to the east of Dévoluy, where fission track ages from basement samples have ages that range from 16 - 4 Ma (D. Seward & M. Ford, pers. comm.). The similarity of the timing of uplift of Pelvoux and the increased exhumation in Dévoluy strongly suggests that the two are related: that is, that the Dévoluy area experienced enhanced exhumation during uplift of Pelvoux. Prior to the uplift of Pelvoux, and following its cessation, Dévoluy experienced more typical rates of exhumation.

10.7. Late Alpine tectonics of the Dévoluy basin

Significant compressional deformation migrated westward across Dévoluy during the early Miocene, as suggested by a fission track age (Fig. 10.18). In southeastern Dévoluy, the deformation was SW- to W-directed, as documented by the orientation of the St. Etienne Syncline and kinematic data associated with the Banards, Grand-Combe, and Palette Klippen. To the north and west in Dévoluy, distinct components of W-directed compression and N-S dextral shear and associated vertical offset are recorded. The W-directed compression is recorded on the Median Dévoluy Thrust, minor associated fault planes, and the major folds in northern Dévoluy. The previously undocumented dextral shear and associated vertical offset is documented by cleavage, fracture, minor fold, and fault kinematic data near the Les Bourrettes and Malmort Faults and in the St-Etienne Shear Zone. When kinematic data from the Median Dévoluy Thrust, the Les Bourrettes and Malmort Faults, and the St-Etienne Fault Zone are considered together, the solution shows pure SW-directed compression (Fig. 10.19). Therefore, regional SW-directed compression is considered to have been partitioned across central Dévoluy into pure shear and wrench components. The small-scale folds within fault blocks of the St-Etienne Fault Zone show that part of the strain was also accommodated within the blocks.

The fault geometries and deformation kinematics associated with the partitioning are compatible with models of local dextral transpression accommodating overall SW-directed compression (e.g., Sanderson & Marchini, 1984; Schreurs, 1993; Tikoff & Teyssier, 1994). In such models, compression is partitioned into (1) shallowly-dipping thrust faults, and (2) steeply-dipping strike-slip faults with reverse dip-slip components that develop in the hanging wall of the thrust faults to accommodate bulk strain. These features correspond well to the respective positions of the Median Dévoluy Thrust and the St-Etienne Fault Zone (Fig. 10.1).

The partitioning is associated with (1) steepening of and (2) decreasing horizontal shortening

on the Median Dévoluy Thrust towards the north (Fig. 10.3). The steepening occurs where the thrust links to the NE-SW oriented, steeply SE dipping Aspres-lès-Corps Fault (Gidon & Pairis, 1976; BRGM, 1980d; Fabre *et al.*, 1986). The decrease in horizontal displacement is considered to have been partially compensated by vertical and strike-slip movements in central Dévoluy and the large-scale folds in northern Dévoluy (Fig. 10.3). However, it is also consistent with a regional northward decrease in shortening along the length of the linked Digne Thrust/Median Dévoluy Thrust system (Gidon & Pairis, 1976; BRGM, 1980d; Fabre *et al.*, 1986). The links to the Aspres-lès-Corps Fault and Digne Thrust are discussed in the following two sections.

10.7.1. The transition from the Median Dévoluy Thrust to the Aspres-lès-Corps Fault

The link between the Aspres-lès-Corps Fault and the Median Dévoluy Thrust is expressed as a gradual steepening of the fault plane to the north. Several branch faults are present where the link occurs. The most important of these faults are the Monestier-d'Ambel Thrust and the Aspres-lès-Corps Fault *sensu stricto* (Fig. 10.21; see also Gidon & Pairis, 1976 and BRGM, 1980d).

Post-Oligocene dextral movement and associated high-angle W-directed thrusting on these faults (Gidon & Pairis, 1976; Pairis *et al.*, 1986; Henry, 1992) was presumably related to the late Alpine deformation in Dévoluy. Although the exact nature of the distribution of the forces is not known, the following observations can be made. (1) The SW-directed deformation in southeastern Dévoluy and its partitioned W-directed and N-S dextral shear components in northern Dévoluy are consistent with dextral movement on the Aspres-lès-Corps Fault (Fig. 10.21) and are therefore considered to be connected by SW-directed movement south of the fault. (2) The NNE-SSW faults of the St-Etienne Fault Zone are subparallel to the dextral Aspres-lès-Corps Fault. Therefore, their orientation and dextral component of displacement probably occurred together with the larger-scale movement on the Aspres-lès-Corps Fault.

Thus, the "link" between the Aspres-lès-Corps Fault system and the Median Dévoluy Thrust appears to have been accommodated by displacement on subsidiary faults. This diffuse accommodation style may also be the cause of the partitioning of SW-directed thrusting into its constituent components, such that commensurately more of the total displacement was taken up on folds and faults in the hanging wall of the Median Dévoluy Thrust than on the thrust plane itself.

10.7.2. The transition from the Median Dévoluy Thrust to the Digne Thrust

The SW-directed compression in Dévoluy is compatible with Mio-Pliocene SW-directed displacement found on the Digne Thrust south of Dévoluy (Ehtechamzadeh-Afchar & Gidon, 1974; Arnaud *et al.*, 1977; Fry, 1989a), and in the Champsaur region east of Dévoluy (Gidon & Pairis, 1986; Ford *et al.*, 1995). Thus, SW-directed compression is considered to have migrated regionally across the Southern Chaînes Subalpines during this time (Pairis *et al.*, 1986; Fry, 1989a).

Despite the similarity in displacement directions, the link from the Median Dévoluy Thrust to the Digne Thrust (Gidon & Pairis, 1976; BRGM, 1980d; Fabre *et al.*, 1986) is problematic because

the Digne Thrust has an estimated 20 km of horizontal displacement (Ehtechamzadeh-Afchar & Gidon, 1974; Arnaud *et al.*, 1977) whereas the Median Dévoluy Thrust accommodates an estimated maximum of 2-3 km of W-directed thrusting (Fig. 10.3). The decrease in displacement may be the result of the branching of the Digne Thrust into (1) a series of splay thrusts at La Saulce, 25 km south of Dévoluy, and (2) N-S oriented reverse faults at Veynes, 10 km south of Dévoluy (Fig. 10.21). These splays, which die out to the north, may accommodate the remaining displacement in a zone of diffuse accommodation. Certainly, several of the faults at Veynes record at least 1 km of horizontal displacement (BRGM, 1974b).

However, the problem of the timing of thrusting remains: it is assumed that emplacement of a 4 km thick thrust sheet, or stack of sheets, in Dévoluy occurred during during the early Miocene, while the most recent displacement on the Digne Thrust postdates the deposition of upper Miocene to upper Pliocene conglomerates (BRGM, 1981).

If the burial was caused by movement on the Median Dévoluy Thrust, then the post-Pliocene thrusting in Digne is probably recorded on one of the splays at La Saulce or Veynes. This hypothesis is reasonable, given the presence of several splay faults with a kilometer or more of displacement south and west of Dévoluy (Fig. 10.20). The timing of movement on these faults is not well-constrained, and could certainly have occurred after the Pliocene.

Conversely, if the burial is associated with emplacement of the Embrunnais-Ubaye nappes in Dévoluy, and minor post-Pliocene thrusting may have occurred on the Median Dévoluy Thrust. This hypothesis is also reasonable, as explained above, if significant erosion of the internal thrust sheet had already occurred by the Pliocene, and post-Pliocene movement carried only the eroded remnant of the thrust sheet. Given that the apatite sample from the footwall of the thrust is interpreted to have been buried 0.72 km (33°) at 4 Ma, and erosion occurred at a rate of 0.18 mm/yr from 4 Ma to present (Fig. 10.6b), then the hanging wall of the Median Dévoluy Thrust sheet would have been 0.36 km thick at 2 Ma (end Pliocene), and subsequent movement would not have reset the fission track age.

No qualitative distinction can be made between these two hypotheses.

10.7.3. Conclusions

Four phases of tectonic activity took place in Dévoluy during the Tertiary:

- (1) ENE-WSW compression, which caused locally intense folding of Senonian sediments, occurred sometime between the late Maastrichtian and the mid-Bartonian (Section 2.2).
- (2) E-W extensional faulting that postdates the folding occurred before the Priabonian (Sections 2.2, 9.1.1).
- (3) Uplift of the western margin of Dévoluy, possibly caused by a blind thrust, occurred in the earliest Oligocene (Section 6.2).
- (4) SW-directed compression occurred during the Miocene, after deposition had ceased in Dévoluy (this chapter). This phase of tectonism included (a) nappe emplacement in south-

eastern Dévoluy that preceded large-scale folding; (b) folding and thrusting of the Tertiary sediments, in which the SW-directed compression was partitioned into components of W-directed compression (the Median Dévoluy Thrust) and N-S dextral strike-slip faulting. At the same time, NE-SW oriented dextral strike-slip faults developed in the hanging wall of the Median Dévoluy Thrust in central Dévoluy to accommodate northward stratigraphic thinning in the hanging wall.

The four phases of deformation correlate well with periods of tectonic activity in the southern Chaînes Subalpines. However, minor NW-directed movements recorded elsewhere in the southern Chaînes Subalpines are not found in Dévoluy.

Chapter 11

THE TECTONIC EVOLUTION OF THE EXTERNAL WESTERN ALPINE ARC

This chapter concerns the implications of the structural and tectonic observations made in Chapter 10 for the geodynamic evolution of the external western Alpine arc, which is still controversial. Most existing models for the formation of the arc fall into three categories: (1) those favoring a radially-forming arc, (2) those favoring partitioning of large-scale tectonic forces into NW- and SW-directed components, and (3) those favoring the presence of two independently active transport directions, one to the WNW-NW and the other to the WSW-SW.

The radial arc models invoke either (1) the presence of a rigid indenter, the relative motion vectors (Platt *et al.*, 1989) or counterclockwise rotation (Gratier *et al.*, 1989; Lacassin, 1989; Vialon *et al.*, 1989) of which caused the divergence, or (2) the NNW-directed emplacement of a large orogenic "pile" that collapsed radially due to gravitational forces (Goguel, 1963; Siddans, 1979). Butler *et al.* (1986) and Butler (1992) have suggested that the orogenic pile experienced sidewall collapse.

Partitioning models propose that pre-existing structural features such as NE-SW oriented zones of crustal weakness in the foreland ("tram line" models of Vialon, 1976; Graham, 1978; Fry, 1989a) or similarly oriented faults within the basement blocks of the Pelvoux-Grandes Rousses-Taillefer-Belledone Massif complex (Henry, 1980, 1992) preferentially partitioned WNW compression into NW- and SW-directed components.

The independent transport models assume that discrete NW and SW transport directions acted through time, and that their combined effects gave rise to the apparent divergence of directions (Fry, 1989a, b; Ford *et al.*, 1995; Bürgisser *et al.*, 1995).

Observations from the area around the bend in the arc support the partitioning or independent transport models, as discussed below.

11.1. Kinematics at the bend of the western Alpine arc

Late Tertiary tectonic transport directions in the external western Alps vary from NW- to SW-directed (Figs. 1.3, 11.1, 11.2). WNW- to NW-directed compression occurred in the northern Chaînes Subalpines (Platt *et al.*, 1989; Coward *et al.*, 1991; Butler, 1992), the Faucon-Turriers-Clamensane region southeast of Dévoluy (Arnaud *et al.*, 1977), and, east of Dévoluy, at Soleil Boeuf and along the eastern side of the Pelvoux Massif (Kerckhove *et al.*, 1978; Gidon & Pairis, 1980-1981; Matthews, 1984; Butler *et al.*, 1986; Ford *et al.*, 1995; Ford, 1996). Significant SW-directed structures are all located in the southern Chaînes Subalpines.

The NW-directed movement in the northern Chaînes Subalpines, tentatively dated as post-Oligocene, changes direction from to 283° in Vercors, at the southern end, to 294° near the Prealps, at the northern

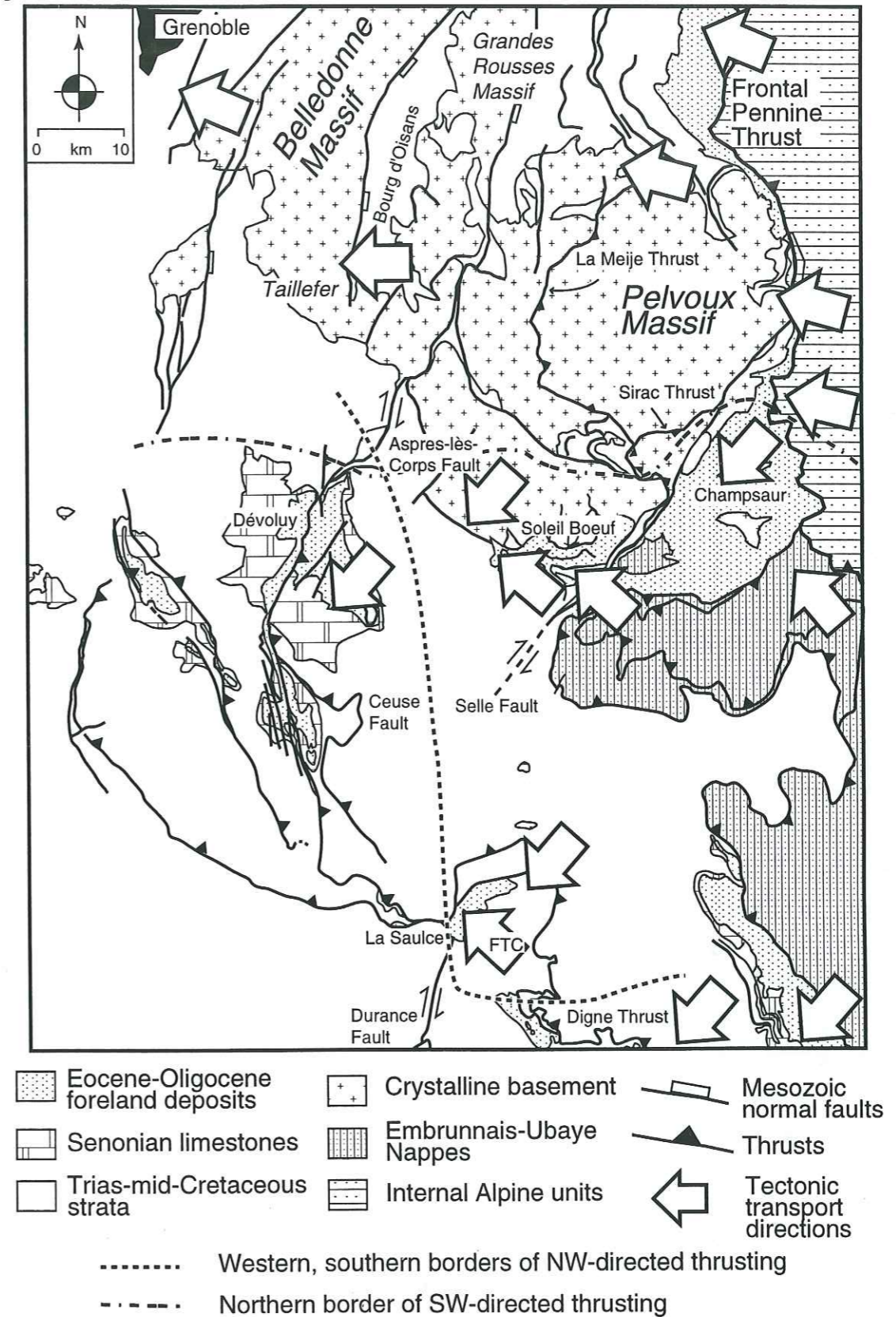


Fig. 11.1. Detailed map showing tectonic transport directions and their interpreted limits in the Pelvoux-Grandes Rousses-Belledone Massif area at the bend in the arc of the external western Alps. Data as in Fig. 1.3 (inset, Fig. 11.2). FTC = Faucon-Turriers-Clamensane.

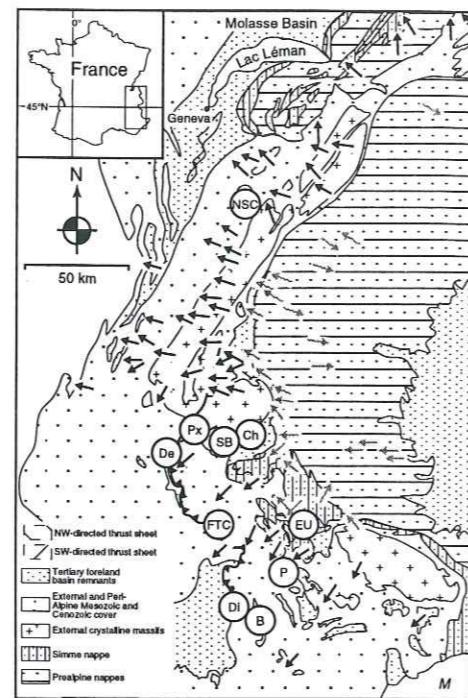
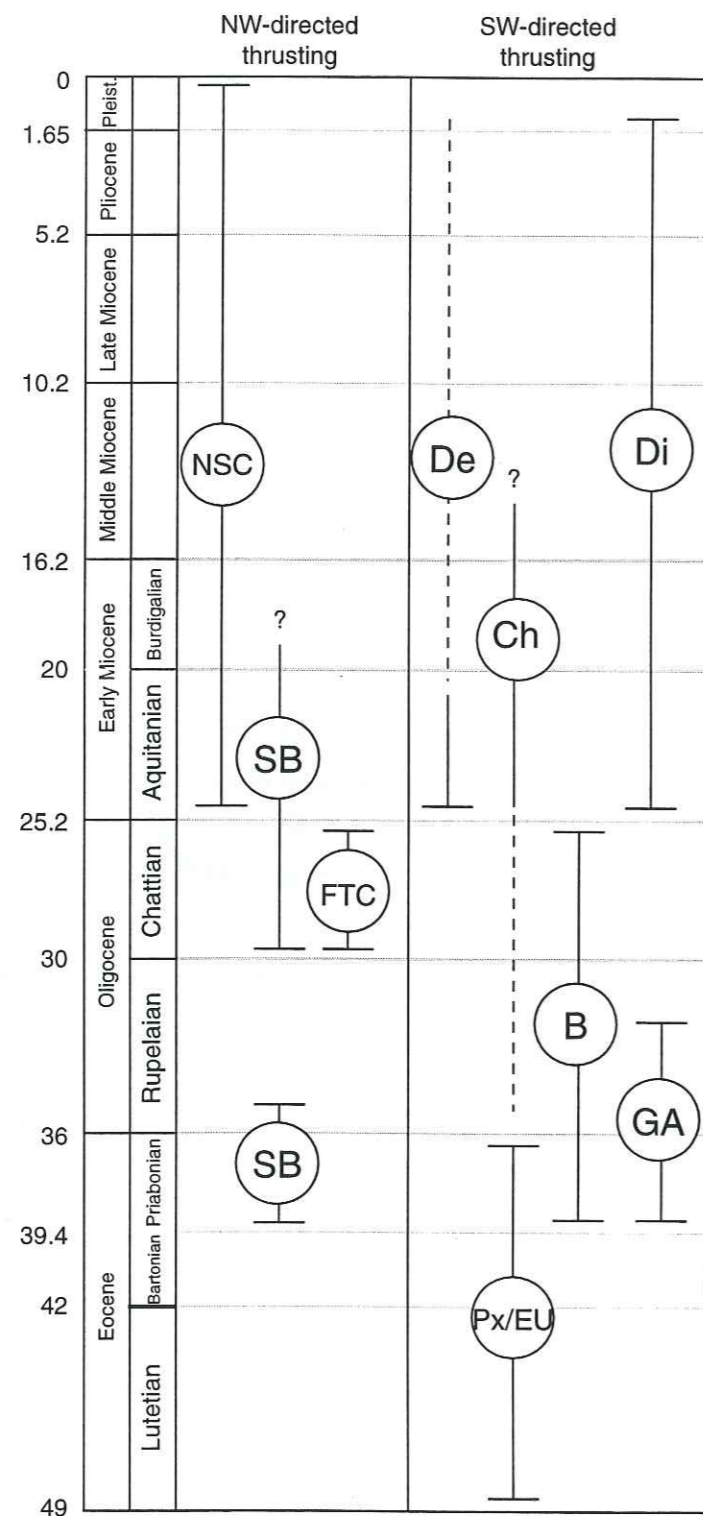


Fig. 11.2. Relative timing of NW- and SW directed compressional events in the Chaînes Subalpines. B: Barrême (Evans, 1987); Ch/Px: Champsaur/SW Pelvoux (Bürgisser *et al.*, 1995); De: Dévoluy (this study); Di: Digne Thrust (Evans, 1987); FTC: Faucon-Turriers-Clamensane (Arnaud *et al.*, 1977); GA: Grès d'Annot basins (Evans, 1987); P/EU: Peyresq/Embrunnais-Ubaye nappes (Apps, 1987 & Evans, 1987 in Fry, 1989a); NSC: northern Chaînes Subalpines (Platt *et al.*, 1989; Butler, 1992); SB: Soleil Boeuf (Gidon & Pairis, 1980-81; Ford, 1996). Time scale of Haq *et al.* (1988). Inset (above) shows locations of areas on a map of tectonic transport directions in the external western Alps (see Fig. 1.3, after Platt *et al.*, 1989).

end (Fig. 11.2; Butler *et al.*, 1986; Butler, 1992). In the southern Chaînes Subalpines, NW-directed deformation at Soleil Boeuf (Fig. 11.2) occurred during deposition of the uppermost Eocene - lowermost Oligocene Champsaur Sandstone (Gidon & Pairis, 1980-1981) and also after the middle Oligocene (Fig. 11.2; Ford *et al.*, 1995; Ford, 1996). The NW movement in the Faucon-Turriers-Clamensane region occurred

during the middle and late Oligocene (Fig. 11.2; Arnaud *et al.*, 1977). There is no evidence of WNW- to NW-directed compression elsewhere in the southern Chaînes Subalpines. Thus, a spatial constraint is placed on the southern and western limits of NW-directed thrusting (Fig. 11.1). Kinematics and displacement estimates for the northern Chaînes Subalpines indicate that the W to WNW shortening was between 70-80 km and 120 km (e.g., Butler, 1984, 1985; Butler *et al.*, 1986; Ménard & Thouvenot, 1986; Mugnier *et al.*, 1987; Gratier *et al.*, 1989; Guellec *et al.*, 1990; Mugnier *et al.*, 1990; Butler, 1992).

The SW-directed structures in the southern Chaînes Subalpines are middle Eocene to Mio-Pliocene in age (Fig. 11.2). The earliest deformation, middle to late Eocene in age, is reported in the Embrunnais-Ubaye nappes (Evans, 1987) and in the Peyresq basin remnant (Fig. 11.2; Apps, 1987 in Fry, 1989a). In the Barrême basin remnant, syndepositional deformation occurred from the Priabonian through the Chattian (Fig. 11.2). Other SW-directed features are post-middle or post-late Oligocene in age, and include thrust and fold structures of the Embrunnais-Ubaye nappes (Kerckhove, 1969; Fry, 1989a), the Digne Thrust (Ehtechamzadeh-Afchar & Gidon, 1974; Arnaud *et al.*, 1977; Fry, 1989a), folds in Champsaur (Vialon *et al.*, 1976; Bürgisser *et al.*, 1995; Ford, 1996), and folds and thrusts in southeastern Dévoluy (Figs. 11.1, 11.2). Minor SW-directed deformation is recorded at Soleil Boeuf, east of Dévoluy (Fig. 1.3; Bürgisser, pers. comm.). SW-directed compression is not recorded in the northern Chaînes Subalpines, except at the south end of the Bornes Massif (south of the Prealpine Klippen), where Butler (1992) reports post-Oligocene SW-directed kinematic indicators related to local thrust-tip effects. Thus, a tentative northern limit to SW-directed thrusting can be inferred (Fig. 11.1). Across the southern Chaînes Subalpines, kinematic data and shortening estimates indicate a northward decrease in WSW-directed shortening (Fry, 1989a) from approximately 20km on the Digne Thrust (Ehtechamzadeh-Afchar and Gidon, 1974; Arnaud *et al.*, 1977) to 2-3 km or less in Dévoluy.

Evidence of W-directed compression in the external Alps is recorded only around the Pelvoux, Grandes Rousses, and Belledone Massifs, where poorly dated (post-Eocene?) thrust kinematics show a spread of directions from 209° to 315° (average = 268°), including several W-directed data (Coward *et al.*, 1991). Cleavage and stretching lineations in the Bourg d'Oisans Syncline (Fig. 11.1) also document "horizontal E-W regional contraction" (de Graciansky *et al.*, 1989, p. 97). Although these data may represent true W-directed compression in this area, figure 3 of Coward *et al.* (1991) appears rather to show two predominant directions of thrusting, to the WNW and WSW-SW. The few other W-directed data are all found in association with the La Meije thrust (Fig. 11.1), which occurs between WNW- and WSW-directed fault blocks, and may therefore represent local strain variations. The lack of a significant component of W-directed movement at the bend in the arc suggests that the distribution of movement vectors around the Pelvoux Massif is not radial, but rather, that there is a distinct break in the kinematic pattern of the arc between NW- and SW-directed transport.

Models that explain the kinematic break include (1) partitioning in the external Alps of W- to WNW-directed movement (e.g., Lacassin, 1989; Platt *et al.*, 1989) of an indenter between the African and European plates ("Apulia", Argand, 1924), and (2) independent NW- and SW-directed transport directions

ahead of Apulia.

11.2. Models

11.2.1. Case 1: Partitioning

In simplified partitioning models, compressional stress oblique to a pre-existing feature such as a fault zone is partitioned into components of movement perpendicular and parallel to the zone (Fig. 11.3a). Odonne & Costa (1991) have shown that across thin-skinned, limited-length transcurrent faults, such models are valid. A second method of partitioning is by block rotation, in which fault blocks within a brittle shear zone rotate to accommodate the oblique regional deformation (e.g., McKenzie & Jackson, 1983, 1986; Fig. 11.3b).

Simple partitioning models assume the zone boundaries are faults (Fig. 11.3a), whereas block rotation models assume a diffuse shear zone, within which the accommodating faults have antithetic senses of strike-slip displacement relative to the larger imposed shear, and dip-slip displacement that is consistent with the principal stress direction (Fig. 11.3b). The fault-bounded blocks in the zone rotate clockwise if the faults are sinistral, and counterclockwise if the faults are dextral.

The following constraints (based on the geologic observations presented in the previous section) were considered in evaluating models to explain the tectonics of the external western Alps. (1) The imposed compressional stress was between 270° (W) and 293° (WNW), in keeping with the W-WNW movement of Apulia (Lacassin, 1989; Platt *et al.*, 1989). (2) The imposed stress was partitioned into slip vectors between 225° (SW) and 270° (W) and between 270° (W) and 315° (NW), the former of which should have less associated shortening than the latter, as occurred in the external Alps. (3) The partitioning occurred across regional NE-SW oriented faults, which experienced dextral strike-slip.

Only the simple partitioning model, in which the plate motion vector of Apulia can be to the W or WNW (shown to the WNW in Fig. 11.3c), satisfies these restrictions. As discussed below, block rotation models do not satisfy the three criteria. The simple partitioning solution is in reasonable agreement with the regional displacement pattern (Fig. 11.3c):

(1) NW-directed compression occurred preferentially west of the NE-SW faults from the Faucon-Turriers-Clamensane area northward (Figs. 1.3, 11.3c). The faults die out northwest of the La Mure Fault in the northern Chaînes Subalpines (Fig. 11.3c), and all compression to the north and west is to the NW (Figs. 1.3, 10.2, 11.3c).

(2) At the bend in the external Alpine arc, in the Belledone-Grandes Rousses-Pelvoux area (Fig. 11.1), NW- and SW-directed compression overlapped where several NE-SW faults occur in close proximity (Fig. 11.3c).

(3) Also in the Belledone-Grandes Rousses-Pelvoux area, blocks bounded by the NE-SW faults rotated in a counterclockwise sense, which is consistent with dextral movement on the faults (Henry, 1992).

(3) In the southern Chaînes Subalpines, SW-directed compression predominated. NW-directed com-

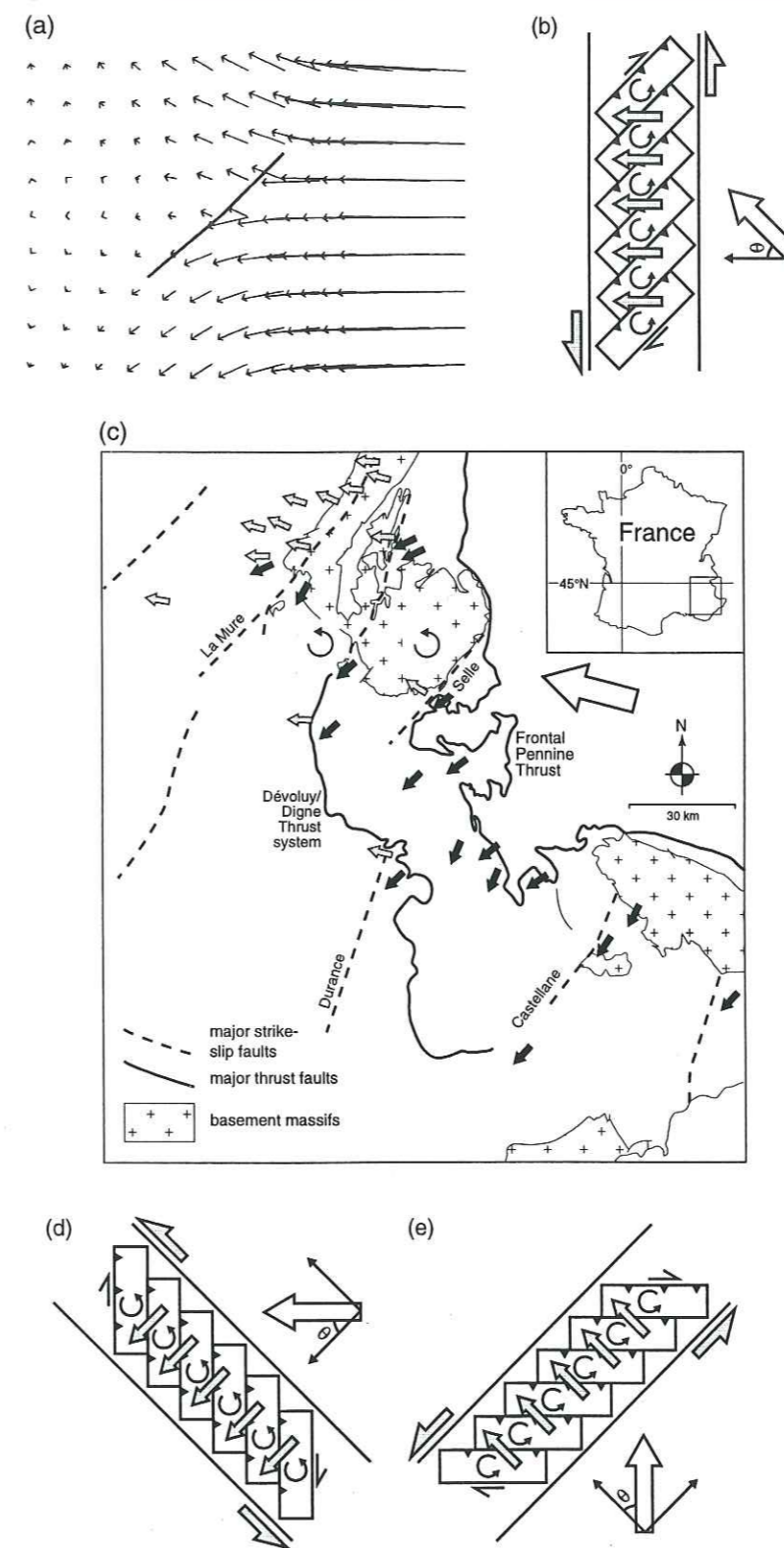


Fig. 11.3. Partitioning models showing the slip vectors generated across a zone of strike-slip faults. (a) General transferral model (after Odonne & Costa, 1991), showing discrete divergence in slip vectors across a thin skinned fault of limited length. (b) Block rotation model (after McKenzie & Jackson, 1986). White arrow = imposed compression; grey arrows = resulting slip vectors; In this model, the faults in the zone of distributed shear are dextral and blocks rotate counterclockwise. (c) Simple partitioning solution for the external western Alps. White arrow = imposed plate vector; grey arrows = NW-directed thrusting; black arrows = SW-directed thrusting. Data from Fig. 1.3. The NW-directed thrusting in the southern Chaînes Subalpines occurs preferentially west of the strike-slip faults (compare with (a)). (d, e) Block rotation models (see text for discussion). Note that the models shown in (b), (d), and (e) do not match the Tertiary kinematics of the external western Alps.

pression only occurred locally, in the vicinity of the Durance and Selle faults (Fig. 11.3c).

The data, then, show that, across the Belledone-Grandes Rousses-Pelvoux area, the movement of Apulia was grossly partitioned into a NW component north of the La Mure Fault and a SW component south of Pelvoux. Local zones of overlapping NW- and SW-directed compression (the Pelvoux and Faucon-Turriers-Clamensane areas) occur between the regional NW- and SW-directed zones. These local zones of overlap appear to confirm the diffuse nature of the shear zone, reflected in the fact that several NE-SW faults occur in close proximity here (Fig. 11.3e). Interestingly, the zones of overlap do not occur at the bend in the external arc, but slightly south of it. The significance of this observation is not yet known.

WNW-directed movement of Apulia (Fig. 11.3c) is considered preferable to W-directed movement (not shown) because Tertiary sediments are thicker in the northern Chaînes Subalpines than in the southern Chaînes Subalpines (see Chapter 9), which probably indicates that the main load of the internal Alps was carried to the WNW and that the southern branch of the foreland basin formed in response to a smaller SW-directed load. WNW-directed movement is also supported by the fact that NW-directed movement is less prevalent in the southern Chaînes Subalpines than in the northern Chaînes Subalpines. This kinematic pattern is more likely if deformation in the southern Chaînes Subalpines occurred in response to side loading of a WNW-moving indenter. If the movement of the indenter were to the west, one would expect a stronger component of partitioning in the southern Chaînes Subalpines, as the W-directed motion would more easily have encountered the faults in the external domain.

A potential weakness of the partitioning models is that they assume that the NE-SW oriented faults acted as thin-skinned, limited faults. However, as they probably represent ancient passive margin faults (Chapter 1), this assumption is not necessarily valid. However, if the faults are passive margin faults, then they would therefore preferentially define the edges of the rigid European block, across which the deformation might be distributed.

Block rotation models do not successfully satisfy the geologic constraints because, when the strike-slip component of the NE-SW oriented faults is dextral, the resulting thrust component is to the W and the boundaries of the deforming zone are oriented N-S (Fig. 11.3b), and when the thrust component is correct (i.e., to the NW or SW), the strike slip faults are oriented E-W or N-S, respectively (Figs. 11.3d, e).

11.2.2. Case 2: Independent Movement

The model invoking two independent compressional directions relies on the previously discussed observation that the WSW to SW thrusting and WNW to NW thrusting were both active in the late Eocene to early Oligocene and after the middle Oligocene through the Mio-Pliocene, and yet are not spatially coincident (Fig. 11.2; refer also to section 11.1). The model considers that compression and loading in the internal Alps caused differential slip on stacked thrust sheets at different structural levels in the external domain. The exact cause of the differential movement is not understood.

The independent motion model requires predominantly SW-directed compression south of the Pelvoux Massif after the mid-Oligocene. This direction of thrusting has been explained previously by lateral expul-

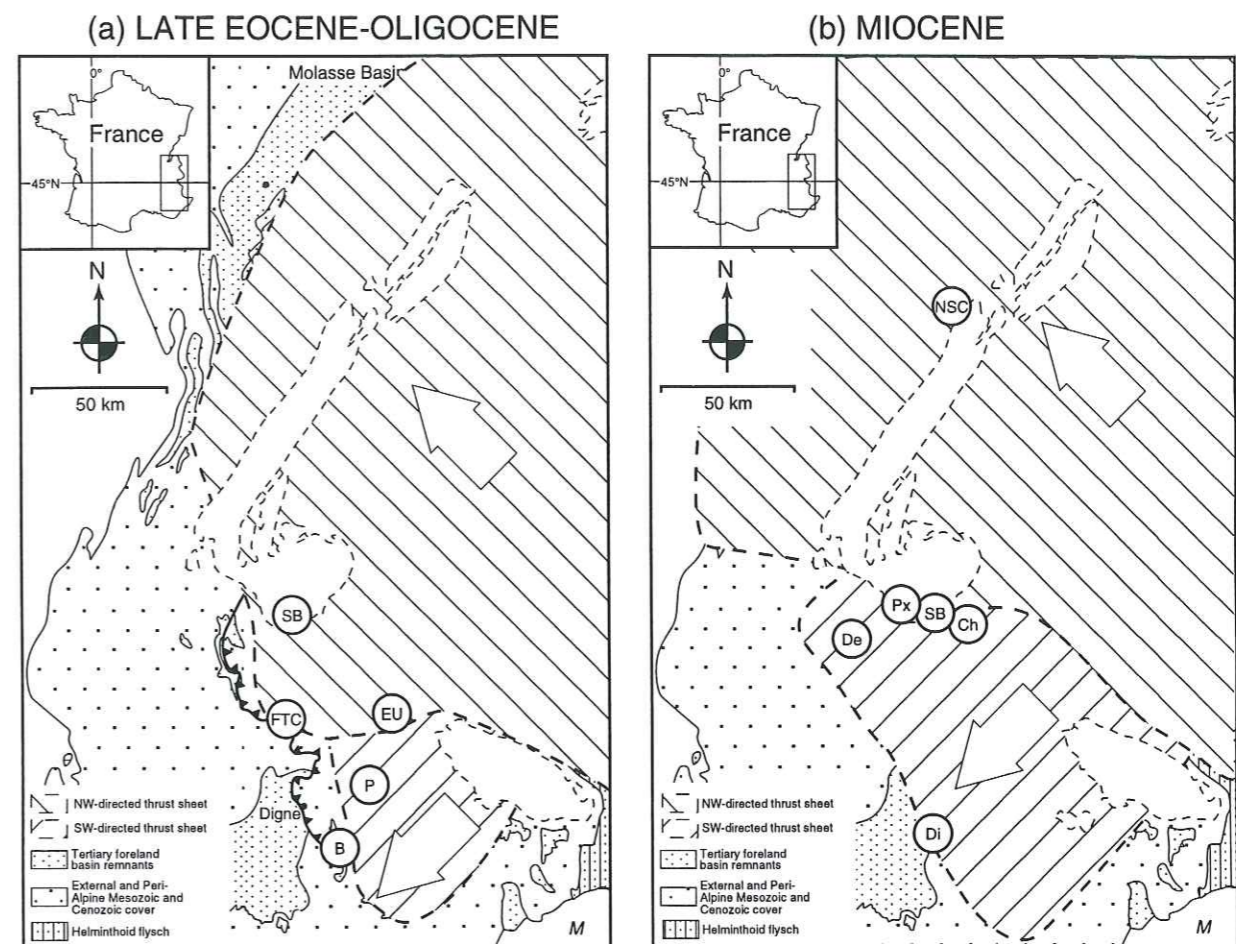


Fig. 11.4. Simplified maps showing hypothetical (a) latest Eocene through Oligocene and (b) Miocene pene-contemporaneous emplacement of NW- and SW-directed thrust sheets. For clarity, these sheets are shown as operating at different structural levels, although the actual emplacement was more complex (Fry, 1989a; Ford, 1996). The Digne Thrust, active during the Miocene, is shown for reference in Fig. 11.4a. Circles show positions of areas shown in Fig. 11.3. Area is the same as in Figs. 1.2, 1.3. The southeast limit of SW thrusting is taken at the edge of the Castellane Fault. M = Mediterranean Sea. The dashed outlines of the basement massifs are provided for reference.

sion (Tapponnier, 1977; Coward *et al.*, 1991, their Figs. 9c, 10b) and sidewall collapse (Butler *et al.*, 1986; Butler, 1992) models, in which overall W-WNW plate movement was buttressed by the NE-SW trending zones, causing the local "escape" of some of the material to the southwest in the southern Chaînes Subalpines.

The following discussion assumes that the two compression directions, which operated at different structural levels at different times, can be simplified to show the two displacement directions as discrete thrust sheets (Fig. 11.4); in reality, the deformation occurred at multiple structural levels through time.

In the late Eocene through the Oligocene, NW-directed movement occurred on thrust sheets that were active in the northern Chaînes Subalpines and the northern part of the southern Chaînes Subalpines (Figs. 11.2, 11.4a). In the southern Chaînes Subalpines, WNW-directed compression, recorded at Soleil Boeuf (Fig. 11.2), was associated with early emplacement of the Embrunnais-Ubaye nappes (Fry, 1989a; Bürgisser *et al.*, 1995; Ford, 1996), and may therefore be associated with similarly directed movements in

the southern Embrunnais-Ubaye nappes (Lawson, 1987 in Fry, 1989a). The relationship between this deformation and the late Oligocene WNW deformation found locally in the Faucon-Turriers-Clamensane region (Fig. 11.2) is poorly constrained. In the southern part of the southern Chaînes Subalpines, relatively smaller thrust sheets accommodated SW-directed movement (Fig. 11.4a).

During the Miocene, NW-directed compression in the northern Chaînes Subalpines and on the north-eastern side of the Pelvoux massif, and SW-directed compression predominated in the southern Chaînes Subalpines (Fig. 11.4b). This probably indicates that the NW-directed deformation had migrated north-westward, allowing SW-directed deformation to migrate across the southern Chaînes Subalpines. The northernmost SW deformation is recorded in Champsaur and Dévoluy. In the Champsaur region, the Embrunnais-Ubaye nappes were carried to the SW, which led to SW-vergent folding (Kerckhove, 1967; Merle & Brun, 1981; Lawson, 1987 in Fry, 1989a; Bürgisser *et al.*, 1995) and prehnite-pumpellyite grade metamorphism in the Champsaur Sandstone (6-8 km burial depth, Waibel, 1990). The SW deformation may have been confined to the north by the Selle Fault (Bürgisser *et al.*, 1995). Dévoluy was probably located at the western limit of the advance of the Embrunnais-Ubaye nappes (Fig. 11.4b; Chapter 10).

The WNW and SW movements may have caused the NE-SW oriented faults of the Mesozoic passive margin to be reactivated as dextral strike-slip faults, which in turn may have caused blocks bounded by the faults (e.g., Pelvoux-Grandes Rousses) to be rotated in a counterclockwise sense (Henry, 1992). However, this hypothesis is tenuous, as there is no *a priori* reason to expect this pattern of deformation.

11.2.3. Discussion

Partitioning and independent movement models both explain the divergent thrusting directions seen in the Chaînes Subalpines. The difference in the models lies in the mechanism causing the divergence. The partitioning models rely on the reactivation of NE-SW oriented faults as transcurrent zones in response to W-WNW directed movement of Apulia, whereas the independent movement model relies on loading and plate-scale compression in the internal Alps to cause two distinct directions to be active more or less simultaneously in the external Alps at different localities and at different structural levels.

The strength of the partitioning models relative to the independent motion model is that the motion of the Apulian microcontinent is an inherent part of the mechanistic solution, in that the Apulian movement vector is redirected in the external Alps by pre-existing NE-SW features. The independent motion model requires a SW movement direction that somehow acted orthogonally to the W-WNW movement of Apulia. Moreover, the independent motion model lacks a convincing mechanism for the differential response of the stacked thrust sheets. Considering this weakness in the independent motion model, the partitioning model is preferable. It should be borne in mind, though, that the partitioning models assume that the NE-SW faults act as thin-skinned faults, which is not necessarily the case. Thus, these models may not be the ideal solution either. More detailed analysis of the partitioning and independent motion models, utilizing analogue and/or computerized forward models, might help to establish the validity of one or

the other model.

11.3. Timing of formation of the external arc

Platt *et al.* (1989) consider the main phase of arc formation as having occurred from 40-15 Ma, when the bulk of the NW- and SW-directed shortening occurred in the external domain. This is consistent with structural kinematic data from the Southern Chaînes Subalpines, where early deformation occurred in the latest Eocene to early Oligocene (e.g., Gidon & Pairis, 1980-1981), and with the observation that the upper Eocene-lower Oligocene turbidites of the western Alpine foreland basin follow an arcuate path, from NW-directed in the Southern Chaînes Subalpines to NE-directed in the Northern Chaînes Subalpines (Sinclair, in press). However, Sinclair (1996, in press) has shown that the shoreline of the Nummulitic Limestone was arcuate from 49-30 Ma, which implies that the incipient foreland basin was already arcuate before tectonic shortening reached the external domain.

11.4. Conclusions

Tectonic transport changes from NW to SW at the bend of the external Alpine arc. However, W-directed transport, which would be expected at the bend of a radially developing arc, occurs only locally, and appears to be related to strain variations in the area. The external western Alpine arc is therefore thought to have formed in response to compression to the NW and SW, which can be explained by either a complex partitioning of deformational forces across NE-SW faults, or by two independent transport directions, but not by a radial sweep of transport from NW to W to SW. Further research should investigate the possibility that the two models may be reconcilable at the large scale.

CONCLUSIONS

Chapter 12 CONCLUSIONS

This study has focused on the sedimentary and structural evolution of the Dévoluy basin, a remnant of the Alpine foreland basin in the southern Chaînes Subalpines of southeastern France, during the Tertiary. Significant tectonism occurred in the Paleocene/Eocene, early Oligocene, and Mio-Pliocene, and orogeny-related sedimentation occurred from the late Eocene through the late Oligocene.

Eocene folding and normal faulting

Before Tertiary sedimentation began, probably at the same time as Eocene folding in Provence, the Mesozoic succession was locally deformed into km-scale, NNW-SSE trending, W-facing folds. The folds are best developed immediately south of the Aspres-lès-Corps Fault, which suggests a period of dextral strike-slip activity on it.

Transgressive carbonate sedimentation (Eocene)

Sedimentation during the late Eocene was carbonate-dominated. The Pierroux Conglomerate, Dévoluy Nummulitic Limestone, and Queyras Marlstone Formations (comprising the Queyras Group) were deposited during this time.

The post-Maastrichtian, pre-Priabonian (Eocene?) Pierroux Conglomerate Formation is interpreted as an alluvial fan system, with both proximal and distal facies preserved. The depocenter of the fan was in northeastern Dévoluy, in the hanging wall of the down-to-the east Median Dévoluy Normal Fault, which was later reactivated in the early Miocene as the Median Dévoluy Thrust. The fan axis and braidplain probably paralleled the fault scarp. The down-to-the-south Pic Grillon Fault in northern Dévoluy was also active during deposition of the conglomerates. Movement on these faults may have been related to activity on the Aspres-lès-Corps Fault system, or could reflect tensional response of the lithosphere to loading in more internal Alpine domains.

The transgressive marine Dévoluy Nummulitic Limestone Formation (Priabonian) consists of a lower conglomerate member and an upper calcarenite member. The lower Nummulitic Conglomerate Member, which records an upsection transition from a shallow marine, high energy shoreface setting to slightly deeper or calmer waters, is interpreted as the composite deposits of a shallow marine, variable energy environment, (upper shoreface, foreshore, or flanks of shallow tidal bars). Deposition occurred at the same time as normal faulting in northern Dévoluy. Notably, the Lucles Fault (orientation = 349-64E; tensional axis = 19-075) shed large blocks of Senonian limestone from the Mt. St-Gicon high into the shallow marine environment. The Nummulitic Calcarenite Member is interpreted as the deposits of fluctuating currents on a medium-energy, ramp-type, deepening carbonate shelf.

The upper Priabonian Queyras Marlstone Formation was deposited in a relatively deep marine (≥ 200 m), hemipelagic setting that was periodically subject to influxes of continental- and/or shelf-derived material in the form of fine-grained sediment plumes and W-flowing sandy turbidity currents. The formation is capped by marly mud- and siltstones that document the first influx of terrigenous debris into the marine foreland

basin, anticipating a transition to siliciclastic-dominated, regressive marine and continental deposition formations (the Souloise Group, consisting of the Souloise Greywacke, St-Disdier Arenite, St-Disdier Siltstone, and Montmaur Conglomerate Formations)

Regressive marine and continental siliciclastic deposition (latest Eocene through Oligocene)

The uppermost Eocene to lowermost Oligocene Souloise Greywacke Formation consists of relatively fine-grained turbidites that record NNW- to NE-directed currents. The turbidity currents probably flowed parallel to a topographic feature such as the axis of the sub-basin or a lateral bounding slope. The formation is interpreted to have been deposited in a shallowing distal fan or distal delta setting.

The lower Oligocene (Rupelian) St-Disdier Arenite Formation was deposited by bidirectional (NE-SW) currents in a medium- to high-energy, upper to middle shoreface setting. A wave-dominated deltaic setting is likely, but cannot be conclusively demonstrated. The base of the formation is a previously unrecognized unconformity that documents uplift and erosion in western Dévoluy before deposition of the formation. The uplift, which probably enhanced shallowing, may have been caused by the propagation of a blind thrust beneath Dévoluy.

The upper Oligocene (Chattian) Upper St-Disdier Siltstone Formation is characterized by a vertical association of subaerial alluvial floodplain deposits, mixed-load fluvial channels, probable crevasse splays, and calichified paleosols characteristic of distal alluvial floodplains. Flow was to the west, but is locally variable, due to the meandering nature of the channels. The Dévoluy floodplain may represent a delta-plain setting or a prograding continental depositional system.

The upper Oligocene (Chattian) Montmaur Conglomerate Formation was deposited either in broad, relatively shallow braided stream channels with poorly-developed margins, or an alluvial fan or fan delta. Flow was to the NW. Inter-channel or finer-grained fan deposits are interbedded with the conglomerates. Overall, the formation probably represents proximal alluvial plain or alluvial fan deposits.

The siliciclastic petrography documents an upsection increase in the amount of internal Alpine debris. The presence of significant amounts of serpentinite, which must have been sourced from an ophiolitic domain, indicates an internal Alpine source area. The St-Disdier Arenite and Siltstone Formations also contain carbonate material that was probably sourced from the uplifting western margin of Dévoluy.

The stratigraphic succession in Dévoluy documents a transition from deepening-up ("underfilled") to shallowing-up ("filled") to continental ("overfilled") conditions within the evolving foreland basin. In the southern Chaînes Subalpines, foreland basin remnants east of Dévoluy record only the underfilled stratigraphy, which typically terminates with a tectonic melange associated with the emplacement of the internal Alpine units. Foreland basin remnants west of Dévoluy record filled and overfilled stratigraphies. These characteristic stratigraphies, which reflect the westward evolution of the foreland basin during its evolution, allow the remnants to be divided into internal, central, and external remnants. Internal remnants occur on the eastern side of the reconstructed basin and record essentially marine conditions. Central remnants, including Dévoluy, preserve the marine to continental transition and were located at the distal edge of the marine basin and the proximal edge of the ensuing continental basin. External remnants are essentially continental and represent the most distal part of the late foreland basin. The deposits in the remnants are diachronous, such that internal remnants are older than external remnants.

Dévoluy is the westernmost and northernmost preserved central remnant in the southern Chaînes Subalpines. Tertiary sedimentary deposits are significantly thicker in the northern Chaînes Subalpines than in the southern Chaînes Subalpines. This difference may indicate that the main load of the internal Alps was carried to the WNW and that the southern branch of the foreland basin formed in response to a smaller SW-directed load. Reconstructions of the shape of the Alpine foreland basin, based on preserved outcrops of the different formations, indicate that the basin was arcuate from its inception, possibly forming in response to this disparate loading in the southern and northern Chaînes Subalpines.

Late Alpine (post-Oligocene) structures

After sedimentation ceased in Dévoluy, the area was deformed, resulting in a locally developed pressure solution cleavage, km-scale folds, the Median Dévoluy Thrust, subvertical N-S and NNE-SSW striking faults that cut through central Dévoluy, and a series of klippen in southeastern Dévoluy.

Cleavage is best developed in the Queyras Marlstone Formation in linear zones within a few tens of meters of faults. Its orientation is strongly dependent on the sense of displacement on the faults, suggesting that it developed in zones of distributed strain around the faults. However, because cleavage in northern and southeastern Dévoluy strikes sub-parallel to large-scale fold axes, faulting and folding are interpreted to have had a close temporal relationship.

Asymmetrical km-scale folds in northern Dévoluy document W-directed compression, whereas those in southeastern Dévoluy document W- and SW-directed compression. These compression directions are consistent with fault kinematic data: the Median Dévoluy Thrust, which cuts Dévoluy from NE to SW, shows top-to-the-W displacement, whereas overturned klippen in southeastern Dévoluy document top-to-the-W and -SW displacement of a second major thrust sheet (the Banards/Grande Combe Thrust).

Tectonically-related burial of the Dévoluy region occurred during the early Miocene, as suggested by an apatite fission track age of 16.2 ± 1.4 Ma from a sample in the St-Disdier Siltstone Formation in the immediate foot wall of the Median Dévoluy Thrust. Assuming a geothermal gradient of $25^\circ\text{C}/\text{km}$, the rock was buried slightly more than 4 km at 21 Ma, indicating that burial occurred at a time-averaged rate of 0.71 mm/yr from the late Oligocene until the late Aquitanian. The depth of burial implies either that the Median Dévoluy Thrust carried other thrust sheets in its hanging wall, or that more internal thrust sheets were emplaced in Dévoluy by 21 Ma, were subsequently eroded, and that the Median Dévoluy Thrust sheet, emplaced later, did not significantly reburied the sediments.

N-S and NNE-SSW oriented subvertical faults in the hanging wall of the Median Dévoluy Thrust in central Dévoluy record dextral strike-slip and down-to-the-west movement in a transpressional system. Movement on these faults is considered to have occurred at the same time as movement on the thrust, and they are interpreted to link at depth to the thrust as a series of high angle dip-slip faults. Furthermore, because dip-slip displacement is greatest where the faults cut major Tertiary fold axes, the faults probably also developed during large-scale folding of the Tertiary strata. The NNE-SSW oriented faults form the St-Etienne Fault Zone, a 2 km wide area that is uplifted relative to both northern and southeastern Dévoluy. Northern Dévoluy is downthrown relative to southeastern Dévoluy across the fault zone, which probably developed as a hanging wall drop fault zone in response to a northward decrease in horizontal displacement on the Median Dévoluy Thrust, from 2 to 3 km in central and southern Dévoluy to less than 100 m where the fault leaves the valley to

the north and links to the major dextral Aspres-lès-Corps Fault. The hanging wall stratigraphy of the Median Dévoluy Thrust thins and the fault cuts abruptly upsection across the fault zone.

It seems probable that SW-directed compression, recorded in SE Dévoluy, was partitioned to the N and W of Dévoluy into distinct components of W-directed compression (the Median Dévoluy Thrust and the major folds in northern Dévoluy) and N-S/NNE-SSW dextral shear and associated vertical offset. The SW-directed compression in Dévoluy is the northernmost such compression found in the Southern Chaînes Subalpines. A regional transition from SW-directed compression on the Digne Thrust, with which the Median Dévoluy Thrust links to the south, to SW-directed dextral strike-slip on the the Aspres-lès-Corps Fault, with which the Median Dévoluy Thrust links to the north, reflects the gradual northward diminution of the SW-directed system to the north.

This observation is significant because Dévoluy is located approximately at the bend in the external Alpine arc, where Tertiary kinematic shortening diverges from SW-directed in the southern Chaînes Subalpines to NW-directed in the northern Chaînes Subalpines. Reasonable models to explain this divergence in the absence of significant W-directed thrusting include regional partitioning of large-scale tectonic forces across NE-SW oriented strike-slip faults, or the occurrence of SW-directed transport independent of overall NNW- or NW-directed transport.

- ALLEN P. A., HOMEWOOD P., WILLIAMS G. (1986). - Foreland basins—an introduction. *In: Allen P. A., Homewood P. (eds.): Foreland Basins. Int. Assoc. Sedimentol. Spec. Pub.*, 8, pp. 199-217
- ALLEN P. A., CRAMPTON S. L., SINCLAIR H. D. (1991). - The inception and early evolution of the North Alpine Foreland Basin, Switzerland. *Basin Res.*, 3, pp. 143-163.
- ALLMENDINGER R. W. (1988-1995). - Stereonet v. 4.9.6. Apple Macintosh computer program.
- ALLMENDINGER R. W., MARRETT R. A., CLADHOUS T. (1989-1994). - FaultKin v. 3.8a. Apple Macintosh computer program.
- ANADON P., CABRERA L., COLOMBO F., MARZO M., RIBA O. (1986). - Syntectonic intraformational unconformities in alluvial fan deposits, eastern Ebro basin margins (NE Spain). *Int. Assoc. Sedimentol. Spec. Pub.*, 8, pp. 259-271.
- APPS, G. M. (1987). - Evolution of the Grès D'Annot basin. Ph. D. thesis, University of Liverpool.
- ARGAND E. (1924). - La tectonique de l'Asie. *Proceedings of the XIIIth International Geological Congress, I* (5), pp. 171-372.
- ARNAUD H., GIDON M., PAIRIS J.-L. (1977). - Précisions sur la structure des chaînes subalpines méridionales dans la région de Faucon-Turriers-Clamensane (Alpes-de-Haute-Provence). *Géol. Alpine*, 53, pp. 5-34.
- ARNAUD M. H. (1974). - Nouvelles données sur la tectonique "antésénionienne" des environs de La Jarjette (Dévoluy occidental). *C. R. Acad. Sci. Fr.*, 278, pp. 697-700.
- AVIGAD D., CHOPIN C., GOFFÉ B., MICHARD A. (1993) - Tectonic model for the evolution of the western Alps. *Geol.*, 21, pp. 659-662.
- BASU A. (1976). - Petrology of Holocene fluvial sand derived from plutonic source rocks: implications to paleoclimatic interpretation. *J. Sed. Petrol.*, 46, pp. 694-709.
- BAUDRIMONT A., DUBOIS R. (1977). - Un bassin mésogéen du domaine péri-alpin: le Sud-Est de la France. *Bull. Centre Rech. Explor. Prod. Elf Aquitaine*, 1, pp. 261-308.
- BERGERAT F. (1987). - Stress fields in the European platform at the time of Africa-Eurasia collision. *Tectonics*, 6, pp. 99-132.
- BLANC C., PAIRIS J.-L., KERCKHOVE C., PERRIAUX J., JEAN S. (1987). - Les flyschs eocènes des unités subbriançonnaises méridionales des nappes de l'Ubaye (Alpes occidentales françaises). *Géol. Alpine Mém. h. s.*, 13, pp. 357-370.
- BODELLE J. (1971). - Les formations nummulitiques de l'arc de Castellane. Thèse d'état, Université de Nice.
- BOGGS S. JR. (1995). - Principles of sedimentology and stratigraphy, Prentice Hall, New Jersey, 774p.
- BOSENCE D. W. H. (1983). - The occurrence and ecology of Recent Rhodoliths - a review. *In: Peyrt T. (ed.): Coated grains, Springer-Verlag, New York, pp. 225-241.*
- BOUMA A. H. (1962). - Sedimentology of some flysch deposits, Elsevier, Amsterdam, 168p.

- BOYER S. E., ELLIOT D. (1982). - Thrust systems. *Bull. Am. Assoc. Petrol. Geol.*, **66**, pp. 1196-1230.
- BRENCHLEY P. J. (1989). - Storm sedimentation. *Geol. Today*, July-August 1989, pp. 133-137.
- BURBANK D., ENGESSER B., MATTER A., WEIDMANN M. (1992). - Magnetostratigraphic chronology, mammalian faunas, and stratigraphic evolution of the Lower Freshwater Molasse, Haute Savoie, France. *Eclogae Geol. Helv.*, **85**, pp. 399-431.
- BÜRGISSER J., FORD M., MECKEL L. D. III (1995). - Kinematics of the western Alpine arc: relations and implications of SW and NW transport directions around the Pelvoux massif. Tectonic Studies Group 26th Annual General Meeting, abstract volume.
- BUTLER R. W. H. (1982). - The terminology of structures in thrust belts. *J. Struct. Geol.*, **4**, pp. 234-239.
- BUTLER R. W. H. (1983). - Balanced cross-sections and their implication for the deep structure of the NW Alps. *J. Struct. Geol.*, **5**, pp. 125-137.
- BUTLER R. W. H. (1984). - Balanced cross-sections and their implications for the deep structure of the NW Alps: reply. *J. Struct. Geol.*, **6**, pp. 607-612.
- BUTLER R. W. H. (1985). - The restoration of thrust systems and displacement continuity around the Mont Blanc Massif, N.W. external Alpine thrust belt. *J. Struct. Geol.*, **7**, pp. 569-582.
- BUTLER R. W. H. (1992). - Thrusting patterns in the NW French Subalpine Chains. *Annales Tectonicae*, **6**, pp. 150-172.
- BUTLER R. W. H., MATTHEWS S. J., PARISH M. (1986). - The NW external Alpine Thrust Belt and its implications for the geometry of the Western Alpine Orogen. In: Ries A. C., Coward, M. P. (eds.): Collision Tectonics. *Geol. Soc. Spec. Pub.*, **19**, pp. 245-260.
- CANT D. J. (1982). - Fluvial lithofacies models and their application. In: Scholle, P. A., Spearing D. (eds.): Sandstone Depositional Systems. *Am. Assoc. Petrol. Geol. Mem.*, **31**, pp. 115-137.
- CHAYES F. (1956). - The Holmes effect and the lower limit of modal analysis. *Mineral. Mag.*, **31**, pp. 276-281.
- CONIGLIO M., DIX G. R. (1992). - Carbonate slopes. In: Walker R.G., James N. P. (eds.): Facies models: response to sea level change, Geol. Assoc. Canada, St. John's, Newfoundland, pp. 349-373.
- COOPER M. A., TRAYNER P. M. (1986). - Thrust surface geometry: implications for thrust-belt evolution and section-balancing techniques. *J. Struct. Geol.*, **8**, pp. 305-312.
- COVEY, M. (1986). - The evolution of foreland basins to steady state: evidence from the western Taiwan foreland basin. In: Allen P. A., Homewood P. (eds.): Foreland Basins. *Int. Assoc. Sedimentol. Spec. Pub.*, **8**, pp. 77-90.
- COWARD M., DIETRICH D. (1989). - Alpine Tectonics-an overview. In: Coward M. P., Dietrich D., Park R. G. (eds.): Alpine Tectonics. *Geol. Soc. Spec. Pub.*, **45**, pp. 1-29.
- COWARD M. P., GILLCHRIST R., TRUDGILL B. (1991). - Extensional structures and their tectonic inversion in the western Alps. In: Roberts A. M., Yielding G., Freeman B. (eds.): The Geometry of Normal Faults. *Geol. Soc. Sp. Pub.*, **56**, pp. 93-112.
- CRAMPTON S. L. E. (1992). - Inception of the Alpine foreland basin: basal unconformity and Nummulitic limestone. Ph. D. thesis, University of Oxford.

- CRAMPTON S. L., ALLEN P. A. (1995). - Recognition of forebulge unconformities associated with early-stage foreland basin development: example from the North Alpine foreland basin. *Bull. Am. Assoc. Petr. Geol.*, **79**, pp. 1495-1514.
- DAHLSTROM C. D. A. (1969). - Balanced cross sections. *Can. J. Earth Sci.*, **6**, pp. 743-747.
- DE GRACIANSKY P. C., DARDEAU G., LEMOINE M., TRICART P. (1989). - The inverted margin of the French Alps and foreland basin inversion. In: Cooper M. A., Williams G. D. (eds.): Inversion Tectonics. *Geol. Soc. Sp. Pub.*, **44**, pp. 87-104.
- DEBELMAS J. (1975). - Réflexiones et hypothèses sur la paléogéographie crétacée des confins alpine-appenninique. *Bull. Soc. Géol. Fr.*, **7/XVII/6**, 1002-1012.
- DEBELMAS J., LEMOINE M. (1970). - The western Alps: paleogeography and structure. *Earth Sci. Rev.*, **6**, pp. 221-256.
- DEBRAND-PASSARD S., COURBOULEIX S., LIENHARDT M. J. (1984). - Synthèse géologique du sud-est de la France. *Mém. BRGM*, **125**, 615 p.
- DECKER J., HELMOLD K. P., INGERSOLL R. V., BULLARD T. F., FORD R. L., PICKLE J. D. (1985). - The effect of grain size on detrital modes: a test of the Gazzi-Dickinson point-counting method: discussion and reply. *J. Sed. Petrol.*, **55**, pp. 618-621.
- DEWEY J. F., HELMAN M. L., TURCO E., HUTTON D. H. W., KNOTT S. D. (1989). - Kinematics of the western Mediterranean. In: Coward M. P., Dietrich D., Park R. G. (eds.): Alpine Tectonics. *Geol. Soc. Spec. Pub.*, **45**, pp. 265-283.
- DICKINSON W. R. (1970). - Interpreting detrital modes of graywacke and arkose. *J. Sed. Petrol.*, **40**, pp. 695-707.
- DICKINSON W. R., SUCZEK C. A. (1979). - Plate tectonics and sandstone composition. *Bull. Am. Assoc. Petrol. Geol.*, **63**, pp. 2164-2182.
- DIEM B. (1986). - Die Untere Meeresmolasse zwischen der Saane (Westschweiz) und der Ammer (Oberbayern). *Eclogae Geol. Helv.*, **79**, pp. 493-559.
- DIETRICH D., CASEY M. (1989). - A new tectonic model for the Helvetic nappes. In: Coward M. P., Dietrich D., Park R. G. (eds.): Alpine Tectonics. *Geol. Soc. Spec. Pub.*, **45**, pp. 47-63.
- DOTT R. H. JR., BOURGEOIS J. (1982). - Hummocky cross-stratification: significance of its variable bedding sequences. *Bull. Geol. Soc. Am.*, **93**, pp. 663-680.
- DUBOIS R. (1962). - Le Nummulitique du Dévoluy (Hautes Alpes). Relations avec les régions voisines. *Bull. Soc. Géol. Fr.*, **7/IV/39**, pp. 612-619.
- DUKE W. L. (1985). - Hummocky cross-stratification, tropical hurricanes and intense winter storms. *Sedimentology*, **32**, pp. 167-194.
- DUNHAM R. J. (1962). - Classification of carbonate rocks according to depositional texture. In: Ham W. E. (ed.): Classification of Carbonate Rocks. *Am. Assoc. Petrol. Geol. Mem.*, **I**, pp. 108-121.
- EHTECHAMZADEH-AFCHAR M., GIDON M. (1974). - Données nouvelles sur la structure de l'extrémité nord de la zone des chevauchements de Digne. *Géologie Alpine*, **50**, pp. 57-69.
- ELLIOTT T., APPS G., DAVIES H., EVANS M., GHIBAUO G., GRAHAM R. H. (1985). - Field excursion B: a structural and sedimentological traverse through the Tertiary foreland basin of the external Alps of south-east France. In: Allen P., Homewood P., Williams G. (eds.): International Sympos-

- sium on Foreland Basins, Excursion Guidebook, Fribourg, Switzerland, 2-4 September, 1985, pp. 39-73.
- EMBRIE, A. F. & KLOVAN, J. E. 1971. A late Devonian reef tract on northeastern Banks Island, Northwest Territories. *Bull. Can. Petrol. Geol.*, **19**, pp. 730-781.
- ENOS P. (1983). - Shelf environment. In: Scholle P. A., Bebout D. G., Moore C. H. (eds.): Carbonate depositional systems. *Am. Assoc. Petrol. Geol. Mem.*, **33**, pp. 267-295.
- ESTEBAN M., KLAPPA C. F. (1983). - Subaerial exposure environment. In: Scholle P. A., Bebout D. G., Moore C. H. (eds.): Carbonate depositional environments. *Am. Assoc. Petrol. Geol. Mem.*, **33**, pp. 1-95.
- EVANS M. J. (1987). - Tertiary sedimentology and thrust tectonics in the southwest Alpine foreland basin, Alpes de Haute-Provence. Ph.D. thesis, University of Wales.
- EVANS M. J., MANGE-RAJETZKY M. (1991). - The provenance of sediments in the Barreine thrust-top basin, Haute-Provence, France. In: Morton A. C., Todd S. P., Haughton P. D. W. (eds.): Developments in Sedimentary Provenance Studies. *Geol. Soc. Spec. Pub.*, **57**, pp. 323-342.
- FABRE P., PAIRIS J.-L. (1984). - Variations de faciès et paléogéographie dans les calcaires nummulitiques des Hautes-Alpes. *10ème R. A. S. T., Bordeaux*, p. 215.
- FABRE P., LAMI A., PAIRIS J.-L., GIDON M. (1985a). - Déformations synsédimentaires paléogènes du Pelvoux au Dévoluy (Alpes externes, France). *Terra Cognita*, **5**, p. 243.
- FABRE P., LAMI A., PAIRIS J.-L., GIDON M. (1985b). - Influence de la paléomorphologie et de la tectonique synsédimentaire sur les dépôts nummulitiques dans les massifs du Dévoluy et du Pelvoux (Alpes externes méridionales). *Rev. Géol. dyn. Géogr. phys.*, **26**, pp. 193-199.
- FABRE P., MÉDUS J., PAIRIS J.-L. (1986). - Caractérisation de l'Eocene et de l'Oligocene marins dans les chaînes subalpines méridionales à l'ouest de Gap (Hautes-Alpes, France). *Eclogae Geol. Helv.*, **79**, pp. 719-730.
- FLANDRIN J. (1966) Sur l'âge des principaux traits structuraux du Diois et des Baronnies. *Bull. Soc. Géol. Fr.*, **7/8**, pp. 376-386.
- FOLK R. L. (1980). - Petrology of sedimentary rocks. Hemphill Publ. Co., Austin, TX, USA, 184 p.
- FONTIGNIE D. (1981). - Géochronologie des galets andésitiques du Conglomérat des Grès du Val d'Illiez du Synclinal de Thônes (Haute-Savoie, France). *Schweiz. Mineral. Petrogr. Mitt.*, **61**, 81-96.
- FONTIGNIE D., Delaloye, M., Vuagnat M. (1987). - Age potassium-argon de galets andésitiques des grès du Champsaur (Hautes-Alpes, France). *Schweiz. Mineral. Petrogr. Mitt.*, **67**, 171-184.
- FORD M. (1996). - Kinematics and geometry of early Alpine basement-involved folds, SW Pelvoux Massif, SE France. *Eclogae Geol. Helv.*, **89**, pp. 269-295.
- FORD M., MECKEL L. D. III, BÜRGISSER J. (1995). - Late Alpine kinematics around the Pelvoux massif, SE France: implications for arc dynamics. *Terra Nova Abstract Volume*, **7/1**, p. 274.
- FORD M., STAHEL U. (1995). - The geometry of a deformed carbonate slope-basin transition: the Ventoux-Lure fault zone, SE France. *Tectonics*, **14**, pp. 1393-1410.
- FRANGIPANE M., SCHMIDT R. (1974). - Point-counting and its errors: a review. *Schweiz. Mineral. Petrogr. Mitteil.*, **54**, pp. 19-31.

- FRY N. (1989a). - Southwestward thrusting and tectonics of the western Alps. In: Coward M. P., Dietrich D., Park R. G. (eds.): Alpine Tectonics. *Geol. Soc. Spec. Pub.*, **45**, pp. 83-109.
- FRY N. (1989b). - Kinematics of the Alpine arc. *J. Geol. Soc. London*, **146**, pp. 891-892.
- GALLOWAY W. E. (1977). - Catahoula Formation of the Texas Coastal Plain: depositional systems, composition, structural development, ground water flow history, and uranium distribution. *University of Texas, Austin, Bur. econ. Geol. Report of Investigations*, **87**.
- GALLOWAY W. E., HOBDAV D. K. (1996). - Terrigenous clastic depositional systems (2nd ed.), Springer Verlag, New York, 489p.
- GAZZI P. (1966). - Sulla determinazione microscopica della composizione mineralogica e granulometrica delle rocce, in particolare delle arenarie e delle sabbie. *Mineral. Petrogr. Acta*, **12**, pp. 61-68.
- GIDON M., PAIRIS J.-L. (1976). - Le rôle des mouvements tectoniques éocènes dans la genèse des structures de l'extrémité NE du Dévoluy et dans celle du chevauchement de Digne. *Géologie Alpine*, **52**, pp. 73-83.
- GIDON M., ARNAUD H., PAIRIS J.-L., APRAHAMIAN J., USELLE J.-P. (1970). - Les déformations tectoniques superposées du Dévoluy méridional (Hautes Alpes). *Géologie Alpine*, **46**, pp. 87-110.
- GIDON M., PAIRIS J.-L. (1980-1981). - Nouvelles données sur la structure des écaillés de Soleil Boeuf (bordure sud du massif du Pelvoux). *Bull. BRGM, Fr.*, **1**, pp. 35-41.
- GILLCHRIST R., COWARD M. P., MUGNIER, J.-L. (1987). - Structural inversion and its controls: examples from the Alpine foreland and the French Alps. *Geodyn. Acta*, **1**, pp. 5-34.
- GLANCEAUD L., D'ALBISSIN M. (1958). - Les phases tectoniques du NE du Dévoluy et leur influence structurale. *Bull. Soc. Géol. Fr.*, **6/VIII/45**, pp. 675-688.
- GOGUEL J. (1963). - L'interprétation de l'arc des Alpes occidentales. *Bull. Soc. Géol. Fr.*, **7/V/3**, pp. 20-33.
- GRAHAM R. H. (1978). - Wrench faults, arcuate fold patterns and deformation in the southern French Alps. *Proc. Geol. Assoc.*, **89**, pp. 125-142.
- GRATIER J.-P., MÉNARD G., ARPIN R. (1989). - Strain-displacement compatibility and restoration of the Chaînes Subalpines of the western Alps. In: Coward M. P., Dietrich D., Park R. G. (eds.): Alpine Tectonics. *Geol. Soc. Spec. Pub.*, **45**, pp. 65-81.
- GUELLEC S., MUGNIER J.-L., TARDY M., ROURE F. (1990). - Neogene evolution of the western Alpine foreland in the light of Eocene data and balanced cross sections. In: Roure F., Heitzmann P., Polino R. (eds.): Deep Structure of the Alps. *Mém. Soc. Géol. Fr.*, **156**, pp. 165-184.
- HAQ B. U., HARDENBOL J., VAIL P. R. (1988). Mesozoic and Cenozoic chronostratigraphy and eustatic cycles. In: Wilgus C. K., Hastings B. S., Posamentier H. W., Ross C. A., Kendall C. G. St. C. (eds.): Sea level changes: an integrated approach. *Soc. Econ. Paleontol. Mineral. Spec. Pub.*, **42**, 71-108.
- HENRY B. (1980). - Contribution à l'étude structurale des propriétés magnétiques de roches magmatiques des Alpes: conséquences structurales, régionales et générales. Thèse, Université de Paris VII.
- HENRY B. (1992). - Structural implications of paleomagnetic data from Pelvoux-Belledune area (French Alps). *Tectonophysics*, **216**, 327-338.

- HERB R. (1988). - Eocene Paläogeographie und Paläotektonik des Helvetikum. *Eclogae Geol. Helv.*, **81**, pp. 611-657.
- HOMWOOD P. (1986). - Geodynamics and palaeogeography of the Western Molasse Basin: a review. *Gior. Geol.*, **48**, pp. 275-284.
- HOMWOOD P., CARON C. (1982). - Flysch of the western Alps. In: Hsü, K. J. (ed.): Mountain Building Processes, Academic Press, London, pp. 157-268.
- HOMWOOD P., ALLEN P. A., WEIDMANN M., FASEL J.-M., LATELIN O. (1985). - Field excursion A: geological excursion to the Swiss Molasse Basin. In: Allen P., Homewood P. A., Williams G. (eds.): International Symposium on Foreland Basins, Excursion Guidebook, Fribourg, Switzerland, 2-4 September 1985, pp. 5-38.
- HOMWOOD P., ALLEN P. A., WILLIAMS G. D. (1986). - Dynamics of the molasse basin of western Switzerland. In: Allen P., Homewood P. (eds.): Foreland basins. *Int. Assoc. Sedimentol. Spec. Pub.*, **8**, pp. 199-217.
- HUYGHE P., MUGNIER J.-L. (1995). - A comparison of inverted basins of the Southern North Sea and inverted structures of the external Alps. In: Buchanan J. G., Buchanan P. G. (eds.): Basin Inversion. *Geol. Soc. Spec. Pub.*, **88**, pp. 339-353.
- INDEN R. F., MOORE C. H. (1983). - Beach environment. In: Scholle P. A., Bebout D. G., Moore C. H. (eds.): Carbonate depositional environments. *Am. Assoc. Petrol. Geol. Mem.*, **33**, pp. 211-265.
- INGERSOLL R. V., BULLARD T. F., FORD R. L., GRIMM J. P., PICKLE J. D., SARES S. W. (1984). - The effect of grain size on detrital modes: a test of the Gazzi-Dickinson point-counting method. *J. Sed. Petrol.*, **54**, pp. 103-116.
- IVALDI J.-P. (1989). - Thermoluminescence et orogénèse: les Alpes occidentales au Paléogène. Thèse habilitation, Institut Polytechnique Méditerranéen.
- JONES B., DESROCHERS A. (1992). - Shallow platform carbonates. In: Walker R. G., James G. (eds.): Facies models: response to sea level changes. *Geol. Soc. Can., St-John's, Newfoundland*, pp. 277-301.
- JORDAN T. E. (1995). - Retroarc foreland and related basins. In: Busby C. J., Ingersoll, R. V. (eds.): Tectonics of sedimentary basins, Blackwell Science, Oxford, pp. 331-362.
- KARNER G. D., WATTS A. B. (1983). - Gravity anomalies and flexure of the lithosphere at mountain ranges. *J. Geophys. Res.*, **88**, pp. 10449-10477.
- KERCKHOVE C. (1969). - La "zone du Flysch" dans les nappes de l'Embrunnais-Ubaye (Alpes occidentales). Thèse d'état, Université de Grenoble, *Géol. Alpine*, **45**, pp. 5-204.
- KERCKHOVE C., DEBELMAS J., COCHONAT P. (1978). - Tectonique du soubassement parautochtone des nappes de l'Embrunnais-Ubaye sur leur bordure occidentale, du Drac au Verdon. *Géol. Alpine*, **54**, pp. 67-82.
- KERCKHOVE C., CARON C., CHAROLLAIS J., PAIRIS J.-L. (1980). - Panorama des séries synorogéniques des Alpes occidentales. *Mém. BRGM.*, **107**, pp. 234-255.
- KING L. M. (1994). - Turbidite to storm transition in a migrating foreland basin: the Kendal Group (Upper Silurian), northwest England. *Geol. Mag.*, **131**, pp. 255-267.
- KNELLER B. C., EDWARDS D. A., MCCAFFREY W. D., MOORE, R. M. M. (1991). - Oblique reflection of turbidity currents. *Geology*, **14**, pp. 250-252.

- LACASSIN R. (1989). - Plate-scale kinematics and compatibility of crustal shear zones in the Alps. In: Coward M. P., Dietrich D., Park R. G. (eds.): Alpine Tectonics. *Geol. Soc. Spec. Pub.*, **45**, pp. 339-352.
- LATELIN O. (1988). - Les dépôts turbiditiques oligocènes d'avant pays entre Annecy (Hte. Savoie) et le Sanetsch (Suisse). Thèse, Université de Fribourg.
- LAUBSCHER H. P. (1965). - Ein kinematisches Modell des Juraufaltung. *Eclogae Geol. Helv.*, **58**, pp. 231-318.
- LAUBSCHER H. P. (1991). - The arc of the western Alps today. *Eclogae Geol. Helv.*, **84**, pp. 631-659.
- LAUBSCHER H., BERNOULLI D. (1982). - History and deformation of the Alps. In: Hsü K. J. (ed.): Mountain Building Processes, Academic Press, London, pp. 169-180.
- LAWSON K. D. (1987). - Thrust geometry and folding in the Alpine structural evolution of Haute Provence. Ph. D. thesis, University College of Swansea.
- LEMCKE K. (1974). - Vertikalbewegungen des vormesozoischen Sockels im nördlichen Alpenvorland vom Perm bis zur Gegenwart. *Eclogae Geol. Helv.*, **67**, pp. 121-133.
- LEMOINE M. (1972). - Rythme et modalités des plissements superposés. *Geol. Rundschau*, **61**, pp. 975-1010.
- LEMOINE M., BAS T., ARNAUD-VANNEAU A., ARNAUD H., DUMONT T., GIDON M., BOURBON M., DE GRACIANSKY P.-C., RUDKIEWICZ J.-L., MÉGARD-GALLI J., TRICART P. (1986) - The continental margin of the Mesozoic Tethys in the Western Alps. *Mar. Petrol. Geol.*, **3**, pp. 179-199.
- LITTLE T. A. (1992). - Development of wrench folds along the Border Ranges fault system, southern Alaska, U.S.A. *J. Struct. Geol.*, **14**, pp. 343-359.
- MATTHEWS S. J. (1984). - Thrust sheet evolution in the Kinlochewe region and of the Moine thrust zone, NW Scotland and the Pelvoux Briançonnais, French Alps. Ph. D. Thesis, University of Leeds.
- MCCUBBIN D. G. (1982). - Barrier-island and strand-plain lithofacies. In: Scholle P. A., Spearing D. (eds.): Sandstone depositional systems. *Am. Assoc. Petrol. Geol. Mem.*, **31**, pp. 247-279.
- MCKENZIE D. P., JACKSON J. A. (1983). - The relationship between strain rates, crustal thickening, paleomagnetism, finite strain and fault movements within a deforming zone. *Earth Planet. Sci. Letters*, **65**, pp. 182-202, and Correction to the above (1984), *ibid.*, **70**, 444.
- MCKENZIE D. P., JACKSON J. A. (1986). - A block model of distributed deformation by faulting. *J. Geol. Soc. London*, **143**, pp. 349-353.
- MECKEL L. D. JR. (1967). - Tabular and trough cross bedding: comparison of dip azimuth variability. *J. Sed. Petrology*, **37**, pp. 80-86.
- MECKEL L. D. III (1995). - Tectonically-forced regression and the transition from carbonate to siliciclastic deposition in the western Alpine foreland basin. *Abs. Vol. Geol. Soc. Am. Ann. Meeting*, p. A-457.
- MECKEL L. D. III., FORD M., BERNOULLI D. (1996). - Tectonic and sedimentary evolution of the Dévoluy Basin, a remnant of the Tertiary western Alpine foreland basin, SE France. *Géol. Fr.*, **1996/2**, pp. 3-26.

- MÉNARD G., THOUVENOT F. (1984). - Écaillage de la lithosphère européenne sous les Alpes occidentales: arguments gravimétriques et sismiques liés à l'anomalie d'Ivrea. *Bull. Soc. Géol. Fr.*, **7/XXVI/5**, pp. 875-884.
- MERCIER J. (1958). - Sur l'âge de la phase tectonique "antesénonienne" a l'W du Dévoluy (Drôme). *Bull. Soc. Géol. Fr.*, **6/VIII/46**, pp. 689-697.
- MERCIER J., NEVEU F. (1956). - Le chevauchement du St-Gicon près de St-Disdier-en-Dévoluy (Hautes Alpes). *C. R. Soc. Géol. Fr.*, **16**, pp. 319-322.
- MERLE O., BRUN J.-P. (1981). - La déformation polyphasée de la nappe du Parpaillon (Flysch à Helminthoïdes): un résultat de la déformation progressive associée à une translation non rectiligne. *C. R. Acad. Sc., Paris*, **292**, 343-346.
- MIALL A. D. (1995). - Collision-related foreland basins. *In: Busby C. J., Ingersoll, R. V. (eds.): Tectonics of Sedimentary Basins*, Blackwell Science, Oxford, pp. 393-424.
- MOUGIN F. (1978). - Contribution à l'étude des sédiments tertiaires de la partie orientale du synclinal d'Annot. Thèse 3^e cycle, Université de Grenoble.
- MUGNIER J.-L., ARPIN R., THOUVENOT F. (1987). - Coupes équilibrées à travers le massif subalpin de la Chartreuse. *Geodin. Acta*, **1**, pp. 123-135.
- MUGNIER J.-L., GUELLEC S., MÉNARD G., ROURE F., TARDY M., VIALON P. (1990). - A crustal scale balanced cross-section through the external Alps deduced from the Ecors profile. *In: Roure F., Heitzmann P., Polino R. (eds.): Deep Structure of the Alps. Mém. Soc. Géol. Fr.*, **156**, pp. 203-216.
- MUGNIER J.-L., ROSETTI J.-P. (1990). - The effects of simplifying assumptions on balanced cross-sections: a view from the Chartreuse Massif. *In: Letonzey J. (ed.): Petroleum and Tectonics in Mobile Belts. Proceedings of the 4th IFP Exploration and Production Research Conference, Bordeaux, France, Nov. 14 - 18, 1988*, pp. 203-216.
- NIGGLI *et al.* (1973). - Carte métamorphique des Alpes à 1:1 000 000^e. Sous-commission pour la cartographie des zones métamorphiques du Monde, Leiden. *Unesco Ed.*, Paris.
- NILSEN T. H. (1982). - Alluvial fan deposits. *In: Scholle P. A., Spearing D. (eds.): Sandstone depositional systems. Am. Assoc. Petrol. Geol. Mem.*, **31**, pp. 49-86.
- ODONNE F., COSTA E. (1991). - Relationships between strike-slip movement and fold trends in thin-skinned tectonics: analogue models. *Tectonophysics*, **228**, 383-391.
- ODONNE F., VIALON P. (1987). - Hinge migration as a mechanism of superposed folding. *J. Struct. Geol.*, **9**, pp. 835-844.
- ORI G. G., FRIEND P. F. (1984). - Sedimentary basins formed and carried piggyback on active thrust sheets. *Geol.*, **12**, pp. 475-478.
- PAIRIS J.-L. (1988). - Paléogène marin et structuration des Alpes occidentales françaises (domaine externe et confins sud-occidentaux du Subbriançonnais). Thèse Docteur ès Sciences, Université Joseph-Fourier (Grenoble, France).
- PAIRIS J.-L., CAMPREDON R., CHARROLAIS J., KERCKHOVE, C. (1983) - Paléogène des Alpes externes. *Groupe d'Etude du Paléogène, Séance du 14 décembre 1983*, 3p.
- PAIRIS J.-L., CAMPREDON R., CHARROLAIS J., KERCKHOVE C. (1984a). - Alpes. *In: Synthèse géologique du sud-est de la France. Mém. BRGM*, **125**, pp. 410-415.

- PAIRIS J.-L., GIANNERINI G., NURY D. (1984b). - Tectonique et sédimentation dans les domaines alpin externe et péri-alpine. *In: Synthèse géologique du sud-est de la France. Mém. BRGM*, **125**, pp. 453-456.
- PAIRIS J.-L., GIDON M., FABRE P., LAMI A. (1986). - Signification et importance de la structuration nummulitique dans les chaînes subalpines méridionales. *C. R. Acad. Sc., Paris*, **303**, pp. 87-92.
- PEMBERTON S. G., MACEachern, J. A., FREY, R. W. (1992). - Trace fossil facies models: environmental and allostratigraphic significance. *In: Walker R. G., James, N. (eds.): Facies models: response to sea level change. Geol. Soc. Can., St. John's, Newfoundland*, pp. 47-72.
- PETTJOHN F. J., POTTER P. E., SIEVER R. (1987). - Sand and sandstone (2nd Ed.), Springer-Verlag, Inc., New York, 553p.
- PIFFNER O. A. (1986). - Evolution of the north Alpine foreland basin in the central Alps. *In: Allen P., Homewood P. (eds.): Foreland basins. Int. Assoc. Sedimentol. Spec. Pub.*, **8**, pp. 219-228.
- PLATT J. P., BEHRMANN J. H., CUNNINGHAM P. C., DEWEY J. F., HELMAN M., PARISH M., SHEPLEY M. G. WALLIS S., WESTON P. J. (1989). - Kinematics of the Alpine arc and the motion history of Adria. *Nature*, **337**, pp. 158-161.
- PLATT N. H., KELLER B. (1992). - Distal alluvial deposits in a foreland basin setting - the Lower Freshwater Molasse (Lower Miocene), Switzerland: sedimentology, architecture and paleosols. *Sedimentology*, **39**, pp. 545-565.
- POLINO R., DAL-PIAZ G. V., GOSSO G. (1990). - Tectonic erosion at the Adria margin and accretionary processes for the Cretaceous orogeny of the Alps. *Mém. Soc. Géol. Fr.*, **156**, pp. 345-367.
- QUINLAN G. M., BEAUMONT C. (1984). - Appalachian thrusting, lithosphere flexure, and the Paleozoic stratigraphy of the eastern interior of North America. *Can. J. Earth Sci.*, **21**, 973-996.
- RAMSAY J. G. (1963). - Stratigraphy, structure and metamorphism of the western Alps. *Proc. Geol. Assoc.*, **74**, 357-391.
- RAMSAY J. G. (1989). - Fold and fault geometry in the western Helvetic nappes of Switzerland and France and its implication for the evolution of the arc of the western Alps. *In: Coward M. P., Dietrich D., Park R. G. (eds.): Alpine Tectonics. Geol. Soc. Spec. Pub.*, **45**, pp. 33-45.
- RAMSAY J. G., HUBER M. I. (1983). - The Techniques of Modern Structural Geology - Volume 1: Strain Analysis, Academic Press, London, 307p.
- RAVENNE C., VIALLY R., RICHÉ P., TRÉMOLIÈRES P. (1987). - Sédimentation et tectonique dans le bassin marin Éocène supérieur-Oligocène des Alpes du sud. *Rev. Inst. Fr. Pétr.*, **42**, pp. 529-553.
- RIBA O. (1976a). - Syntectonic unconformities of the Alto Cardener, Spanish Pyrenees, a genetic interpretation. *Sed. Geol.*, **15**, pp. 213-233.
- RIBA (1976b). - Tectogenèse et sédimentation: deux modèles des discordances syntectoniques pyrénéennes. *Bull. BRGM*, **4**, pp. 383-401.
- RICOU L. E., SIDDANS A. W. B. (1986). - Collision tectonics in the Western Alps. *In: Ries A. C., Coward M. P. C. (eds.): Collision tectonics. Geol. Soc. Spec. Pub.*, **19**, pp. 229-244.
- RUBIN D. M. (1987). - Cross-bedding, bedforms, and paleocurrents. *Soc. Econ. Paleontol. Min. Concepts in Sedimentology and Paleontology*, **1**, 187p.
- SANDERSON D. J., MARCHINI W. R. D. (1984). - Transpression. *J. Struct. Geol.*, **6**, pp. 449-458.

- SCHREURS G. (1993). - Analogue modelling using X-ray computed tomography analysis: oblique shortening and oblique extension experiments. *Inst. Fr. Pétrole Report*, 40467.
- SCHUMM S. A. (1977). - The Fluvial System, Wiley & Sons, New York, 338p.
- SCHWAB F. L. (1986). - Sedimentary "signatures of foreland basin assemblages: real or counterfeit? In: Allen P., Homewood P. (eds.): Foreland basins. *Int. Assoc. Sedimentol. Spec. Pub.*, 8, pp. 395-410.
- SEILACHER A. (1978). - Use of trace fossil assemblages for recognizing depositional environments: trace fossil concept. In: Society of Economic Paleontologists and Mineralogists Short Course, 5, pp. 167-181.
- SIDDANS A. W. B. (1979). - Arcuate fold and thrust patterns in the Subalpine Chains of Southeast France. *J. Struct. Geol.*, 1, pp. 117-126.
- SINCLAIR H. D. (1989). - The North Helvetic Flysch of E Switzerland: foreland basin architecture and modelling. Ph. D. Thesis, University of Oxford.
- SINCLAIR H. D. (1993). - High resolution stratigraphy and facies differentiation of the shallow marine Annôt Sandstones, south-east France. *Sedimentology*, 40, pp. 955-978.
- SINCLAIR H. D. (1996). - Plan-view curvature of foreland basins and its implications for the paleostrength of the lithosphere underlying the western Alps. *Basin. Res.*, 8, 173-182.
- SINCLAIR H. D. (in press). - Tectono-stratigraphic model for underfilled peripheral foreland basins: an Alpine perspective. *Bull. Geol. Soc. Amer.*
- SINCLAIR H. D., ALLEN P. A. (1992). - Vertical vs. horizontal motions in the Alpine orogenic wedge: stratigraphic response in the foreland basin. *Basin Res.*, 4, 215-233.
- SINCLAIR H. D., COAKLEY B. J., ALLEN P. A., WATTS A. B. (1991). - Simulation of foreland basin stratigraphy using a diffusion model of mountain belt uplift and erosion: an example from the central Alps, Switzerland. *Tectonics*, 10, pp. 599-620.
- STAMPFLI G. M. (1993). - Le Briançonnais, terrain exotique dans les Alpes? *Eclogae Geol. Helv.*, 86, pp. 1-45.
- STANLEY D. J. (1975). - Submarine canyon and slope sedimentation (Grès d'Annot) in the French Maritime Alps. IX Congress Int. Sedimentol., Nice, France, 129 p.
- STOW D. A. V., SHANMUGAM, G. (1980). - Sequence of structures in fine-grained turbidites: comparison of recent deep-sea and ancient flysch sediments. *Sed. Geol.*, 25, 23-42.
- SUTTNER L. J., BASU A., INGERSOLL R. V., BULLARD T. F., FORD R. L., PICKLE J. D. (1985). - The effects of grain size on detrital modes: a test of the Gazzi-Dickinson point-counting method: discussion and reply. *J. Sed. Petr.*, 55, pp. 616 - 618.
- TAPPONNIER P. (1977). - Evolution tectonique du système Alpin en Méditerranée: poinçonnement et écrasement rigide-plastique. *Bull. Soc. Géol. Fr.*, 19/4, 437-460.
- TIKOFF B., TEYSSIER C. (1994). - Strain modeling of displacement-field partitioning in transpressional orogens. *J. Struct. Geol.*, 16, pp. 1575-1588.
- TRIGART P. (1984). From passive margin to continental collision: a tectonic scenario for the western Alps. *Am. Jour. Sci.*, 284, pp. 97-120.

- TRÜMPY R. (1976). - Du Pèlerin aux Pyrénées. *Eclogae Geol. Helv.*, 69, 249-264.
- TRÜMPY R. (1980). - Geology of Switzerland, part A: An Outline of the Geology of Switzerland, Wepf and Co., Basel, 104 p.
- TUCKER M. E., WRIGHT V. P. (1988). - Carbonate sedimentology, Blackwell Scientific Publications, Oxford, 482 p.
- VAN DER PLAS L. (1962). - Preliminary note on the granulometric analysis of sedimentary rocks. *Sedimentology*, 1, pp. 145-157.
- VIALLY R. (1994). - The southern French Alps Paleogene basin: Subsidence modeling and geodynamic implications. *Sp. Pub. Eur. Assoc. Petrol. Geosci.*, 4, 281-293.
- VIALON P. (1974). - Les déformations synschisteuses superposées en Dauphine. Leur place dans la collision des éléments du socle préalpin. *Schweiz. Mineral. Petrogr. Mitt.*, 54, pp. 663-690.
- VIALON P. (1976). - L'arc alpin occidental: orientation des structures primitivement. *Eclogae Geol. Helv.*, 69, pp. 509-519.
- VIALON P., BOUDOU J., GAMOND J.-F., PLOTTO P., ROBERT J.-F. (1976). - L'arc des Alpes occidentales: une zone de "transformation continentale" ou glissement senestre? Présentation d'un modèle des déformations. *Réunion annuelle des Sciences de la Terre*, 4, p. 391.
- VIALON P., ROCHETTE P., MÉNARD, G. (1989). - Indentation and rotation in the western Alpine arc. In: Coward M. P., Dietrich D., Park R. G. (eds.): Alpine Tectonics. *Geol. Soc. Spec. Pub.*, 45, pp. 329-338.
- WAIBEL A. F. (1990). - Sedimentology, petrographic variability, and very-low-grade metamorphism of the Champsaur Sandstone (Paleogene, Hautes-Alpes, France): evolution of volcanoclastic foreland turbidites in the external western Alps. Thèse Docteur ès Sciences de la Terre, Université de Genève, Switzerland.
- WAIBEL A. F. (1993). - Nature and plate-tectonic significance of orogenic magmatism in the European Alps: a review. *Schweiz. Mineral. Petrogr. Mitt.*, 73, pp. 391-405.
- WILLIAMS H., TURNER F. J., GILBERT, C. M. (1954). - Petrology, Freeman, San Francisco, 406p.
- WILSON J. L., JORDAN C. (1983). - Middle shelf environment. In: Scholle P. A., Bebout D. G., Moore C. H. (eds.): Carbonate depositional environments. *Am. Assoc. Petrol. Geol. Mem.*, 33, pp. 297-343.
- WINKLER W. (1988). - Mid to early Late Cretaceous flysch and melange formations in the western part of the Eastern Alps: palaeotectonic implications. *Jahrb. Geol. Bundesanst. Wien*, 131, pp. 341-389.
- WOODWARD N. B., BOYER S. E., SUPPE J. (1989). - Balanced geological cross-sections: an essential technique in geological research and exploration. *Am. Geophys. Union Short Course in Geology*, 6, 132p.

Maps consulted

- Carte Géologique de la France à 1:50000 (Bureau de Recherches Géologiques et Minières)
- BRGM (1957). - Puget-Théniers. Feuille XXXVI-41 (946).

- BRGM (1966)- *Fayence*. Feuille XXXV-43 (998).
- BRGM (1967a). - *Allos*. Feuille XXXV-40 (919).
- BRGM (1967b). - *St-Martin-Vésubie-Le Boréon*. Feuille XXXVII-41-40 (947).
- BRGM (1968). - *Menton-Nice*. Feuille XXXVII-42-43.
- BRGM (1970a). - *Grasse-Cannes*. Feuille XXXVI-43-44 (999).
- BRGM (1970b). - *St-Etienne de Tinée*. Feuille XXXVI-40 (920).
- BRGM (1971). - *Gap*. Feuille XXXIII-38.
- BRGM (1974a). - *Barcelonnette*. Feuille XXXV-39 (895).
- BRGM (1974b). - *Mens*. Feuille XXXII-37 (844).
- BRGM (1976). - *Castellane*. Feuille XXXV-42 (971).
- BRGM (1978a). - *Larche*. Feuille XXXVI-39 (896).
- BRGM (1978b). - *Moustiers-Ste-Marie*. Feuille XXXIV-42 (970).
- BRGM (1980a). - *Entrevaux*. Feuille XXXV-41 (945).
- BRGM (1980b). - *Orcières*. Feuille XXXIV-37 (846).
- BRGM (1980c). - *Roquesteron*. Feuille XXXVI-42 (972).
- BRGM (1980d). - *St-Bonnet*. Feuille XXXIII-37 (845).
- BRGM (1981). - *Digne*. Feuille XXXIV-41 (944).

Point counting of thin sections of clastic rock samples from Dévoluy was selected as the preferred method to determine the clastic content because it allows the provenance schemes of Dickinson (1970) to be utilized. However, point counting is a problematic method because it does not account for the effects of grain size-dependent variations in mineralogy (van der Plas, 1962). This shortcoming was addressed by selecting medium-grained samples whenever possible. An additional problem is that the method gives a volumetric modal estimate of component grains (Chayes, 1956), which gives less accurate compositional distributions than a number frequency estimate (van der Plas, 1962, Winkler, 1988). Therefore, the usefulness of point counting for provenance determination has been questioned (Winkler, 1988). Nevertheless, the advantage of utility within an accepted and established provenance scheme (Dickinson, 1970) were considered to outweigh the additional precision obtained in a number frequency analysis such as ribbon counting (usually < 10%, according to Winkler, 1988).

Dickinson's (1970) provenance scheme utilizes the Gazzi-Dickinson point-counting method (Gazzi, 1966; Dickinson, 1970), in which all sand-sized grains (0.063 - 2 mm), whether they occur within lithic fragments or not, are counted as individual mineral grains (i.e., a quartz grain within a granitic clast is counted as a quartz grain, and not as an igneous lithic clast; however, carbonate and fine-grained siliciclastic sedimentary lithic clasts are counted as the respective clasts). This method reduces the effects of grain size on composition, thereby allowing samples from the same source, but with different grain sizes or with different amounts of weathering, to be placed in the same category.

An alternative approach (the "traditional" method of, e.g., Basu, 1976) considers sand-sized grains within lithic fragments to be part of the lithic fragment (i.e., a quartz grain within a granitic clast is not counted, but rather, the igneous lithic fragment is counted). This method assumes that compositional variation is an inherent effect of grain size: that is, as lithic fragments of a rock are broken down, the composition of the sediment changes fundamentally, and that this evolution is a critical and distinguishing aspect of the rock. Ingersoll *et al.* (1984) have documented the apparent compositional differences which result from the use of one or the other method.

In this study, sand-sized minerals within larger lithic fragments were counted according to the "traditional" method (i.e., as lithic fragments). Clearly, this introduces a component of error when utilizing Dickinson's (1970) ternary diagrams. However, I believe that the "traditional" method gives improved interpretive ability in provenance studies (cf. Decker *et al.*, 1985; Suttner & Basu, 1985), and that the introduced error is negligible because the quantity of sand-sized minerals in lithic fragments was always significantly less than that of the stable minerals.

Twelve categories were used in point counting. These are defined below.

POINT COUNTING CATEGORIES

Monocrystalline quartz (Q_m): All single quartz grains with straight extinction. Quartz grains with straight extinction within a larger grain were included in the corresponding lithic category (L_v , L_s , or L_t).

Polycrystalline quartz (Q_p): All quartz grains having either (i) more than one sub-grain with distinct, but irregular, subgrain boundaries, or (ii) strongly undulose extinction; this definition includes "metamorphic" quartz (Folk 1980) and sedimentary chert, but does not include unstable lithic fragments composed of quartz, such as quartzite or metaquartzite. When these were discernible, the grain was counted in the corresponding lithic category.

Plagioclase feldspar (F_p): Plagioclase feldspar was etched with 50% hydrofluoric acid and stained red with barium chloride and amaranth. Individual grains were counted as plagioclase, while grains within a lithic fragment were counted as part of the corresponding lithic fragment (typically, L_v or L_s).

Potassium feldspar (F_k): Orthoclase feldspar was etched with 50% hydrofluoric acid and stained yellow with sodium cobalt nitrite. Individual grains were counted as K-feldspar, while grains within a lithic fragment were counted as part of the corresponding lithic fragment (typically, L_v or L_s).

Igneous lithic fragment (L_v): Comprises detrital plutonic igneous fragments (e. g., granite) and extrusive igneous fragments with a fine-grained groundmass and distinct phenocrysts.

Carbonate lithic fragment (L_c): Detrital carbonate grains with distinct grain boundaries. Typically micritic, but also including grains in which fossils or other carbonate grains are recognizable. Includes lime mudstone, wackestone, packstone, grainstone, and crystalline carbonate material (terminology of Dunham, 1962). Differentiated from matrix (Ma) by the distinct grain boundaries.

Siliciclastic lithic fragment (L_s): Detrital sedimentary grains of shale, siltstone, or fine-grained sandstone. These fragments are assumed to be extrabasinal (after Dickinson & Suczek, 1976), so they are included in the counts of lithic fragments.

Metamorphic lithic fragment (L_m): Detrital grains with clear evidence of metamorphism (usually a metamorphic cleavage).

Microcrystalline lithic fragment (L_{mx}): All lithic fragments too fine-grained to determine the parent lithology. Might include shale, metashale, aphanitic igneous fragments, or (micro)cryptocrystalline igneous fragments. Because the parent lithology was undiscernible, these fragments were only included in counts of total lithics (TL ; see below).

Serpentinite (S): Because of the unusually high content of serpentinite in many of the siliciclastic rocks of Dévoluy, this rock fragment, which occasionally stains red with the plagioclase stain, was counted separately. In my scheme, serpentinite is considered to be a meta-volcanic fragment. Therefore, in triangular plots including igneous lithics, it was included in the L_v count.

Miscellaneous ($Misc$): All identifiable grains not included in another category. Includes heavy mineral species, micas, metamorphic and igneous minerals other than quartz, feldspar, or serpentinite), opaque grains, carbonaceous debris, fossils, glauconite, unidentified grains, cement, matrix, and replaced grains. These grains were excluded from the total point count sum (see below).

GAZZI-DICKINSON CATEGORIES

Total points counted (T_{All}): The sum total of all points counted, including miscellaneous ($Misc$) grains. Because of the inclusion of miscellaneous grains, T_{All} was not used in calculating the corrected percentages of constituent grains in the sample. That total (TOT) is described below.

Total grains (TOT): The sum total of grains counted with genetic and comparative significance. Therefore:

$$TOT = (T_{All}) - (Misc).$$

To ensure a reasonably small counting error (van der Plas, 1962), $TOT \approx 300$.

Total quartz (Q): The total quartz in the sample is calculated as the sum of all stable quartzose grains. That is:

$$Q = (Q_m + Q_p).$$

Total feldspar (F): The total feldspar in the sample is calculated as the sum of all stable feldspar grains. That is:

$$F = (F_k + F_p).$$

Unstable lithic fragments (L): The sum of unstable lithic grains:

$$L = (L_c + L_s + L_v + L_m + L_{mx} + S),$$

where serpentinite (S) is considered a meta-volcanic lithic clast.

Total lithics (Lt): The total lithic components in the sample are the sum of unstable lithic fragments and stable quartzose lithic fragments. The sum is calculated as follows:

$$Lt = L + Q_p.$$

Total unstable sedimentary lithic fragments (LS): The sum of unstable sedimentary lithic clasts:

$$LS = L_c + L_s.$$

The results of the petrographical analysis are shown in Table A-I.

